EOS Data Products Handbook

Volume 2

ACRIMSAT • Aqua • Jason-1 • Landsat 7
• Meteor 3M/SAGE III •
QuikScat • QuikTOMS • VCL

EOS Data Products Handbook

Volume 2

ACRIMSAT
- ACRIM III

Aqua
- AIRS
- AMSR-E
- AMSU-A
- CERES
- HSB
- MODIS

Jason-1
- DORIS
- JMR
- Poseidon-2

Landsat 7
- ETM+

Meteor 3M
- SAGE III

QuikScat
- SeaWinds

QuikTOMS
- TOMS

VCL
- MBLA

EOS Data Products Handbook

Volume 2

Editors

Claire L. Parkinson
NASA Goddard Space Flight Center

Reynold Greenstone
Raytheon ITSS

Design and Production

Sterling Spangler
Raytheon ITSS

For Additional Copies:

EOS Project Science Office
Code 900
NASA/Goddard Space Flight Center
Greenbelt, MD 20771
eos.nasa.gov

Phone: (301) 867-2037
Internet: leon_middleton@ssaihq.com

NASA Goddard Space Flight Center
Greenbelt, Maryland

Printed October 2000

Acknowledgments

Special thanks are extended to Michael King for guidance throughout and to the many additional individuals who also provided information necessary for the completion of this second volume of the EOS Data Products Handbook. These include most prominently Stephen W. Wharton and Monica Faeth Myers, whose tremendous efforts brought about Volume 1, and the members of the science teams for each of the instruments covered in this volume.

Support for production of this document, provided by William Bandeen, Jim Closs, Steve Graham, and Hannelore Parrish, is also gratefully acknowledged.

Abstract

The *EOS Data Products Handbook* provides brief descriptions of the data products that will be produced from a range of missions of the Earth Observing System (EOS) and associated projects. Volume 1, originally published in 1997, covers the Tropical Rainfall Measuring Mission (TRMM), the Terra mission (formerly named EOS AM-1), and the Data Assimilation System, while this volume, Volume 2, covers the Active Cavity Radiometer Irradiance Monitor Satellite (ACRIMSAT), Aqua, Jason-1, Landsat 7, Meteor 3M/Stratospheric Aerosol and Gas Experiment III (SAGE III), the Quick Scatterometer (QuikScat), the Quick Total Ozone Mapping Spectrometer (QuikTOMS), and the Vegetation Canopy Lidar (VCL) missions. Volume 2 follows closely the format of Volume 1, providing a list of products and an introduction and overview descriptions of the instruments and data processing, all introductory to the core of the book, which presents the individual data product descriptions, organized into 11 topical chapters. The product descriptions are followed by five appendices, which provide contact information for the EOS data centers that will be archiving and distributing the data sets, contact information for the science points of contact for the data products, references, acronyms and abbreviations, and a data products index.

Table of Contents

Foreword

This is Volume 2 in a planned three-part series known as the Earth Observing System (EOS) Data Products Handbook (DPH). Each of the three volumes in the series will contain product descriptions for the science data products that are, or will be, available as standard products from sensors on existing and planned EOS satellites. The objective of the information presented in the series of Handbooks is to promote a broader understanding of how EOS data products can be used to contribute to and facilitate science research that will lead to improved monitoring and analysis of Earth phenomena, and ultimately to improved understanding and prediction of global climate change.

DPH Volume 1 is dedicated to data products from instruments of the first era of EOS platforms, the Tropical Rainfall Measuring Mission (TRMM) and Terra (formerly known as AM-1). The reader is therefore referred to Volume 1 for information on the TRMM precipitation-related instrument products derived from the TRMM Microwave Imager (TMI), the Precipitation Radar (PR), the Visible Infrared Scanner (VIRS) and the Lightning Imaging Sensor (LIS). TRMM also carried the Clouds and the Earth's Radiant Energy System (CERES) instrument, and its products will be found in Volume 1 as well. There are also products based on the analyses performed by the Goddard Data Assimilation Office (DAO).

The instruments on board Terra are the Advanced Spaceborne Thermal Emission and Reflection Radiometer (ASTER), Clouds and the Earth's Radiant Energy System (CERES), the Multi-Angle Imaging Spectroradiometer (MISR), the Moderate Resolution Imaging Spectroradiometer (MODIS), and the Measurements of Pollution in the Troposphere (MOPITT). All standard products for these instruments are described in Volume 1.

This Volume 2 of the DPH brings us to the era featuring the second major EOS mission, Aqua (formerly PM-1) and includes product descriptions not only for the instruments on board Aqua but also for those instruments flying in the same era on missions not included in Volume 1. The additional missions and their sensors are ACRIMSAT (Active Cavity Irradiance Monitor, ACRIM III), Jason-1 (Doppler Orbitography and Radiopositioning Integrated by Satellite, DORIS; Jason Microwave Radiometer, JMR; and a radar altimeter, Poseidon-2), Landsat 7 (Enhanced Thematic Mapper +, ETM+), Meteor 3M/SAGE III (Stratospheric Aerosol and Gas Experiment, SAGE III), QuikScat (SeaWinds), QuikTOMS (Total Ozone Mapping Spectrometer, TOMS), and Vegetation Canopy Lidar (VCL, Multi-Beam Laser Altimeter, MBLA).

The Aqua instruments whose products are featured in Volume 2 are: Atmospheric Infrared Sounder (AIRS), Advanced Microwave Sounding Unit-A (AMSU-A), Humidity Sounder for Brazil (HSB), Advanced Microwave Scanning Radiometer-E (EOS version, AMSR-E), Clouds and the Earth's Radiant Energy System (CERES), and Moderate Resolution Imaging Spectroradiometer (MODIS).

Note that there has been a deliberate plan to have CERES fly on three missions, TRMM, Terra, and Aqua, with the intent of achieving maximum near-simultaneous coverage but at different viewing angles of Earth's radiances and clouds.

Processing Level – Data set processing level is referred to throughout this document (see definitions on facing page). Level 1 data (radiances, brightness temperatures, etc.) require knowledge regarding the instrument calibration and characterization, agreed-upon algorithms, and computer processing capability for conversion from Level 0 (unprocessed raw data in counts). Level 2 data measure the biogeophysical properties of Planet Earth derived from the calibrated and geolocated Level 1 data using scientific remote sensing principles.

Level 3 (mapped/gridded) and Level 4 (modeled) products can be used by interdisciplinary scientists to combine data from different areas of knowledge without necessarily having to know the details or undertake all of the processing that would otherwise be necessary (to process Level 1 to Level 3 or 4). The availability of Level 3 and 4 data is a major advantage of the EOS Data and Information System (EOSDIS) in promoting data usage from outside the science field in which the data were generated. Some data sets are being produced and archived in both a Level 2 (unmapped) and Level 3 (mapped and/or temporally sampled) form.

Access to the actual data from the EOS instruments can be obtained most readily through the EOS Distributed Active Archive Centers (DAACs), and they are listed in Appendix A of this volume. In addition, names and addresses of key investigators are to be found in Appendix B: Points of Contact. Other information concerning all the EOS instruments can be found in the 1999 EOS Reference Handbook, which can be found, along with Volume 1 of the Data Products Handbook, by accessing the EOS Project Science Office home page at http://eos.nasa.gov/.

As was typical of the information supplied in Volume 1, the information supplied here in Volume 2 has primarily been obtained from the principal investigators of the various instruments or from key staff members of the science teams for the instruments. We are extremely grateful to all the many contributors who have made it possible for us to assemble this material. We hope the information contained here will be of great use to a wide variety of potential users.

Michael D. King
EOS Senior Project Scientist

Level 0 - Reconstructed unprocessed instrument/payload data at full resolution; any and all communications artifacts (e.g., synchronization frames, communications headers) removed.

Level 1A - Reconstructed unprocessed instrument data at full resolution, time-referenced, and annotated with ancillary information, including radiometric and geometric calibration coefficients and georeferencing parameters (i.e., platform ephemeris) computed and appended, but not applied, to the Level 0 data.

Level 1B - Level 1A data that have been processed to sensor units (not all instruments have a Level 1B equivalent).

Level 2 - Derived geophysical variables at the same resolution and location as the Level 1 source data.

Level 3 - Variables mapped on uniform space-time grid scales, usually with some completeness and consistency.

Level 4 - Model output or results from analyses of lower level data (e.g., variables derived from multiple measurements).

List of Data Products

(Organized by Mission Name)

ACRIMSAT
- ACRIM III

Aqua
- AIRS
- AMSR-E
- AMSU-A
- CERES
- HSB
- MODIS

Jason-1
- DORIS
- JMR
- Poseidon-2

Landsat 7
- ETM+

Meteor 3M
- SAGE III

QuikScat
- SeaWinds

QuikTOMS
- TOMS

VCL
- MBLA

Mission	Instrument	Data Set	Proc. Level	Prod. ID	Chapter	Page #
ACRIMSAT	***ACRIM III***	Radiometric Products	1, 2		Radiance/ Reflectance and Irradiance Products	*51*
Aqua	***AIRS***	Level 1A Radiance Counts	1A	AIR 01	Radiance/ Reflectance and Irradiance Products	*52*
	AIRS	Level 1B Calibrated, Geolocated Radiances	1B	AIR 02	Radiance/ Reflectance and Irradiance Products	*52*
Aqua	***AIRS/ AMSU-A/HSB***	Trace Constituent Product	2	AIR 03	Atmospheric Chemistry	*126*
	AIRS/ AMSU-A/HSB	Cloud Product	2	AIR 04	Cloud and Aerosol Properties and Radiative Energy Fluxes	*91*
	AIRS/ AMSU-A/HSB	Humidity Product	2	AIR 05	Precipitation and Atmospheric Humidity	*75*
	AIRS/ AMSU-A/HSB	Surface Analysis Product	2	AIR 06	Surface Temperatures of Land and Oceans, Fire Occurrence, and Volcanic Effects	*155*
	AIRS/ AMSU-A/HSB	Atmospheric Temperature Product	2	AIR 07	Atmospheric Temperatures	*134*
	AIRS/ AMSU-A/HSB	Ozone Product	2	AIR 08	Atmospheric Chemistry	*126*
	AIRS/ AMSU-A/HSB	Level 2 Cloud-Cleared Radiances	2	AIR 09	Radiance/ Reflectance and Irradiance Products	*53*
	AIRS/ AMSU-A/HSB	Flux Product	2	AIR 10	Cloud and Aerosol Properties and Radiative Energy Fluxes	*92*
Aqua	***AMSR-E***	Columnar Cloud Water	2,3	AE_Ocean, AE_DyOcn, AE_WkOcn, AE_MoOcn	Cloud and Aerosol Properties and Radiative Energy Fluxes	*94*
	AMSR-E	Columnar Water Vapor	2,3	AE_Ocean, AE_DyOcn, AE_WkOcn, AE_MoOcn	Precipitation and Atmospheric Humidity	*79*
Aqua	***AMSR-E***	Level 2A Brightness Temperatures	2	AE_L2A	Radiance/ Reflectance and Irradiance Products	*53*

Mission	Instrument	Data Set	Proc. Level	Prod. ID	Chapter	Page #
Aqua	***AMSR-E***	Rainfall - Level 2	2	AE_Rain	Precipitation and Atmospheric Humidity	*76*
	AMSR-E	Rainfall - Level 3	3	AE_RnGd	Precipitation and Atmospheric Humidity	*78*
	AMSR-E	Sea Ice Concentration	3	AE_SI25	Snow and Ice Cover	*207*
	AMSR-E	Sea Ice Temperatures	3	AE_SI25	Snow and Ice Cover	*209*
	AMSR-E	Sea Surface Temperature	2,3	AE_Ocean	Surface Temperatures of Land and Oceans, Fire Occurrence, and Volcanic Effects	*157*
	AMSR-E	Sea Surface Wind Speed	2,3	AE_Ocean, AE_DyOcn, AE_WkOcn, AE_MoOcn	Winds	*142*
	AMSR-E	Snow Depth on Sea Ice	3	AE_SI12	Snow and Ice Cover	*208*
	AMSR-E	Snow-Water Equivalent and Snow Depth	3	AE_DySno, AE_5Dsno, AE_MoSno	Snow and Ice Cover	*210*
	AMSR-E	Surface Soil Moisture	2,3	AE_Land, AE_Land3,	Vegetation Dynamics, Land Cover, and Land Cover Change	*169*
	AMSU-A	Level 1A Radiance Counts	1A	AMS 01	Radiance/ Reflectance and Irradiance Products	*54*
	AMSU-A	Level 1B Calibrated, Geolocated Radiances	1B	AMS 02	Radiance/ Reflectance and Irradiance Products	*55*
Aqua	***CERES***	Bi-Directional Scans Product	0,1	CER/BDS	Radiance/ Reflectance and Irradiance Products	*55*
	CERES	ERBE-like Instantaneous TOA Estimates	2	CER/ES-8	Cloud and Aerosol Properties and Radiative Energy Fluxes	*96*
	CERES	ERBE-like Monthly Regional Averages (ES-9) and ERBE-like Monthly Geographical Averages (ES-4)	3	CER/ES-4, CER/ES-9	Cloud and Aerosol Properties and Radiative Energy Fluxes	*97*

Mission	Instrument	Data Set	Proc. Level	Prod. ID	Chapter	Page #
Aqua	***CERES***	Single Scanner TOA/ Surface Fluxes and Clouds	2	CER/SSF	Cloud and Aerosol Properties and Radiative Energy Fluxes	*99*
	CERES	Clouds and Radiative Swath	2	CER/CRS	Cloud and Aerosol Properties and Radiative Energy Fluxes	*101*
	CERES	Monthly Gridded Radiative Fluxes and Clouds	3	CER/FSW	Cloud and Aerosol Properties and Radiative Energy Fluxes	*103*
	CERES	Synoptic Radiative Fluxes and Clouds	3	CER/SYN	Cloud and Aerosol Properties and Radiative Energy Fluxes	*104*
	CERES	Monthly Regional Radiative Fluxes and Clouds (AVG) and Monthly Zonal and Global Radiative Fluxes and Clouds (ZAVG)	3	CER/AVG, CER/ZAVG	Cloud and Aerosol Properties and Radiative Energy Fluxes	*105*
	CERES	Monthly Gridded TOA/ Surface Fluxes and Clouds	3	CER/SFC	Cloud and Aerosol Properties and Radiative Energy Fluxes	*107*
Aqua	***CERES***	Monthly TOA/Surface Averages	3	CER/ SRBAVG	Cloud and Aerosol Properties and Radiative Energy Fluxes	*108*
	HSB	Level 1A Radiance Counts	1A	HSB 01	Radiance/ Reflectance and Irradiance Products	*57*
	HSB	Level 1B Calibrated, Geolocated Radiances	1B	HSB 02	Radiance/ Reflectance and Irradiance Products	*57*
Aqua	***MODIS***	Level 1A Radiance Counts	1A	MOD 01	Radiance/ Reflectance and Irradiance Products	*58*
	MODIS	Level 1B Calibrated, Geolocated Radiances	1B	MOD 02	Radiance/ Reflectance and Irradiance Products	*58*
	MODIS	Geolocation Data Set	1B	MOD 03	Radiance/ Reflectance and Irradiance Products	*60*

Mission	Instrument	Data Set	Proc. Level	Prod. ID	Chapter	Page #
Aqua	***MODIS***	Aerosol Product	2	MOD 04	Cloud and Aerosol Properties and Radiative Energy Fluxes	*109*
	MODIS	Total Precipitable Water	2	MOD 05	Precipitation and Atmospheric Humidity	*80*
	MODIS	Cloud Product	2	MOD 06	Cloud and Aerosol Properties and Radiative Energy Fluxes	*112*
	MODIS	Atmospheric Profiles	2	MOD 07	Precipitation and Atmospheric Humidity; Atmospheric Temperatures	*82* *136*
	MODIS	Level 3 Atmosphere Products	3	MOD 08	Cloud and Aerosol Properties and Radiative Energy Fluxes	*115*
	MODIS	Surface Reflectance; Atmospheric Correction Algorithm Products	2	MOD 09	Vegetation Dynamics, Land Cover, and Land Cover Change	*170*
	MODIS	Snow Cover	2,3	MOD 10	Snow and Ice Cover	*211*
	MODIS	Land Surface Temperature (LST) and Emissivity	2,3	MOD 11, 11comb, 11adv	Surface Temperatures of Land and Oceans, Fire Occurrence, and Volcanic Effects	*159*
	MODIS	Land Cover Type	3	MOD 12	Vegetation Dynamics, Land Cover, and Land Cover Change	*171*
	MODIS	Vegetation Indices	3	MOD 13	Vegetation Dynamics, Land Cover, and Land Cover Change	*173*
	MODIS	Thermal Anomalies – Fires	2,3	MOD 14	Surface Temperatures of Land and Oceans, Fire Occurrence, and Volcanic Effects	*161*
	MODIS	Leaf Area Index and Fraction of Photosynthetically Active Radiation – Moderate Resolution	4	MOD 15	Vegetation Dynamics, Land Cover, and Land Cover Change	*176*

Mission	Instrument	Data Set	Proc. Level	Prod. ID	Chapter	Page #
Aqua	***MODIS***	Surface Resistance and Evapotranspiration	4	MOD 16	Vegetation Dynamics, Land Cover, and Land Cover Change	*178*
	MODIS	Vegetation Production and Net Primary Production	4	MOD 17	Vegetation Dynamics, Land Cover, and Land Cover Change	*179*
	MODIS	Normalized Water-Leaving Radiance	2,3	MOD 18	Radiance/ Reflectance and Irradiance Products	*60*
	MODIS	Pigment Concentration	2,3	MOD 19	Phytoplankton and Dissolved Organic Matter	*190*
	MODIS	Chlorophyll Fluorescence	2,3	MOD 20	Phytoplankton and Dissolved Organic Matter	*193*
	MODIS	Chlorophyll *a* Pigment Concentration	2,3	MOD 21	Phytoplankton and Dissolved Organic Matter	*195*
	MODIS	Photosynthetically Active Radiation	2,3	MOD 22	Radiance/ Reflectance and Irradiance Products	*62*
	MODIS	Suspended Solids Concentration	2,3	MOD 23	Phytoplankton and Dissolved Organic Matter	*190*
	MODIS	Organic Matter Concentration	2,3	MOD 24	Phytoplankton and Dissolved Organic Matter	*190*
	MODIS	Coccolith Concentration	2,3	MOD 25	Phytoplankton and Dissolved Organic Matter	*197*
Aqua	***MODIS***	Ocean Water Attenuation Coefficient	2,3	MOD 26	Phytoplankton and Dissolved Organic Matter	*190*
	MODIS	Ocean Primary Productivity	4	MOD 27	Phytoplankton and Dissolved Organic Matter	*198*
	MODIS	Sea Surface Temperature	2,3	MOD 28	Surface Temperatures of Land and Oceans, Fire Occurrence, and Volcanic Effects	*162*
	MODIS	Sea Ice Cover	2,3	MOD 29	Snow and Ice Cover	*213*

Mission	Instrument	Data Set	Proc. Level	Prod. ID	Chapter	Page #
Aqua	***MODIS***	Phycoerythrin Concentration	2,3	MOD 31	Phytoplankton and Dissolved Organic Matter	*200*
	MODIS	Processing Framework and Match-up Database	2	MOD 32	Radiance/ Reflectance and Irradiance Products	*63*
	MODIS	Cloud Mask	2	MOD 35	Cloud and Aerosol Properties and Radiative Energy Fluxes	*118*
	MODIS	Absorption Coefficients	2,3	MOD 36	Phytoplankton and Dissolved Organic Matter	*195*
	MODIS	Aerosol Optical Depth	2,3	MOD 37	Radiance/ Reflectance and Irradiance Products	*60*
	MODIS	Clear-Water Epsilon	2,3	MOD 39	Radiance/ Reflectance and Irradiance Products	*64*
	MODIS	Burn Scars	4	MOD 40	Surface Temperatures of Land and Oceans, Fire Occurrence, and Volcanic Effects	*161*
	MODIS	Surface Reflectance BRDF/ Albedo Parameter	3	MOD 43	Vegetation Dynamics, Land Cover, and Land Cover Change	*180*
	MODIS	Vegetation Cover Conversion	4	MOD 44	Vegetation Dynamics, Land Cover, and Land Cover Change	*182*
	MODIS	Snow and Sea Ice Albedo	3	MODISALB	Snow and Ice Cover	*214*
Jason-1	***JMR***	Columnar Water Vapor Content	2		Precipitation and Atmospheric Humidity	*85*
	Poseidon-2	Normalized Radar Backscatter Coefficient and Wind Speed	2		Winds	*143*
	Poseidon-2	Significant Wave Height	2		Sea Surface Height and Ocean Wave Dynamics	*150*

Mission	Instrument	Data Set	Proc. Level	Prod. ID	Chapter	Page #
Jason-1	***Poseidon-2***	Total Electron Content	2		Atmospheric Chemistry	*127*
	Poseidon-2/ JMR/DORIS	Sea Surface Height	2		Sea Surface Height and Ocean Wave Dynamics	*149*
Landsat-7	***ETM+***	Raw Digital Numbers	0R	L70R	Radiance/ Reflectance and Irradiance Products	*66*
	ETM+	Calibrated Radiances	1R	L71R	Radiance/ Reflectance and Irradiance Products	*67*
	ETM+	Calibrated Radiances	1G	L71G	Radiance/ Reflectance and Irradiance Products	*68*
Meteor 3M/SAGE	***SAGE III***	Atmospheric Slant-Path Transmission Product	1B	SAGE III 1B	Radiance/ Reflectance and Irradiance Products	*69*
	SAGE III	Aerosol and Cloud Data Products	2	SAGE III/ 01, 02	Cloud and Aerosol Properties and Radiative Energy Fluxes	*120*
	SAGE III	Water Vapor Products	2	SAGE III 03	Precipitation and Atmospheric Humidity	*86*
	SAGE III	NO_2, NO_3, O_3, and OClO Data Products	2	SAGE III/ 04, 05, 06, 07	Atmospheric Chemistry	*128*
	SAGE III	Temperature and Pressure Data Products	2	SAGE III 08	Atmospheric Temperatures	*138*
QuikScat	***SeaWinds***	Grouped and Surface-Flagged Backscatter and Attenuations in 25 km Swath Grid	2A		Winds	*145*
	SeaWinds	Normalized Radar Cross-Section and Ancillary Data	1B		Winds	*144*
	SeaWinds	Ocean Wind Vectors in 25 km Grid	3		Winds	*145*
	SeaWinds	Ocean Wind Vectors in 25 km Swath Grid	2B		Winds	*145*

Mission	Instrument	Data Set	Proc. Level	Prod. ID	Chapter	Page #
QuikTOMS	***TOMS***	Aerosol Product	3	Aerosol	Cloud and Aerosol Properties and Radiative Energy Fluxes	*122*
	TOMS	Ozone Product	3	Ozone	Atmospheric Chemistry	*129*
VCL	***MBLA***	Geolocated Ground Elevations	2		Vegetation Dynamics, Land Cover, and Land Cover Change	*184*
	MBLA	Geolocated Canopy-Top Heights	2		Vegetation Dynamics, Land Cover, and Land Cover Change	*186*
	MBLA	Geolocated Vertical Distribution of Intercepted Surfaces	2		Vegetation Dynamics, Land Cover, and Land Cover Change	*185*

Introduction

ACRIMSAT
- ACRIM III

Aqua
- AIRS
- AMSR-E
- AMSU-A
- CERES
- HSB
- MODIS

Jason-1
- DORIS
- JMR
- Poseidon-2

Landsat 7
- ETM+

Meteor 3M
- SAGE III

QuikScat
- SeaWinds

QuikTOMS
- TOMS

VCL
- MBLA

Introduction

Background and Context

The Earth Observing System (EOS) is an international program, centered within NASA's Earth Science Enterprise, to address fundamental issues regarding Earth system science through collection and analysis of satellite data. The program involves numerous individual satellite missions, teams of scientists to develop and apply techniques to convert the satellite data to meaningful geophysical products, and an extensive EOS Data and Information System (EOSDIS) to process, archive, and distribute the data products. To assist potential users of the EOS data, the *EOS Data Products Handbook* is meant as a convenient reference on the data products being produced from the EOS and associated missions.

The current, second volume of the *Data Products Handbook* provides information regarding the data products from the Active Cavity Radiometer Irradiance Monitor Satellite (ACRIMSAT), Aqua, Jason-1, Landsat 7, Meteor 3M/SAGE III, the Quick Scatterometer (QuikScat), the Quick Total Ozone Mapping Spectrometer (QuikTOMS), and the Vegetation Canopy Lidar (VCL) missions. Volume 1 (Wharton and Myers, 1997) covers the data products from the Tropical Rainfall Measuring Mission (TRMM), Terra (formerly named EOS AM-1), and the Data Assimilation System; and Volume 3 is scheduled to cover the data products from the Gravity Recovery and Climate Experiment (GRACE), Earth Observing 1 (EO-1), the Ice, Clouds, and Land Elevation Satellite (ICESat), the Solar Radiation and Climate Experiment (SORCE), Pathfinder Instruments for Cloud and Aerosol Spaceborne Observations-Climatologie Etendue des Nuages et des Aerosols (PICASSO-CENA), CloudSat, the International Space Station SAGE III, and Aura. Because two of the instruments, the Clouds and the Earth's Radiant Energy System (CERES) and the Moderate Resolution Imaging Spectroradiometer (MODIS), are on both the Terra and Aqua missions, with CERES being on TRMM as well, their data products are covered in both Volumes 1 and 2. Hence the descriptions in this volume of the CERES and MODIS products repeat some of the material in Volume 1, as well as providing updates where appropriate. Amongst the updates, in this volume some of the data product descriptions are illustrated by actual CERES and MODIS images from the Terra and TRMM missions, something that was not possible in the original printing of Volume 1, which was published prior to the TRMM and Terra satellite launches.

This volume can be used either as a source for determining what data products are being produced from the eight missions covered or, for individuals seeking information on specific products, as a reference providing specifics and contact information on those products. In the latter case, individuals seeking information about a particular data product should turn to the Data Products Index in Appendix E or to the expanded listing of the data products, with product IDs, immediately following the Table of Contents and Foreword, to find the appropriate page numbers for the desired product.

Volume Synopsis

Volume 2 follows closely the format of Volume 1, beginning with a list of products and an introduction and overview descriptions of the instruments and data processing, followed by the core of the book, which presents the individual data product descriptions. The data products are grouped into the following 11 topical chapters:

- Radiance/Reflectance and Irradiance Products
- Precipitation and Atmospheric Humidity
- Cloud and Aerosol Properties and Radiative Energy Fluxes
- Atmospheric Chemistry
- Atmospheric Temperatures
- Winds
- Sea Surface Height and Ocean Wave Dynamics
- Surface Temperatures of Land and Oceans, Fire Occurrence, and Volcanic Effects
- Vegetation Dynamics, Land Cover, and Land Cover Change
- Phytoplankton and Dissolved Organic Matter
- Snow and Ice Cover.

Each topical chapter begins with a short overview that discusses the relationship of the chapter's subject matter to global change issues, overviews the products presented in the chapter, indicates some of the product interdependencies and product heritages, and lists suggested relevant readings.

The data product sections are mostly 1- or 2-page summaries, divided into short subsections on:

- Product Description
- Research and Applications
- Data Set Evolution (from precursor data sets)
- Suggested Reading
- A boxed product summary highlighting the following specifics about the data product:
  - Coverage (the portion of the globe covered)

- Spatial/Temporal Characteristics (space and time resolutions)
- Wavelengths or Frequencies (for the products in the chapter titled "Radiance/Reflectance and Irradiance Products")
- Key Science Applications
- Key Geophysical Parameters
- Processing Level (indicating processing levels as defined in the Foreword)
- Product Type (indicating whether the product is a standard product or a research product and whether the computer coding for it will be available at-launch or post-launch; standard products are routinely processed for each applicable data acquisition, whereas research products are not)
- Maximum File Size
- File Frequency
- Primary Data Format
- Browse Available (indicating whether or not a browse is available, what type of browse is available, or a location for browse information)
- Additional Product Information (indicating a web site for the information)
- DAAC (for the product's data archival and distribution)
- Science Team Contact/Contacts (with the full contact information provided in Appendix B).

Not all the product descriptions contain each of the items in the above list, as in some cases the item is not applicable and in others the relevant information was not available at the time of printing. Most contain most of the items, however, and some additionally contain illustrative material. More detailed information about the data products and the theory and background behind their derivation is in the respective Algorithm Theoretical Basis Documents (ATBDs), available over the internet at the EOS Project Science Office Home Page (http://eos.nasa.gov). This site also contains electronic versions of both Volumes 1 and 2 of the *Data Products Handbook*.

Following the data product descriptions are five appendices, providing contact information for the EOS data centers that will be archiving and distributing the data sets to the user community (Appendix A), contact information for the science points of contact for the data products (Appendix B), references (Appendix C), acronyms and abbreviations (Appendix D), and a data products index (Appendix E).

Data Availability

The data products described in the *EOS Data Products Handbook* will be archived and distributed through the various Distributed Active Archive Centers (DAACs) of the EOS Data and Information System (EOSDIS). Contact information for these DAACs is included in Appendix A. It is hoped that these data will be widely used, and although the data are not copyrighted, it is requested that researchers publishing results using EOS data sets include an acknowledgment along the lines of:

Data used in this research include data produced through the funding of NASA's Earth Science Enterprise (ESE) Earth Observing System (EOS) program.

Furthermore, publications using data provided by EOSDIS should include the following:

Data used in this research include data provided to the authors by the NASA-funded EOS Data and Information System archive at [insert the name of the appropriate DAAC].

Further Information Sources

The reader is referred to Volume 1 (Wharton and Myers, 1997) for information about the TRMM and Terra data products and additional background on the objectives of the *EOS Data Products Handbook*. The reader is further referred to the *MTPE/EOS Reference Handbook* (Asrar and Greenstone, 1995) and the *1999 EOS Reference Handbook* (King and Greenstone, 1999) for background on NASA's Earth Science Enterprise (formerly called Mission to Planet Earth) and for details on the entire EOS program, including its scope, purposes, individual mission elements and instruments, science teams, interdisciplinary science investigations, and educational outreach programs. Finally, the reader is referred to the *Science Strategy for the Earth Observing System* (Asrar and Dozier, 1994) and the *EOS Science Plan* (King, 1999) and its accompanying Executive Summary (Greenstone and King, 1999) for details on the science issues being addressed by the EOS program and the approaches being used.

Suggested Reading

(full references are listed in Appendix C)

Asrar, G., and J. Dozier, 1994.

Asrar, G., and R. Greenstone, 1995.

Greenstone, R., and M.D. King, 1999.

King, M.D., 1999.

King, M.D., and R. Greenstone, 1999.

Wharton, S.W., and M.F. Myers, 1997.

Instrument Descriptions and Data Processing Overviews

ACRIMSAT
- ACRIM III

Aqua
- AIRS
- AMSR-E
- AMSU-A
- CERES
- HSB
- MODIS

Jason-1
- DORIS
- JMR
- Poseidon-2

Landsat 7
- ETM+

Meteor 3M
- SAGE III

QuikScat
- SeaWinds

QuikTOMS
- TOMS

VCL
- MBLA

Overview

The data products described in this volume are derived from the data of eight satellite missions and 15 satellite instruments. Of the 15 instruments, six are scheduled to fly on board the Aqua satellite, three are scheduled to fly on board Jason-1, and one each is scheduled to fly on board the Active Cavity Radiometer Irradiance Monitor Satellite (ACRIMSAT), Landsat 7, Meteor 3M/SAGE III, Quick Scatterometer (QuikScat), Quick Total Ozone Mapping Spectrometer (QuikTOMS), and Vegetation Canopy Lidar (VCL) satellites. Of the eight missions, ACRIMSAT, Landsat 7, and QuikScat were launched in 1999, while the other five are all scheduled for launch in 2001 or 2002. The table entitled "Satellite missions covered in this volume" (below) provides further information about the eight missions. Briefly, in alphabetical order the 15 instruments are:

- The Active Cavity Radiometer Irradiance Monitor III (ACRIM III), aimed at monitoring the total solar irradiance with a high level of precision. ACRIM III is on board ACRIMSAT, launched in December 1999. It continues the long-term measurements of the total amount of solar energy arriving at the Earth begun with the precursor ACRIM I and ACRIM II instruments, launched in 1980 and 1991 on the Solar Maximum Mission (SMM) and the Upper Atmosphere Research Satellite (UARS), respectively.

- The Advanced Microwave Scanning Radiometer for EOS (AMSR-E), a 12-channel microwave radiometer provided by Japan and aimed at monitoring a range of hydrologic variables including water vapor, cloud liquid water, rainfall, sea surface temperature and sea ice temperature, sea ice concentration, snow depth on sea ice, snow water equivalent over land, and soil moisture. Surface variables will be monitored at a coarse spatial resolution (ranging approximately from 5 to 56 km) but will be obtainable day and night and under almost all weather conditions. AMSR-E will be on the Aqua satellite.

- The Advanced Microwave Sounding Unit (AMSU-A), a 15-channel microwave sounder designed pri-

Mission	*Orbit Type*	*Altitude*	*Equatorial crossing time*	*Launch date or scheduled month*
Landsat 7	Sun-synchronous, 98.2° inclination	705 km	10:05 a.m., descending node	April 15, 1999
QuikScat	Sun-synchronous, 98.6° inclination	803 km	5:55 a.m., ascending node	June 19, 1999
ACRIMSAT	Sun-synchronous 98.13° inclination	685 km	10:50 a.m., descending node	December 20, 1999
Jason-1	Circular, non-sun-synchronous, 66° inclination	1336 km	----------	February 2001
Meteor 3M/ SAGE III	Sun-synchronous, 99.5° inclination	1020 km	9:30 a.m., ascending node	March 2001
QuikTOMS	Sun-synchronous, 97.3° inclination	800 km	10:30 a.m.,	April 2001 descending node
Aqua	Sun-synchronous, 98.2° inclination	705 km	1:30 p.m.,	July 2001 ascending node
VCL	Circular, non-sun-synchronous, 67° inclination	390-410 km	----------	May 2002

Satellite missions covered in this volume

marily to obtain temperature profiles in the upper atmosphere (especially the stratosphere) and to provide a cloud-filtering capability for tropospheric temperature observations. The first AMSU was launched in May 1998 on board the National Oceanic and Atmospheric Administration's (NOAA's) NOAA 15 satellite. The EOS AMSU-A will be on board the Aqua satellite, as part of a closely coupled triplet of instruments including also the AIRS and HSB.

- The Atmospheric Infrared Sounder (AIRS), an advanced sounder containing 2378 infrared channels and four visible/near-infrared channels, aimed at obtaining highly accurate temperature profiles within the atmosphere plus a variety of additional Earth/atmosphere products. AIRS will be on board the Aqua satellite, as the highlighted instrument in the AIRS/AMSU-A/HSB triplet centered on measuring accurate temperature and humidity profiles throughout the atmosphere.

- The Clouds and the Earth's Radiant Energy System (CERES), a 3-channel radiometer measuring shortwave radiation in the wavelength band 0.3-5 μm, longwave radiation in the band 8-12 μm, and total radiation from 0.3 μm to over 100 μm. These data will be used to determine radiative fluxes and balances, and, in combination with MODIS data, detailed information about clouds. The first CERES was launched on the Tropical Rainfall Measuring Mission (TRMM) in November 1997; the second and third CERES were launched on the Terra satellite in December 1999; and the fourth and fifth CERES will be on board the Aqua satellite.

- The Doppler Orbitography and Radiopositioning Integrated by Satellite (DORIS), a precise orbit determination system measuring the doppler shift of radiofrequency signals transmitted from ground-based beacons at 2.03625 GHz and 401.25 MHz. The 2.03625 GHz measurements are for precise doppler determinations, while the 401.25 MHz measurements are for ionospheric corrections. A DORIS is on board the TOPEX/Poseidon mission, and an updated version is scheduled to fly on board the Jason-1 satellite.

- The Enhanced Thematic Mapper Plus (ETM+), an 8-band imaging radiometer aimed at providing high spatial resolution, multispectral images of the sunlit land surface, using visible, near-infrared, shortwave infrared, and thermal infrared wavelength bands, along with a panchromatic band. The ETM+ is on board the Landsat 7 satellite, launched in April 1999. It is an enhanced version of the Thematic Mapper (TM) on board earlier Landsat satellites.

- The Humidity Sounder for Brazil (HSB), a 4-channel microwave sounder provided by Brazil and aimed at obtaining humidity profiles throughout the atmosphere. The HSB will be on board the Aqua satellite, as the instrument in the AIRS/AMSU-A/HSB triplet that will allow humidity measurements even under conditions of heavy cloudiness and haze.

- The Jason-1 Microwave Radiometer (JMR), a 3-frequency microwave radiometer measuring brightness temperatures at 18.7, 23.8, and 34 GHz. The primary objective of the JMR is to measure total water vapor along the path viewed by the Poseidon-2 altimeter, both for range correction for the Poseidon-2 topography measurements and for determining atmospheric columnar water vapor content. JMR will be on board the Jason-1 satellite.

- The Moderate Resolution Imaging Spectroradiometer (MODIS), a 36-band spectroradiometer measuring visible and infrared radiation and obtaining data that will be used to derive products ranging from vegetation, land surface cover, and ocean chlorophyll fluorescence to cloud and aerosol properties, fire occurrence, snow cover on the land, and sea ice cover on the oceans. The first MODIS instrument was launched on board the Terra satellite in December 1999, and the second MODIS will be on board the Aqua satellite.

- The MultiBeam Laser Altimeter (MBLA), a five-beam laser instrument to measure the heights of vegetation canopies and land surface topographies and to provide the first global inventory of the vertical structure of the Earth's forests. The measurements are expected to enable by far the most accurate estimates of the global forest biomass. MBLA is scheduled to fly on the VCL mission, the first mission of NASA's Earth System Science Pathfinder (ESSP) program.

- Poseidon-2, a dual-frequency radar altimeter aimed at mapping the topography of the sea surface and measuring ocean wave height and wind speed, thereby allowing monitoring of the global ocean circulation and more precise determinations of the large-scale coupling between the oceans and atmosphere. Poseidon-2 is being provided by France

(Overview, continued)

and is an enhanced version of the Poseidon-1 instrument flown on TOPEX/Poseidon, launched in 1992. Poseidon-2 will be on board the Jason-1 satellite.

- SeaWinds, a Ku-band scatterometer aimed primarily at measuring near-surface wind velocities over the global oceans under almost all weather and cloud conditions and secondarily at providing information for vegetation classification and ice-type monitoring. SeaWinds is a follow-on to the NASA Scatterometer (NSCAT), which flew on the Japanese Advanced Earth Observing Satellite (ADEOS) in 1996-1997. The first SeaWinds is on board QuikScat, launched in June 1999, and the second SeaWinds is scheduled for ADEOS II.

- The Stratospheric Aerosol and Gas Experiment III (SAGE III), an Earth limb-scanning grating spectroradiometer aimed at retrieving global profiles of atmospheric aerosols, ozone, water vapor, nitrogen oxides, chlorine dioxide, temperature, and pressure. SAGE III is an enhanced version of the earlier Stratospheric Aerosol Measurement II (SAM II), SAGE I, and SAGE II instruments, launched in 1978, 1979, and 1984 on board Nimbus 7, the Applications Explorer Mission 2 (AEM 2), and the Earth Radiation Budget Satellite (ERBS), respectively. It will fly on board the Russian Meteor 3M satellite, with an additional SAGE III instrument scheduled to fly on board the International Space Station.

- The Total Ozone Mapping Spectrometer (TOMS), a six-band instrument measuring ultraviolet radiation with the primary objective of continuing the daily global (sunlit) mapping of total column atmospheric ozone, thereby monitoring the degeneration and/or regeneration or stabilization of the Earth's protective ozone layer. TOMS also measures aerosols and sulfur dioxide, the latter enabling monitoring of volcanic eruption plumes. Several TOMS instruments have flown, the first launched in October 1978 on the Nimbus 7 satellite and two others launched in 1996 on ADEOS and in 1996 on Earth Probe TOMS. An additional TOMS will fly on board QuikTOMS.

Greater detail on each of the instruments is provided in the remainder of this chapter, arranged alphabetically according to mission name.

ACRIM III

Active Cavity Radiometer Irradiance Monitor

Sustained changes in the total solar irradiance (TSI) smaller than 0.25% may have been the prime causal factor for significant climate change in the past, on time scales of centuries to millennia. The long-range objective of TSI monitoring is to provide a precision database for comparison with the climate record that will be capable of resolving systematic variability of a tenth of one percent on time scales of a century. The continuation of the climate TSI database during solar cycle 23, establishment of its precise relationship to previous and successive components of the database, and analysis of TSI variability on all time scales with respect to the climatological and solar physics significance constitute the primary objectives of the ACRIM experiment.

The primary approach of the experiment is observational: to monitor the variability of total solar irradiance, extending the NASA high-precision solar total irradiance variability database into solar cycles 23 and 24. This database has been compiled as part of NASA's Earth radiation budget 'principal thrust' responsibility in the National Climate Program. ACRIM flight experiments have provided the precision database from the peak of solar cycle 21 (1980) to the present, except for a two-year gap between the end of the SMM/ACRIM I (1989) mission and the beginning of the UARS/ACRIM II (1991) mission.

The detection of subtle solar luminosity variability during solar cycles 21, 22, and 23 underscores the need to extend the irradiance database indefinitely with maximum precision. There may be other luminosity variabilities with longer periodicities and/or proportionately larger amplitudes that could have significant climatic implications. Subtle trends in the total irradiance of as little as 0.1% per century could eventually produce the extreme range of climates known to have existed in the past, from warm periods without permanent ice, to the great ice ages. Accumulation of a database capable of detecting such trends will necessarily require the results of many individual solar-monitoring experiments. If these experiments last an average of half a decade each, about the maximum that can be expected from today's technology, they will have to be related with a precision smaller than 10 parts per million (ppm).

A careful measurement strategy will be required to sustain adequate precision for the database since the uncertainty of current satellite instrumentation on an absolute basis is inadequate for this purpose (no better than +/- 0.1%). An approach must be used that relates successive solar-monitoring experiments at a precision level defined by the operation of the instrumentation. Overlapping flights and comparing the observations accomplishes this. A relative precision of less than 5 ppm is achievable for the data from overlapped solar monitors with the current state-of-the-art, given sufficient comparison observations.

The principal remaining uncertainty for the "overlap strategy" is the degradation of solar-monitor sensors during extended missions. Calibration of degradation, using redundant sensors in phased operation, can sustain the precision of the long-term TSI database at the level of 10 ppm or less. Considerable effort will be expended to implement the degradation comparisons and to compare with preceding (UARS/ACRIM II and SOHO/VIRGO) and succeeding (TSIM) TSI experiments.

Level 0 TSI data are first processed to Level 1 by conversion to SI units of watts per square meter (W/m^2) at the satellite. The satellite TSI is then reconciled to 1 Astronomical Unit using the Solar Elevation, Azimuth, and Range computation of the Satellite Tool Kit software (Analytical Graphics, Inc.), based on ACRIMSAT's NORAD two-line orbital elements. The primary archived data products are Level 2 shutter cycle and daily means. The time scale of the shutter cycle means is 2.048 minutes.

As summarized in the figure on the following page, the ACRIM III experiment has been deployed on ACRIMSAT, a dedicated small satellite. A ground station at the Table Mountain Observatory of the Jet Propulsion Laboratory (JPL) controls ACRIMSAT and will be the downlink site for Level 0 science data. The Level 0 data will be provided via the Internet to the Science Team's Science Computing Facility (SCF)/Science Investigator-led Processing System (SIPS) in Coronado, California. Level 0 data, ancillary data, and Level 2 results will be provided to the Langley DAAC by the ACRIM III Science Team SIPS.

ACRIMSAT Home Pages

Science:
http://acrim.com

Satellite and Instrument:
http://acrim.jpl.nasa.gov/

Key ACRIM III Facts

Selected for flight on ACRIMSAT, launched December 20, 1999

Heritage: ACRIM I, ACRIM II

Contains three active cavity radiometer type IV sensors

Measures total solar irradiance

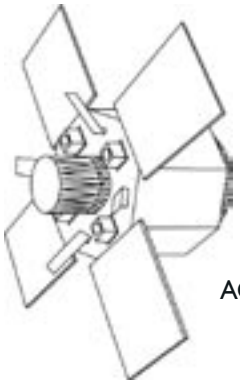

ACRIMSAT

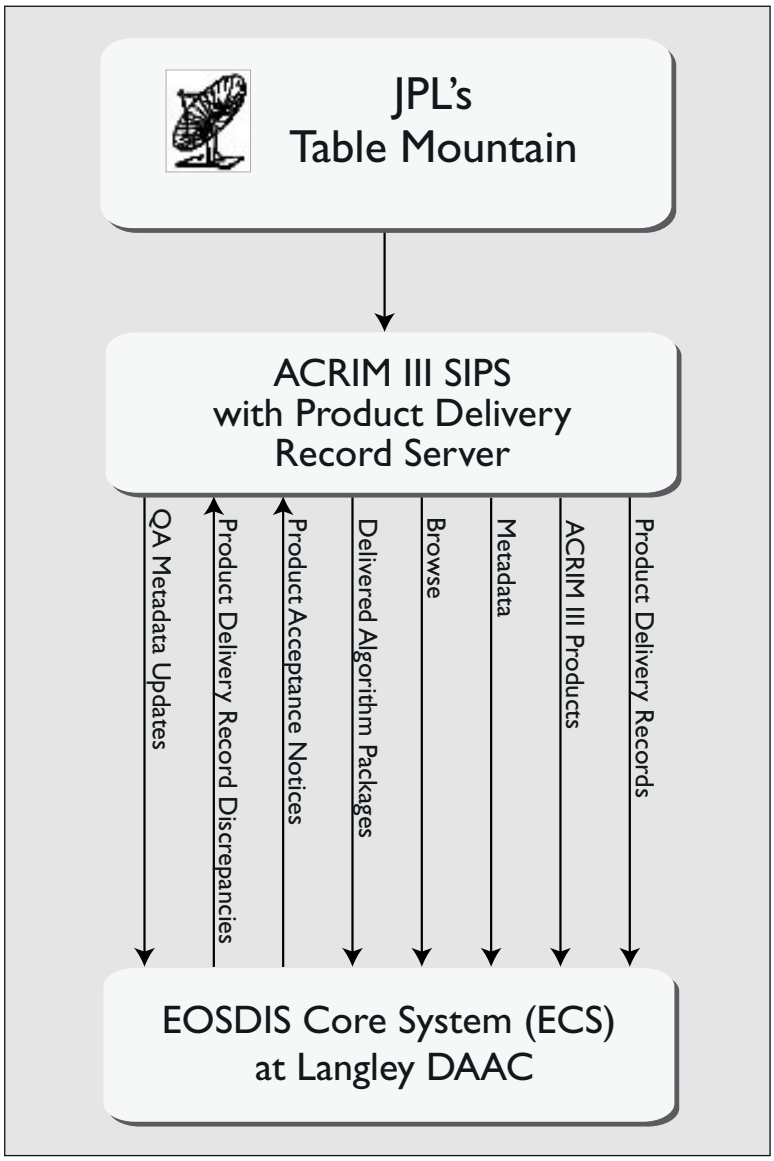

ECS-ACRIM III SIPS Functional Interface

AIRS/AMSU-A/HSB

- *Atmospheric InfraRed Sounder (AIRS)*
- *Advanced Microwave Sounding Unit (AMSU-A)*
- *Humidity Sounder for Brazil (HSB)*

AIRS is a high-resolution infrared (IR) sounder selected to fly on the EOS Aqua platform with two operational microwave sounders, AMSU-A and HSB. Measurements from the three instruments will be analyzed jointly to filter out the effects of clouds from the IR data in order to derive clear-column air-temperature profiles and surface temperatures with high vertical resolution and accuracy. Together, these three instruments constitute an advanced operational sounding system whose data will:

a) improve global modeling efforts and numerical weather prediction;
b) enhance studies of the global energy and water cycles, the effects of greenhouse gases, and atmosphere-surface interactions; and
c) facilitate monitoring of climate variations and trends.

AIRS measures upwelling radiances in 2378 spectral channels covering the IR spectral band, 3.74 micrometers to 15.4 micrometers. A set of four channels in the visible/Near-IR (VIS) observes wavelengths from 0.4 to 1.0 micrometers to provide cloud cover and spatial-variability characterization. The microwave sounders provide sea ice concentration, snow cover, and additional temperature-profile information as well as precipitable water and cloud liquid-water content. If cloud cover is too great for IR retrievals, the microwave (MW) measurements alone will provide a coarse, low-precision atmospheric-temperature profile and surface characterization.

The figure on page 23 provides an overview of the data processing architecture and the products which originate at the various stages.

Three independent Product Generation Executives (PGEs), one each for AIRS/VIS, AMSU-A, and HSB, execute at the DAAC to ingest Level 0 data to produce Level 1A geolocated science data counts and engineering parameters in Hierarchical Data Format (HDF) swath format.

Four independent PGEs, one for each instrument, execute at the DAAC to ingest Level 1A data to produce a Level 1B calibrated IR radiance product, a microwave brightness temperature product, and associated calibration coefficients. The AIRS L1B PGE also produces a subset data file of selected cloudy IR radiances for ingest by the AIRS L1B daily browse PGE. The AIRS and AMSU-A/HSB L1B daily browse PGEs subsequently produce browse products from this subset file and the L1B brightness temperature product data.

A combined AIRS/AMSU-A/HSB/VIS Level 2 PGE executes at the DAAC to ingest the Level 1B data products and ancillary data and to produce Level 2 standard products and support products, all in HDF swath format. A Level 2 subset data file is also produced for ingest by the Level 2 daily browse PGE. This daily browse PGE produces browse products from this subset file as well as summary data to be ingested by follow-on Level 2 pentad and Level 2 monthly browse PGEs. All browse PGEs are executed at the DAAC.

Quality Assurance (QA) Support Products are produced at the Team Leader Science Computing Facility (TLSCF) in HDF swath format for a fraction of the total data set and are used to monitor the operation of the instrument and validate the retrieval algorithm and products.

The microwave Level 1B data sets and Level 2 standard products are ingested at the TLSCF along with the ancillary radiosonde observations (RAOBS) to produce a daily statistic by comparison of profiles observed by radiosondes with spatially and temporally matched retrieval profiles.

The combined Level 2 PGE consists of three major retrieval stages:

- Microwave-Only Retrieval
- Cloud Clearing
- Combined MW/IR/VIS Retrieval

The Microwave-Only Retrieval employs only the AMSU-A and HSB data in combination with an ancillary general circulation model (GCM) (providing general climatology and accurate surface pressure) and a digital elevation model (DEM) (providing topography and land/water fractions) to retrieve atmospheric temperature, water vapor, and liquid-water profiles as well as surface skin temperature and microwave spectral surface emissivity. A rain flag is also produced. These profiles are passed to the combined MW/IR/VIS retrieval as an initial guess. In the event of rain or overwhelming cloud cover, the combined retrieval is not attempted and the MW-Only Retrieval is passed through to the standard product.

The Cloud Clearing Stage employs MW and selected IR channels to estimate the clear-column IR radiances for all IR channels. It also employs IR window channels to retrieve the surface skin temperature, emissivity, and reflectivity. The temperature and water-vapor profiles are corrected for the effects of the clouds. This rapid stage produces reasonably accurate AIRS/AMSU-A products that are suitable

(AIRS/AMSU-A/HSB Overview, continued)

for assimilation into operational numerical weather prediction models.

The Combined MW/IR/VIS Retrieval Stage recursively refines the temperature and water-vapor profiles and surface parameters, while retrieving ozone and multiple cloud-layer parameters and calculating uncertainties for all retrieved parameters. If a profile is rejected, a new retrieval is produced, starting from the Microwave-Only product and utilizing the AMSU-A/HSB channels together with those AIRS channels which are insensitive to cloud effects. The final profiles and improved clear-column radiances for all IR channels are passed to the standard product.

AIRS Home Page

http://www-airs.jpl.nasa.gov

Key AIRS/AMSU-A/HSB Facts

Selected for flight on Aqua

Heritage: HIRS/MSU

AIRS is a high-spectral-resolution, grating infrared sounder operated in a cross-track-scanning mode; AMSU-A and HSB are both multi-channel microwave radiometers

Provides global atmospheric temperature and humidity profiles, ozone burden, cloud emissivity, cloud-top temperatures and pressures, and surface skin temperature and emissivity

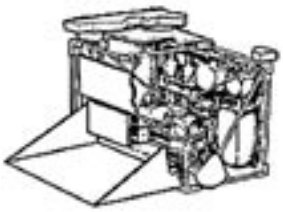

AIRS

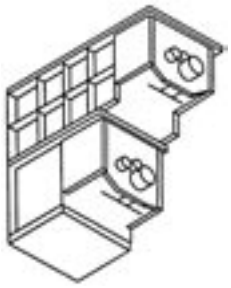

AMSU-A

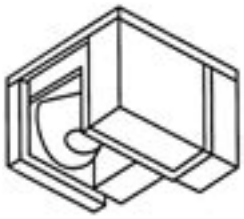

HSB

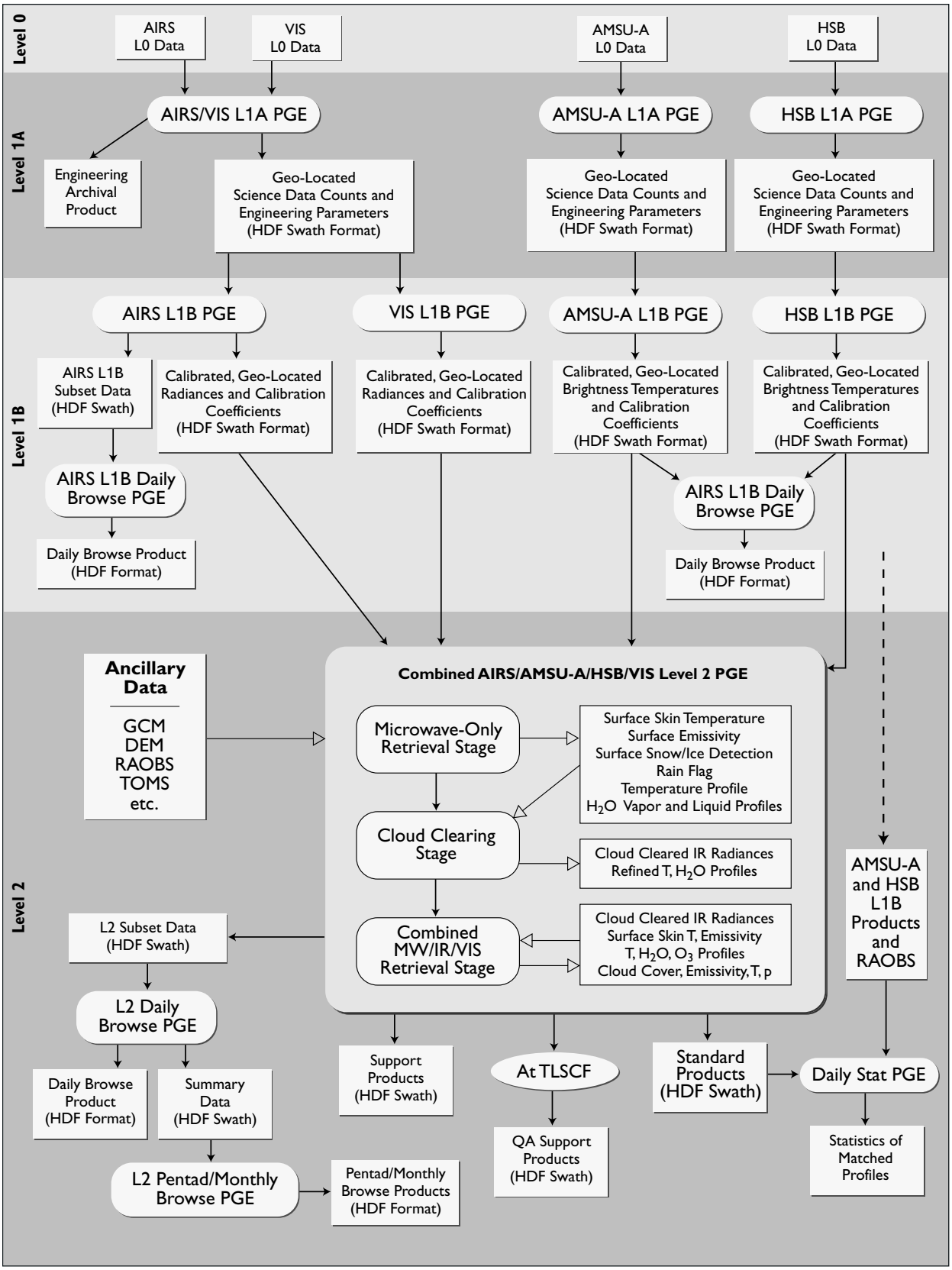

AIRS/AMSU-A/HSB Data Processing Architecture and Products

AMSR-E

Advanced Microwave Scanning Radiometer for EOS

AMSR-E will be carried aboard the EOS Aqua satellite and will monitor a range of hydrologic processes critical to our knowledge of climate variability. A unique capability of AMSR-E, versus the other EOS instruments, is its ability to make most of its measurements through cloud cover. Over the ocean, the instrument will measure rainfall, cloud-water and water-vapor abundance, sea ice parameters, sea surface temperature, and near-surface wind speed. Over land, vegetation amounts, snow cover, and soil wetness will be monitored. AMSR-E will provide unprecedented detail and accuracy in the global, all-weather measurement of these variables and thereby will allow a more-complete understanding of climate variability, ultimately enabling better climate prediction.

The instrument is a twelve-channel, six-frequency, total power passive-microwave radiometer system. It measures brightness temperatures at 6.925, 10.65, 18.7, 23.8, 36.5, and 89.0 GHz. Vertically and horizontally polarized measurements are taken at all channels. The Earth-emitted microwave radiation is collected by an offset parabolic reflector 1.6 meters in diameter that scans across the Earth along an imaginary conical surface, maintaining a constant Earth incidence angle of 55° and providing a swath width of 1445 km. The reflector focuses radiation into an array of six feedhorns which then carry the radiation to radiometers for measurement. Calibration is accomplished with observations of the cosmic background radiation and an on-board warm target. Spatial resolution of the individual measurements varies from 5.4 km at 89 GHz to 56 km at 6.9 GHz.

The AMSR-E will provide instantaneous measurements for the following data products:

- Level 2 rainfall over ocean (land) with an accuracy of 1 mm/hr (2 mm/hr) or 20% (40%), whichever is greater, at a spatial resolution of 5.4 km.
- Level 3 monthly rainfall averages over ocean (land) with an accuracy of 1 mm/day (2 mm/day) or 20% (40%), whichever is greater, at a spatial resolution of 5° latitude × 5° longitude.
- Sea surface temperature, through most clouds, with an accuracy of 0.5° C at two different spatial resolutions: 56 and 38 km.
- Total integrated water vapor over the ocean with an accuracy of 1.0 mm at a resolution of 24 km.
- Total integrated cloud water over the ocean with an accuracy of 0.02 mm at a resolution of 12 km.
- Sea surface wind speed with an accuracy of 1.0 m/s at two resolutions: 38 and 24 km.
- Surface soil moisture with an accuracy of 0.06 gm/cm^3 in low-vegetation areas (biomass less than 1.5 kg/m^2), at a grid spacing of 25 km and a spatial resolution of 56 km.
- Sea ice concentration at two resolutions (SSM/I grid): 12.5 and 25 km.
- Snow depth over sea ice at a resolution of 12.5 km.
- Sea ice temperature at a resolution of 25 km.
- Snow-cover water equivalent over land.

AMSR-E Home Page:

http://www.ghcc.msfc.nasa.gov/AMSR

Key AMSR-E Facts

Selected for flight on EOS Aqua spacecraft

Heritage: Nimbus 7 and Seasat SMMR, DMSP SSM/I

Multi-frequency, dual polarization conically scanning passive-microwave radiometer

Measures hydrologic processes

AMSR-E

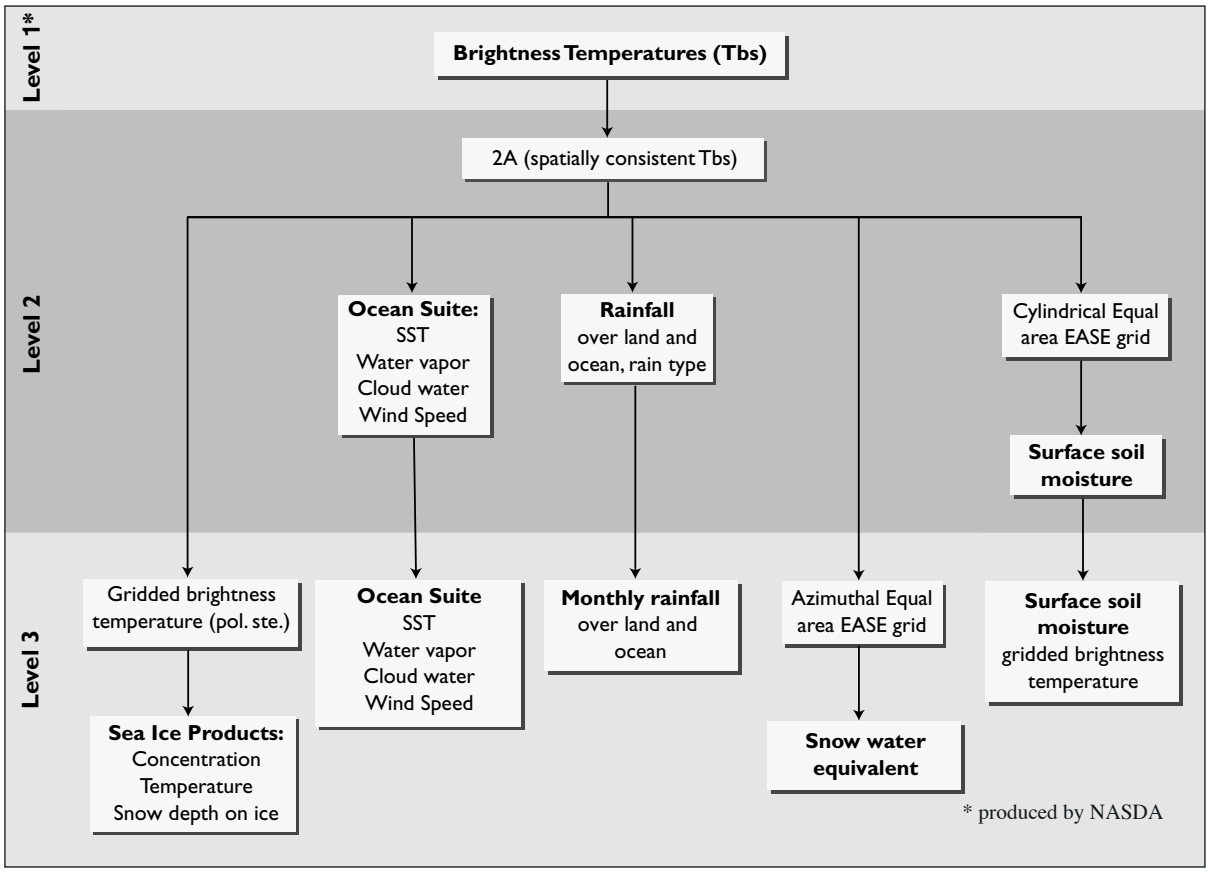

AMSR-E Standard Products

CERES

Clouds and the Earth's Radiant Energy System

The U.S. Global Change Research Program classifies the role of clouds and radiation as its highest scientific priority (CEES, 1994). There are many excellent summaries of the scientific issues (IPCC, 1992; Hansen *et al*., 1993; Ramanathan *et al*., 1989; Randall *et al*., 1989, Wielicki *et al*., 1995) concerning the role of clouds and radiation in the climate system. These issues naturally lead to a requirement for improved global observations of both radiative fluxes and cloud physical properties. The CERES Science Team, in conjunction with the EOS Investigators Working Group representing a wide range of scientific disciplines from oceans, to land processes, to atmosphere, has examined these issues and proposed an observational system with the following objectives:

1) For climate-change analysis, provide a continuation of the ERBE record of radiative fluxes at the top of the atmosphere (TOA), analyzed using the same algorithms that produced the existing ERBE data.

2) Double the accuracy of estimates of radiative fluxes at TOA and the Earth's surface.

3) Provide the first long-term global estimates of the radiative fluxes within the Earth's atmosphere.

4) Provide cloud-property estimates which are consistent with the radiative fluxes from the surface to the top of the atmosphere.

To accomplish these goals, the CERES data products are divided into three major categories, as shown in the figure on the following page: ERBE-like Products (top row), CERES Surface/TOA Products (middle row), and CERES Surface/TOA/Atmosphere (bottom row).

The ERBE-like products address the first objective of long-term continuity of the ERBE TOA fluxes. The TOA/Surface Products address the second objective and attempt to provide the most direct tie between surface radiative-flux estimates and TOA flux measurements. The TOA/Surface/Atmosphere products focus on the last two objectives and attempt to derive an internally consistent set of atmosphere, cloud, and surface-to-TOA radiative fluxes, all within the context of a state-of-the-art radiative-transfer model. In this last case, the observed TOA fluxes are used as a direct constraint on the model calculations in order to implicitly account for non-plane-parallel and other poorly modeled atmospheric radiative effects. As in ERBE, CERES radiative fluxes will be separately determined for both clear- and cloudy-sky conditions.

One of the major advances of CERES over ERBE is the availability of high spatial and spectral resolution cloud imagers for cloud masking, cloud height, and cloud-optical-property determination (i.e., VIRS on TRMM, MODIS on Terra and Aqua). A second major advance is the use of one CERES scanner in a cross-track mode (global spatial coverage) and a second scanner in a rotating-azimuth-plane mode (complete angular sampling of viewing zenith and azimuth). The rotating-azimuth-plane scanner data will be combined with nearly simultaneous cloud-imager data to develop a new set of improved empirical models of the SW and LW anisotropy of radiation as a function of surface and cloud type. While it is estimated to take two years of these data to develop new angular models, they are expected to reduce instantaneous TOA flux errors by a factor of three from the ERBE levels.

A detailed listing of the CERES data products and their individual parameters can be found in the CERES Data Products Catalog (http://asd-www.larc.nasa.gov/DPC/DPC.html). Documentation of the Release 1 CERES analysis algorithms can be found in the CERES Algorithm Theoretical Basis Documents (ATBDs) Volumes 0 through 12, where each volume covers one of the CERES Data Products and its associated technical algorithms (http://eospso.gsfc.nasa.gov/atbd/cerestables.html). A summary of the CERES experiment can be found in Wielicki *et al*., *Bulletin of the American Meteorological Society*, May, 1996.

CERES Home Page

http://asd-www.larc.nasa.gov/ceres/docs.html

Key CERES Facts

Selected for flight on TRMM, Terra, and Aqua

Heritage: ERBE

Broadband, scanning radiometer capable of operating in cross-track mode, or rotating plane mode (bi-axial scanning)

Measures Earth's radiation budget and atmospheric radiation from the top of the atmosphere to the surface

First instrument (cross-track scanning) will essentially continue the ERBE mission; the second (biaxially scanning) will provide angular radiance information that will improve the accuracy of angular models used to derive the Earth's radiative balance

Dual scanners on Aqua

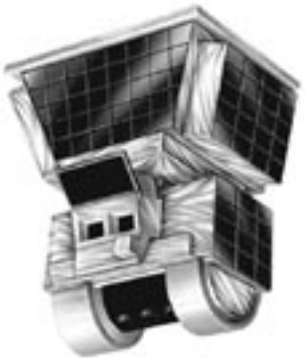

CERES

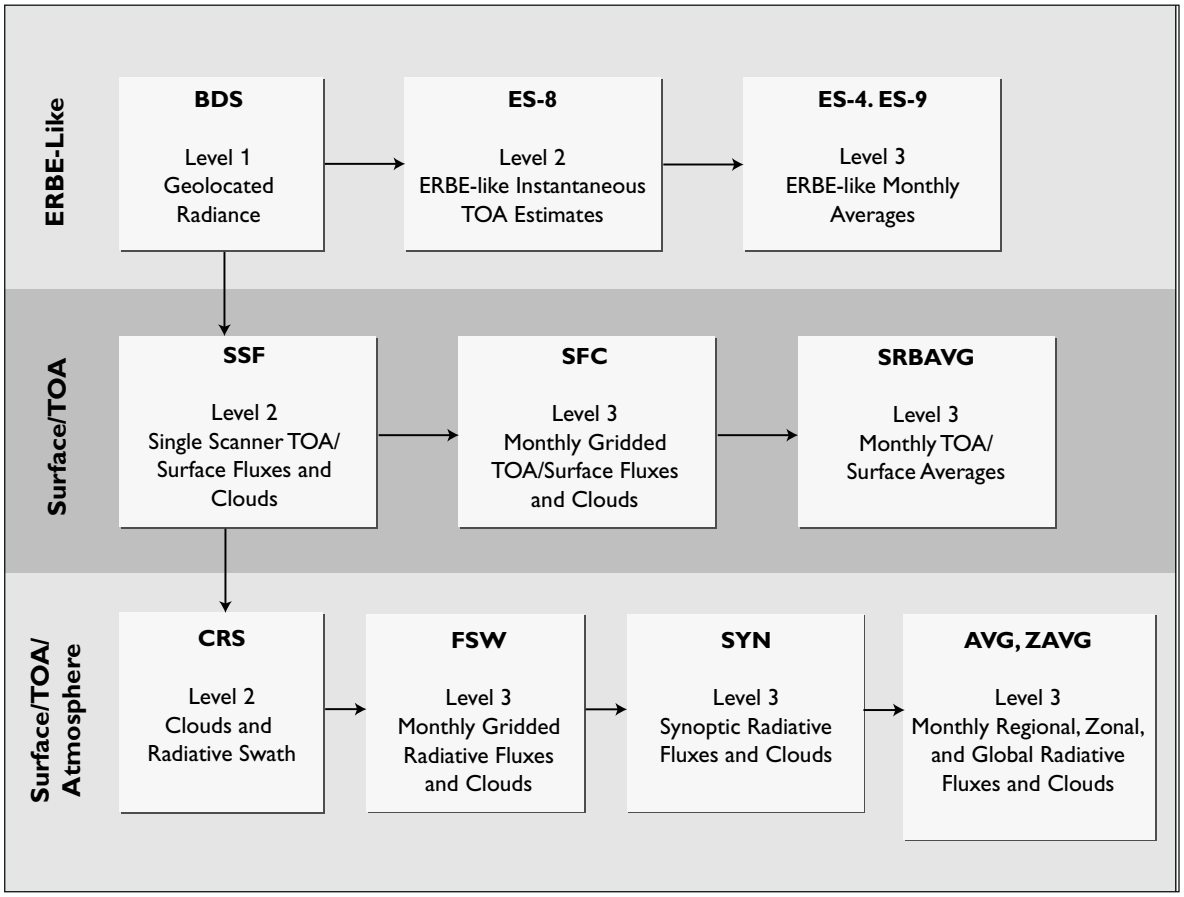

CERES Data Processing Architecture and Products

MODIS

Moderate Resolution Imaging Spectroradiometer

MODIS is an EOS facility instrument designed to measure biological and physical processes on a global basis every one to two days. Slated for both the Terra and Aqua satellites, the instrument will provide long-term observations from which to derive an enhanced knowledge of global dynamics and processes occurring on the surface of the Earth and in the lower atmosphere. This multidisciplinary instrument will yield simultaneous, congruent observations of high-priority atmospheric (cloud cover and associated properties), oceanic (sea-surface temperature and chlorophyll), and land-surface features (land-cover changes, land-surface temperature, and vegetation properties). The instrument is expected to make major contributions to the understanding of the global Earth system, including interactions between land, ocean, and atmospheric processes.

The MODIS instrument employs a conventional imaging-radiometer concept, consisting of a cross-track scan mirror and collecting optics, and a set of linear detector arrays with spectral interference filters located in four focal planes. The optical arrangement will provide imagery in 36 discrete bands from 0.4 to 14.5 μm, selected for diagnostic significance in Earth science. The spectral bands will have spatial resolutions of 250 m, 500 m, or 1 km at nadir; signal-to-noise ratios of greater than 500 at 1-km resolution (at a solar zenith angle of 70°); and absolute irradiance accuracies of ±5 percent from 0.4 to 3 μm (2 percent relative to the Sun) and 1 percent or better in the thermal infrared (3 to 14.5 μm). MODIS instruments will provide daylight reflection and day/night emission spectral imaging of any point on the Earth at least every two days, operating continuously.

Many MODIS products are made over time intervals ranging from about one week to a month or a season. These products will be better suited for use by investigators interested in seasonal phenomena. In some cases these products are made to reduce data volume; in others they are made to provide cloud-free coverage within a defined time period. Because the ground track of the EOS spacecraft follows a 16-day repeat cycle, and because there may be biases in the multiday data sets based on viewing geometry at specific locations, the MODIS "week" has been defined as an 8-day period. The land and ocean data products are based upon 8-day weeks beginning on January 1 of each year. The atmosphere products are also based on 8-day weeks, but these begin with the first 8-day period of the Aqua MODIS sensor that is concurrent with the Terra MODIS schedule and run in an unbroken sequence thereafter. Thus, the land and ocean weeks will not, in general, coincide with the atmosphere weeks.

MODIS will provide specific global data products, which include the following:

- Surface temperature with 1-km resolution, day and night, with absolute accuracy of 0.2 K for oceans and 1 K for land;
- Ocean color, defined as ocean-leaving spectral radiance within 5 percent from 415 to 653 nm, enabled by atmospheric correction from near-infrared sensor channels;
- Chlorophyll fluorescence within 50 percent at surface-water concentrations of 0.5 mg m^{-3};
- Concentrations of chlorophyll *a* within 35%;
- Vegetation/land-surface cover, conditions, and productivity
  - Net primary productivity, leaf-area index, and intercepted photosynthetically active radiation
  - Land cover type, with change detection and identification
  - Vegetation indices corrected for atmosphere, soil, and directional effects;
- Snow cover and sea ice cover;
- Land-surface reflectance (atmospherically corrected) with bidirectional reflectance and albedo;
- Cloud cover with 250-m resolution by day and 1,000-m resolution at night;
- Cloud properties characterized by cloud-droplet phase, optical thickness, droplet size, cloud-top pressure, and emissivity;
- Aerosol properties defined as optical thickness, particle size, and mass transport;
- Fire occurrence, size, and temperature;
- Global distribution of precipitable water; and
- Cirrus-cloud cover.

The data-product descriptions in the main part of this handbook refer to MODIS spectral bands by number. These are all defined in the table on the following page.

MODIS Home Page
http://ltpwww.gsfc.nasa.gov/MODIS/MODIS.html

Key MODIS Facts

Selected for flight on Terra and Aqua missions

Heritage: AVHRR, HIRS, Landsat TM, and Nimbus 7 CZCS

Medium-resolution, multi-spectral, cross-track-scanning radiometer

MODIS

Primary Use	Band	Center Wavelength (nm)	Bandwidth (nm)	Pixel Size (m)	L_{typ}	SNR @ L_{typ}
Land/Cloud/Aerosol Boundaries	1	645.0	48.0	250	21.8	129.0
	2	856.5	38.4	250	24.7	200.8
Land/Cloud/Aerosol Properties	3	465.6	18.8	500	35.3	243.4
	4	553.6	19.8	500	29.0	228.3
	5	1241.6	24.0	500	5.4	74.0
	6	1629.1	28.6	500	7.3	270.4
	7	2114.1	55.7	500	1.0	111.1
Ocean Color/ Phytoplankton/ Biogeochemistry	8	411.3	14.8	1000	44.9	880.4
	9	442.0	9.7	1000	41.9	838.0
	10	486.9	10.6	1000	32.1	802.5
	11	529.6	12.0	1000	27.9	754.1
	12	546.8	10.3	1000	21.0	750.0
	13	665.5	10.1	1000	9.5	913.5
	14	676.8	11.3	1000	8.7	1087.5
	15	746.4	9.9	1000	10.2	600.0
	16	866.2	15.5	1000	6.2	516.7
Atmospheric Water Vapor	17	904.0	35.0	1000	10.0	166.7
	18	935.5	13.6	1000	3.6	57.1
	19	935.2	46.1	1000	15.0	250.0
Cirrus Clouds	26	1383.0	35.0	1000	6.0	150.0

Primary Use	Band	Center Wavelength (µm)	Bandwidth (µm)	Pixel Size (m)	$L_{typ}(T_{typ})$	SNR @ L_{typ} = $L_{typ}/NE\Delta L^{typ}$
Surface/Cloud	20	3.785	.19	1000	0.45(300K)	900.0
Temperature	21	3.990	.08	1000	2.38(335K)	203.4
	22	3.970	.09	1000	0.67(300K)	837.5
	23	4.056	.09	1000	0.79(300K)	987.5
Atmospheric Temperature	24	4.472	.09	1000	0.17(250K)	141.7
	25	4.545	.09	1000	0.59(275K)	453.8
Water Vapor	27	6.752	.25	1000	1.16(240K)	252.2
	28	7.334	.33	1000	2.18(250K)	641.2
Cloud Properties	29	8.518	.35	1000	9.58(300K)	2661.1
Ozone	30	9.737	.30	1000	3.69(250K)	444.6
Surface/Cloud Temperature	31	11.017	.54	1000	9.55(300K)	2808.8
	32	12.032	.52	1000	8.94(300K)	1824.5
Cloud Top Altitude	33	13.359	.31	1000	4.52(260K)	452.0
	34	13.675	.33	1000	3.76(250K)	298.4
	35	13.907	.33	1000	3.11(240K)	220.6
	36	14.192	.29	1000	2.08(220K)	106.7

SNR = Signal-to-Noise Ratio
NE = Noise Equivalent
L_{typ} (in W/m²-µm-sr) = Spectral radiance at typical conditions for this product
T_{typ} = Temperature at typical conditions for this product

MODIS Spectral Band Properties

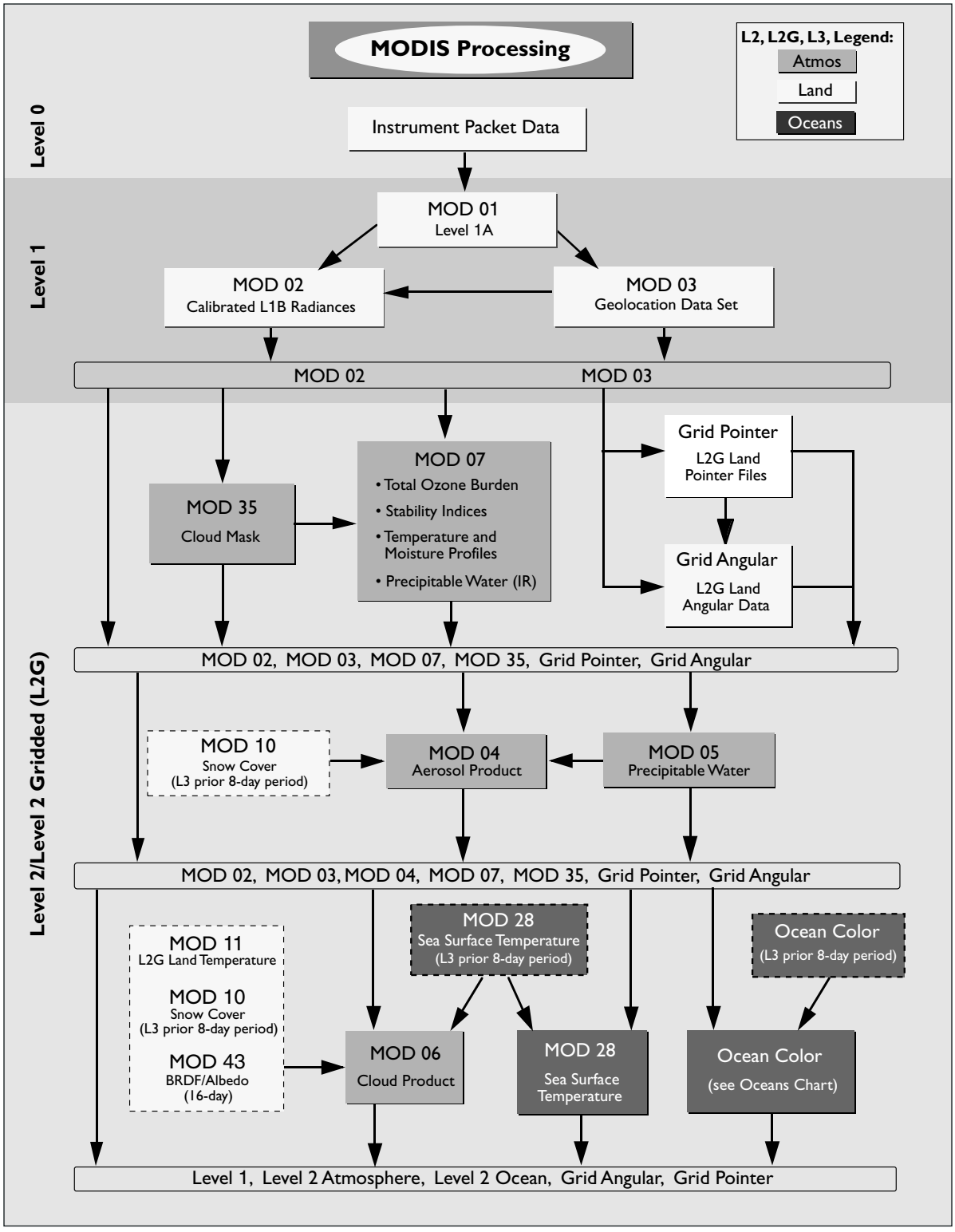

MODIS Data Processing Architecture and Products, general

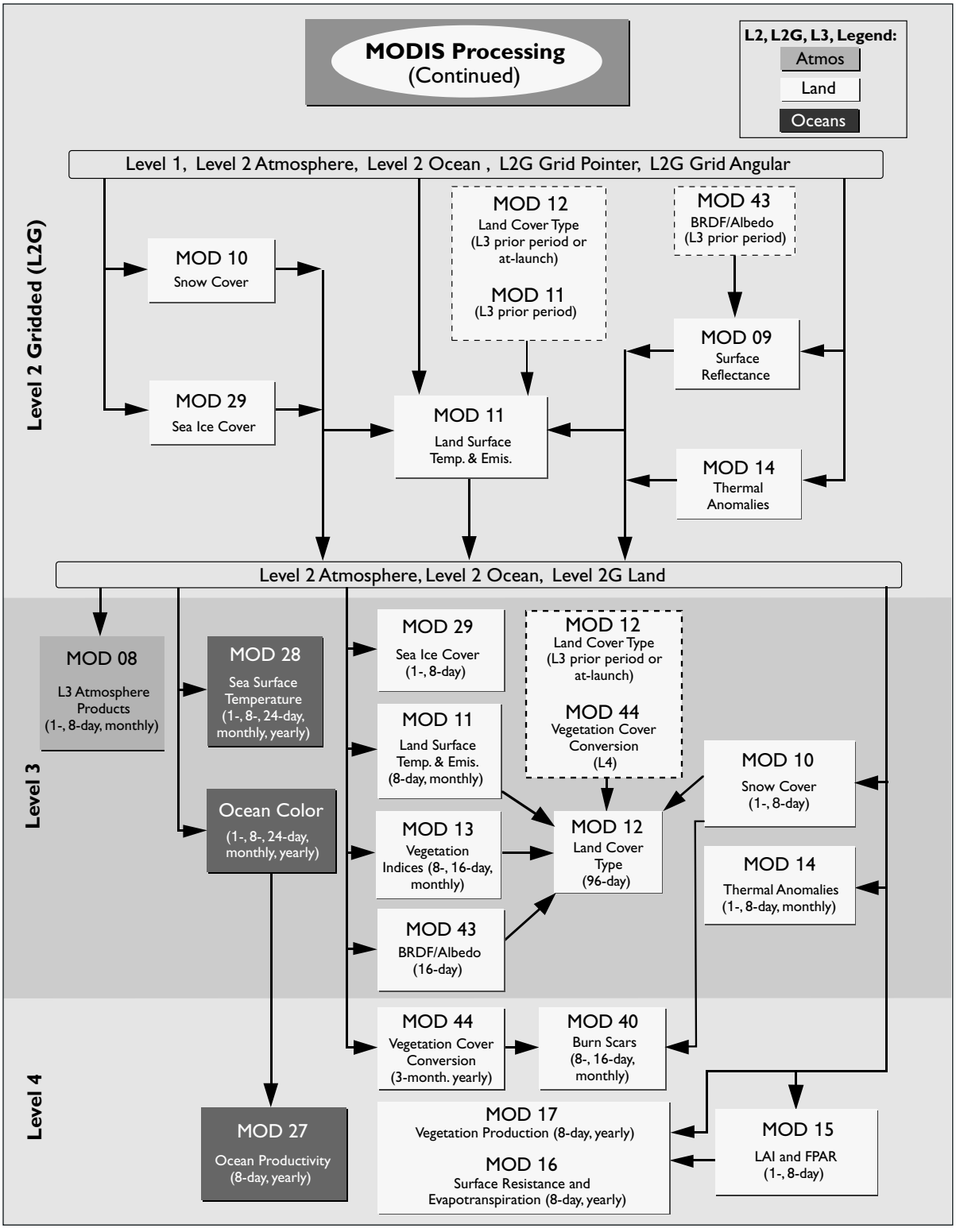

MODIS Data Processing Architecture and Products, general (continued)

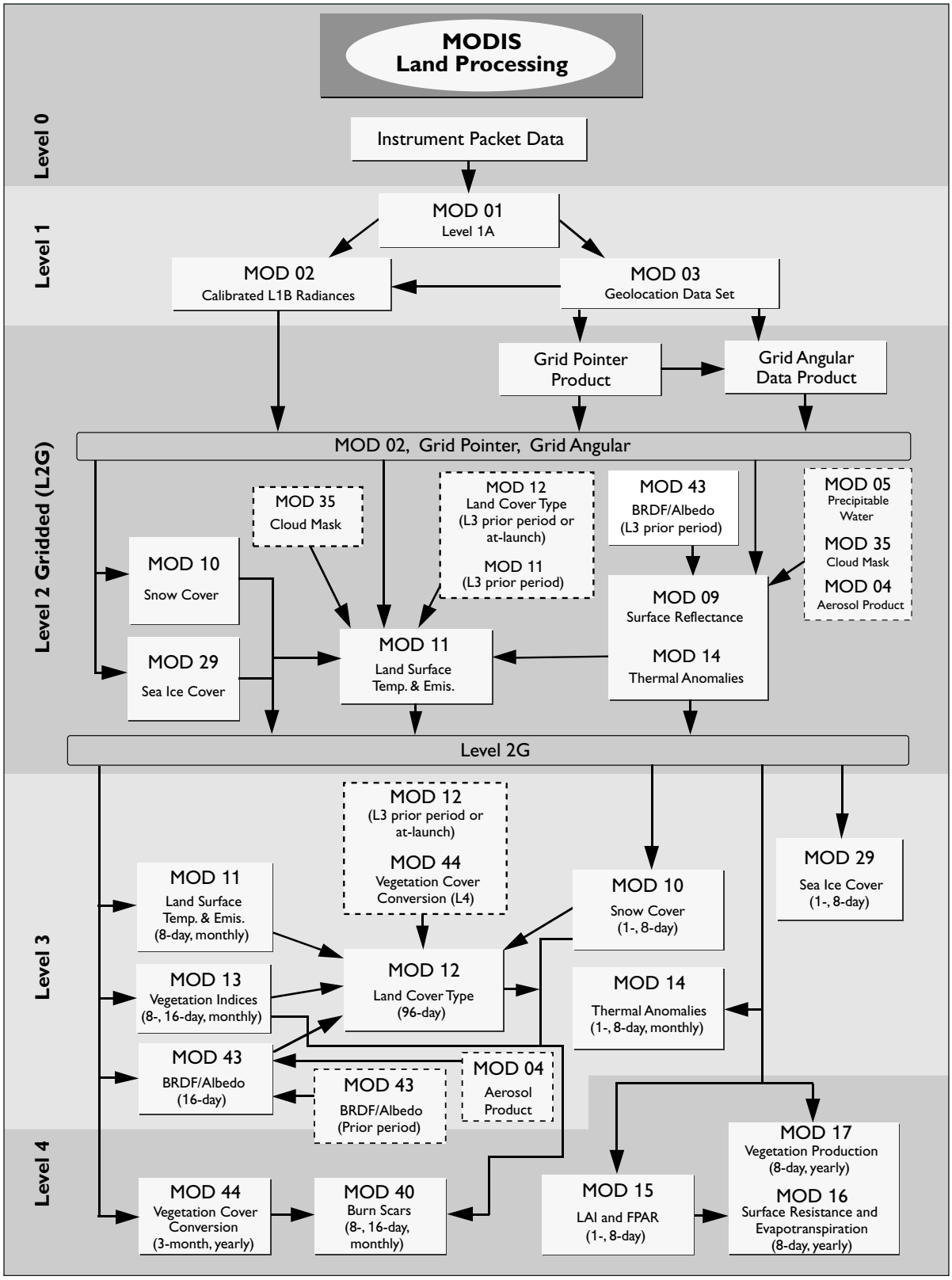

MODIS Data Processing Architecture and Products, land

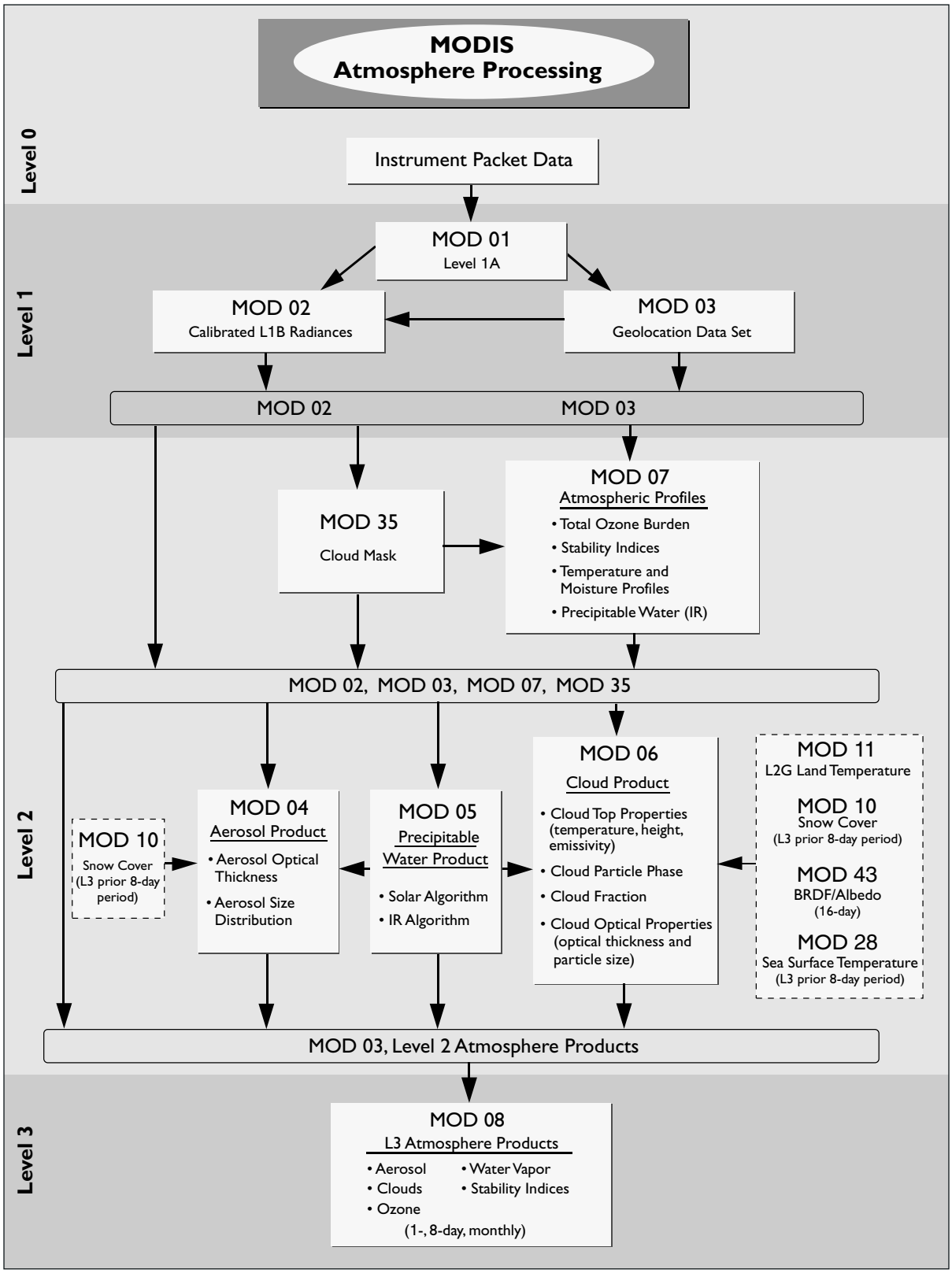

MODIS Data Processing Architecture and Products, atmosphere

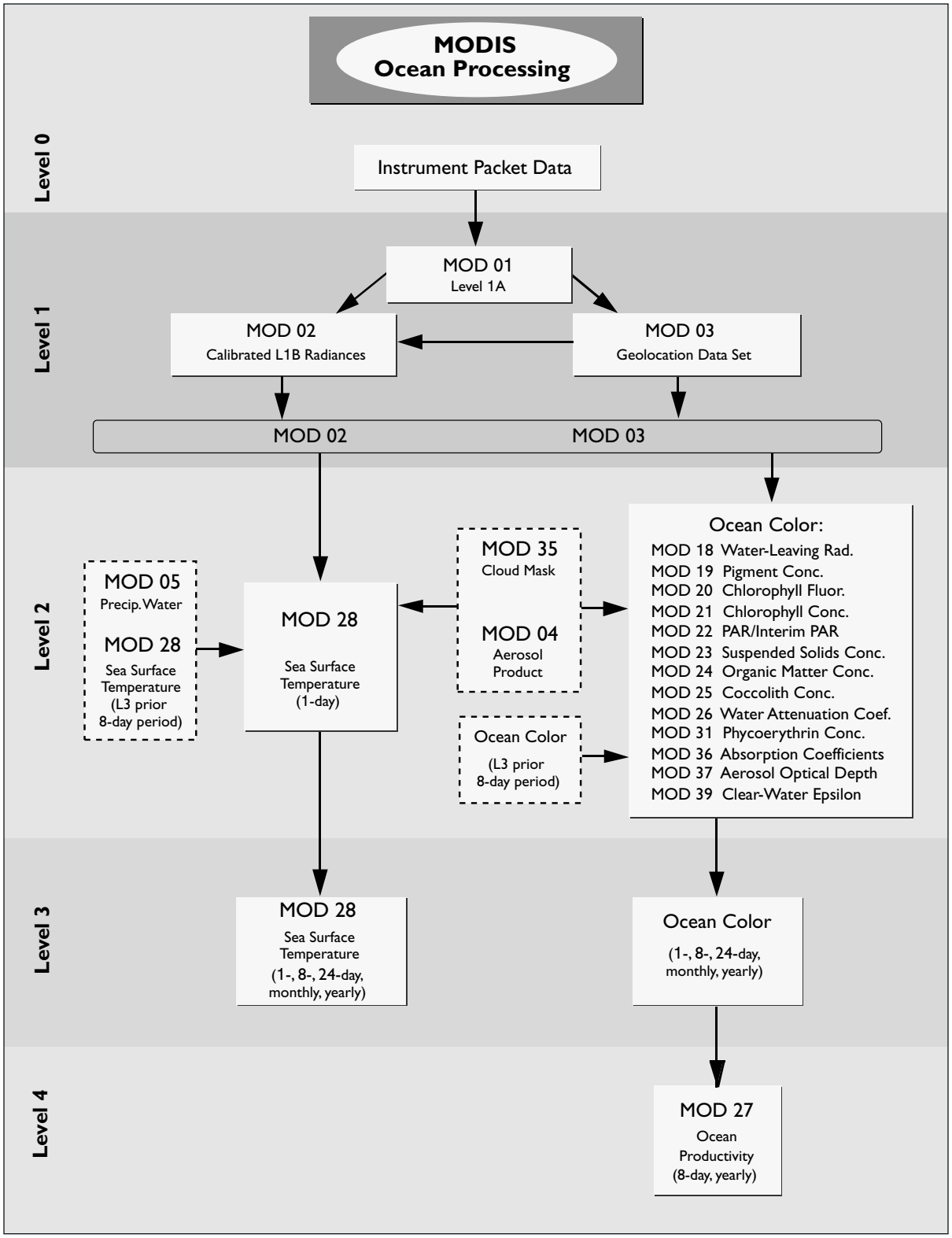

MODIS Data Processing Architecture and Products, oceans. A complete set of these products will be produced for both Terra and Aqua MODIS sensor data. In addition, a merged Terra/Aqua MODIS Ocean product set will be produced at Levels 3 and 4 in the post-Aqua launch period.

Poseidon-2/JMR/DORIS

Jason-1 is a follow-on mission to TOPEX/Poseidon (T/P) to continue high-accuracy measurement of the sea surface topography of the world's oceans. The mission's measurements will be used to study: 1) the global ocean circulation and its variability in relation to climate variability, 2) the global ocean wave field, and 3) the global radar backscatter in relation to sea state and gas exchange with the atmosphere. The data are organized as sequential records along the ground track of the satellite. Each record contains all the information regarding the instrument's measurements averaged over a period close to one second of flight time, including the measurements of sea surface height, wave height, radar backscatter cross-section, and wind speed, along with a host of auxiliary data, including atmospheric, geophysical, and instrumental corrections as well as other relevant information such as ocean-tide model products and atmospheric-pressure products.

The Jason-1 mission was defined in a way that allows an optimum continuation of the T/P scientific mission and fulfillment of the long-term observation requirements. The satellite is designed for a minimum duration of three years, with a potential for an additional two years. Every 10 days, it will overfly within 1 km the reference T/P ground-tracks (66° inclination, 1336 km orbit), measuring sea level with the same or better accuracy than T/P. The Jason-1 payload includes a similar package as for T/P. CNES (Centre National d'Etudes Spatiales) provides the Poseidon-2 altimeter, which is a solid-state, low-power-consumption, low-mass instrument. It is derived from the Poseidon-1 altimeter of T/P but works at two frequencies (13.6 GHz and 5.3 GHz) to enable an ionospheric correction accuracy in accordance with the required error budget. The DORIS Precise Orbit Determination system, whose ultimate performance has been demonstrated on T/P, is also provided by CNES. JPL/NASA is responsible for developing the 3-frequency Jason-1 Microwave Radiometer (JMR) which will be used to compute the troposphere path-delay correction with the required accuracy. A TurboRogue Space GPS Receiver and a Laser Retroreflector Array, also provided by JPL/NASA, will contribute to the Precise Orbit Determination effort. The US Delta II vehicle will be used to launch the Jason-1 satellite, jointly with the TIMED satellite, from the Vandenberg Air Force Base.

The raw engineering Jason-1 data will be recorded on board the satellite, then transmitted to the ground when over-flying the two main telemetry stations located in Aussagel (near Toulouse, France) and in Poker-Flat (Alaska). One backup station is located at the Wallops Flight Facility in Virginia. In addition to these Earth terminals, the control ground system will include a Satellite Control Center located in CNES and a Project Operation Control Center (POCC) at JPL. The mission ground system will be responsible for instrument programming/monitoring as well as scientific product generation and distribution. It will comprise: 1) a CNES center called SSALTO (Segment Sol Multimission Altimetry and Orbitography), which will work not only for Jason-1, but also for other DORIS missions and the Envisat altimeter mission, and 2) a NASA center, which is part of the JPL POCC and derived from the T/P ground system.

The Geophysical Data Records (GDRs) will constitute the final and fully validated products. They will be systematically delivered to data users within 30 days and eventually archived as permanent records. They will contain, at a rate of one record per second, the best estimates of range measurement, the time tag and Earth location, plus the best associated instrumental and environmental corrections and the most accurate orbit altitude. All these parameters will be validated during the verification phase of the mission, covering the first 6-8 months after launch. The GDR, structured in a way similar to what has been used with T/P, will contain the following additional geophysical parameters: wave-height, sigma-naught and derived wind speed, atmospheric surface pressure, tides, mean sea surface, and the geoid. The altimeter radar instrument bias and drift and the relative bias between T/P and Jason-1 time series will be provided. For specific applications (over ocean, coastal areas, lake, land, or ice), the Sensor Geophysical Data Records (SGDR), containing waveforms, will be made available to users.

The Interim GDRs (IGDRs) and Operational Sensor Data Records (OSDR) will support near-real-time applications, including mesoscale and coastal applications, climate forecasting, and marine meteorology. Wind speed, significant wave-height (SWH), and their forecasts are of interest to many activities related to maritime industries. The key requirement for operational use of altimetric data in models is to provide the data within a very short time period. IGDRs will be delivered within three days, mainly for mesoscale and climate applications. They will contain the same parameters as GDRs, but not fully validated and not necessarily in their ultimate precision. OSDRs will be provided within three hours, mainly for supporting marine meteorology applications. They will contain, at a rate of one record per second, all parameters needed for such applications. OSDR products will

have a lower accuracy than IGDR products, as they are based on on-board processing for radar altimetry and orbit determination (DORIS navigator). SWH and wind speed will have respective accuracies of 10% or 0.5 m (whichever is greater) and 2 m/s.

Jason-1 Home Page

http://topex-www.jpl.nasa.gov/jason1/

Key Poseidon-2/JMR/DORIS Facts

Selected for flight on Jason-1

Heritage: Poseidon-1, TMR, and DORIS on TOPEX/Poseidon

Poseidon-2 is a dual-frequency solid-state radar altimeter (13.6 GHz and 5.3 GHz); JMR is a 3-frequency microwave radiometer; DORIS is a 2-frequency receiver measuring signals received from ground-based beacons

Provides high-accuracy global observations of ocean topography, wave height, and wind speed, plus, from the JMR, columnar water vapor content and, from Poseidon-2, total electron content

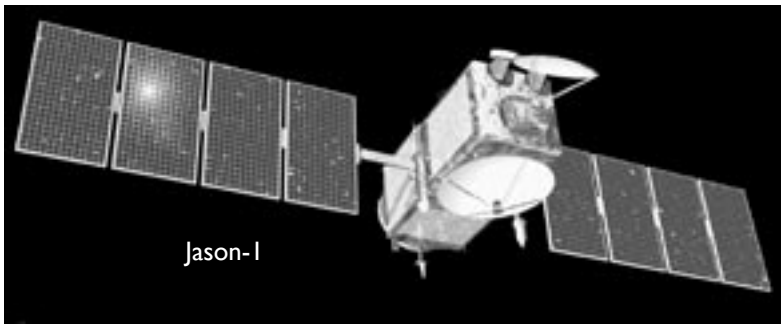

ETM+

Enhanced Thematic Mapper Plus

The Enhanced Thematic Mapper Plus (ETM+) has flown on the Landsat 7 satellite as of 15 April 1999, and provides synoptic, repetitive, multispectral, high-resolution, digital imagery of the Earth's land surfaces. Since 1972, the Landsat Program has provided calibrated land-surface digital imagery to a broad user group including the agricultural community, global change researchers, state and local governments, commercial users, international users, and the military. The Landsat 7 mission will extend the database of the Earth's surface into the next century.

The ETM+ instrument is an improved version of the Thematic Mapper instruments that flew on Landsat 4 and 5. Like the earlier instruments, the ETM+ will acquire data for six visible, near-infrared, and shortwave infrared spectral bands at a spatial resolution of 30 meters.

The ETM+ instrument also incorporates a 15-meter resolution panchromatic band as well as improved ground resolution for the thermal infrared band (60 m vs. 120 m). Incorporation of in-flight full- and partial-aperture solar calibration will improve the overall radiometric accuracy to 5 percent. The ETM+ will provide data that are sufficiently consistent in terms of acquisition geometry, spatial resolution, spectral characteristics, and calibration with previous Landsat data to meet requirements for global change research.

The Landsat 7 satellite operates in a circular, sun-synchronous orbit with an inclination of 98.2°, an altitude of 705 km, and a descending node equatorial crossing time of 10:00 AM plus or minus 15 minutes. This orbit allows Landsat 7 to precede the Terra satellite by 30 minutes along a common ground track. The 185 km swath of coverage provided by the ETM+ field-of-view affords a global view every 16 days.

ETM+ data will be used primarily to characterize and monitor change in land cover and land-surface processes. The high spatial resolution and seasonal global coverage of ETM+ will allow improved assessment of both the rates of land cover change, and the local processes responsible for those changes. Deforestation, ecosystem fragmentation, agricultural productivity, glacier dynamics, coastal hazards, and volcano monitoring are all science targets for ETM+. The common orbit with Terra offers additional opportunities for data fusion with the data from the ASTER, MISR, and MODIS sensors.

The mission will generate and periodically refresh a global archive with substantially cloud-free, sunlit data. To facilitate this objective, a long-term acquisition plan has been devised to ensure maximal global data acquisition, taking into account vegetation seasonality, cloud cover, and instrument gain.

Data stored on board, as well as real-time continental U.S. data, will be downlinked to the Landsat 7 ground station located at the EROS Data Center (EDC) in South Dakota. Data received at the EDC will be processed for archiving and distribution by the Land Processes DAAC. All data received at EDC will be available at L0R (no radiometric calibration; limited geometric correction). In addition, a subset of these scenes can be processed to Level 1 (radiometric and geometric corrections applied).

ETM+/Landsat Home Page

http://landsat.gsfc.nasa.gov/

Key ETM+ Facts

Selected for flight on Landsat 7, launched April 15, 1999

Heritage: Landsat 4, 5 and 6

Imaging radiometer with 7 spectral bands from visible to thermal infrared plus a panchromatic band; 16-day repeat cycle

Provides high spatial resolution, multispectral images of the sunlit land surface

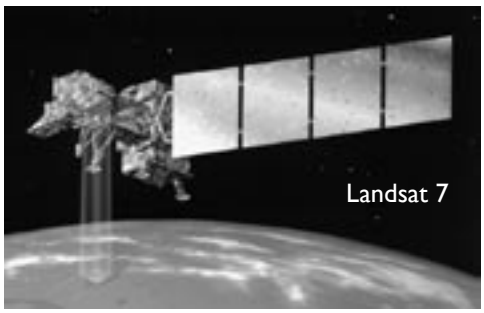

SAGE III

Stratospheric Aerosol and Gas Experiment III

The SAGE III instrument is designed to enhance our understanding of natural and human-derived atmospheric processes by providing accurate long-term measurements of the vertical structure of aerosols, clouds, temperature, ozone, water vapor, and other important trace gases (NO_2, NO_3, and OClO) in the upper troposphere and stratosphere. The instrument is mounted on board the Russian Meteor 3M spacecraft and is scheduled for launch in March 2001. The SAGE III instrument has a design that has been advanced over that of its predecessors, permitting measurements during both solar and lunar occultation events. For the SAGE III instrument on Meteor 3M, solar events will occur between 50°N and 80°N and between 30°S and 60°S. Lunar occultation events will be limited to periods when the lunar disk is more than 50% illuminated. These measurement opportunities, however, will extend over all latitudes.

The SAGE III data processing function converts the instrument's Level 0 data into Level 1B and Level 2 data products. The procedure involves the conversion of instrument responses to solar or lunar flux, at 70-to-80 wavelengths between 290 and 1550 nm, into vertical profiles of the molecular density of gaseous species, aerosol extinction at eight wavelengths, temperature, and pressure. This procedure consists of two main parts: the transmission algorithm and the inversion algorithm, as illustrated in the figure on the following page.

The function of the transmission algorithm is to calibrate the radiance data and to produce multi-wavelength slant-path transmission profiles from time sequences of radiometric and engineering measurements by the SAGE III instrument. This process can be separated into five components: data screening, position registration, wavelength registration, radiance calibration, and data grouping and statistics.

The inversion algorithm converts the multi-wavelength slant-path transmission data from the transmission algorithm into vertical profiles of molecular density for SAGE III-measured gas species, aerosol extinction at eight wavelengths, and atmospheric temperature and pressure. Procedures such as the multiple linear regression (MLR) technique and the Marquardt nonlinear least-squares algorithm are used in the retrieval algorithm to produce the Level 2 data products. The detailed algorithm is discussed in the SAGE III ATBDs.

The SAGE III data processing algorithm has been developed at the NASA Langley Research Center (LaRC). Routine processing of the SAGE III data will be performed at the SAGE III Scientific Computing Facility (SCF) at LaRC. All products will be delivered to the Langley Distributed Active Archive Center (DAAC) for archive and public distribution.

SAGE III Home Page

http://www-sage3.larc.nasa.gov/

Key SAGE III Facts

Selected for flights on the Russian Meteor 3M satellite and on the International Space Station

Heritage: SAM II, SAGE I, and SAGE II

Multi-spectral sun/moon-looking photometer

Provides long-term global ozone and aerosol data

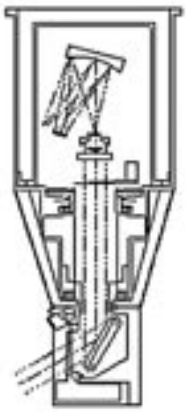

SAGE III

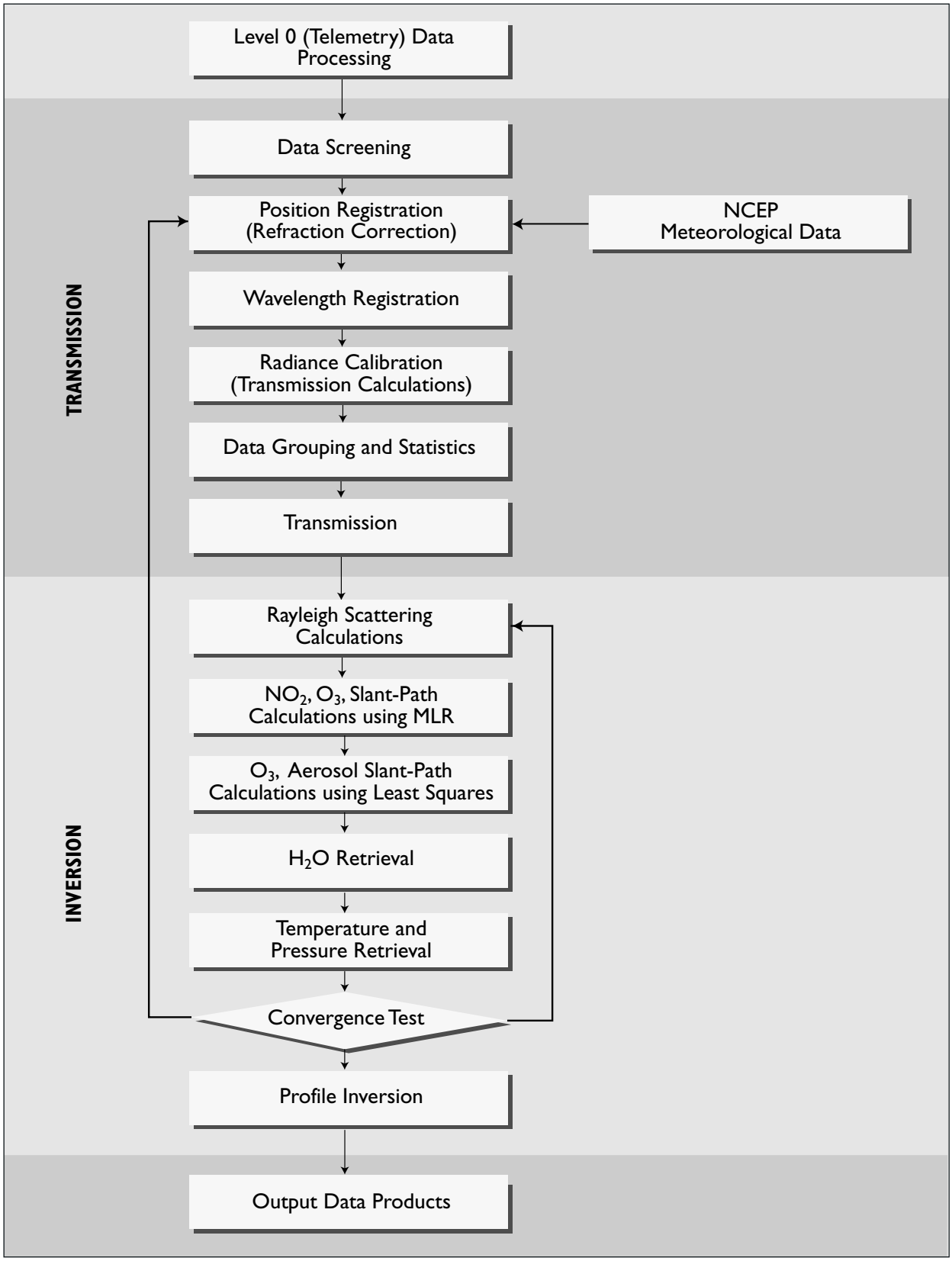

SAGE III Data Processing Architecture and Products

SeaWinds

The SeaWinds instruments are specialized microwave radars designed to make moderate-resolution, broad-swath measurements of global radar backscatter and ocean-surface wind speed and direction under nearly all-weather conditions. SeaWinds vector-wind measurements are critical for investigating and modeling upper-ocean circulation, marine meteorological processes, and large-scale air-sea interaction and climate. The data are provided to the U.S. National Oceanic and Atmospheric Administration (NOAA) and the EOS Data Assimilation Office (DAO) in near-real-time for use in regional and global weather prediction and marine forecasting. NOAA distributes near-real-time SeaWinds wind-velocity data to international operational weather prediction centers.

The SeaWinds radar backscatter cross-section measurements over land provide information on vegetation type and both seasonal and interannual change. Measurements over continental and sea-ice-covered areas are used to monitor ice extent and freeze/melt processes on diurnal through interannual time scales.

SeaWinds is a dual, conically scanning pencil-beam radar operating at 13.4 GHz. Vertically polarized backscatter cross-section measurements at ~54° incidence angle are acquired over an 1800-km-wide swath centered on the satellite subtrack. Horizontally polarized data are acquired over a concentric 1400-km-wide swath at ~46° incidence angle. The antenna spins at 18 rpm, yielding measurements with 25-×-35-km IFOV. Modulation of the transmitted pulses allows extraction of cross-section data with ~6-×-25-km spatial resolution. SeaWinds vector-wind measurements are obtained with 25-km resolution across nearly the entire swath, and cover more than 90% of the global, ice-free oceans daily.

Significant ground processing is required to extract accurate backscatter cross-section and vector-wind measurements from raw SeaWinds radar measurements. The surface normalized radar cross-section is calculated from the received power and knowledge of the viewing geometry and instrument characteristics. Over the ocean, backscattering results primarily from centimetric ocean roughness elements whose amplitudes and directional distributions are in local equilibrium with the local wind. The ocean backscatter cross-section thus varies with wind speed and direction relative to the radar beam. Vector-wind measurements are thus obtained by combining multiple, near-simultaneous, collocated backscatter measurements acquired from different viewing geometries as the satellite passes overhead. SeaWinds ocean vector-wind products include flags to indicate the presence of contamination resulting from heavy rain conditions.

Two SeaWinds instruments will be flown in the first set of EOS missions. The QuikScat mission, with SeaWinds as the sole science instrument, was launched on 19 June 1999 and has been returning high-quality data since 19 July 1999. A second SeaWinds will be launched in late 2001 as part of the National Space Development Agency (NASDA) of Japan's ADEOS-II mission; this mission will also include a broad-swath, multi-channel microwave radiometer (an AMSR). A subset of the ADEOS AMSR measurements will be used in the ADEOS SeaWinds processing to provide atmospheric corrections and advanced rain flagging to supplement the autonomous SeaWinds flags and to enhance the accuracy of the vector-wind measurements. The figure on the following page outlines the complete SeaWinds processing chain and standard products.

SeaWinds Homepage

http://winds.jpl.nasa.gov/

Key SeaWinds Facts

Selected for flights on QuikScat, launched June 19, 1999, and the Japanese ADEOS II satellite

Heritage: SEASAT, NSCAT

Ku-band scatterometer

Provides near-surface wind velocities over the oceans, plus information for vegetation classification and ice-type investigations

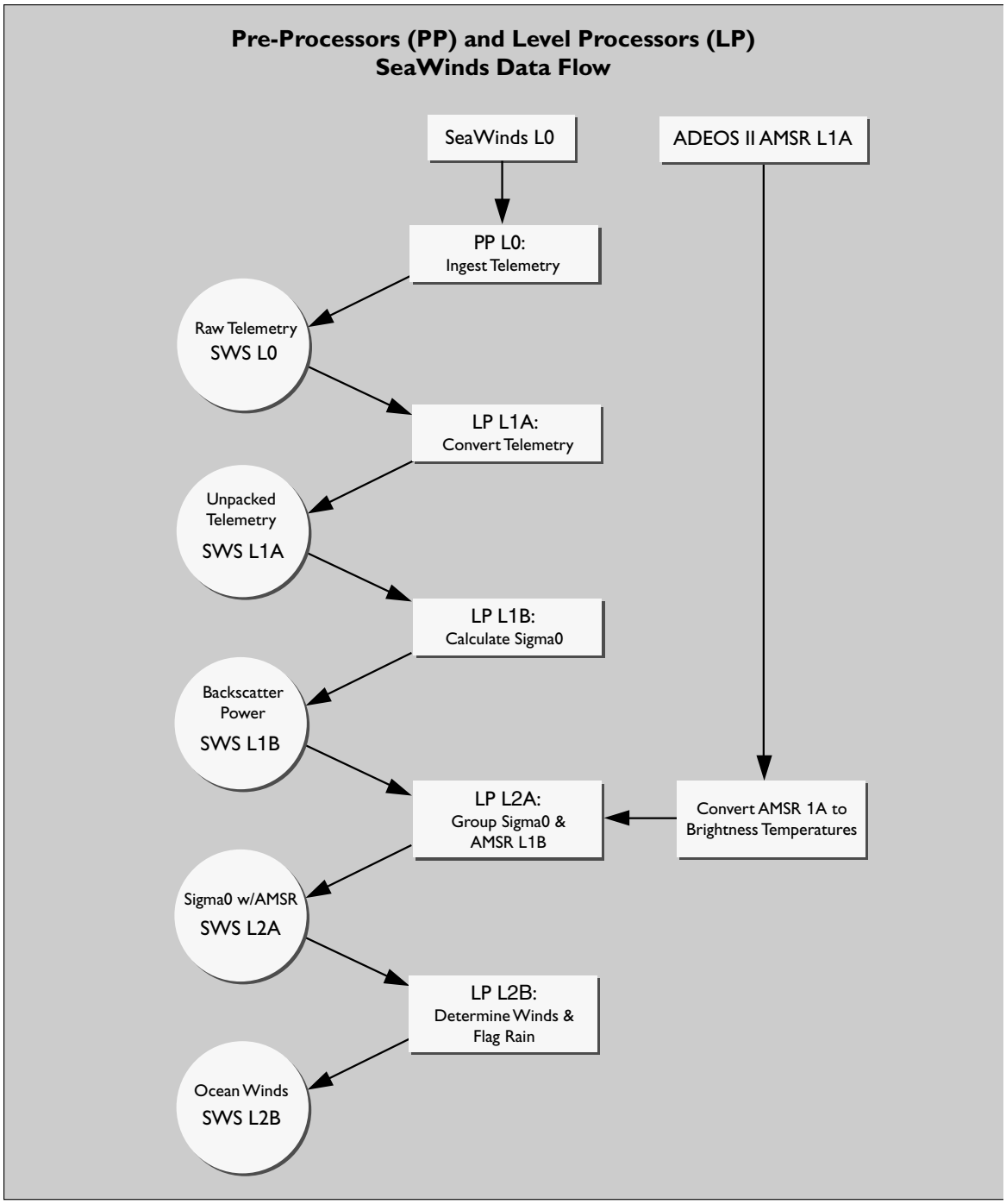

SeaWinds Data Processing Architecture and Products

TOMS

Total Ozone Mapping Spectrometer

The QuikTOMS mission is to continue daily mapping of the global distribution of the Earth's total column of atmospheric ozone with the Total Ozone Mapping Spectrometer Flight Model 5 (TOMS-FM5). TOMS-FM5 was scheduled to be launched in the year 2000 aboard a Russian satellite, but that mission was terminated in April 1999. Because of the requirement for monitoring changes in the ozone layer, NASA had to formulate a new mission to fly TOMS-5 in a very short time. The continuous observation of the global ozone past the year 2000 is critical in order to monitor the expected recovery of ozone as levels of chlorofluorocarbons (CFCs) decrease from their current maximum as a result of the Montreal Protocol limits. The planned three-year QuikTOMS mission is intended to provide overlap with the current Earth Probe TOMS, launched in July 1996, and with the Ozone Monitoring Instrument (OMI), scheduled for launch on Aura in 2003.

The main objectives of QuikTOMS are: 1) the determination of long term change in global total ozone level, 2) the understanding of the processes related to the "ozone hole" formation and local anomalies in the equatorial region, and 3) improved understanding of processes that govern the generation, depletion, and distribution of global total ozone. Additional objectives are: the detection and measurement of volcanic ash clouds and sulfur dioxide gas, the detection and measurement of aerosol and pollution plumes, and the estimation of surface ultraviolet irradiance

TOMS-5 is a f/5 single grating Ebert-Fastie type monochromator with multiple exit slits for six different wavelengths. The nominal center wavelength values of the six bands are 308.6, 312.5, 317.5, 322.3, 331.2, 360 nm, and the nominal bandwidth for each band is 1.2 nm. The wavelength is selected with a chopper wheel near the slit plate that gates the pair of the entrance and exit slits for each wavelength band. The instantaneous field of view (IFOV) of TOMS-5 is 3° × 3°, which projects to approximately 42 km × 42 km at the subsatellite point on the Earth for the 800 km satellite altitude. TOMS-5 scans ±18 scenes from the nadir in a 3° interval to cover approximately 2300 km cross track.

The TOMS instrument records daily global measurements of total column ozone, aerosols, Erythemal UV exposure, and reflectivity. In the event of a volcanic eruption it can also measure sulfur dioxide in the eruption plume.

Data are provided in a gridded 1° latitude by 1.25° longitude format. All data processing will be done at the Science Operations Center at NASA Goddard Space Flight Center, Greenbelt, Maryland.

QuikTOMS Home Page

http://toms.gsfc.nasa.gov/.

Key TOMS Facts

Selected for flights on:
Nimbus 7, launched October 24, 1978;
Meteor 3, launched August 15, 1991;
ADEOS I, launched August 17, 1996;
Earth Probe, launched July 2, 1996; and
QuikTOMS

Heritage: the earlier TOMS instruments

Six-band monochromator

Provides global daytime measurements of total column ozone, aerosols, Erythemal ultraviolet exposure, and reflectivity

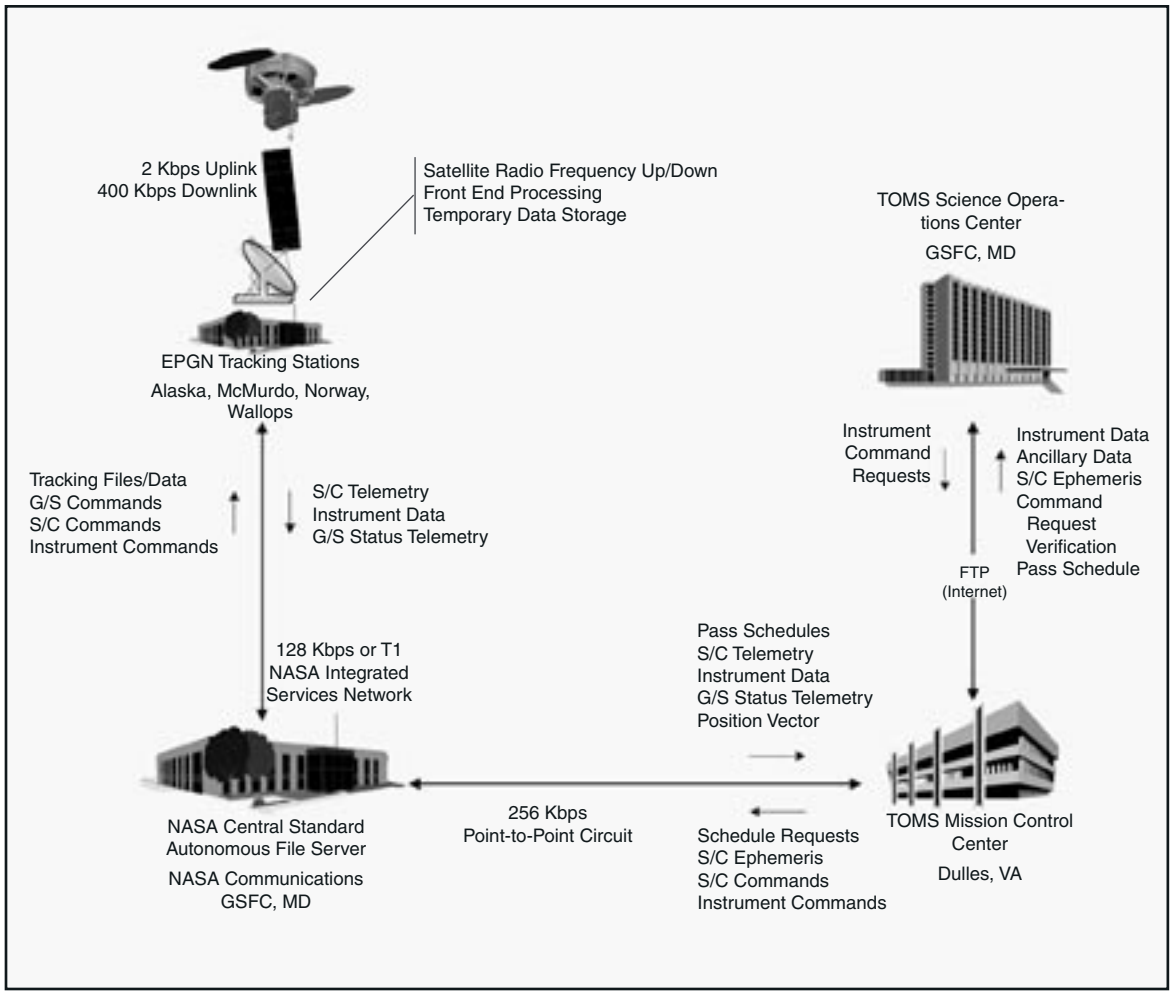

QuikTOMS Data Processing Architecture

MBLA

MultiBeam Laser Altimeter

The Vegetation Canopy Lidar (VCL) is the first selected mission of NASA's new Earth System Science Pathfinder (ESSP) program. The related data products listed in this handbook are derived from the Multi-Beam Laser Altimeter (MBLA), the instrument that will fly on the VCL platform. The principal goal of VCL is the characterization of the three-dimensional structure of the Earth: in particular, canopy vertical and horizontal structure and land-surface topography. Its primary science objectives are: land cover characterization for terrestrial ecosystem modeling, monitoring and prediction; land cover characterization for climate modeling and prediction; and production of a global reference data set of topographic spot heights and transects. VCL will provide unique data sets for understanding important environmental issues including climatic change and variability, biotic erosion, and sustainable land use, and will dramatically improve our estimation of global biomass and carbon stocks, fractional forest cover, forest extent and condition. Furthermore, it will provide canopy data critical for biodiversity studies as well as for natural hazard and climate studies. Scheduled for launch in late 2000, VCL is an active lidar remote sensing system consisting of a five-beam instrument with 25-m contiguous along-track resolution. The five beams are in a circular configuration 8 km across, and each beam traces a separate ground track spaced 2 km apart, eventually producing 2-km coverage between 67° N and S latitude. VCL's core measurement objectives are: 1) canopy top heights; 2) vertical distribution of intercepted surfaces, e.g., leaves and branches; and 3) ground-surface topographic elevations. These measurements are used to derive a variety of science data products, including canopy heights, canopy vertical distribution, and ground elevations gridded at various temporal and spatial resolutions.

The VCL standard data products will be produced by the VCL Data Center (VDC). The VDC consists of three major science-processing subsystems. These science subsystems are:

- Altimeter Return Echo Analysis System (AREAS) will process the altimeter waveform acquired with each laser shot. These waveforms will be used to determine the range to the canopy top and ground, provide information on the Vertical Distribution of Intercepted Surfaces (VDIS), and perhaps deliver other information, e.g., reflectance, useful in the characterization of the surface spot being ranged to. For example, the laser data can be used to identify water, unvegetated land surfaces, surface slopes, terrain roughness, and related information.

- The VCL Precision Geolocation System (VPGS) will be responsible for providing precise orbital ephemeris information for VCL through the proper modeling of the forces acting on the satellite, reduction and analysis of the GPS, Satellite Laser Ranging (SLR), and laser-altimeter data, and incorporation of specialized orbit-determination methodologies. The system will also utilize the altimeter ranges acquired over the ocean during times of special-pointing, off-nadir spacecraft maneuvers to derive pointing corrections for the spacecraft's attitude and laser instrument offsets due to mounting and thermal effects, and to geolocate the spot on the surface being ranged to. This orbit-position and spacecraft-attitude information will be interpolated to the time of each VCL altimeter range to locate the surface footprint while retaining the level of accuracy in the geolocation and pointing solutions. The VPGS will also process the raw star tracker, gyro, and magnetometer data to provide improved attitude information in support of the pointing solution.

- The Level 3 Products Generation Subsystem. This science processing system, of less complexity, is a gridding package which will generate the mission's Level 3 data products, using a variety of windowing, averaging, and parsing strategies.

The VDC also supports other important functions, which include:

- Processing data received from telemetry packets into various science and intermediate products. This includes unpacking and uncompressing telemetry to provide gyro/attitude, star tracker, GPS receiver, GPS NAV orbit, and MBLA waveform data at Level 0.

- Support expedient data delivery (through both a subscription and random ordering capability) and specialized analysis functions and flexibility needed by the Science Team to verify system performance, improve processing algorithms, calibrate instruments, and add value to the processing approaches as the mission evolves.

- Provide all required data and data product distribution to the EROS Data Center in Sioux Falls, South Dakota, which is designated as the DAAC interface with the outside science community.

(MBLA Overview, continued)

- Provide on-site data archiving, information management, and data-management functions.
- Perform gridding, and visualization functions to assist the Science Team in their evaluation of these data and provide interim and final higher level data products for testing and accuracy assessment and distribution to the EROS Data Center.
- Provide data back-up and security management to protect the VDC and its data holdings from unauthorized use and catastrophic failure/events.
- Acquire all data sets in a timely and regular fashion externally located from the VDC which are needed to support AREAS, pointing, and orbit processing. This includes Earth-orientation information, solar and magnetic flux, SLR data, snow cover grids, sea state, and like information.
- Provide on-line/near-line access to all subsidiary data sets which are needed to process, characterize, and evaluate data products. This includes DEM, urban masks, land/ocean masks, surface-type/ characterization files, surface-slope masks, etc.

VCL Home Page

http://www.inform.umd.edu/geog/vcl

Key MBLA Facts

Selected for flight on VCL, the first mission of NASA's ESSP program

Heritage: Shuttle Laser Altimeter (SLA), Mars Orbiter Laser Altimeter (MOLA), Laser Vegetation Imaging Sensor (LVIS)

Laser altimeter system using five, 1064 nm-wavelength lasers in a circular configuration

Measures the three-dimensional structure of the Earth, in particular canopy vertical and horizontal structure and land surface topography

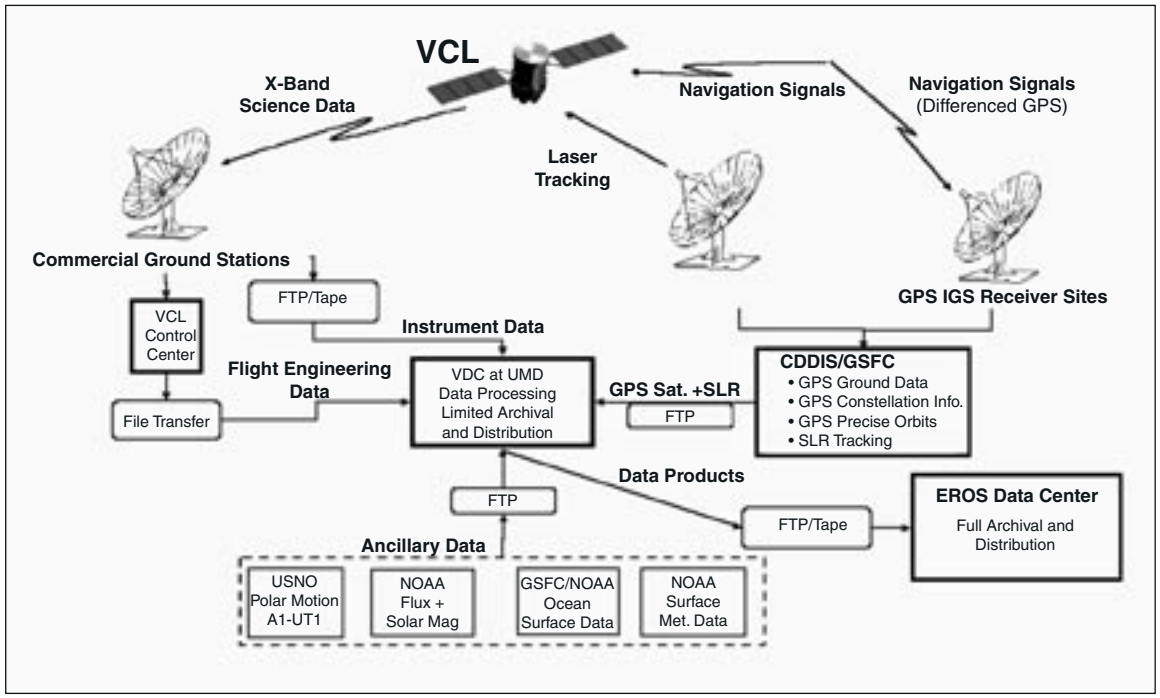

VDC System Context within the VCL Mission

Radiance/Reflectance and Irradiance Products

ACRIMSAT
- ACRIM III

Aqua
- AIRS
- AMSR-E
- AMSU-A
- CERES
- HSB
- MODIS

Landsat 7
- ETM+

Meteor 3M
- SAGE III

Radiance/Reflectance and Irradiance Products – An Overview

Relationship to Global Change Issues

Remote sensing of the Earth and its atmosphere requires the detection of electromagnetic radiation, something that has been done effectively from satellites for a wide range of wavelengths and wavelength bands from the ultraviolet to the microwave. Instruments used to detect this radiation can be broadly classified as either passive or active, the distinction being based on whether the instruments carry only detectors or detectors plus electromagnetic radiation sources. The fundamental products of passive and active remote sensing instruments can be classified as radiance/reflectance products, irradiance products, or radar/lidar products. Radiance products are a measure of the radiant flux per unit area and solid angle originating from an Earth scene. Reflectance products are a measure of the incoming radiant flux reflected from an Earth scene, usually measured using a reference target of known reflectance. Reflectance products can be converted to radiance products provided that an accurate solar-irradiance spectrum is available or is measured. Irradiance products are a measure of radiant flux incident on a surface per unit area of that surface. Products that can be classified in the radar category are produced by active remote sensing instruments. Examples of these instruments in this volume are microwave radar, such as SeaWinds on the QuikScat satellite, and lidar instruments, such as MBLA on the VCL satellite. For all products, the geophysical parameters derived from the fundamental instrument measurements drive the selection of instrument operating wavelengths and bandpasses.

The derivation of accurate higher order, geophysical data products used in global change studies depends on the accuracy and precision of the fundamental products. Accuracy and precision in the fundamental instrument products are sought through careful prelaunch and on-orbit instrument calibration and characterization and through precise geolocation of those products. Moreover, the need for accurate geophysical data over the time frame of decades requires that fundamental instrument products be calibrated between successive versions of the same instrument on different platforms and between synergistic instruments operating in similar or different wavelength regions.

Product Overview

Radiance/Reflectance: Calibrated and geolocated radiance/reflectance products are generated by passive remote sensing instruments designed to measure 1) emitted thermal and microwave radiation from the Earth and its atmosphere in the 2.5-to-100- micrometer wavelength and the 6-to-89-GHz frequency regions, and/or 2) solar radiation reflected from the Earth's land, ocean, cryosphere, and atmosphere in the 0.3-to-2.5-micrometer wavelength region.

On the EOS Aqua platform, radiances will be measured from the visible through microwave wavelength regions by the MODIS, CERES, AIRS, AMSU-A, HSB, and AMSR-E instrument suite. Radiance products will be generated by the first five of these instruments. The AMSR-E instrument will make calibrated, geolocated radiance measurements, but will produce a brightness temperature as its fundamental product made available to the remote sensing community. The MODIS instrument team plans to generate a reflectance product in addition to a radiance product. These radiance/reflectance and brightness temperature products will be used to generate higher order geophysical products used in the study of atmospheric radiation, cloud formation, atmospheric temperatures and humidities, precipitation, radiative balance, snow, sea ice, sea surface temperature, land vegetation, and ocean productivity.

The Landsat 7 ETM+ instrument produces radiances from the visible through infrared in seven spectral bands. The ETM+ spectral coverage, coupled with its small footprint on the Earth, facilitates high-resolution remote sensing studies of the Earth's surface.

The QuikTOMS instrument will make high-resolution measurements of upwelling ultraviolet radiance in six spectral bands between 0.309 and 0.360 micrometers. These radiance measurements will be used in studies of the atmospheric ozone layer.

The JMR instrument on Jason-1 will make microwave radiance measurements in three channels between 18 and 34 GHz. These measurements will be used to determine atmospheric water concentrations and to perform path-delay corrections for the Poseidon-2 altimeter on board the Jason-1 platform.

Irradiance: Remote sensing instruments that produce irradiance products measure radiant flux incident per unit instrument-aperture area. Irradiance measurements include solar irradiance, in which solar flux is measured directly, and irradiance reflected or scattered through interaction with the Earth and its atmosphere. Irradiance-measuring instruments are typically passive remote sensing instruments.

ACRIM III is a solar-irradiance-measuring instrument which, with its predecessor instruments, has contributed greatly to the long-term solar-irradiance database. ACRIM III is an active cavity radiometer that measures total solar irradiance in the 0.001-to-1000- micrometer wavelength range. ACRIM measurements have been, and will continue to be, of paramount importance in monitoring the variability of total solar irradiance in climatic interactions between the Sun and the Earth.

The SAGE III instrument measures the ratio of Earth-occulted solar and lunar irradiance transmitted through the Earth's atmosphere to the un-occulted solar and lunar irradiance. SAGE III will not produce an irradiance product but will produce a transmission-based product, the slant-path optical depth, at a number of wavelengths from 0.29 to 1.55 micrometers. These optical depths will be used to retrieve a number of atmospheric constituent concentrations and parameters as a function of altitude. These measurements include O_3, H_2O, NO_2, NO_3, OClO, air density, and atmospheric aerosols.

Product Interdependency and Continuity with Heritage Data

The accuracy and precision of higher order geophysical data products is directly dependent on the accuracy and precision of the fundamental radiance/reflectance, irradiance, and radar products. Fundamental products of high accuracy and precision are produced by mechanically, optically, and electronically well-designed instruments that have been completely calibrated and characterized prelaunch and whose calibrations are carefully monitored while in orbit. The importance of cross-calibration of remote sensing instruments is amplified for those instances in which a product from one instrument is needed for a product derived from the data of another instrument, either to generate products or to improve the accuracy and precision of products. A good example of the use of data from multiple instruments to produce data products of high quality is the AIRS, AMSU-A, HSB instrument suite. Collocated microwave measurements from AMSU-A in the 27-to-89 GHz channels and from HSB in the 89-to-183 GHz channels will be directly used to increase the accuracy of AIRS atmospheric temperature retrievals under partly cloudy conditions. Additional examples of product interdependency are the use of MODIS scene classification in processing CERES radiance data and the use of collocated AMSR-E precipitation and atmospheric water-vapor measurements in improving the accuracy of QuikScat retrievals of wind velocities.

Long-term monitoring of instrument on-orbit calibration and performance is necessary to produce the long time series remote sensing data products needed in global climate-change studies. Ideally, data products measured by identical or different versions of the same instrument on successive platforms should produce continuous, seamless data products. Careful calibration of generations of instruments is of fundamental importance in the generation of useful long-term remote sensing data products. In addition, the production of high-quality, long-term data products is facilitated when future generations of remote sensing instruments share a strong heritage with predecessor instruments. The instruments addressed in this second volume of the Data Products Handbook take advantage of invaluable lessons learned from heritage instruments. The instruments highlighted in this volume and their heritage instruments are listed on the next page.

Suggested Reading

Brest, C.L., and S.N. Goward, 1987.

Chomko, R., and H.R. Gordon, 1998.

Evans, R.H., and H.R. Gordon, 1994.

Foukal, P.A., and J.L. Lean, 1990.

Gillespie, A.R. *et al.*, 1986.

Lee III, R.B. *et al.*, 1996.

Robinson, W.D. *et al.*, 1992.

Slater, P.N. *et al.*, 1987.

Smith, G.L. *et al.*, 1986.

Wielicki, B.A. *et al.*, 1998.

Willson, R.C., and A.V. Mordvinov, 1999.

DPH2 Instrument	Heritage Instruments
ACRIM III	ACRIM I/SMM, ACRIM II/UARS
AIRS	HIRS
AMSR-E	SSM/I, TMI/TRMM
AMSU-A	MSU, AMSU-A/NOAA K
CERES	ERB, ERBE, CERES/TRMM, CERES/Terra
DORIS	DORIS/SPOT-2, DORIS/ TOPEX/Poseidon
ETM+	TM/Landsat 4, TM/Landsat 5
HSB	MSU
JMR	TMR/TOPEX/Poseidon
MBLA	Various airborne lidars
MODIS	AVHRR, CZCS, MODIS/Terra
Poseidon-2	GEOSAT, ERS-1, TOPEX/Poseidon
TOMS	TOMS/Nimbus 7, TOMS/EP, TOMS/ADEOS
SeaWinds	S-193/Skylab, SASS/SEASAT, AMI/ERS-1, NSCAT/ADEOS
SAGE III	SAM/Apollo-Soyuz, SAM II/ Nimbus 7, SAGE I/AEM II, SAGE II/ERBS

Instruments highlighted in this volume (DPH2, for Data Products Handbook, Volume 2) and their heritage instruments

ACRIM III Radiometric Products

Product Description

ACRIM III uses three redundant cavity pyrheliometers to monitor the total solar irradiance (TSI) with state-of-the-art precision. One sensor monitors full time; a second is compared to the first, monthly; and a third is compared with the other two every third month, as a calibration for solar-exposure-induced degradation. TSI precision will be better than 20 ppm over ACRIM III's 5-year mission lifetime. Overlapping comparisons with preceding (UARS/ACRIM II and SOHO/VIRGO) and succeeding (TIM/SIM) TSI monitors will be made that are essential for database continuity.

The Level 1A data product (not archived) will consist of the experiment data converted to watts per square meter in the International System of units (SI) at the ACRIMSAT satellite.

Level 1B data will be Level 1A corrected for shutter offsets, pointing errors, temperature dependencies, and other minor instrumental effects.

Level 1C data will be the calculated TSI time-ordered series in units of watts per square meter for each ACRIM shutter-open cycle as observed *in situ* by the ACRIM instrument on ACRIMSAT. The basic time resolution will therefore be an average TSI centered on 131.076-second intervals.

Level 2 data will be Level 1C corrected to 1 Astronomical Unit. The satellite TSI is reconciled to 1 Astronomical Unit using the Solar Elevation, Azimuth and Range computation of the Satellite Tool Kit software (Analytical Graphics, Inc.) based on ACRIMSAT's NORAD two-line orbital elements. The primary archived data products are Level 2 shutter cycle and daily means. The time scale of the shutter cycle means is 2.048 minutes.

Suggested Reading

Beer, J. *et al.*, 1991.

Eddy, J. A., 1976.

Foukal, P. A., and J. L. Lean, 1988.

Foukal, P. A., and J. L. Lean, 1990.

Hays, J.D. *et al.*, 1976.

Hickey, J.R. *et al.*, 1980.

Lee III, R.B. *et al.*, 1995.

Willson, R.C., 1984.

Willson, R.C., 1997.

Willson, R.C., and A.V. Mordvinov, 1999.

Willson, R.C. *et al.*, 1981.

Woodard, M., and R. Noyes, 1985.

ACRIM III Radiometric Products Summary

Coverage: N/A

Processing Level: 1, 2

Product Type: Standard, at-launch

Maximum File Size: 1.2 MB

File Frequency: 1/day

Primary Data Format: HDF-EOS

Browse Available: Daily Solar Irradiance Graphs (10 MB)

Additional Product Information: http://eosweb.larc.nasa.gov/PRODOCS/acrimIII/table_acrimIII.html

DAAC: NASA Langley Research Center

Science Team Contact: R. C. Willson

AIRS Level 1A Radiance Counts (AIR 01)

Product Description

This Level 1A data set contains geolocated counts for 2378 infrared channels and 4 visible/near-infrared channels, along with engineering and spacecraft ancillary data.

The Level 1A data are used as input for calibration and processing. Quality indicators are added to the data to indicate instrument mode and missing or otherwise bad data.

Infrared and visible observations are made during both the day and the night portions of the orbits.

This product includes all AIRS infrared and visible data in counts from all channels and all detector views (Earth, space, and calibrated-source views). Included also are engineering data in engineering units, geolocation data, and spacecraft ancillary data.

AIRS Level 1A Radiance Counts Summary

Coverage: Global

Spatial/Temporal Characteristics:
Infrared: 13.5 km FOV at nadir/twice daily (daytime and nighttime)
Visible: 2.3 km FOV at nadir/twice daily (daytime and nighttime)

Wavelengths:
Infrared: 2378 channels (3.74-4.61 µm, 6.20-8.22 µm, 8.8-15.4 µm)
Visible/Near-Infrared: 4 channels (0.40-0.44 µm, 0.58-0.68 µm, 0.71-0.93 µm, 0.48-0.95 µm)

Product Type: Standard, at-launch

Maximum File Size: 75 MB (total size of 4 files)

File Frequency: 240/day for each of 4 files

Primary Data Format: HDF-EOS

Browse Available: No

Additional Product Information:
http://www-airs.jpl.nasa.gov/

DAAC: NASA Goddard Space Flight Center

Science Team Contact:
H. H. Aumann

AIRS Level 1B Calibrated, Geolocated Radiances (AIR 02)

Product Description

This Level 1B data set contains calibrated and geolocated radiances for 2378 infrared channels and 4 visible/near-infrared channels, along with engineering, calibration, and spacecraft ancillary data. The units of radiance for infrared channels are mW/(m^2 cm sr). The units of radiance for visible/near-infrared channels are W/(m^2 μm sr).

Infrared and visible/near-infrared observations are made during both the day and the night portions of the orbits.

This product includes all AIRS IR and visible/near-infrared data in radiance units from all channels and all detector views (Earth, space, and calibrated-source views). Included also are engineering and spacecraft ancillary data, quality flags, error estimates, and calibration coefficients.

AIRS Level 1B Calibrated, Geolocated Radiances Summary

Coverage: Global

Spatial/Temporal Characteristics:
Infrared: 13.5 km FOV at nadir/twice daily (daytime and nighttime)
Visible: 2.3 km FOV at nadir/twice daily (daytime and nighttime)

Wavelengths:
Infrared: 2378 channels (3.74-4.61 µm, 6.20-8.22 µm, 8.8-15.4 µm)
Visible/Near-Infrared: 4 channels (0.40-0.44 µm, 0.58-0.68 µm, 0.71-0.93 µm, 0.48-0.95 µm)

Product Type: Standard, at-launch

Maximum File Size: 147 MB (total size of 2 files)

File Frequency: 240/day for each of 2 files

Primary Data Format: HDF-EOS

Browse Available: Yes

Additional Product Information:
http://www-airs.jpl.nasa.gov/

DAAC: NASA Goddard Space Flight Center

Science Team Contact:
H. H. Aumann

AIRS/AMSU-A/HSB Level 2 Cloud-Cleared Radiances (AIR 09)

Product Description

The Cloud-Cleared Radiance product is included in the Level 2 retrieval data granules and is geolocated to an AMSU-A footprint.

This Level 2 data set contains calibrated and geolocated radiances for 2378 infrared channels. The units of radiance are mW/(m^2 cm sr).

This product includes all AIRS infrared data in radiance units from all channels. The cloud-cleared radiances from Earth views are the radiances that would have been observed by the IR detectors if there were no clouds in the field of view.

AIRS/AMSU-A/HSB Level 2 Cloud-Cleared Radiances Summary

Coverage: Global

Spatial/Temporal Characteristics:
40.6-km FOV at nadir/
twice daily (daytime and nighttime)

Wavelengths:
Infrared: 2378 channels within
3.74-4.61 µm, 6.20-8.22 µm,
and 8.8-15.4 µm

Product Type: Standard, at-launch

Maximum File Size: 14 MB

File Frequency: 240/day

Primary Data Format: HDF-EOS

Browse Available: Yes

Additional Product Information:
http://www-airs.jpl.nasa.gov/

DAAC: NASA Goddard Space Flight Center

Science Team Contacts:
H. H. Aumann
J. Susskind

AMSR-E Level 2A Brightness Temperatures

Product Description

Due to diffraction, radiometers of differing frequencies using a common antenna do not generally produce equivalent gain patterns on the Earth's surface. Consequently, direct comparison of such observations is complicated by the fact that the measurements do not describe identical locations. The Level 2A algorithm will alleviate this problem by producing several spatially consistent data sets of brightness temperatures, corresponding to the footprint sizes of the 6.9, 10.7, 18.7, 23.8, 36.5, and 89-GHz observations. These six sets of antenna patterns are referred to as resolutions 1 through 6 of the Level 2A data set, corresponding to footprint sizes of approximately 56, 38, 21, 24, 12, and 5 km, respectively. Observations will be produced at spatial intervals of approximately 10 km, except at 89 GHz, for which the spatial interval is 5 km. The Level 2A product will serve as input for all AMSR-E standard Level 2 algorithms.

Research and Applications

The resampling that is done during Level 2A processing is a logical first step for most types of geophysical retrievals. Bringing the AMSR-E observations to a common spatial resolution will improve the retrieval accuracy for those algorithms requiring multi-spectral observations.

Data Set Evolution

For previous microwave radiometers such as SSM/I, individual investigators employed various resampling schemes in order to do geophysical retrievals (see Suggested Reading). For AMSR-E, we will be providing the resampled brightness temperatures as a standard data product.

Suggested Reading

Farrar, M. R., and E. A. Smith, 1992.

Farrar, M. R. *et al.*, 1994.

Poe, G. A., 1990.

Robinson, W. D. *et al.*, 1992.

Stogryn, A., 1978.

(AMSR-E Level 2A Brightness Temperatures, continued)

AMSR-E Level 2A Brightness Temperatures Summary

Coverage: Global

Spatial/Temporal Characteristics: Swath pixels at resolutions from 5 to 56 km

Key Science Applications: Input to all AMSR-E standard Level 2 algorithms

Key Geophysical Parameters: Brightness temperatures at common resolutions

Processing Level: 2

Product Type: Standard, at-launch

Maximum File Size: 86 MB

File Frequency: 29/day

Primary Data Format: HDF-EOS

Browse Available: Accompanies data product

Additional Product Information:
http://wwwghcc.msfc.nasa.gov/AMSR/html/amsr_products.html

DAAC: National Snow and Ice Data Center

Science Team Contacts:
F. J. Wentz
P. Ashcroft

AMSU-A Level 1A Radiance Counts (AMS 01)

Product Description

This Level 1A data set contains geolocated counts for 15 microwave channels, along with engineering and spacecraft ancillary data.

The Level 1A data are used as input for calibration and processing. Quality indicators are added to the data to indicate instrument mode and missing or otherwise bad data.

Microwave observations are made during both the day and the night portions of the orbits.

This product includes all AMSU-A microwave data in counts from all channels and all detector views (Earth and space views). Included also are engineering data in engineering units, spacecraft ancillary data, and geolocation data.

AMSU-A Level 1A Radiance Counts Summary

Coverage: Global

Spatial/Temporal Characteristics:
40.6-km FOV at nadir/twice daily (daytime and nighttime)

Center Frequencies (MHz):
23800, 31400, 50300, 52800, 53596±115, 54400, 54940, 55500, 57290.344, 57290.344±217, 57290.344±322.4±48, 57290.344±322.4±22, 57290.344±322.4±10, 57290.344±322.4±4.5, 89000

Processing Level: 1A

Product Type: Standard, at-launch

Maximum File Size: 1 MB

File Frequency: 240/day

Primary Data Format: HDF-EOS

Additional Product Information:
http://orbit-net.nesdis.noaa.gov/crad/st/amsuclimate/index.html

DAAC: NASA Goddard Space Flight Center

Science Team Contact:
H. H. Aumann

AMSU-A Level 1B Calibrated, Geolocated Radiances (AMS 02)

Product Description

This Level 1B data set contains calibrated and geolocated radiances for 15 microwave channels, along with engineering, calibration, and spacecraft ancillary data. The radiances are expressed as brightness temperatures in K. Accuracy of radiances varies from channel to channel and is expected to be approximately ±1.5 K absolute and ±0.5 K relative.

Microwave observations are made during both the day and the night portions of the orbits.

This product includes all AMSU-A microwave data in counts from all channels and all detector views (Earth, space, and calibrated-source views). Included also are engineering and spacecraft ancillary data, quality flags, error estimates, and calibration coefficients.

AMSU-A Level 1B Calibrated, Geolocated Radiances Summary

Coverage: Global

Spatial/Temporal Characteristics:
40.6-km FOV at nadir/twice daily (daytime and nighttime)

Center Frequencies (MHz):
23800, 31400, 50300, 52800, 53596±115, 54400, 54940, 55500, 57290.344, 57290.344±217, 57290.344±322.4±48, 57290.344±322.4±22, 57290.344±322.4±10, 57290.344±322.4±4.5, 89000

Processing Level: 1B

Product Type: Standard, at-launch

Maximum File Size: 1 MB

File Frequency: 240/day

Primary Data Format: HDF-EOS

Browse Available: Daily global browse images

Additional Product Information:
http://orbit-net.nesdis.noaa.gov/crad/st/amsuclimate/index.html

DAAC: NASA Goddard Space Flight Center

Science Team Contact:
H. H. Aumann

CERES Bi-Directional Scans Product (BDS)

Product Description

The Bi-Directional Scans (BDS) Product contains 24 hours of instantaneous Level 1B Clouds and the Earth's Radiant Energy System (CERES) data for a single scanner instrument. The BDS contains instantaneous radiance measurements recorded every 0.01 second for views of space, internal calibration, solar calibration, and Earth. It contains all elevation scan modes, which include the normal Earth scan and the short Earth scan modes and both the fixed and rotating azimuth-plane scan modes. The BDS also contains Level 0 raw (unconverted) science and instrument data as well as the geolocation of the radiance measurements. The BDS product contains additional data not found in the Level 0 input file, including converted satellite position and velocity data, celestial data, converted digital status data, and parameters used in the equations for radiance count conversions.

A complete listing of parameters for this data product can be found in the CERES Data Products Catalog at http://asd-www.larc.nasa.gov/DPC/DPC.html, and detailed definitions of each parameter can be found in the CERES Collection Guide at http://asd-www.larc.nasa.gov/ceres/collect_guide/list.html.

Research and Applications

These radiance data products are the primary inputs to all the CERES product algorithms. The spacecraft ephemeris and sensor telemetry are inputs to this subsystem, which uses instrument calibration coefficients to convert the spacecraft telemetry inputs into geolocated filtered radiances and housekeeping data into engineering units.

Data Set Evolution

The BDS product algorithm operates on the Level 0 reformatted raw sensor counts and produces calibrated radiances in the three channels. The steps in the processing are: 1) Convert the raw housekeeping telemetry into engineering units; 2) calculate the geographical location of the CERES footprints; 3) revise the radiometric detector count conversion coefficients when required; 4) convert the radiometric detector signals into filtered radiances; and 5) archive the BDS standard products.

Documentation on the BDS algorithms can be found in the CERES ATBD for Subsystem 1.0, in PDF format, at http://eospso.gsfc.nasa.gov/atbd/cerestables.html.

Suggested Reading

Hoffman, L. H. *et al*., 1987.

Jarecke, P. J. *et al*., 1991.

Lee III, R. B. *et al*., 1996.

Priestley, K. J. *et al*., 2000.

Smith, G. L. *et al*., 1986.

Wielicki, B. A. *et al*., 1998.

CERES Bi-Directional Scans Product Summary

Coverage: Global

Spatial/Temporal Characteristics: 20 km at nadir/0.01 second

Key Geophysical Parameters: Filtered total, shortwave, and window radiances, geolocation data

Processing Level: 0, 1

Product Type: Standard, at-launch

Maximum File Size: 900 MB

File Frequency: 1/day

Primary Data Format: HDF

Browse Available: No

Additional Product Information: http://eosweb.larc.nasa.gov/PRODOCS/ceres/table_ceres.html

DAAC: NASA Langley Research Center

Science Team Contacts:
R. B. Lee
K. J. Priestley

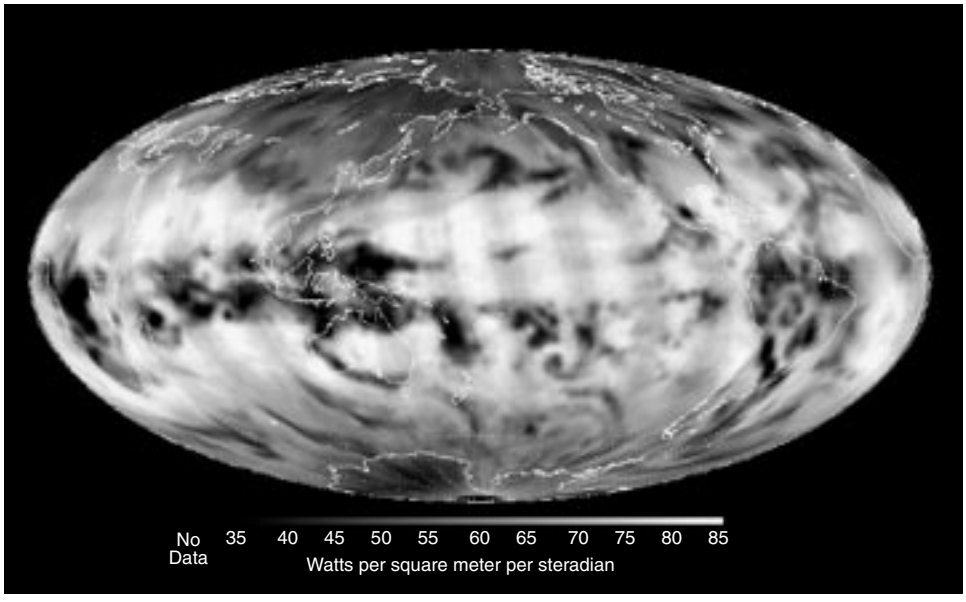

Bi-Directional Scans Product: Nighttime total channel radiance measurements taken from the CERES instrument on Terra on February 28, 2000.

HSB Level 1A Radiance Counts (HSB 01)

Product Description

This Level 1A data set contains geolocated counts for 4 microwave channels, along with engineering and spacecraft ancillary data.

The Level 1A data are used as input for calibration and processing. Quality indicators are added to the data to indicate instrument mode and missing or otherwise bad data.

Microwave observations are made during both the day and the night portions of the orbits.

This product includes all HSB microwave data in counts from all channels and all detector views (Earth and space views). Included also are engineering data, in engineering units, spacecraft ancillary data, and geolocation data.

HSB Level 1A Radiance Counts Summary

Coverage: Global

Spatial/Temporal Characteristics:
13.5-km FOV at nadir/
twice daily (daytime and nighttime)

Center Frequencies (MHz):
150000, 183310±1000, 183310±3000, 183310±7000

Processing Level: 1A

Product Type: Standard, at-launch

Maximum File Size: 1 MB

File Frequency: 240/day

Primary Data Format: HDF-EOS

Additional Product Information:
http://www.dss.inpe.br/programas/hsb/ingl/Produto/Default.htm

Science Team Contact:
H. H. Aumann

HSB Level 1B Calibrated, Geolocated Radiances (HSB 02)

Product Description

This Level 1B data set contains calibrated and geolocated radiances for 4 microwave channels, along with engineering, calibration, and spacecraft ancillary data. The radiances are expressed as brightness temperatures in K. Accuracy of radiances varies from channel to channel and is expected to be approximately ±1.0 K absolute and ±0.6 K relative.

Microwave observations are made during both the day and the night portions of the orbits.

This product includes all HSB microwave data in counts from all channels and all detector views (Earth, space, and calibrated-source views). Included also are engineering and spacecraft ancillary data, quality flags, error estimates, and calibration coefficients.

HSB Level 1B Calibrated, Geolocated Radiances Summary

Coverage: Global

Spatial/Temporal Characteristics:
13.5-km FOV at nadir/
twice daily (daytime and nighttime)

Center Frequencies (MHz):
150000, 183310±1000, 183310±3000, 183310±7000

Processing Level: 1B

Product Type: Standard, at-launch

Maximum File Size: 2 MB

File Frequency: 240/day

Primary Data Format: HDF-EOS

Browse Available: Daily global browse images

Additional Product Information:
http://www.dss.inpe.br/programas/hsb/ingl/Produto/Default.htm

Science Team Contact:
H. H. Aumann

MODIS Level 1A Radiance Counts (MOD 01)

Product Description

This Level 1A data set contains counts for 36 MODIS channels, along with raw instrument engineering and spacecraft ancillary data. The Level-1A data are used as input for geolocation, calibration, and processing. Quality indicators are added to the data to indicate missing or bad pixels and instrument modes. Visible, SWIR, and NIR measurements are made during daytime only, while radiances for TIR are measured during both the day and the night portions of the orbit. This product includes all MODIS data in digitized (counts) form for all bands, all spatial resolutions, all time tags (converted), all detector views (Earth, solar diffuser, spectroradiometric calibration assembly, black body, and space view), and all engineering and ancillary data.

MODIS Level 1A Radiance Counts Summary

Coverage: Global

Spatial/Temporal Characteristics: 0.25, 0.5, and 1 km resolutions/ daily (daytime and nighttime)

Wavelengths: 20 channels 0.4-3.0 µm, 16 channels 3-15 µm

Processing Level: 1A

Product Type: Standard, at-launch

Maximum File Size: 534 MB

File Frequency: 288/day

Primary Data Format: HDF-EOS

Additional Product Information: http://daac.gsfc.nasa.gov/CAMPAIGN_DOCS/MODIS/rad_geo_products.html

DAAC: NASA Goddard Space Flight Center

Science Team Contact: V.V. Salomonson

MODIS Level 1B Calibrated, Geolocated Radiances (MOD 02)

Product Description

The Level 1B data set contains calibrated and geolocated at-aperture radiances for 36 bands generated from MODIS Level 1A sensor counts (MOD 01). The radiances are in $W/(m^2 \mu m\, sr)$. In addition, Earth BRDF may be determined for the solar reflective bands (1-19, 26) through knowledge of the solar irradiance (e.g., determined from MODIS solar-diffuser data, and from the target-illumination geometry). Additional data are provided, including quality flags, error estimates, and calibration data.

Visible, SWIR, and NIR measurements are made during daytime only, while radiances for TIR are measured continuously. Only Channels 1 and 2 have 250-m resolution, Channels 3-7 have 500-m resolution, and the rest have 1-km resolution.

MODIS Level 1B Calibrated, Geolocated Radiances Summary

Coverage: Global

Spatial/Temporal Characteristics: 0.25, 0.5, and 1 km resolutions/daily (daytime and nighttime)

Wavelengths: 20 channels 0.4-3.0 µm, 16 channels 3-15 µm

Processing Level: 1B

Product Type: Standard, at-launch

Maximum File Size: 345 MB (1 km), 276 MB (500 m), 287 MB (250 m)

File Frequency: 288/day (1 km), 144/day (500 m), 144/day (250 m)

Primary Data Format: HDF-EOS

Additional Product Information: http://daac.gsfc.nasa.gov/CAMPAIGN_DOCS/MODIS/rad_geo_products.html

DAAC: NASA Goddard Space Flight Center

Science Team Contact: B.W. Guenther

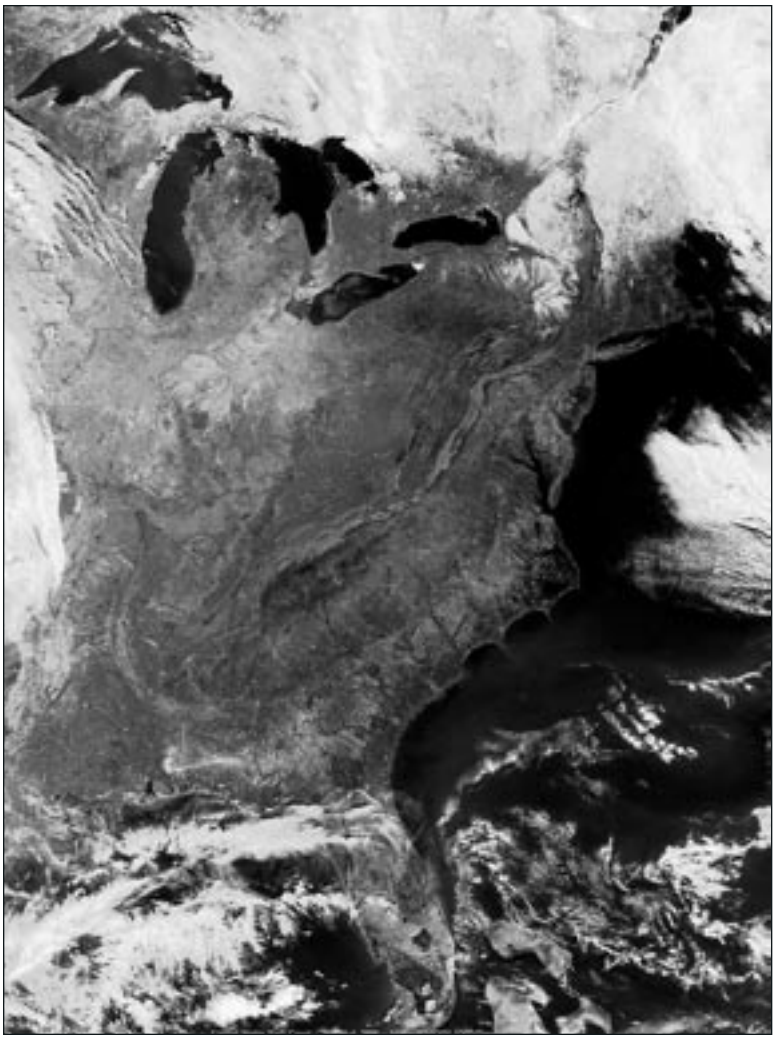

View of eastern North America on March 6, 2000, obtained from data of the MODIS instrument on Terra.

MODIS Geolocation Data Set (MOD 03)

Product Description

The MODIS Geolocation product contains geodetic coordinates, ground elevation, and solar and satellite zenith, and azimuth angle for each MODIS 1-km sample. These data are provided as a 'companion' data set to the Level 1B calibrated radiances and the Level 2 data sets to enable further processing. These geolocation fields are determined using the spacecraft attitude and orbit, instrument telemetry, and a digital elevation model.

MODIS Geolocation Data Set Summary

Coverage: Global

Spatial/Temporal Characteristics:
1 km resolution/daily (daytime and nighttime)

Wavelengths: n/a

Processing Level: 1B

Product Type: Standard, at-launch

Maximum File Size: 60 MB

File Frequency: 288/day

Primary Data Format: HDF-EOS

Additional Product Information:
http://daac.gsfc.nasa.gov/CAMPAIGN_DOCS/MODIS/rad_geo_products.html

DAAC: NASA Goddard Space Flight Center

Science Team Contacts:
V.V. Salomonson
E. J. Masuoka

MODIS Normalized Water-Leaving Radiance (MOD 18) and Aerosol Optical Depth (MOD 37)

Product Description

This Level 2 and Level 3 product contains ocean water-leaving radiances for 7 of the 36 wavelengths/spectral bands (Bands 8 through 14, 412 through 681 nm) of MODIS. These are the "ocean" bands; the water-leaving radiances in these bands are used to derive nearly all of the MODIS ocean products. In addition, another key parameter generated by the algorithm is provided as product MOD 37: Aerosol Optical Depth. The Level 2 product is provided daily at 1-km resolution for cloud-free pixels, while the Level 3 product is provided daily, 8-day weekly, monthly, and yearly. The product constraints are that only cloud-free pixels are used (with Sun glitter below a threshold), and all valid pixels are outside a distance threshold from land. The product availability is at-launch.

Research and Applications

Normalized Water-Leaving Radiance is the radiance that would exit the ocean in the absence of the atmosphere, if the Sun were at the zenith. It is used in the bio-optical algorithms to estimate chlorophyll a concentration and ocean primary productivity on a global scale. The algorithm evolved from experience from the CZCS experiment, which proved the feasibility of measuring ocean color from space. Extensive testing of the algorithm is being conducted using SeaWiFS imagery and will be continued using the Terra and Aqua MODIS instruments. This is the fundamental product for recovering most of the MODIS ocean products.

Data Set Evolution

Inputs to the algorithm are the Level 1 radiances in Bands 8-14, screened for clouds and land, and estimates of the surface wind speed, atmospheric pressure, and ozone concentration derived from National Centers for Environmental Prediction (NCEP, formerly the NMC) products. The success of the algorithm depends on the accurate characterization of the atmospheric effect, which for water typically constitutes 90 percent of the at-satellite radiance. The algorithm includes single scattering, multiple

scattering effects, and whitecap removal, and uses six types of ancillary data. There are three major sources of uncertainty in the product: 1) The candidate aerosol models chosen to describe the aerosol may be unrepresentative of the natural aerosol, 2) there is uncertainty in the estimate of the whitecap reflectance/radiance, and 3) there is uncertainty in the sensor's radiometric calibration. Efforts to reduce these uncertainties include development of improved aerosol models, direct measurements of the properties of oceanic whitecaps, and utilization of the Marine Optical Buoy (MOBY) calibration site to improve radiometric calibration. The product will be validated by comparing simultaneous surface-based measurements (including drifting-buoy radiometers) and MODIS-derived values at a set of locations.

Suggested Reading

Chomko, R., and H. R. Gordon, 1998.

Deschamps, P. Y. *et al*., 1983.

Evans, R. H., and H. R. Gordon, 1994.

Gordon, H. R., 1997.

Gordon, H. R., and D. K. Clark, 1981.

Gordon, H. R., and A. Y. Morel, 1983.

Gordon, H. R., and M. Wang, 1994.

Gordon, H. R. *et al*., 1997.

MODIS Normalized Water-Leaving Radiance and Aerosol Optical Depth Product Summary

Coverage: Global ocean surface, clear-sky only

Spatial/Temporal Characteristics: 1 km/daily (Level 2), 4.6 km, 36 km, 1°/daily, 8-day, monthly, yearly (Level 3)

Key Science Applications: Ocean chlorophyll, ocean productivity

Key Geophysical Parameters: Water-leaving radiances in the ocean bands, aerosol optical depth

Processing Level: 2, 3

Product Type: Standard, at-launch

Maximum File Size: 88 MB (Level 2); 640 MB binned, 134 MB mapped (Level 3)

File Frequency: 144/day (Daily Level 2); 7/day (Daily Level 3), 7/8-day (8-day Level 3),7/month (Monthly Level 3), 7/year (Yearly Level 3)

Primary Data Format: HDF-EOS

Additional Product Information: http://modis-ocean.gsfc.nasa.gov/dataprod.html

DAAC: NASA Goddard Space Flight Center

Science Team Contact: H. R. Gordon

MODIS Photosynthetically Active Radiation (PAR-MOD 22)

Product Description

This Level 2 and 3 product consists of four related parameters which describe the irradiance at the ocean surface. The first is Downwelling Solar Irradiance, which is the incident irradiance just above the sea surface in each of the visible MODIS ocean bands (8, 9, 10, 11, 12, 13, 14). The second is Instantaneous Photosynthetically Active Radiation (IPAR), which is the total downwelling flux of photons just below the sea surface at the instant MODIS views the pixel, integrated over the wavelength range of 400-to-700 nm. The third is PAR, which is the irradiance averaged over an entire day. Since measurements are only available at the time MODIS views the pixel, this parameter is estimated from IPAR by the algorithm. The product is produced at 1 km daily for Level 2 and gridded at 4.6 km, 36 km, and 1° daily, 8-day weekly, monthly, and yearly for Level 3. The fourth is ARP (Absorbed Radiation by Phytoplankton) averaged over the first optical depth. This parameter is critical for calculation of fluorescence efficiency, a product useful for conditioning phytosynthesis models (MOD 23).

Research and Applications

This product is critical for determining photosynthetic rate of growth of phytoplankton and primary ocean production. Downwelling irradiance is needed as an input to the chlorophyll *a* algorithm (MOD 21), and it is used to convert the normalized water-leaving radiance values (MOD 18) into remote sensing reflectance values. A series of irradiance models specific for terrigenous aerosols have been available; however, the aerosol characteristics of these models differ greatly in size and optical characteristics from marine aerosols. The irradiance model of Gregg and Carder (1990) uses a mixture of marine and terrigenous aerosols and forms the basis for the algorithm for the MODIS PAR product.

Data Set Evolution

Product generation begins with solar-irradiance data at 1-nm resolution taken from the revised Neckel and Labs data and corrected for Earth-Sun distance for the current day. Atmospheric correction is made for the effects of scattering, absorption by ozone, absorption by gas, and water vapor. This spectrum is then binned and weighted appropriately to give the irradiance in each of the MODIS ocean bands. Next, the below-surface values are computed and summed to give IPAR. Inputs to the algorithm are Water-Leaving Radiance (MOD 18), PAR (MOD 22) and Absorption Coefficients (MOD 36).

Suggested Reading

Gordon, H. R., and M. Wang, 1994.

Gregg, W. W., and K. L. Carder, 1990.

Iqbal, M., 1983.

Paltridge, G. W., and C. M. R. Platt, 1976.

MODIS Photosynthetically Active Radiation Summary

Coverage: Global ocean surface, clear-sky only

Spatial/Temporal Characteristics: 1 km/daily (Level 2); 4.6 km, 36 km, 1°/daily, 8-day, monthly, yearly (Level 3)

Key Science Applications: Ocean chlorophyll, productivity

Key Geophysical Parameters: Photosynthetically available irradiance

Processing Level: 2, 3

Product Type: Validation, at-launch

Maximum File Size: 83 MB (Level 2); 640 MB binned, 134 MB mapped (Level 3)

File Frequency: 144/day (Daily Level 2); 2/day (Daily Level 3), 2/8-day (8-day Level 3), 2/month (Monthly Level 3), 2/year (Yearly Level 3)

Primary Data Format: HDF-EOS

Browse Available: 36 km sample imagery available at the Goddard DAAC (Level 3 only)

Additional Product Information: http://modis-ocean.gsfc.nasa.gov/dataprod.html

DAAC: NASA Goddard Space Flight Center

Science Team Contacts:
K. Carder
W. Esaias
M. Abbott

MODIS Processing Framework and Match-up Database (MOD 32)

Product Description

This Level 2 product consists of the calibration data set to be used in the generation of all the MODIS Oceans products. It consists of a database which contains *in situ* observations of ocean parameters matched with satellite measurement data. This match-up database will initially be populated with existing ocean-surface data matched temporally and spatially with CZCS and AVHRR data and with SeaWiFS data as they are obtained and then MODIS data post-launch. The product includes the definition of the processing framework in which all the MODIS ocean-product algorithms will operate. It is produced daily and supports ocean products at 1 km, but the product itself does not have a spatial resolution.

Research and Applications

This is a calibration product for MODIS ocean processing. It is used through a vicarious calibration scheme to update MODIS radiometric calibration coefficients, which directly relate MODIS Level 1A raw counts to Level 2 calibrated water-leaving radiances, and to monitor long-term performance of the MODIS instrument. MOD 32, as a match-up database, is also used to validate derived ocean geophysical parameters such as SST and for quality control of the ocean-team retrievals.

Data Set Evolution

Heritage programs provide the basis for MODIS algorithms. A program developed for the Pathfinder ocean SST product forms the framework for analyzing AVHRR-derived SST, algorithm development and validation, and application of the match-up database. Development for ocean-color algorithms is based on experience gained in the transition from CZCS to SeaWiFS algorithms. Development of the SeaWiFS program involves integration of algorithms generated by H. Gordon (atmospheric correction) and K. Carder (chlorophyll). In addition, daily validity tests are being developed through collaboration of the SeaWiFS cal/val team and our group. The *in situ* records are first temporally matched against the

(MODIS Processing Framework and Match-up Database, continued)

AVHRR extractions. AVHRR data for the match-up database were extracted for 3 × 3 pixel boxes centered at each *in situ* sea-surface-temperature-measurement location. Sea-surface observations are from two main types of platforms: moored buoys and drifting buoys. After the SeaWiFS and Pathfinder programs are validated using actual sensor data, they will be converted from a scalar to a parallel implementation and coded using the FORTRAN 90 language and EOS coding standards. Code for the MODIS algorithms initially will be based on SeaWiFS and Pathfinder programs. These implementations will evolve to support product production for the MODIS ocean investigators and will be coded using a combination of the C and FORTRAN 90 programming languages and EOS coding standards.

Suggested Reading

Evans, R. H., and H. R. Gordon, 1994.

Gordon, H. R., 1987.

Gordon, H. R., and A. Y. Morel, 1983.

Slater, P. N. *et al.*, 1987.

Smith, R. C., and W. H. Wilson, 1981.

MODIS Processing Framework and Match-up Database Summary

Coverage: Global ocean surface

Spatial/Temporal Characteristics: 1 km/daily

Key Science Applications: Ocean chlorophyll, ocean productivity, all ocean products

Key Geophysical Parameters: Match-up databases, water-leaving radiances, *in situ* measurements

Processing Level: 2

Product Type: Standard, at-launch

Science Team Contact:
R. H. Evans
H. R. Gordon

MODIS Clear-Water Epsilon (MOD 39)

Product Description

This product provides a single parameter, the ratio of clear-water-leaving radiance at 531 nm to that at 667 nm and is called the clear-water epsilon. This quantity relates directly to the iron content of aerosols over clear waters mostly in the ±35° latitude range. The Level 2 product is produced daily, at 1-km spatial resolution, whereas the Level 3 product is produced daily, 8-day weekly, monthly, and yearly, at 4.6 km, 36 km, and 1° resolution.

Research and Applications

The primary purpose of this algorithm is to estimate aerosol iron content over ocean waters. The aerosol iron influences the validity of other MODIS products. The secondary objective is to flag instances when normalized water-leaving-radiance retrievals may need adjustment due to aerosol absorption at blue and green wavelengths. Such errors will affect chlorophyll *a* calculations. The third objective is to provide a check on the Angstrom exponent derived at red and infrared wavelengths. The algorithm is valid for pigment concentrations up to 2 mg/m^3. When pigment concentrations are larger than this, the algorithm can no longer be applied. A research algorithm is planned post-launch that will use a coupled ocean-atmosphere radiance model to address, interactively, aerosols in high-pigment water.

Data Set Evolution

The algorithm is based on methods developed for obtaining clear-water epsilon values from CZCS data. Modifications for the MODIS algorithm include extension of the clear-water concept to include waters with higher pigment concentrations and modification of the values of the normalized water-leaving radiance at 520, 550, and 670 nm for CZCS to the slightly different MODIS bands by means of the water-absorption curve. Product validation will use SeaWiFS data in the pre-launch period and MODIS data post-launch. Scattering and optical-thickness data plus ship data of water-leaving radiances will be acquired to test the clear-water radiance assumptions. This is an interim validation product which may not be archived.

Suggested Reading

Carder, K. L. *et al*., 1991.

Gordon, H. R., 1978.

Gordon, H. R., and D. K. Clark, 1981.

Gordon, H. R., and A. Y. Morel, 1983.

Gordon, H. R., and M. Wang, 1994.

MODIS Clear-Water Epsilon Summary

Coverage: Global ocean surface, clear-sky only

Spatial/Temporal Characteristics: 1 km/daily (Level 2); 4.6 km, 36 km, 1°/daily, 8-day, monthly, yearly (Level 3)

Key Science Applications: Aerosol iron estimation, water-leaving radiance correction

Key Geophysical Parameters: Clear-water epsilon, aerosol iron content

Processing Level: 2, 3

Product Type: Validation, at-launch

Maximum File Size: 88 MB (Level 2); 865 MB binned, 134 MB mapped (Level 3)

File Frequency: 144/day (Daily Level 2); 36/day (Daily Level 3), 36/8-day (8-day Level 3), 36/month (Monthly Level 3), 36/year (Yearly Level 3)

Primary Data Format: HDF-EOS

Browse Available: 36 km sample imagery available at the Goddard DAAC (Level 3 only)

Additional Product Information: http://modis-ocean.gsfc.nasa.gov/dataprod.html

DAAC: NASA Goddard Space Flight Center

Science Team Contact: K. Carder

ETM+ L70R Raw Digital Numbers

Product Description

This Level 0R data set contains raw digital numbers from the eight channels of the ETM+ instrument. The data are in 8-bit form. Ephemeris profiles and other information required for radiometric correction and geometric rectification accompany the image bands. Descriptive information and data quality metrics are also included in the product metadata.

Data are collected during the day over land. Some nighttime acquisitions are made. The ETM+ is commanded to collect all channels simultaneously. Radiometric calibration is performed using ground testing and in-flight data. The instrument has three onboard calibrators: a partial-aperture solar calibrator, a full-aperture solar calibrator, and an internal- lamp calibrator. Data from the calibrators are ground processed and used to update pre-launch calibration coefficients for bands 1 through 5, 7, and 8. An onboard blackbody source is used to update the calibration of band 6. All parameters required for radiometric and geometric processing are included in the Calibration Parameter File (CPF). The most current CPF accompanies the product.

The ETM+ is similar to other EOS radiance imagers, and data from this instrument may be used for a variety of terrestrial and atmospheric research studies. First, however, the data must be radiometrically corrected. Band 6 radiances can be converted to brightness temperatures for thermal studies.

ETM+ L70R Raw Digital Numbers Summary

Coverage: 233 orbits, each having a 185-km swath width

Spatial/Temporal Characteristics: 30 meter (bands 1-5, 7), 60 meter (band 6), 15 meter (band 8)

Wavelengths: .45-.52, .53-.61, .63-.69, .78-.90, 1.55-1.75, 10.4-12.5, 2.09-2.35, .52-.90 µm

Product Type: Standard, at-launch

Maximum File Size: 450 MB

File Frequency: 250/day

Primary Data Format: HDF-EOS

Secondary Data Format: Fast, GeoTIFF

Browse Available: Yes

Additional Product Information: http://eosdatainfo.gsfc.nasa.gov/eosdata/landsat7/dataproducts.html

DAAC: EROS Data Center

Science Team Contact: D. L. Williams

ETM+ L71R Calibrated Radiances

Product Description

This Level 1R data set contains calibrated radiances in $W/(m^2 \mu m\ sr)$ from the eight channels of the ETM+ instrument. The data are scaled to 16-bit integers. The data can be converted back to radiance units by dividing pixel values by 100. Ephemeris profiles and other information required for geometric rectification accompany the image bands. Descriptive information and data quality metrics are also included in the product metadata.

Data are collected during the day over land. Some nighttime acquisitions are made. The ETM+ is commanded to collect all channels simultaneously. Radiometric calibration is performed using ground testing and in-flight data. The instrument has three onboard calibrators: a partial-aperture solar calibrator, a full-aperture solar calibrator, and an internal lamp calibrator. Data from the calibrators are ground processed and used to update pre-launch calibration coefficients for bands 1 through 5, 7, and 8. An onboard blackbody source is used to update the calibration of band 6. Processing to compensate for undesirable image artifacts is performed, but the data are not geometrically corrected or resampled.

The ETM+ is similar to other EOS radiance imagers, and data from this instrument may be used for a variety of terrestrial and atmospheric research studies. Band 6 radiances can be converted to brightness temperatures for thermal studies.

ETM+ L71R Calibrated Radiances Summary

Coverage: 233 orbits, each having a 185-km swath width

Spatial/Temporal Characteristics: 30 meter (bands 1-5, 7), 60 meter (band 6), 15 meter (band 8)

Wavelengths: .45-.52, .53-.61, .63-.69, .78-.90, 1.55-1.75, 10.4-12.5, 2.09-2.35, .52-.90 µm

Product Type: Standard, at-launch

Maximum File Size: 900 MB

File Frequency: 250/day

Primary Data Format: HDF-EOS

Secondary Data Format: Fast, GeoTIFF

Browse Available: Yes

Additional Product Information: http://eosdatainfo.gsfc.nasa.gov/eosdata/landsat7/dataproducts.html

DAAC: EROS Data Center

Science Team Contact: D. L. Williams

ETM+ L71G Calibrated Radiances

Product Description

This Level 1G data set contains calibrated radiances in $W/(m^2 \mu m\ sr)$ from the eight channels of the ETM+ instrument. The data are scaled to 8-bit integers. The data can be converted back to radiance units by applying radiometric correction coefficients. These are included in the Fast-formatted product. Descriptive information and data-quality metrics are also included in the product metadata.

Data are collected during the day over land. Some nighttime acquisitions are made. The ETM+ is commanded to collect all channels simultaneously. Radiometric calibration is performed using ground testing and in-flight data. The instrument has three onboard calibrators: a partial-aperture solar calibrator, a full-aperture solar calibrator, and an internal- lamp calibrator. Data from the calibrators are ground processed and used to update pre-launch calibration coefficients for bands 1 through 5, 7, and 8. An onboard blackbody source is used to update the calibration of band 6. Processing to compensate for undesirable image artifacts is performed, and the data are geometrically corrected and resampled according to user-specified parameters.

The ETM+ is similar to other EOS radiance imagers, and data from this instrument may be used for a variety of terrestrial and atmospheric research studies. Band 6 radiances can be converted to brightness temperatures for thermal studies.

ETM+ L71G Calibrated Radiances Summary

Coverage: 233 orbits, each having a 185-km swath width

Spatial/Temporal Characteristics: 30 meter (bands 1-5, 7), 60 meter (band 6), 15 meter (band 8)

Wavelengths: .45-.52, .53-.61, .63-.69, .78-.90, 1.55-1.75, 10.4-12.5, 2.09-2.35, .52-.90 µm

Product Type: Standard, at-launch

Maximum File Size: 600 MB

File Frequency: 250/day

Primary Data Format: HDF-EOS

Secondary Data Format: Fast, GeoTIFF

Browse Available: Yes

Additional Product Information: http://eosdatainfo.gsfc.nasa.gov/eosdata/landsat7/dataproducts.html

DAAC: EROS Data Center

Science Team Contact: D. L. Williams

SAGE III Atmospheric Slant-Path Transmission Product (SAGE III 1B)

Product Description

This Level 1B product (SAGE III 1B) consists of atmospheric slant-path transmission profiles at 85 spectral channels in 0.5-km intervals from sea level to 100-km height. The estimated uncertainty for each transmission value is also included. These data have been geolocated and normalized to the exo-atmospheric solar measurements so that independent retrieval can be performed on these data sets to produce Level 2 atmospheric species profiles.

SAGE III Atmospheric Slant-Path Transmission Product Summary

Coverage: 30 solar events per day, 15 northern high latitude, 15 southern high latitude.

Spatial/Temporal Characteristics:
Altitude resolution: 0.5 km vertical

Wavelengths: 290 nm to 1550 nm, 85 wavelengths/30 events per day

Processing Level: 1B

Product Type: Standard, at-launch

Maximum File Size: 0.21 MB

File Frequency: 196/week

Primary Data Format: HDF-EOS, Big Endian IEEE Binary

Browse Available: Yes

Additional Product Information:
http://eosweb.larc.nasa.gov/PRODOCS/sage3/table_sage3.html

DAAC: NASA Langley Research Center

Science Team Contact:
W. P. Chu

Precipitation and Atmospheric Humidity

Aqua
- AIRS
- AMSR-E
- AMSU-A
- HSB
- MODIS

Jason-1
- JMR

Meteor 3M
- SAGE III

Precipitation and Atmospheric Humidity – An Overview

Relationship to Global Change Issues

NASA now recognizes the combined water and energy cycle as one of five key Earth-science disciplines. The latent heat associated with the phase transitions of water is a significant, in some cases the dominant, portion of the energy flux in the atmosphere. Monitoring precipitation and other forms of water is critical to obtaining hydrological-cycle parameterizations needed for developing and improving global climate models and detecting climate change. The processes that generate rainfall are central to the dynamical, biological, and chemical processes in the atmosphere, in the oceans, and on the land surfaces; and space-based measurement is the only practical means to an accurate documentation of global rainfall.

The AMSR-E instrument on Aqua is designed to provide greatly improved measurements of rain rates over both land and ocean compared to current methods at high latitudes and to extend the temporal coverage of the Tropical Rainfall Measuring Mission (TRMM) in the tropics. TRMM has been referred to as a 'flying rain gauge.' Due to the lack of a precipitation radar on the Aqua platform, the rain measurements from Aqua will not provide the same insight as provided by TRMM. The use of physically based algorithms will nonetheless offer the opportunity to take understandings acquired through the combined radar/radiometer system on TRMM and apply them to AMSR-E. The final product thus offers a large contribution to the World Climate Research Programme's (WCRP's) rain climatology initiative.

Microwave measurements are particularly well suited to the measurement of water in all its phases. AMSR-E, in addition to rain rates, will also be used to derive total integrated water vapor, total integrated cloud water, soil moisture, snow cover, and sea ice coverage. The AIRS/AMSU-A/HSB instruments, also on Aqua, will be used to determine the vertical profiles of water vapor and will allow estimation of precipitation rates over land and sea.

From Jason-1, JMR data will be used to obtain columnar water vapor content; and from Meteor 3M, SAGE III data will be used to obtain water-vapor concentration, water-vapor mixing ratios, and relative humidities, as well as total-column water vapor.

This chapter describes the EOS products that support the monitoring of precipitation and atmospheric humidity. Although the majority of global precipitation occurs in the tropics, between latitudes 30°N and 30°S, extratropical precipitation also affects global climate change, the global heat balance, and the global water cycle. To understand and predict large variations in weather and climate, it is critical to understand the coupling between the atmosphere and the underlying oceans, which cover 70% of the Earth's surface.

Precipitation: Atmospheric circulation transports both energy and water, moving heat from the tropics to polar regions. Water, evaporated from the oceans and the land surface, falls as rain or snow, often in places far removed from its point of origin. Rainfall variability is influenced by wind and pressure patterns and storm tracks and in turn influences aspects of the underlying surface, such as sea surface temperature. Fluctuations in rainfall amounts impact climate on both short-term and long-term time scales. In fact, variation in rainfall is considered by some to be the primary means by which climate changes will impact human welfare.

The long-term, time-averaged circulation and precipitation fields show large-scale features associated with the annual evolution of the monsoons, trade-wind systems, and oceanic convergence zones. Large-scale features are also evident on a monthly and seasonal scale. Interannual variability is dominated by tropical Pacific ocean-atmosphere interactions associated with the ENSO cycle, whose major swings occur at irregular intervals of 2-7 years and are associated with pronounced year-to-year precipitation variations over large areas of the Earth. The large-scale spatial coherence and systematic evolution of both interseasonal and interannual tropical precipitation anomalies is of great significance to seasonal climate prediction. They are also important to the development of optimum sampling strategies for estimating accumulated precipitation over periods of a few weeks to a few months.

Humidity: The atmosphere gains water through evaporation from ocean and land areas, transpiration from vegetation, and sublimation from ice and snow. Once in the atmosphere, the water vapor is transported both vertically and horizontally by local and larger-scale atmospheric circulations, thereby being redistributed. In general, there is a net outflow of atmospheric moisture from the tropics, where sea surface temperatures are high and the warm atmosphere can support large amounts of water vapor, to higher latitudes. At all latitudes, condensation occurs when the air becomes saturated and clouds form, after which precipitation returns the water, in the form of rain or snow, to the surface. Current numerical weather prediction models give interesting but inconsistent results about the future distribution of precipitation.

Humidity is a local measure of the amount of water vapor in the atmosphere. Water-vapor concentration depends on temperature, which determines the total amount of water per unit volume that the atmosphere can support without saturation, as well as evaporation. The greater the temperature, the greater is the amount of water vapor that the atmosphere can support, and consequently, in the large-scale, water-vapor amounts decrease from equator to pole and with increasing altitude. Furthermore, water amounts are generally less over the continents than over the oceans, the oceans providing the overwhelmingly larger water source for evaporation. Superimposed on these large-scale patterns are smaller variations of water-vapor amounts that determine locally the formation and properties of clouds and rainfall.

Product Overview

The products included in this chapter are produced by the AMSR-E, AIRS/AMSU-A/HSB, and MODIS instruments on Aqua, the JMR instrument on Jason-1, and the SAGE III instrument on Meteor 3M. The product list includes both instantaneous and time-averaged entries. Among the instantaneous products, land and ocean rainfall are generated separately in the AMSR-E data processing because of the different physics accessible to the retrieval process. The products are generated through a single algorithm that determines the nature of the background and adjusts accordingly in a manner transparent to the data user. The user need only be aware that the background significantly affects the accuracy of the results from AMSR-E. Both the land and ocean components of the algorithm have a long heritage and history of numerous improvements.

The Level 3 AMSR-E product aggregates the instantaneous rainfall retrieval and also generates an independent estimate of the monthly rainfall over the oceans based on a simpler, and presumably more robust, algorithm that makes use of the statistical properties of rainfall. The independent method only works over the ocean; there is no parallel algorithm for the land areas.

The Level 2 AIRS/AMSU-A/HSB precipitation-rate retrievals have 50-km spatial resolution and differ from AMSR-E products in their heavy reliance on opaque atmospheric bands near 54 and 183 GHz, which reduces surface effects and tends to yield comparable accuracies over both land and sea. Humidity profiles will be generated from the AIRS/AMSU-A/HSB data with a global root-mean-square (rms) accuracy of ±10% in 2-km layers from the surface to the 200 mb pressure level.

MODIS products include total precipitable water (MOD 05) and atmospheric water vapor profiles (MOD 07), both processed at Level 2. SAGE III products include water vapor concentration and volume mixing ratios, both with a vertical resolution of 0.5 km and both processed at Level 2.

Product Interdependency and Continuity with Heritage Data

The heritage of the measurement of rainfall with passive-microwave measurements began with the 1972 launch of Nimbus 5 carrying the 19.35-GHz Electrically Scanning Microwave Radiometer (ESMR), which was used for the first retrievals of oceanic rainfall. The launch of the dual-polarized 37-GHz version of ESMR on Nimbus 6 in 1975 enabled early exploration of the mapping, if not measurement, of rain over land. The discovery of the importance of scattering by ice particles from the NASA Convair 990 aircraft in the mid-1970s paved the way for the Special Sensor Microwave/Imager (SSM/I) on the Defense Meteorological Satellite Program (DMSP) satellite, which was first launched in 1987. The SSM/I has been used for the routine production of oceanic rainfall data sets for more than a decade and for extensive research in algorithm development.

The TRMM satellite, which was launched in 1997, carries a microwave radiometer, the TRMM Microwave Imager, or TMI, of very similar capability to AMSR-E as far as rain is concerned. It also carries the first precipitation radar to be flown in space. This combination has enabled detailed examination of the assumptions in the microwave retrieval of rainfall. The non-sun-synchronous orbit of TRMM has additionally enabled the exploration of the impact of the diurnal cycle of rainfall on totals derived from sensors on sun-synchronous spacecraft such as DMSP and Aqua. Level 2 and Level 3 rainfall products have been routinely produced from TRMM. Thus, between DMSP and TRMM we have global coverage of rainfall extending back to 1987.

Heritage data for the MODIS water vapor profiles include the HIRS and TOVS data, while heritage data for the MODIS precipitable water calculations come from the AVIRIS instrument on an ER-2 aircraft, MODIS being the first satellite instrument to use near-IR bands along with IR bands to retrieve total precipitable water. Heritage data for the JMR water vapor products come from the TOPEX/Poseidon Microwave Radiometer; and heritage data for the SAGE III water vapor products come from the earlier SAGE instruments, SAGE I and SAGE II.

Suggested Reading

Chang, A. T. C. *et al*., 1993.

Ferraro, R. R, 1997.

Kummerow, C. *et al*., 1998.

Olson, W. *et al*., 1999.

Rosenkranz, P. W., 1998.

Smith, E. A. *et al*., 1998.

Staelin, D. H., and F. W. Chen, 2000.

AIRS/AMSU-A/HSB Humidity Product (AIR 05)

Product Description

The AIRS Humidity Product (AIR 05) is Level 2 data providing tropospheric column water-vapor profiles, total precipitable water, cloud liquid-water content, precipitation flags, and cloud-ice flags.

A microwave-only retrieval algorithm is first applied to estimate atmospheric temperature and surface temperature and to derive the total precipitable water, cloud liquid-water content, precipitation, and cloud-ice states. A combined microwave and infrared retrieval algorithm is then applied to refine these quantities and to derive the atmospheric column water-vapor profile and burden.

The product is generated daily (day and night) at AMSU-A FOV resolution, with some information at AIRS FOV resolution.

Research and Applications

Water vapor is the most variable, radiatively active constituent of the atmosphere and the main contributor to the greenhouse effect. In addition to being the primary gaseous absorber of both longwave and shortwave radiation, water vapor is also connected to the prediction of cloudiness that controls the Earth's radiation budget. Water vapor in the lower troposphere is the primary determinant of moist convective activities and of convective precipitation under unstable atmospheric conditions. Boundary-layer water vapor is also important for calculation of latent heat flux, which plays a role in the exchange of energy between the Earth's surface and the atmosphere. Existing observational knowledge is insufficient to meet even the simplest requirements of general circulation models (GCMs). High-spectral-resolution observations by AIRS will provide improved accuracy over the entire globe. The AIRS humidity profile will be a significant quantity for data assimilation to improve numerical weather prediction.

Data Set Evolution

The column water-vapor profiles are derived from selected AIRS radiances in the 6.3-μm water-vapor band (in the regions 1234 cm^{-1} to 1612 cm^{-1} and 2606 cm^{-1} to 2657 cm^{-1}) and the 11-μm windows, which are sensitive to the water-vapor continuum. The radiance measured in these channels depends on atmospheric and surface temperature and the distribution of humidity in the atmosphere.

The 6.3-μm channels are more sensitive to humidity in the middle and upper troposphere, while the narrow channels in the 11-μm continuum are more sensitive to humidity in the lower troposphere. Simultaneous determination of surface temperature and spectral emissivity is essential for obtaining an accurate low-level water-vapor distribution.

The total precipitable water, cloud liquid-water content, and precipitation flags are derived from AMSU-A and HSB radiances. The AMSU-A window channels will also be used to provide information on sea ice concentration and snow cover.

The humidity-profile rms error is expected to be ±10% for precipitable water in 2-km layers from the surface to 200 mb. The rms error of total precipitable water is expected to be ±20%.

HSB channels in the 183-GHz water-vapor line are used to improve the accuracy of atmospheric humidity profiles and total precipitable water vapor.

Data validation will be accomplished through comparison of the retrieved water-vapor profiles with simultaneous water-vapor measurements by: 1) ground-based Raman lidar, 2) *in situ* research-quality radiosondes, 3) Lidar Atmospheric Sensing Experiment (LASE) on the NASA DC-8 aircraft, and 4) NPOES Airborne Sounder Testbed-Interferometer (NASTI) on the NASA ER-2 aircraft. Locations will be DoE ARM/CART and other EOS instrument-validation sites.

Suggested Reading

Aumann, H. H., and C. Miller, 1995.

Aumann, H. H. *et al.,* 1999.

Chahine, M. T. *et al.*,1997c.

Fleming, H. F. *et al.*, 1986.

Grody, N. C. *et al.*, 1980.

Haskins, R. D. *et al.*, 1997.

Hofstadter, M. *et al.*, 1999.

Janssen, M. A. 1993.

Kuo, C. C. *et al.,* 1994.

Lambrigtsen, B., 1996.

Rosenkranz, P. W., 1995.

Rosenkranz, P. W., 1998.

Smith, W. L., and H. M. Woolf, 1976.

Susskind, J. *et al.*, 1993.

Susskind, J. *et al*., 1998.

Wilheit, T. T., 1990.

AIRS/AMSU-A/HSB Humidity Product Summary

Coverage: Global

Spatial/Temporal Characteristics: 40.6 km FOV at nadir; 2-km vertical layers, surface to tropopause/twice daily (daytime and nighttime)

Key Science Applications: Global moisture transport; hydrological cycle; climatology

Key Geophysical Parameters: Atmospheric column water-vapor profile and burden; total precipitable water; cloud liquid-water content, precipitation flag; cloud-ice flag

Processing Level: 2

Product Type: Standard, at-launch; precipitation flag is a research product, post-launch

Maximum File Size: 5 MB

File Frequency: 240/day

Primary Data Format: HDF-EOS

Browse Available: Yes

Additional Product Information: http://www-airs.jpl.nasa.gov/

DAAC: NASA Goddard Space Flight Center

Science Team Contacts:
J. Susskind
P.W. Rosenkranz
D. H. Staelin

AMSR-E Rainfall – Level 2

Product Description

This product contains surface rainfall and its classification into convective and stratiform components. This information is obtained by matching the observed brightness temperatures to a database of *a priori* cloud profiles derived from a variety of sources including cloud dynamical models as well as ground-based radars. This *a priori* information is then used in a Bayesian inversion scheme to derive a linear combination of profiles that most resembles the observed brightness temperatures. Despite differences, the Land and Ocean algorithms have been combined into a single framework to insure communication between the algorithm components. The Level 2 product has not been resampled; scan time, latitude, longitude, and scan line/pixel number are included for each pixel in this product.

This product uses the Level 2A AMSR-E brightness temperatures as input. There is also a Level 3 AMSR-E rainfall product, which uses the Level 2 product over land directly for accumulations but uses the Level 2 product over ocean only as a means of independent validation.

Research and Applications

The research objectives of this product include

- Improve the availability of high-quality rainfall products and latent-heat-release estimates over the globe.
- Validate and improve models that promote the understanding of the formation and organization of convection and their interactions with the ocean and ambient atmosphere and the climate system; and
- Advance understanding of the Earth's global energy and water cycles by determining how rainfall and its variability influence global circulation.

Data Set Evolution and Applications

The AMSR-E instantaneous rainfall product is very similar to the TRMM TMI rainfall algorithm. There is also a parallel version of this algorithm running for the DMSP SSM/I sensor. There is a long heritage for

this rainfall algorithm, the physical nature of which makes the transition from these previous sensors to AMSR-E straightforward.

Suggested Reading

Hong, Y. *et al.*, 1999.

Kummerow, C. *et al.,* 1996.

AMSR-E Rainfall – Level 2 Summary

Coverage: 70°N-70°S ice-free and snow-free land and ocean

Spatial/Temporal Characteristics: Satellite orbit track, 5-km resolution

Key Geophysical Parameters: Rainfall, rainfall type (Convective/Stratiform)

Processing Level: 2

Product Type: Standard, at-launch

Maximum File Size: 18 MB

File Frequency: 29/day

Primary Data Format: HDF-EOS

Browse Available: Accompanies data product

Additional Product Information: http://wwwghcc.msfc.nasa.gov/AMSR/html/amsr_products.html

DAAC: National Snow and Ice Data Center

Science Team Contacts:
R. Ferraro (Level 2 Land)
C. Kummerow (Level 2 Ocean)

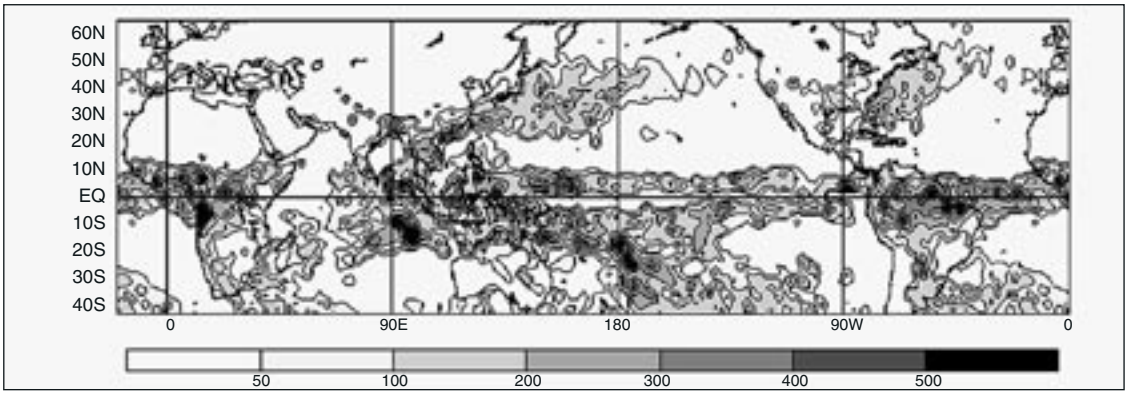

Passive-Microwave Satellite Global Monthly Rainfall Estimates for April 2000, derived from data from the DMSP SSM/I based on a similar algorithm to the algorithm that will be used for Level 2 rainfall estimates from AMSR-E data. This image illustrates the global rainfall patterns that will be produced from AMSR-E. Units are mm/month.

AMSR-E Rainfall – Level 3

Product Description

This product consists of mean monthly rainfall amounts over 5° × 5° cells. Retrievals over ocean are independent of the Level 2 algorithm. Monthly accumulations over land use the Level 2 land product as input. Over oceans, this approach sacrifices some of the accuracy of the instantaneous retrieval in order to minimize assumptions that might contaminate a climate record of rainfall. The frequency of occurrence of rain intensities in different rate categories over a specified area can be plotted as a histogram or as a smoothed curve that fits the histogram. This product is obtained by considering histograms of 19-GHz, 21-GHz, and 19-21 GHz combinations. Monthly rainfall indices are computed by statistically matching the histograms with the model-calculated probability density functions (pdf). The main purpose of this product is to provide a robust baseline of surface-rainfall rates. There is no equivalent independent method for estimating rainfall over land, and the Level 2 product is therefore used as input to the pdf scheme.

This Level 3 rainfall product uses the Level 2A AMSR-E brightness temperatures as well as the AMSR-E Level 2 rainfall product as input. The Level 3 product uses the Level 2A brightness temperatures to estimate rainfall independently over oceans and the Level 2 rainfall product over land to compute monthly accumulations.

Research and Applications

This product is designed to advance understanding of the Earth's global energy and water cycles by determining how rainfall and its variability influence global circulation. A reliable measurement of rainfall, particularly over the oceans, will provide the long-term record needed to distinguish natural variability from any anthropogenic changes.

Data Set Evolution

The AMSR-E instrument is very similar to the TRMM TMI and the DMSP SSM/I. The algorithm over oceans will be a slight modification of the algorithm for the TMI standard product and the WMO Global Precipitation Climatology Project (GPCP) algorithm applied to SSM/I. Data are already available from these algorithms for the period since 1987.

Suggested Reading

Chang, A. T. C. *et al.*, 1999.

Wilheit, T. T. *et al.*, 1991.

AMSR-E Rainfall – Level 3 Summary

Coverage: 70˚N-70˚S

Spatial/Temporal Characteristics: 5˚ × 5˚/ monthly

Key Geophysical Parameters: Rainfall amount and statistics

Processing Level: 3

Product Type: Standard, at-launch

Maximum File Size: 0.016 MB

File Frequency: 1/month

Primary Data Format: HDF-EOS

Browse Available: Accompanies data product

Additional Product Information: http://wwwghcc.msfc.nasa.gov/AMSR/html/amsr_products.html

DAAC: National Snow and Ice Data Center

Science Team Contact: T. T. Wilheit

AMSR-E Columnar Water Vapor

Product Description

The columnar water vapor derived from the AMSR-E microwave radiances is a measure of the total vertically integrated water vapor in the marine atmosphere. It is expressed in units of millimeters, which represent the depth of the column of liquid water that would result if the vapor were to precipitate completely. The spatial resolution of this product is 24 km, and its expected rms accuracy at this resolution is 1.0 mm. This product is available for clear and cloudy conditions and up-to-moderate rain rates. The product will be produced for individual pixels across the AMSR-E swath (Level 2) as well as an Earth-gridded product (0.25° in latitude and longitude) averaged daily, weekly, and monthly (Level 3).

Research and Applications

Column water vapor is a critical component coupling the atmosphere and oceans, transporting energy in the form of latent heat from the ocean surface to the atmosphere, where it is released through condensation. Furthermore, water vapor is the Earth's principal greenhouse gas, trapping sufficient heat to maintain the average surface temperature above freezing, and therefore is responsible for the habitability of the planet. Within the context of global-change studies, the possibility of positive feedback between anthropogenic carbon dioxide and water vapor has become a particularly active research area, largely due to model predictions of significant amplification of greenhouse heat trapping by concomitant rises in atmospheric water vapor. Sensitive and accurate long-term measurements of spatial and temporal variability in this quantity also constitute, along with measurements of air and sea-surface temperature, a valuable geophysical data set for monitoring global change.

Data Set Evolution

The water-vapor retrieval algorithm is based on experience gained from previous microwave radiometers, including SMMR, SSM/I, and TMI. In particular, the SSM/I has demonstrated the ability of microwave radiometers to measure water vapor to an accuracy of about 1 mm. For 35,000 SSM/I overflights of radiosondes (1987-1991), the rms difference between the SSM/I and radiosonde water vapor is 3.9 mm, with most of this difference being due to the spatial-temporal mismatch between the point radiosonde observation and the 25-km SSM/I footprint. Computer simulations show that the true rms accuracy of the microwave water-vapor retrievals is about 1 mm. The AMSR-E retrievals should be more accurate than those from SSM/I because AMSR-E has a dual-polarization water-vapor channel whereas SSM/I only had vertical polarization. Also, the AMSR-E water-vapor signal will not saturate in the tropics because its water-vapor channel is at 23.8 GHz rather than at the center of the water-vapor absorption line (22.235 GHz). (SSM/I operated at 22.235 GHz and experienced partial saturation in the tropics.)

Suggested Reading

Alishouse, J. C. *et al.*, 1990.

Chahine, M. T., 1992.

Chang A. T. C., and T. T. Wilheit, 1979.

Chang, H. D. *et al.*, 1984.

Grody, N. C., 1976.

Liu, W. T. *et al.*, 1992.

Ramanathan, V., 1988.

Staelin, D. H. *et al.*, 1976.

Wentz, F. J., 1997.

(AMSR-E Columnar Water Vapor, continued)

AMSR-E Columnar Water Vapor Summary

Coverage: Global ocean surface, clear and cloudy skies and up-to-moderate rainfall rates

Spatial/Temporal Characteristics:
Level 2: swath pixels at 20-km resolution
Level 3: 0.25° latitude-longitude grid/daily, weekly, and monthly

Key Science Applications: Climate variability, air-sea interaction, radiation balance, hydrological cycle

Key Geophysical Parameters: Columnar water vapor

Processing Level: 2, 3

Product Type: Standard, post-launch

Maximum File Size: 10 MB

File Frequency: 29/day

Primary Data Format: HDF-EOS

Browse Available: Accompanies data product

Additional Product Information:
http://wwwghcc.msfc.nasa.gov/AMSR/html/amsr_products.html

DAAC: National Snow and Ice Data Center

Science Team Contact:
F. J. Wentz

MODIS Total Precipitable Water (MOD 05)

Product Description

The MODIS Precipitable Water product (MOD 05) consists of column water-vapor amounts. During the daytime, a near-infrared algorithm is applied over clear land areas of the globe and above clouds over both land and ocean. Over clear ocean areas, water-vapor estimates are provided over the extended glint area. An infrared algorithm for deriving atmospheric profiles is also applied both day and night for Level 2.

The Level 2 data are generated at the 1-km spatial resolution of the MODIS instrument using the near-infrared algorithm during the day, and at 5 × 5 1-km pixel resolution both day and night using the infrared algorithm when at least nine FOVs are cloud free. The infrared-derived precipitable water vapor is generated as one component of product MOD 07, and simply added to product MOD 05 for convenience.

The solar retrieval algorithm relies on observations of water-vapor attenuation of reflected solar radiation in the near-infrared MODIS channels so that the product is produced only over areas where there is a reflective surface in the near IR.

Research and Applications

The near-infrared total-column precipitable water is very sensitive to boundary-layer water vapor since it is derived from attenuation of reflected solar light from the surface. This data product is essential to understanding the hydrological cycle, aerosol properties, aerosol-cloud interactions, energy budget, and climate. Of particular interest is the collection of water-vapor data above cirrus cloudiness, which has important applications to climate studies. MODIS will also provide finer horizontal-scale atmospheric water-vapor gradient estimates than are currently available from the Polar-orbiting Operational Environmental Satellites (POES).

Data Set Evolution

The solar-column water-vapor parameter is derived from the attenuation by water vapor of near-IR solar radiation. Techniques employing ratios of water-vapor-absorbing channels 17, 18, and 19 with the atmospheric window channels 2 and 5 are used. The ratios remove partially the effects of variation of surface reflectance with wavelength and result in the atmospheric water-vapor transmittances. The column-water-vapor amounts are derived from the

transmittances based on theoretical radiative-transfer calculations and using look-up-table procedures. MODIS is the first space instrument to use near-IR bands together with the traditional IR bands to retrieve total precipitable water. Experience in this retrieval is based on an AVIRIS instrument aboard an ER-2 aircraft. Atmospheric water vapor should be determined with an accuracy of 5-10%.

The thermal column water-vapor parameter is derived by integrating the moisture profile through the atmospheric column. Other, split-window, methods also exist. This class of techniques uses the difference in water-vapor absorption that exists between channel 31 (11 μm) and channel 32 (12 μm).

Data validation will be conducted by comparing these data with water-vapor measurements from the National Weather Service (NWS) radiosonde network, from ground-based upward-looking microwave radiometers, from a ground-based GPS network, and from a ground-based sunphotometer network. Quality control will be performed in two dimensions. The first will be comparisons of specific validation sites across as many different climatic and geographic regions as possible. The second will be a statistical analysis of the entire data set.

The related MODIS Cloud product ATBDs can be found in PDF format at http://eos.nasa.gov/atbd/modistables.html.

Suggested Reading

Gao, B. C., and A. F. H. Goetz, 1990.

Gao, B. C. *et al*., 1993a,b.

Green, R. O., and J. E. Conel, 1995.

Jedlovec, G. J., 1987.

Kaufman, Y. J., and B. C. Gao, 1992.

King, M. D. *et al*., 1992.

Kleepsies, T. J., and L. M. McMillan, 1984.

MODIS Total Precipitable Water Summary

Coverage: Global

Spatial/Temporal Characteristics: Varies with retrieval technique; 1 km near-infrared daylight only, and 5 km infrared day and night

Key Science Applications: Hydrological cycle climatology, effect on aerosol and clouds, atmospheric correction, characterization of the atmosphere

Key Geophysical Parameters: Atmospheric total column water vapor

Processing Level: 2

Product Type: Standard, at-launch

Maximum File Size: 15 MB

File Frequency: 288/day

Primary Data Format: HDF-EOS

Browse Available:
http://modis-atmos.gsfc.nasa.gov/MOD05_L2/sample.html

Additional Product Information:
http://modis-atmos.gsfc.nasa.gov/MOD05_L2/index.html

Science Team Contacts:
B. C. Gao
Y. J. Kaufman
D. Tanré
W. P. Menzel

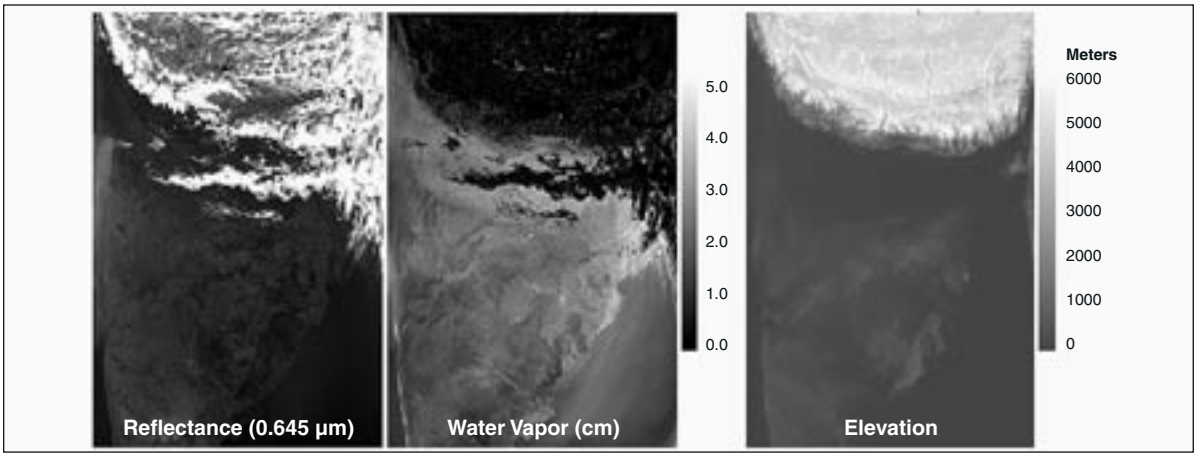

Sample Columnar Atmospheric Water Vapor from Terra MODIS data from the vicinity of Tibet and India on March 2, 2000, at UTC 0525. These results are derived from data from channels located within and around the 0.94-μm water vapor band. The left panel shows an image processed from MODIS channels centered at 0.645 μm. The lower part of the scene covers portions of India and the nearby Indian Ocean. The upper part of the scene covers Nepal and part of the Tibetan Plateau. The middle panel shows the MODIS column water vapor. The right panel shows the corresponding image of surface elevations. It is seen from these images that column water vapor values vary significantly with surface elevation.

MODIS Atmospheric Profiles (MOD 07)

Product Description

The MODIS Atmospheric Profiles product (MOD 07) consists of several parameters: they are total-ozone burden, atmospheric stability, temperature and moisture profiles, and atmospheric water vapor. All of these parameters are produced day and night for Level 2 at 5 × 5 1-km pixel resolution when at least 9 FOVs are cloud free.

The MODIS total-ozone burden is an estimate of the total-column tropospheric and stratospheric ozone content. The MODIS atmospheric stability consists of three daily Level 2 atmospheric stability indices. The Total Totals (TT), the Lifted Index (LI), and the K index (K) are each computed using the infrared temperature- and moisture-profile data, also derived as part of MOD 07. The MODIS temperature and moisture profiles are produced at 20 vertical levels for temperature and 15 levels for moisture. A simultaneous direct physical solution to the infrared radiative-transfer equation in a cloudless sky is used. The MODIS atmospheric water-vapor product is an estimate of the total tropospheric column water vapor made from integrated MODIS infrared retrievals of atmospheric moisture profiles in clear scenes.

Research and Applications

Total-column ozone estimates at MODIS resolution are required by MODIS investigators developing atmospheric correction algorithms. This information is crucial for accurate land and ocean-surface-parameter retrievals. Furthermore, strong correlations have been found to exist between the meridional gradient of total ozone and the wind velocity at tropopause levels, providing the potential to predict the position and intensity of jet streams. Total-column ozone monitoring is also important due to the potential harm to the environment caused by anthropogenic depletion of ozone.

Atmospheric instability measurements are predictors of convective-cloud formation and precipitation. The MODIS instrument offers an opportunity to characterize gradients of atmospheric stability at high resolution and greater coverage. Radiosonde-derived stability indices are limited by the coarse spacing of the point-source data, too large to pinpoint local regions of probable convection.

Atmospheric temperature and moisture sounding data at high spatial resolution from MODIS and high- spectral-resolution sounding data from AIRS will provide a wealth of new information on atmospheric structure in clear skies. The profiles will be used to correct for atmospheric effects for some of the MODIS products (e.g., sea-surface and land-surface temperatures, ocean aerosol properties, water-leaving radiances, and PAR) as well as to characterize the atmosphere for global greenhouse studies.

Total-column precipitable-water estimates at MODIS resolution are required by MODIS investigators developing atmospheric-correction algorithms. This information is crucial for accurate land and ocean surface-parameter retrievals. MODIS will also provide finer horizontal-scale atmospheric water-vapor gradient estimates than are currently available from the POES satellites.

Data Set Evolution

One of two ozone-retrieval methods developed using the HIRS will be chosen as best suited for application with MODIS data. Both use a first-guess perturbation method and radiances from MODIS channel 30 (9.6 μm) to solve the radiative-transfer equation. The perturbations are with respect to some *a priori* conditions that may be estimated from climatology, regression, or, more commonly, from an analysis or forecast provided by a numerical model. The MODIS cloud-mask product (MOD 35) will also be used to screen for clouds.

Atmospheric-stability estimates will be derived from the MODIS temperature and moisture retrievals contained in this product. Layer temperature and moisture values may be used to estimate the temperature lapse rate of the lower troposphere and the low-level moisture concentration.

Temperature and moisture profile retrieval algorithms are adapted from the International TOVS Processing Package (ITPP), taking into account MODIS' lack of stratospheric channels and far higher horizontal resolution. The profile retrieval algorithm requires calibrated, navigated, and coregistered 1-km FOV radiances from MODIS channels 20, 22-25, 27-29, and 30-36. The MODIS cloud mask (MOD 35) is used for cloud screening. The algorithm also requires NCEP model analyses of temperature and moisture profiles as a first guess and an NCEP analysis of surface temperature and pressure.

Several algorithms for determining atmospheric water vapor, or precipitable water, exist. It is most directly achieved by integrating the moisture profile through the atmospheric column. Other, split-window, methods also exist. This class of techniques

uses the difference in water-vapor absorption that exists between channel 31 (11 μm) and channel 32 (12 μm).

Data validation will be conducted by comparing results to *in situ* radiosonde measurements, NOAA HIRS operational retrievals, GOES sounder operational retrievals, NCEP analyses, and retrievals from the AIRS/AMSU-A/HSB instrument package on the Aqua platform. A field campaign using a profiler network in the central U.S. and an aircraft equipped with the MODIS Airborne Simulator (MAS) will be initiated in the first year after launch. Quality control will consist of manual and automatic inspections, with regional and global mean temperatures at 300, 500, and 700 hPa monitored weekly, along with 700 hPa dew-point temperatures. For total ozone, data validation will consist of comparing the TOMS retrievals, as well as operational NOAA ozone estimates from HIRS, to the MODIS retrievals.

Suggested Reading

Hayden, C. M., 1988.

Houghton, J. T. *et al.*, 1984.

Jedlovec, G. J., 1987.

Kleepsies, T. J., and L. M. McMillan, 1984.

Ma, X. L. *et al.*, 1984.

Prabhakara, C. *et al.*, 1970.

Shapiro, M. A. *et al.*, 1982.

Smith, W. L., and F. X. Zhou, 1982.

Smith, W. L. *et al.*, 1985.

Sullivan, J. *et al.*, 1993.

MODIS Atmospheric Profiles Summary

Coverage: Global, clear-sky only

Spatial/Temporal Characteristics: 5 km

Key Science Applications:

- Ozone: atmospheric correction, prediction of cyclogenesis, anthropogenic ozone depletion
- Atmospheric stability: atmospheric correction, prediction of convective cloudiness and precipitation, characterization of the atmosphere
- Soundings: atmospheric correction algorithm development and use, characterization of the atmosphere
- Total-column water vapor: atmospheric-correction algorithm development and use, characterization of the atmosphere

Key Geophysical Parameters: Total-column ozone, atmospheric stability (Total Totals, Lifted Index, and K index), atmospheric profiles of temperature and moisture, atmospheric total-column water vapor

Processing Level: 2

Product Type: Standard, at-launch

Maximum File Size: 28 MB

File Frequency: 288/day

Primary Data Format: HDF-EOS

Browse Available:
http://modis-atmos.gsfc.nasa.gov/MOD07_L2/sample.html

Additional Product Information:
http://modis-atmos.gsfc.nasa.gov/MOD07_L2/index.html

Science Team Contact:
W. P. Menzel

Atmospheric Temperature at 500 hPa

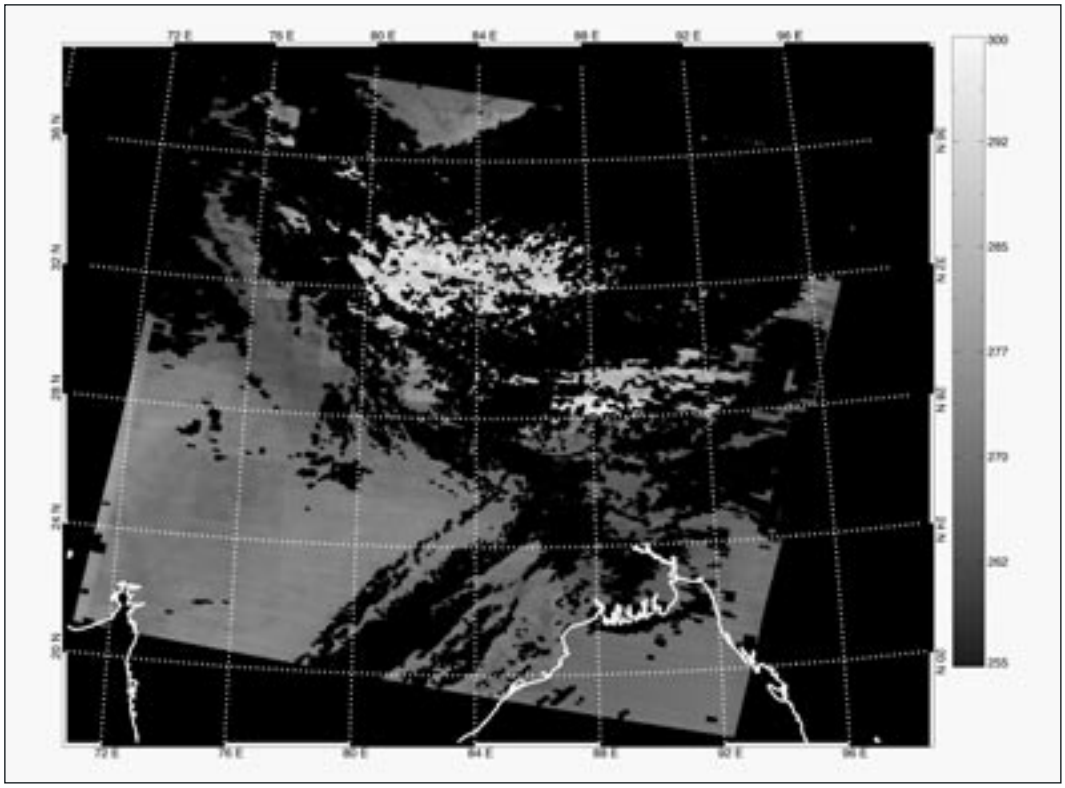

Total Column Precipitable Water Vapor

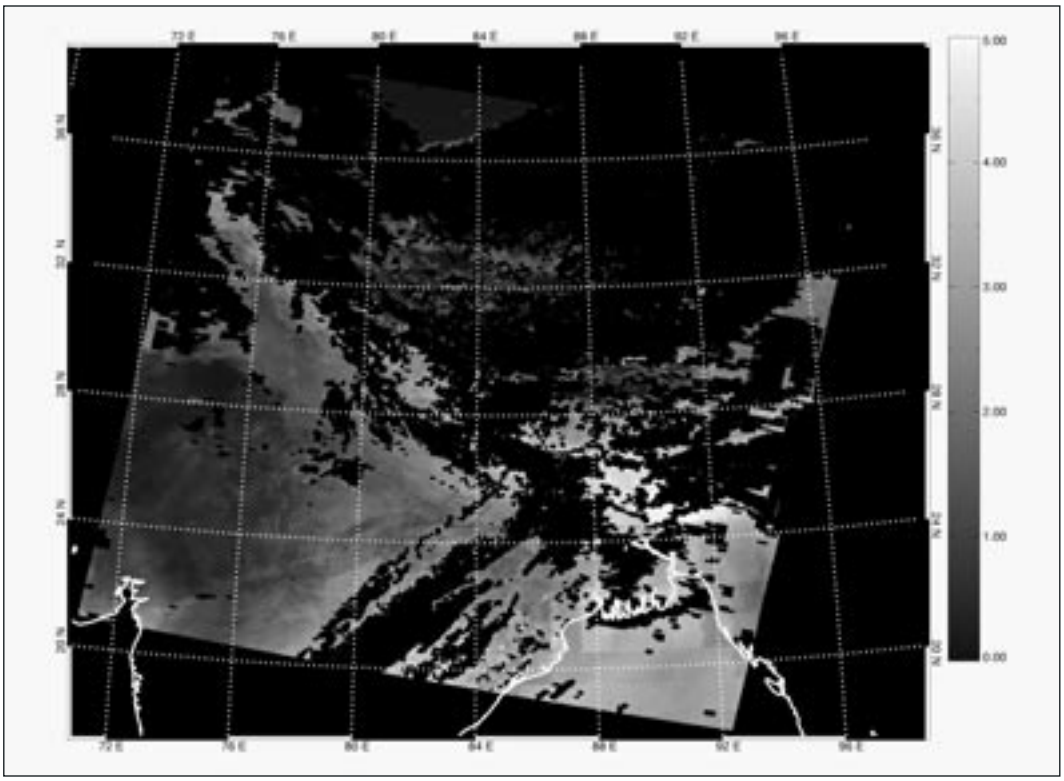

Level 2 MODIS Atmospheric Temperature (K) at 500 hPa (upper panel) and Level 2 MODIS Total Column Precipitable Water Vapor (cm) (lower panel), both derived from data taken over the Himalayas and Northern India at 5:25 UTC on April 19, 2000, from the MODIS instrument on Terra.

JMR Columnar Water Vapor Content

Product Description

This Level 2 product provides the measurement of the total atmospheric columnar water vapor content (in g/cm^2) made by the Jason-1 Microwave Radiometer (JMR). The measurement is repeated every 9.9 days along a set of fixed ground tracks. The satellite makes 127 revolutions of the Earth every 9.9 days. The coverage of the measurement is limited from 66° S to 66° N due to the 66° inclination of the satellite's orbit plane. The longitudinal distance between the ground tracks is [315·cos(latitude)] km, i.e., 315 km at the equator, 223 km at 45°, and 128 km at 66°. This product is used to generate gridded Level 3 products by various Jason-1 Science Working Team members. Two kinds of product are available: The Interim Geophysical Data Record (IGDR) is available 3 days after the data collection, while the GDR, based on a more precisely determined orbit, is available 30 days after the data collection.

Research and Applications

Water vapor is the most important greenhouse gas in the atmosphere. It plays a large role in keeping the Earth at a temperature suitable for intelligent life. Furthermore, information on the content of water vapor and its variability is important for the study of climate in other ways as well. For example, the water vapor measurement made by the TOPEX Microwave Radiometer was used to study the relationship between the 1997-98 El Niño and the variability of total water vapor content of the Earth.

Data Set Evolution

The JMR measures the brightness temperature of the sea surface at three frequencies: 18.7, 23.8, and 34 GHz. These measurements are used to compute the range delay of radar altimeter signals due to the water vapor in the atmosphere as well as the total columnar water vapor content. The antenna temperatures measured by JMR are first converted into brightness temperatures of the sea surface at the three frequencies. The brightness temperatures are then used to compute the total water vapor content along the path of the JMR line of sight. The primary heritage for the JMR water vapor product is the corresponding product derived from the data of the TOPEX/Poseidon Microwave Radiometer, launched in 1992.

Suggested Reading

Haines, B. J., and Y. E. Bar-Sever, 1998.

Nerem, R. S. *et al*., 1999.

Ruf, C. S. *et al*., 1994.

JMR Columnar Water Vapor Content Summary

Coverage: Ocean areas from 66° S to 66° N.

Spatial/Temporal Characteristics: 6.2-km resolution along-track every 9.9 days; [315·cos(latitude)] km longitudinal track spacing

Key Science Applications: Greenhouse gas monitoring, climate change

Key Geophysical Parameters: Atmospheric columnar water vapor content

Processing Level: 2

Product Type: Standard, at-launch

Maximum File Size: 1.5 MB

File Frequency: 25/day

Primary Data Format: Binary

Browse Available: Yes

Additional Product Information: http://www-aviso.cnes.fr

DAAC: Jet Propulsion Laboratory

Science Team Contacts:
L.-L. Fu
Y. Ménard

SAGE III Water Vapor Products (SAGE III 03)

Product Description

The SAGE III Water Vapor Products (SAGE III 03 at Level 2) consist of H_2O concentration (number density in units of molecules/cm^3) and volume mixing ratio (ppmv) at each measurement location with a vertical resolution of 0.5 km. The water-vapor products are retrieved from the solar-occultation measurements of slant-path absorption using 29 contiguous subchannels between 933.19 nm and 960.12 nm, spaced at approximately 1 nm with a resolution of about 1.4 nm.

Since temperature profiles will also be measured by SAGE III, utilizing the oxygen A-band absorption spectra in the wavelength region 759-771 nm, relative humidities can be derived accordingly, using the SAGE III-retrieved water-vapor profiles and temperature profiles.

Research and Applications

SAGE III water-vapor profiles will provide complementary measurements to those of other EOS instruments. With its vertical resolution of 0.5 km, SAGE III water-vapor products are necessary for unraveling the issues associated with troposphere-stratosphere water-vapor exchange. Since the occultation measurements are relatively immune to drift in instrument performance, SAGE III-retrieved water-vapor profiles are invaluable for helping to validate observations from the other EOS-system instruments. Furthermore, given the long-term reliability and self-calibration capabilities of the SAGE instruments, SAGE III may be in a position to evaluate water-vapor trends in the upper troposphere and lower stratosphere during a time period when considerable warming due to increased emissions of human-derived greenhouse gases may occur.

SAGE III Water Vapor Products Summary

Coverage: 30 solar events per day, 15 northern high latitude, 15 southern high latitude

Spatial/Temporal Characteristics: 0.5 km vertical resolution

Key Science Applications: Greenhouse effect, global warming, validation of climate models, convective cloud studies, weather-forecast initialization, tropospheric chemistry, stratospheric chemistry

Key Geophysical Parameters: Water-vapor concentration, water-vapor mixing ratios, relative humidities, total-column water vapor, moisture content

Processing Level: 2

Product Type: Standard, at-launch

Maximum File Size: 0.05 MB

File Frequency: 196/week

Primary Data Format: HDF-EOS, Big Endian IEEE Binary

Browse Available: Yes

Additional Product Information: http://eosweb.larc.nasa.gov/PRODOCS/sage3/table_sage3.html

DAAC: NASA Langley Research Center

Science Team Contact: E.-W. Chiou

Cloud and Aerosol Properties and Radiative Energy Fluxes

Aqua
- AIRS
- AMSR-E
- AMSU-A
- CERES
- HSB
- MODIS

Meteor 3M
- SAGE III

QuikTOMS
- TOMS

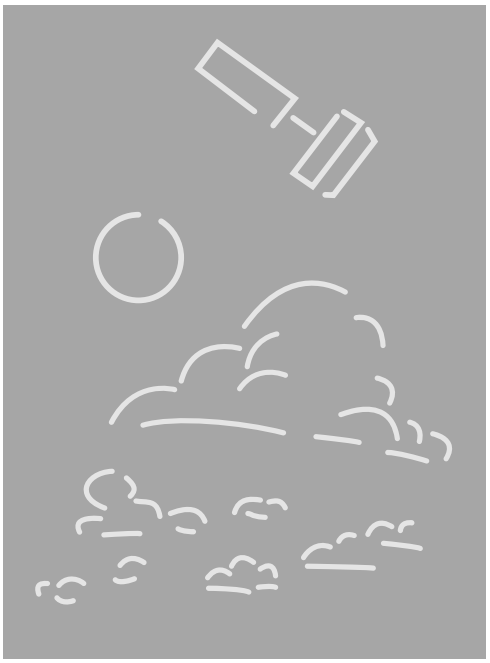

Cloud and Aerosol Properties and Radiative Energy Fluxes – An Overview

Relationship to Global Change Issues

Clouds and aerosols play a significant role in modifying the flow of energy to and from the Earth's surface. Hence, measuring and understanding clouds and aerosols are among the keys to predicting climate change and to testing global climate models. The technology for measuring radiative fluxes, cloud properties, and aerosol properties from space is now sufficiently advanced that these measurements can be used to improve significantly our ability to address such critical global change issues as whether clouds act as a positive or negative feedback mechanism as climate changes and whether aerosols will offset some of the expected warming from increasing greenhouse gases.

In many cases, cloud and/or aerosol studies using the data from the missions highlighted in this volume will benefit from instruments on other satellite missions as well. In particular, versions of the CERES instrument will be operating on the TRMM, Terra, and Aqua platforms and will function synergistically in conjunction with VIRS and TMI (on TRMM), MODIS and MISR (on Terra), and MODIS and AMSR-E (on Aqua). Similarly, the MODIS instruments on Terra and Aqua will complement each other by providing morning and afternoon measurements, respectively.

Clouds: A first step in examining clouds from space is to determine their distribution through the atmosphere, i.e, where they are and what their dimensions are. Once clouds are identified and mapped, cloud properties such as effective particle size, thermodynamic phase (water, ice), cloud-top properties, and optical thickness (all of which help determine how much radiation passes through them) may be measured. The MODIS, AIRS/AMSU-A/HSB, and AMSR-E instruments on the EOS Aqua platform, the SAGE III instrument on the Meteor 3M platform, the MODIS, MISR, and ASTER instruments on the EOS Terra platform (see Volume 1), and the VIRS and TMI instruments on TRMM (see Volume 1) will provide these key cloud measurements. The daily observations from these instruments also provide the sampling needed to drive and verify climate models. In the longer term, advances are expected in the vertical distribution of clouds using the active lidar and cloud radar data from the PICASSO-CENA and CloudSat missions flying in formation with Aqua starting in 2003.

Aerosols: Aerosols are suspended particles in the atmosphere such as dust, sulfate, smoke, and many others. Their measurement is an important element in describing energy transmission through the atmosphere. Uncertainties regarding aerosols result in their being a significant source of uncertainty in climate modeling. They affect cloud microphysics by acting as condensation nuclei, thereby affecting cloud radiative properties. They also interact directly with solar radiation, thus affecting the radiative balance; and the geographic locations of anthropogenic aerosols are also important considerations in their impact on climate. In addition, stratospheric aerosols play a role in the ozone depletion issue through heterogeneous chemistry. Aerosol products described here, derived from MODIS on Aqua, and those from MODIS and MISR on Terra, will provide new information on aerosol formation, distribution, and sinks over both the land and ocean. Aerosol data from SAGE III on Meteor 3M will provide altitude profiles of aerosols and polar stratospheric cloud information from the upper troposphere through the stratosphere in the high-latitude regions. In the longer term, advances are expected in determining the vertical distribution of aerosols in the troposphere using the active lidar on the PICASSO-CENA mission.

Radiation: The flow of radiation from the Sun to the Earth and its absorption, reflection, and emission within the Earth system determine the energy balance of the Earth and hence have a significant effect on the nature of life on Earth as well. The information from products describing optical and physical properties of clouds and aerosols is combined with broadband radiation measurements from CERES and AIRS to provide estimates of solar and infrared radiative fluxes, which in turn determine the heating and cooling of the Earth and the atmosphere. The radiation estimates needed to do this are both shortwave and longwave fluxes at the surface and at the top of the atmosphere, both downwelling and upwelling, so that the net flow can be determined. Also, fluxes must be distinguished between cloudy- and clear-sky regions, and the fluxes over a series of elevation intervals are needed to test atmospheric models. Improved knowledge of the vertical distribution of radiative fluxes will be obtained by the addition of PICASSO-CENA and CloudSat data, with these platforms flying in formation with Aqua.

Product Overview

CERES will continue the fifteen-year record of radiation-budget information produced by the ERBE

program. As with Terra, starting 6 months after the launch of Aqua (following instrument and analysis validation), the CERES science team will begin production of ERBE-like data products. These top-of-the-atmosphere (TOA) fluxes will use the ERBE analysis algorithms to allow consistent comparisons to historical ERBE data. Furthermore, the data from the first 24 months after the Terra and Aqua launches will be used to develop a new set of CERES angular distribution models (ADMs). These ADMs are used to convert broadband CERES radiances, i.e., radiative energy at a single viewing direction, into estimates of broadband hemispheric fluxes. The CERES rotating-azimuth-plane scan mode will be used along with the cloud properties derived using VIRS and MODIS data to derive new and much more accurate ADMs. Beginning 30 months after launch, these more accurate CERES estimated TOA fluxes will be produced in addition to the ERBE-like products. Finally, starting 36 months after launch, CERES will routinely provide estimates of radiative fluxes at the surface and at a selected number of levels within the atmosphere. The number of atmospheric levels will depend on the accuracies determined during post-launch validation.

All the CERES products except the ERBE-like products are classified as "post-launch" for the reasons discussed above. The AMSR-E product in this chapter is also post-launch, while the AIRS/AMSU-A/HSB, MODIS, SAGE III, and TOMS products are "at-launch."

The cloud products fall into two classes: 1) cloud detection and delineation, and 2) cloud properties. Cloud detection and delineation produces masks indicating where clouds exist and information on layering and overlap to give a geometric picture of global cloud coverage. Cloud properties include optical thickness, temperature, liquid-water content, ice-water content, particle radius, cloud-top altitude, and phase, all of which relate to the radiative transmission, reflection, and emission of the clouds.

The CERES cloud-detection process uses observations from VIRS on TRMM and MODIS on Terra and Aqua to produce a global binary mask indicating the presence or absence of a cloud in each imager pixel mapped to the CERES fields of view. The MODIS cloud mask (MOD 35) is a global product that provides a probability that a view of the Earth is obstructed by clouds and an indication of whether cloud shadow is detected. It also provides information on land/sea presence and day/night conditions.

MODIS cloud-property parameters include particle size and phase, optical thickness, cloud-top height, emissivity and temperature, and cloud fraction in a region, all of which support specific MODIS science tasks that complement the radiation studies and products from other instruments. CERES cloud properties include cloud-layer mapping, cloud-top and cloud-base pressure, infrared emissivity, liquid-water path, particle radius, and cloud overlap, all derived from MODIS or VIRS data and remapped onto the broadband CERES fields of view for studies of the Earth's radiative-energy distribution. AIRS/AMSU-A/HSB cloud properties include cloud-top pressure, temperature, and cloud spectral properties, while AMSR-E data will be used to derive columnar cloud water.

Aerosol properties are provided by SAGE III on Meteor 3M, TOMS on QuikTOMS, and MODIS (MOD 04) on Aqua. Aerosols must be accounted for during the retrieval of surface and atmospheric parameters for maximum accuracy. The MODIS aerosol products include aerosol optical thickness, aerosol size distribution, and aerosol sources and sinks; SAGE III products include multi-spectral extinction profiles of aerosols with high vertical resolution from the upper troposphere through the stratosphere; and TOMS products include an aerosol index derived from backscattered ultraviolet radiances. These various aerosol products will aid both in understanding the role of aerosols in the climate system and in improving corrections for aerosol effects in the retrieval of surface parameters.

Radiant energy flux products from CERES include the radiative fluxes downward and upward at the top of the atmosphere, at the Earth's surface, and at selected intermediate altitudes, as well as the net flux, which is used to determine the radiation budget. This budget in turn determines the overall heating and cooling of the atmosphere and the Earth's surface and hence has a central role in climate changes. The CERES radiation algorithms use the cloud and aerosol products in the calculations for determining how much solar radiation is transmitted, reflected, and absorbed in the cloud/atmosphere/Earth-surface system. They are thus critical in the monitoring of global climate.

Product Interdependency and Continuity with Heritage Data

There is significant interdependency both amongst the products described in this chapter and between these products and data from other sources. In many cases, output data from one instrument become input ancillary data for another, as in the case of MODIS and/or TRMM data being used in the calculation of CERES cloud products. Further, the cloud distributions will be used in cloud masks for surface products.

(Cloud and Aerosol Properties and Radiative Energy Fluxes – An Overview, continued)

The AIRS/AMSU-A/HSB cloud products build on the heritage of HIRS/MSU, the AMSR-E products on the heritage of SMMR, SSM/I, and TMI, the CERES products on the heritage of ERBE, the MODIS products on the heritage of AVHRR, the SAGE III products on the heritage of SAM II, SAGE I, and SAGE II, and the QuikTOMS products on the heritage of earlier TOMS instruments. In the case of CERES, several data products use ERBE algorithms to ensure continuity with the extensively analyzed ERBE data set. Similarly, the SAGE III data will be used to derive aerosol products with an algorithm similar to the SAGE II algorithm, to ensure continuity of the SAGE aerosol products. The continuation of existent data records will assist the determination of long-term trends and the analysis of the role of clouds, aerosols, and radiative energy fluxes in global climate and climate change.

Suggested Reading

Barkstrom, B. R., 1984.

Coakley, J. *et al.*, 1983.

Di Girolamo, L., and R. Davis, 1994.

Diner, D. J. *et al.*, 1991.

Dubovik, O. *et al.*, 2000.

Goodman, A. H., and A. Henderson-Sellers, 1988.

Hansen, J. *et al.*, 1993.

Holben, B. N. *et al.*, 1992.

Kaufman, Y. J., and C. Sendra, 1988.

Kaufman, Y. J. *et al.*, 1997a,b.

King, M. D., 1987.

King, M. D. *et al.*, 1992.

King, M. D. *et al.*, 1999.

Ramanathan, V., 1986.

Ramanathan, V., 1987.

Ramanathan, V. *et al.*, 1989.

Randall, D. A. *et al.*, 1989.

Remer, L. A., and Y. J. Kaufman, 1998.

Remer, L. A. *et al.*, 1997.

Remer, L. A. *et al.*, 1998.

Sohn, B.-J., and F. R. Robertson, 1993.

Solomon, S. *et al.*, 1997.

Tanré, D. *et al.*, 1996.

Wang, M., and H. R. Gordon, 1994.

Wielicki, B. A. *et al.*, 1995.

Wielicki, B. A. *et al.*, 1996.

Wielicki, B. A. *et al.*, 1998.

AIRS/AMSU-A/HSB Cloud Product (AIR 04)

Product Description

The AIRS Cloud Product (AIR 04) employs microwave, infrared, and visible observations to determine the physical and radiative cloud properties within an AMSU-A field of view (FOV).

The product consists of cloud-top pressure for up- to-two cloud layers within an AMSU-A FOV, effective fractional cloud-cover values for each AIRS footprint and cloud type, and the ratio of the spectral emissivity at a number of frequencies to that at 11 μm for the top cloud layer. The effective fractional cloud cover is the product of the geometrical fractional cloud cover and the 11-μm cloud emissivity.

Cloud parameters are retrieved for each AIRS footprint, regardless of whether a microwave/infrared (MW/IR) temperature profile can be successfully retrieved.

The product is generated daily (day and night) at AMSU-A FOV resolution, with some information at AIRS FOV resolution.

A visible cloud product is available at AIRS footprint resolution during daylight. The product consists of cloud amount (distinguishing between high and low clouds) and variability index within the AMSU-A footprint.

Research and Applications

Cloud parameters are important for studying interannual variability, and cloudiness is the principal modulating factor on shortwave- and longwave-radiation fluxes. Because of their high spatial and temporal variability, the effect of clouds is important over a wide range of spatial and temporal scales. Most current estimates of cloud amount (fractional cloud cover) are based on observations made at the ground. The accuracy of these values is doubtful except for zero or 100% cloudiness. Several definitions of cloudiness from space have been proposed. The definition considered appropriate for sounders such as AIRS emphasizes that clouds are the forcing parameters that make the observed infrared radiance differ from clear-column radiance.

The AIRS effective fractional cloud cover derived from the MW/IR retrieval is effective for longwave- flux calculations only and involves the cloud emissivity. Shortwave fluxes require effective cloud fractions utilizing the cloud albedo as well as the geometric cloud fraction.

Data Set Evolution

Radiances are cloud cleared to remove the effects of clouds on the radiance, enabling geophysical parameters to be determined for the clear portion of the scene. Assuming these parameters are valid over the entire scene, a set of cloud parameters is found which, when substituted in the radiative-transfer equations, best matches the observations for a number of channels used to determine cloud properties. The geophysical parameters used to determine the cloud parameters are from the AIRS solution for the AMSU- A footprint, whether it is a combined MW/IR solution in the case of accepted retrievals, or a primarily MW solution in the case of rejected MW/IR profiles.

Visible observations are made at 2-km resolution during day portions of the orbits to determine a visible cloud amount (distinguishing between high and low clouds) and variability index within the AMSU-A footprint. Visible observations made during the night portions of the orbits are expected to consist only of noise, except where bright moonlight or man-made sources are present. Visible information is combined to achieve AIRS IR spatial resolution.

Data validation will be accomplished through comparison of the retrieved cloud parameters with correlative data sets from satellite imagers (AVHRR and its derivatives).

Suggested Reading

Aumann, H. H., and C. Miller, 1995.

Aumann, H. H. *et al.*, 1999.

Chahine, M. T., 1977.

Chahine, M. T., 1982.

Chahine, M. T. *et al.*, 1977.

Chahine, M. T. *et al.*, 1997a,b,c.

Hofstader, M. *et al.*, 1999.

Lambrigsten, B., 1996.

Susskind, J. *et al.*, 1997.

Susskind, J. *et al.*, 1998.

(AIRS/AMSU-A/HSB Cloud Product, continued)

AIRS/AMSU-A/HSB Cloud Product Summary

Coverage: Global

Spatial/Temporal Characteristics: Resolution of AMSU-A FOV (40.6 km at nadir); some parameters at AIRS FOV (13.5 km at nadir)/once or twice daily (varies with parameter)

Key Science Applications: Cloud parameterization, climate modeling, and monitoring; AIRS cloud-cleared radiances

Key Geophysical Parameters:
- Fraction of FOV obscured by clouds and number of resolved cloud formations
- Cloud-top pressure, temperature, and cloud spectral properties

Processing Level: 2

Product Type: Standard, at-launch (spectral emissivity is a research product)

Maximum File Size: 5 MB

File Frequency: 240/day

Primary Data Format: HDF-EOS

Browse Available: Yes

Additional Product Information: http://www-airs.jpl.nasa.gov/

DAAC: NASA Goddard Space Flight Center

Science Team Contacts:
M.T. Chahine
J. Susskind

AIRS/AMSU-A/HSB Flux Product (AIR 10)

Product Description

The AIRS Flux Product is included in the Level 2 retrieval data granules and is geolocated to an AMSU-A footprint.

AIRS radiative fluxes consist of clear-column radiances, total Outgoing Longwave Radiation (OLR), net surface longwave flux, and net surface shortwave flux.

Clear-column radiances represent the radiances which would have gone to space at the angle of observation if no clouds were present in the field of view, and they are the radiances used to compute the final AIRS products. Clear-column radiances are produced for each AMSU-A footprint in which a successful combined MW/IR retrieval can be produced. This occurs in most cases of up to 80% cloudiness in the AMSU-A footprint and is expected roughly two thirds of the time.

Clear-column radiances at different zenith angles should not be averaged together to produce time-mean values because of their substantial zenith-angle dependence.

OLR is a function of surface and atmospheric conditions, particularly cloud-top pressure and cloud amount. OLR will be produced for every AIRS footprint. OLR is important for studying interannual variability and has been used as a proxy for precipitation.

When compared to other measures of OLR, such as those from CERES, OLR from AIRS also serves as a validation for the detailed AIRS surface and atmospheric products. Net surface longwave flux is the difference between the longwave flux leaving the surface, which depends only on surface parameters, and longwave flux striking the surface, which depends on atmospheric parameters, including cloud-base pressure. This is not a retrieved parameter. Consequently, net surface longwave flux is more difficult to compute than OLR and is a research product. One value will be produced for each AMSU-A footprint.

Net shortwave flux is the difference between the shortwave flux reaching the surface and that reflected by the surface. The downwelling shortwave flux is a function of the sun irradiance and the atmospheric properties, mostly those of clouds (cloud cover and cloud optical depth). The upwelling shortwave flux depends on the downwelling flux and the surface albedo.

Research and Applications

The study of the global hydrologic cycle and its coupling to the energy cycle is key to understanding the major driving forces of the Earth's climate system. AIRS will measure the major components of these driving forces, including the thermal structure of the surface and atmosphere, amount and height of clouds, outgoing longwave infrared radiation, and distribution of atmospheric water vapor.

If the net radiative energy flux at the top of the atmosphere (TOA) is combined with the net radiative energy flux at the Earth's surface, the net atmospheric radiative cooling is obtained. The atmospheric radiative cooling is the net effect of the infrared emission by the atmosphere, the absorption by the atmosphere of infrared radiation emitted by the Earth's surface, and the absorption by the atmosphere of solar radiation.

AIRS/AMSU-A/HSB will measure the spectral changes in the longwave radiation going to space. Knowledge of the changes is needed to monitor the effects of trace gases on global warming.

AIRS super-window channels will be able to observe the surface with minimum spectral contamination by the atmosphere. In addition, AIRS narrow spectral channels in the short-wavelength infrared region will observe the atmospheric layers above the Earth's surface with the highest vertical resolution possible with passive remote sensing. The observations will enable investigations of the fluxes of energy and water vapor between the atmosphere and the surface, as well as studies of their effect on climate.

Data Set Evolution

The AIRS Flux product is derived by integrating the observed radiances in the infrared and near infrared.

Determination of the AIRS clear-column radiances is the most important step in the AIRS retrieval process. The methodology implicitly assumes that geophysical parameters in all nine AIRS footprints within an AMSU-A footprint are otherwise homogeneous except for varying amounts of up to eight different types of cloud formations. With this assumption, the clear-column radiances for all channels are given as linear combinations of the observed radiances in those channels in the nine fields of view, with an unknown set of channel-independent coefficients, one for each cloud formation.

Radiances in selected AIRS cloud-clearing channels, together with all the microwave radiances, are used to determine the coefficients for each AMSU-A footprint. Error estimates are computed theoretically for each channel for each profile. Surface temperature and emissivity variations within the AMSU-A footprint will contribute to the error in the clear-column radiances.

The procedure to compute OLR and downward flux is analogous to the procedure used with HIRS2/MSU sounding data. Radiative-transfer calculations are done separately for a number of spectral bands as a function of the retrieved surface-skin temperature, band surface emissivity, temperature-water-vapor-ozone profile, and cloud parameters including band cloud spectral emissivity. The calculation in each band is done at a band effective zenith angle, different for upwelling and downwelling flux, and multiplied by π to give total band flux. These are added together to give the total OLR or downwelling longwave flux.

The procedure to compute the downwelling and upwelling shortwave flux employs a radiative-transfer model that uses the broad AIRS VIS/IR channel 4, surface albedo, aerosol optical depth, and integrated water vapor as input. The surface albedo is computed from AIRS Channel 4 clear-sky radiances using the same radiative-transfer model. Clear-sky detection is achieved using a combination of AIRS Channel 1 and, for regions covered by land surfaces, normalized difference vegetation index (NDVI) computed by differencing AIRS Channels 2 and 3.

Data validation will be accomplished through checking the internal consistency of the Level 2 retrieval and vicarious validation of AIRS and near-IR radiances against *in situ* measurements at DoE ARM/CART sites, Baseline Upper Air Network (BUAN) sites, and dedicated MODIS and ASTER validation sites.

Suggested Reading

Aumann, H. H. *et al*., 1999.

Chahine, M. T. *et al*., 1977.

Gautier, C., and M. Landsfeld, 1997.

Hofstadter, M. *et al*., 1999.

Lambrigsten, B., 1996.

Mehta, A., and J. Susskind, 1999.

(AIRS/AMSU-A/HSB Flux Product, continued)

AIRS/AMSU-A/HSB Flux Product Summary

Coverage: Global

Spatial/Temporal Characteristics: AMSU-A FOV resolution (40.6 km at nadir)/twice daily

Key Science Applications: Radiation budget, climate modeling

Key Geophysical Parameters:
- Clear-column radiance
- TOA outgoing longwave spectral radiative flux
- Spectral features in longwave fluxes, both land and ocean
- Net surface longwave fluxes, both land and ocean
- Net surface and TOA outgoing shortwave fluxes, both land and ocean
- Surface albedo

Processing Level: 2

Product Type: Research, at-launch

Maximum File Size: 5 MB

File Frequency: 240/day

Primary Data Format: HDF-EOS

Browse Available: Yes

Additional Product Information: http://www-airs.jpl.nasa.gov/

DAAC: NASA Goddard Space Flight Center

Science Team Contacts:
J. Susskind
C. Gautier

AMSR-E Columnar Cloud Water

Product Description

The columnar cloud water (L) derived from the AMSR-E microwave radiances is a measure of the total vertically integrated liquid cloud water in the marine atmosphere. It is expressed in units of millimeters, which represent the depth of the column of liquid water that would result if the cloud were to precipitate completely. The spatial resolution of this product is 12 km, and its expected rms accuracy at this resolution is 0.02 mm. The product only includes the liquid-water contribution due to cloud droplets, and does not include the larger raindrops. Cloud droplets are typically smaller than 100 μm, whereas raindrops can reach sizes up to several millimeters. At microwave frequencies, the radiative characteristics of cloud droplets and raindrops are quite different. Hence when rain is present, the accuracy of the cloud product degrades due to the difficulty in separating the cloud water from the rain water. The product will be produced for individual pixels across the AMSR-E swath (Level 2) as well as an Earth-gridded product (0.25° in latitude and longitude) averaged daily, weekly, and monthly (Level 3).

Research and Applications

Clouds remain one of the most poorly understood constituents of the climate system, primarily because of their complex morphology and highly variable radiative effects. They have significant effects on the planetary radiation balance through both their high albedo in the visible and the direct absorption and re-emission of outgoing longwave radiation. Clouds contribute to both positive greenhouse feedback from increased solar absorption and heat trapping and negative feedback from increases in albedo and radiative cooling. Formation of clouds is directly related to the conversion of latent heat to sensible heat, and is strongly correlated with the distribution of atmospheric heating. Additionally, advection of cloud water is critical in the redistribution of water through precipitation, forming a major link in the global hydrological cycle, which is a major driving force in the Earth's climate. Due to the difficulties involved in treating their manifold effects accurately, clouds are generally regarded as the weak link in most current state-of-the-art models of climate, making improvements in the observational cloud data sets of particular importance.

Data Set Evolution

The cloud-water retrieval algorithm is based on experience gained from previous microwave radiometers, including SMMR, SSM/I, and TMI. In particular, the SSM/I has demonstrated the ability of microwave radiometers to measure the cloud content over the world's oceans. Unfortunately, there is no reliable "ground truth" with which to validate the cloud-water algorithm. Hence, we rely on computer simulations and statistical analyses to assess the performance of the algorithm. The AMSR-E L retrievals should be more accurate than SSM/I retrievals because AMSR-E has two additional sets of dual-polarization channels at 6.9 and 10.7 GHz, which help separate the cloud signal from the wind signal and remove cross-talk due to varying sea-surface temperature.

Suggested Reading

Grody, N. C., 1976.

Liu, G., and J. Curry, 1993.

Ramanathan, V. *et al*., 1989.

Staelin, D. H. *et al*., 1976.

Trenberth, K. E., 1998.

Webster, P. J., 1994.

Weng, F., and N.C. Grody, 1994.

Wentz, F. J., 1997.

Wentz, F. J., and R. W. Spencer, 1998.

AMSR-E Columnar Cloud Water Summary

Coverage: Global ocean surface, clear and cloudy skies and light rainfall

Spatial/Temporal Characteristics:
Level 2: swath pixels at 12-km resolution
Level 3: 0.25° latitude-longitude grid/daily, weekly, and monthly

Key Science Applications: Climate variability, air-sea interaction, radiation balance, hydrological cycle

Key Geophysical Parameters: Columnar cloud water

Processing Level: 2, 3

Product Type: Standard, post-launch

Maximum File Size: 10 MB

File Frequency: 29/day

Primary Data Format: HDF-EOS

Browse Available: Accompanies data product

Additional Product Information:
http://wwwghcc.msfc.nasa.gov/AMSR/html/amsr_products.html

DAAC: National Snow and Ice Data Center

Science Team Contact:
F. J. Wentz

CERES ERBE-like Instantaneous TOA Estimates (ES-8)

Product Description

The ERBE-like Instantaneous TOA Estimates (ES-8) product contains 24 hours of instantaneous CERES data for a single scanner instrument. The ES-8 product contains filtered radiances recorded every 0.01 seconds for the total, shortwave (SW), and window (WN) channels and the unfiltered SW, longwave (LW), and WN radiances. The SW and LW radiances at spacecraft altitude are converted to top-of-the-atmosphere (TOA) fluxes with a scene-identification algorithm and Angular Distribution Models (ADMs), which are "like" those used for the Earth Radiation Budget Experiment (ERBE). The TOA fluxes, scene identification, and angular geometry are included in the ES-8 product.

A complete listing of parameters for this data product can be found in the CERES Data Products Catalog at http://asd-www.larc.nasa.gov/DPC/DPC.html and detailed definitions of each parameter can be found in the CERES Collection Guide at http://asd-www.larc.nasa.gov/ceres/collect_guide/list.html.

Research and Applications

This product is a CERES-produced equivalent to the instantaneous fluxes derived from the ERBE scanners on ERBS, NOAA-9, and NOAA-10. ES-8 flux data are directly comparable to ERBE fluxes and thus effectively extend the time series of ERBE flux measurements, allowing global-change experiments to continue using ERBE algorithms without the errors associated with comparing fluxes estimated by two different algorithms. Improved TOA flux-estimation algorithms for CERES (using improved ADMs and VIRS/MODIS cloud identification) are available in the Single-Scanner Footprint (SSF) product. Producing the two versions of TOA fluxes will allow continuity with the previous ERBE data along with improved accuracy of CERES TOA flux data.

Data Set Evolution

The ERBE-like Inversion Subsystem consists of algorithms that convert filtered radiometric measurements to instantaneous flux estimates at the TOA. The basis for this procedure is the ERBE Data Management System, which produced TOA fluxes from the ERBE scanning radiometers. The system consists of algorithms for Spectral Correction, Observed Scene Type, Radiance-to-Flux Conversion using Angular Distribution Models, and finally the Regional Averaging algorithm, which produces regional fluxes. A linear-estimation scheme is used to relate the filtered and unfiltered radiances. Ancillary parameter files are required for processing, including ADMs and spectral correction coefficients for converting filtered radiances to unfiltered radiances.

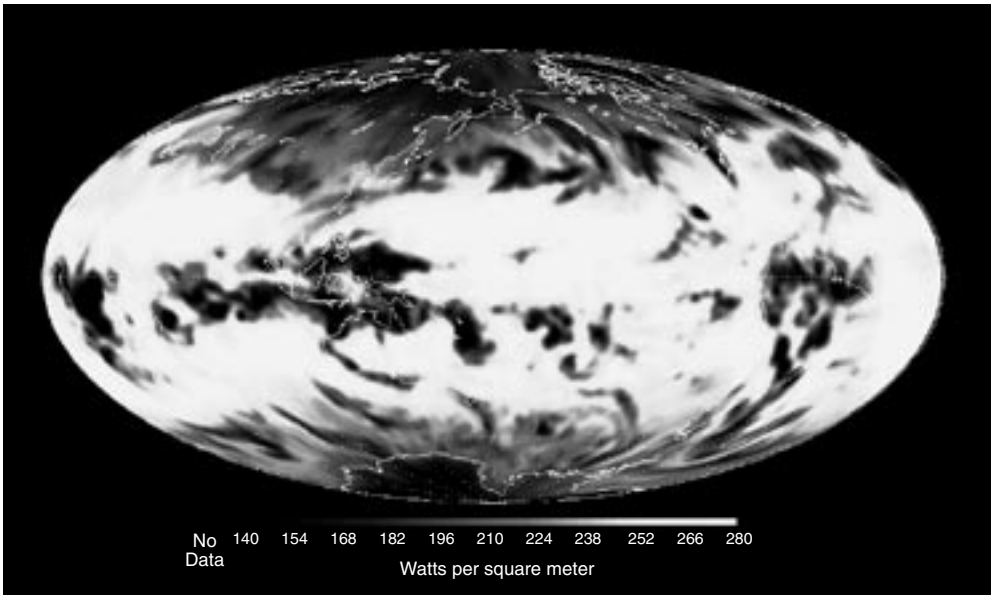

CERES ERBE-like Instantaneous TOA Estimates: TOA longwave flux measurements taken from the CERES instrument on Terra on February 28, 2000.

Documentation on the ES-8 algorithms can be found in CERES ATBD Subsystem 2.0, in PDF format, at http://eospso.gsfc.nasa.gov/atbd/cerestables.html.

Suggested Reading

Avis, L. M. *et al*., 1984.

Barkstrom, B. R., and G. L. Smith, 1986.

Smith, G. L. *et al*., 1986.

Wielicki, B. A. *et al*., 1998.

CERES ERBE-like Instantaneous TOA Estimates Summary

Coverage: Global

Spatial/Temporal Characteristics: 20 km at nadir/0.01 second

Key Geophysical Parameters: TOA SW, LW fluxes and radiances, scene type

Processing Level: 2

Product Type: Standard, at-launch

Maximum File Size: 490 MB

File Frequency: 1/day

Primary Data Format: HDF

Browse Available: No

Additional Product Information: http://eosweb.larc.nasa.gov/PRODOCS/ceres/table_ceres.html

DAAC: NASA Langley Research Center

Science Team Contacts:
R. N. Green
N. G. Loeb

CERES ERBE-like Monthly Regional Averages (ES-9) and ERBE-like Monthly Geographical Averages (ES-4)

Product Description

The ERBE-like Monthly Regional Averages (ES-9) product contains a month of space-and-time-averaged CERES data for a single scanner instrument. The ES-9 product is also produced for combinations of scanner instruments. All instantaneous shortwave and longwave fluxes at the top of the atmosphere (TOA) from the CERES ES-8 product for a month are sorted by 2.5° spatial regions, by day number, and by the local hour of observation. The mean of the instantaneous fluxes for a given region-day-hour bin is determined and recorded in the ES-9 product along with other flux statistics and scene information. For each region, the daily average flux is estimated from an algorithm that uses the available hourly data, scene identification data, and diurnal models. This algorithm is "like" the algorithm used for the Earth Radiation Budget Experiment (ERBE). The ES-9 product also contains hourly average fluxes for the month and an overall monthly average for each region. These average fluxes are given for both clear-sky and total-sky scenes.

The ERBE-like Monthly Geographical Averages (ES-4) product contains a month of space-and-time-averaged CERES data for a single scanner instrument. The ES-4 product is also produced for combinations of scanner instruments. For each observed 2.5-degree spatial region, the daily average, the hourly average over the month, and the overall monthly average of shortwave and longwave fluxes at the TOA from the CERES ES-9 product are spatially nested up from 2.5° regions to 5° and 10° regions, to 2.5°, 5°, and 10° zonal averages, and to global monthly averages. For each nested area, the albedo and net flux are given. For each region, the daily average flux is estimated from an algorithm that uses the available hourly data, scene-identification data, and diurnal models. This algorithm is "like" the algorithm used for the ERBE.

A complete listing of parameters for these data products can be found in the CERES Data Products Catalog at http://asd-www.larc.nasa.gov/DPC/DPC.html, and detailed definitions of each parameter can be found in the CERES Collection Guide at http://asd-www.larc.nasa.gov/ceres/collect_guide/list.html.

(CERES ERBE-like Monthly Regional Averages and ERBE-like Monthly Geographical Averages, continued)

Research and Applications

These products provide an equivalent of the ERBE-based radiation-balance component of inputs to global climate models, which were developed as part of, or over the same period, as the ERBE program and will allow continuation of this research while new algorithms are developed for CERES data.

The ES-9 and ES-4 products are equivalent to their ERBE analogs (S-9, and S-4) and effectively extend the time series of ERBE flux measurements through the EOS era. Various spatial scales are provided to simplify intercomparisons with earlier Nimbus and ERBE non-scanner time series.

Data Set Evolution

These data sets are generated using heritage ERBE algorithms operating on inputs from CERES calibrated Level 1 data and ancillary data. Data processing uses CERES Subsystem 3.0, which temporally interpolates CERES measurements using linear interpolation over oceans and half-sine-curve fit over land and desert regions. Monthly and monthly-hourly means are then computed using the combination of observed and interpolated values.

Documentation on the algorithms used to create the data products can be found in CERES ATBD Subsystem 3.0, in PDF format, at http://eos.nasa.gov/atbd/cerestables.html.

Suggested Reading

Brooks, D. R. *et al.*, 1986.

Harrison, E. F. *et al.*, 1990a,b.

Harrison, E. F. *et al.*, 1995.

Ramanathan V. *et al.*, 1989.

Wielicki, B. A. et al., 1998.

CERES ES-9 and ES-4 Products Summary

Coverage: Global

Spatial/Temporal Characteristics: 2.5°, 5.0°, 10.0°, region and zone, global/monthly (by day and hour)

Key Geophysical Parameters: TOA shortwave and longwave radiant flux, scene type, albedo, solar incidence, cloud condition

Processing Level: 3

Product Type: Standard, at-launch

Maximum File Size: 27 MB (ES-4), 1100 MB (ES-9)

File Frequency: 1/month

Primary Data Format: HDF

Browse Available: No

Additional Product Information: http://eosweb.larc.nasa.gov/PRODOCS/ceres/table_ceres.html

DAAC: NASA Langley Research Center

Science Team Contact: D. F. Young

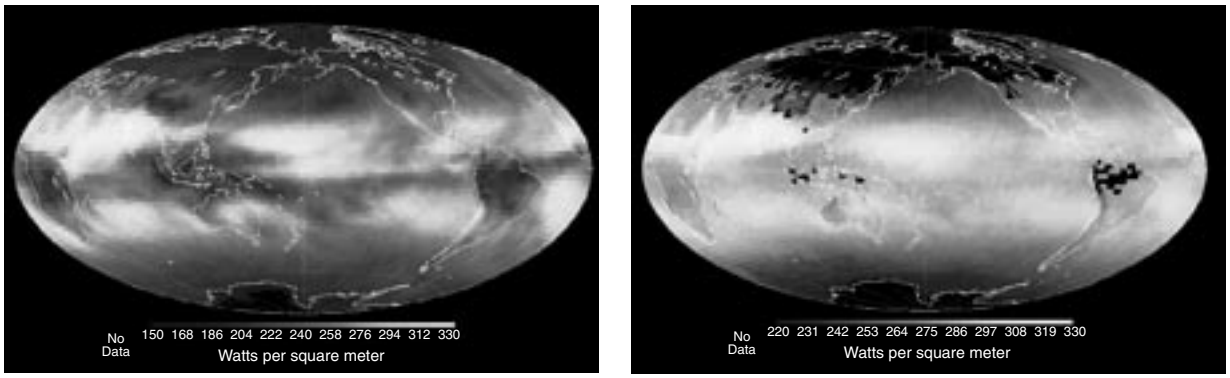

(Left) Sample CERES ERBE-like Monthly Geographical Averages, presenting the TOA longwave flux for March 2000. (Right) Sample CERES ERBE-like Monthly Regional Average, presenting the TOA clear-sky longwave flux for March 2000. Both images are from data from the Terra CERES.

CERES Single Scanner TOA/ Surface Fluxes and Clouds (SSF)

Product Description

The Single Scanner Footprint TOA/Surface Fluxes and Clouds (SSF) product contains one hour of instantaneous CERES data for a single scanner instrument. The SSF combines instantaneous CERES data with scene information from a higher-resolution imager such as the Visible/Infrared Scanner (VIRS) on TRMM or MODIS on Terra and Aqua. Scene identification and cloud properties are defined at the higher imager resolution and these data are averaged over the larger CERES footprint. For each CERES footprint, the SSF contains the number of cloud layers, and for each layer, the cloud amount, height, temperature, pressure, optical depth, emissivity, ice and liquid-water path, and water-particle size. The SSF also contains the CERES filtered radiances for the total, shortwave (SW), and window (WN) channels and the unfiltered SW, longwave (LW), and WN radiances. The SW, LW, and WN radiances at spacecraft altitude are converted to top-of-the-atmosphere (TOA) fluxes based on the imager-defined scene. These TOA fluxes are used to estimate surface fluxes. Only footprints with adequate imager coverage are included on the SSF, which is much less than the full set of footprints on the CERES ES-8 product.

A complete listing of parameters for this data product can be found in the CERES Data Products Catalog at http://asd-www.larc.nasa.gov/DPC/DPC.html, and detailed definitions of each parameter can be found in the CERES Collection Guide at http://asd-www.larc.nasa.gov/ceres/collect_guide/list.html. The algorithms are described in CERES ATBDs 4.0-4.6, located, in PDF format, at http://eospso.gsfc.nasa.gov/atbd/cerestables.html.

Research and Applications

This product generates the basic data on radiation and cloud characteristics needed by the hourly, monthly, gridding, averaging, and radiation-budget algorithms producing many of the CERES output products.

Data Set Evolution

This product is the first step in the sequence of processes from the geolocated radiances to estimates of the global radiation budget.

The SSF analysis uses coarse-spatial-resolution broadband radiance data from CERES, matched with simultaneous high-spatial-resolution narrow-band radiance data from MODIS on Aqua.

Analysis proceeds in six basic steps:

1) Cloud masking and clear-sky map update;
2) Cloud height and layering determination;
3) Cloud-optical-property determination;
4) Convolution of imager pixel-level cloud/surface properties with the CERES point-spread function for each CERES field of view;
5) Use of convolved cloud/surface properties to select a broadband anisotropic model for conversion of CERES radiance to TOA flux; and

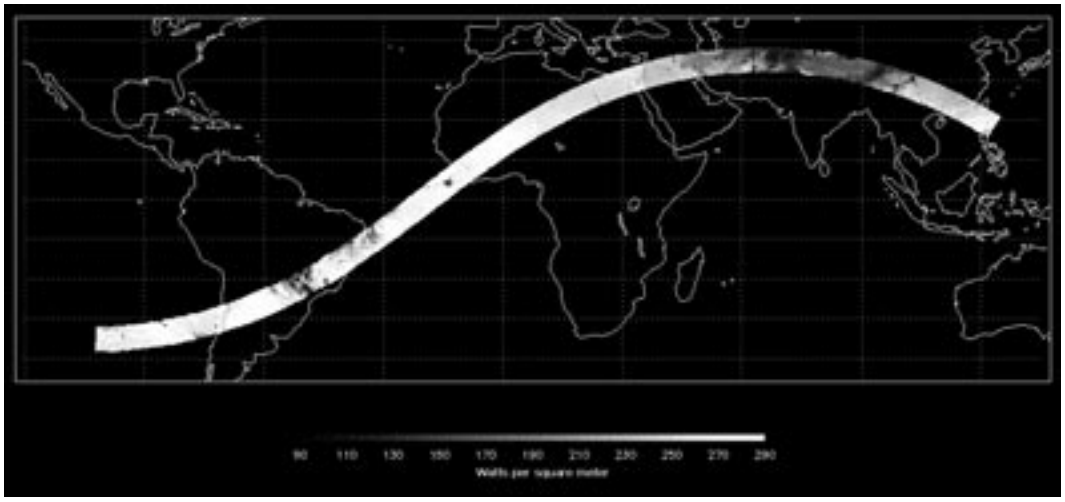

CERES Single Scanner Footprint TOA Longwave Flux from the TRMM Satellite on March 1, 1998, hour 23. This hourly product contains data within the area viewed by the VIRS imager on TRMM. For the corresponding Terra and Aqua CERES images, the area coverage is defined by the respective MODIS instruments.

(CERES Single Scanner TOA/Surface Fluxes and Clouds, continued)

6) Estimation of radiative fluxes at the surface, using theoretical/statistical relationships to TOA fluxes.

The SSF data product contains the matched cloud and radiative-flux data, which will also be used for later determination of radiative fluxes within the atmosphere.

Suggested Reading

Baum, B. A. *et al*., 1995a,b.

Dong, X. *et al*., 1999.

Green, R. N., and B. A. Wielicki, 1995.

Green, R. N. *et al*., 1995.

Minnis, P. *et al*., 1995.

Minnis, P. *et al*., 1998.

Minnis, P. *et al*., 1999.

Wielicki, B. A. *et al*., 1995.

Wielicki, B. A. *et al*., 1998.

Young, D. F. *et al*., 1998.

CERES Single Scanner TOA/Surface Fluxes and Clouds Summary

Coverage: Global

Spatial/Temporal Characteristics: 20 km at nadir/0.01 second

Key Geophysical Parameters: Radiance and flux (TOA and surface); cloud and clear-sky statistics, optical depth, infrared emissivity, liquid-water path, ice-water path, cloud-top pressure, cloud effective pressure, cloud temperature and cloud height, cloud-bottom pressure, water and ice-particle radius

Processing Level: 2

Product Type: Standard, post-launch

Maximum File Size: 260 MB

File Frequency: 1/hour

Primary Data Format: HDF

Browse Available: No

Additional Product Information: http://eosweb.larc.nasa.gov/PRODOCS/ceres/table_ceres.html

DAAC: NASA Langley Research Center

Science Team Contact: P. Minnis

CERES Clouds and Radiative Swath (CRS)

Product Description

The Clouds and Radiative Swath (CRS) product contains one hour of instantaneous CERES data for a single scanner instrument. The CRS contains all of the CERES SSF product data. For each CERES footprint on the SSF the CRS also contains vertical flux profiles evaluated at four levels in the atmosphere: the surface, 500-, 70-, and 1-hPa. The CRS fluxes and cloud parameters are adjusted for consistency with a radiative-transfer model, and adjusted fluxes are evaluated at the four atmospheric levels for both clear-sky and total-sky.

A complete listing of parameters for this data product can be found in the CERES Data Products Catalog at http://asd-www.larc.nasa.gov/DPC/DPC.html.

Research and Applications

The surface and atmospheric radiation budget (SARB) is the primary driver of the hydrological cycle and the general circulation of the atmosphere. Anthropogenically induced changes in the radiatively active trace gases and aerosols will affect the SARB and will therefore force a climate response. The 68 radiance and radiant flux and cloud parameters provided by this product are inputs to higher level algorithms which produce gridded, averaged flux and cloud-property products. This product contains a further enhancement of the basic data on radiation and cloud characteristics from SSF needed for determination of the amount of energy passing from space through the atmosphere to the Earth and flowing from the Earth back to space, which is provided by products SRBAVG, AVG, and ZAVG. It is a global product and is used as the input to the hourly gridded computation of surface, multiple atmosphere levels, and TOA radiative fluxes.

The analysis algorithms are described in CERES ATBD Subsystem 5.0, which can be found in PDF format at http://eospso.gsfc.nasa.gov/atbd/cerestables.html.

An example of the radiative-flux profile, expressed in terms of the radiative diabatic heat rate, is given in the figure on the following page. The local-scale CERES/ARM/GEWEX Experiment (CAGEX) provides a prelaunch window to this component of CERES with on-line access to input data, calculated fluxes, and validating measurements (see http://snowdog.larc.nasa.gov:8081/cagex.html).

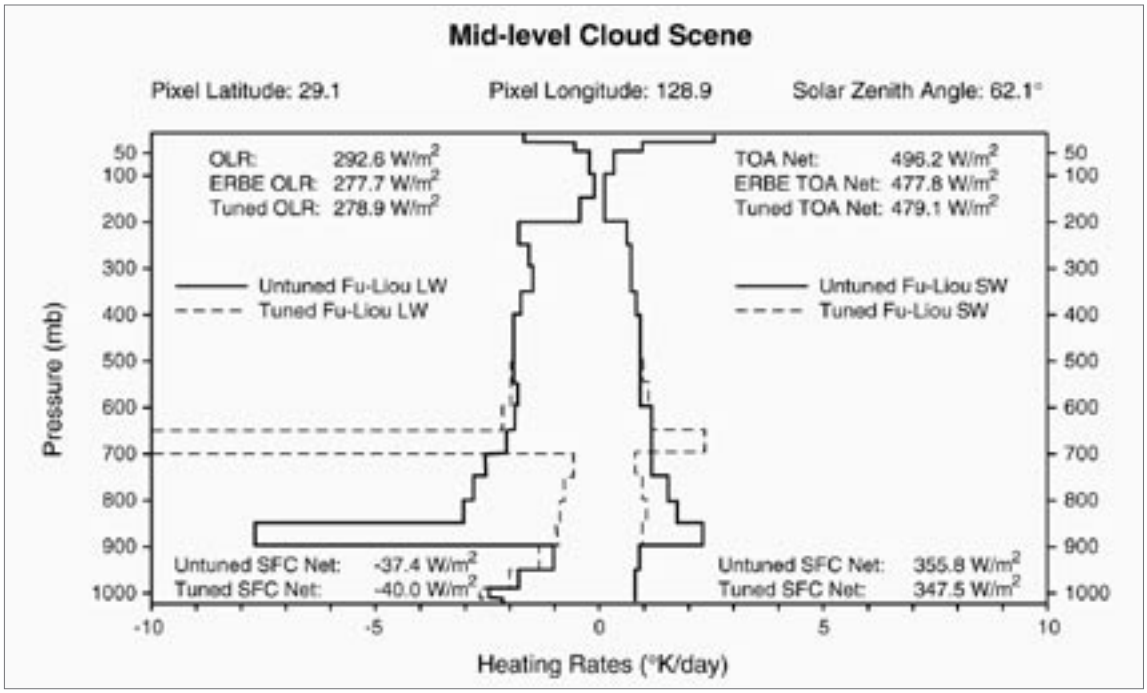

Longwave and Shortwave Heating Rates over one ERBE footprint containing low clouds. The figure shows for both LW and SW the fluxes at the TOA (as untuned Fu-Liou values, ERBE observations, and tuned Fu-Liou values), fluxes at the surface (as untuned Fu-Liou values and tuned Fu-Liou values), and heating rates (untuned are solid and tuned are dashed).

Data Set Evolution

The inputs to this product come from the SSF product, and the cloud parameters are further corrected and adjusted. The TOA and surface values are corrected for satellite and cloud effects to produce observed TOA and tuned surface estimates. This data set is tailored to provide the needed inputs to the hourly gridded flux and surface radiation budget Level 3 product, FSW.

Suggested Reading

Charlock, T. P., and T. L. Alberta, 1996.

Charlock, T. P. *et al*., 1993.

Charlock, T.P . *et al*., 1995.

Fu, Q., and K. Liou, 1993.

Liou, K.-N., 1992.

Whitlock, C. H. *et al*., 1995.

Wielicki, B. A. *et al*., 1998.

Wu, M., and L.-P. Chang, 1992.

CERES Clouds and Radiative Swath Summary

Coverage: Global

Spatial/Temporal Characteristics: 20 km at nadir/0.01 second

Key Geophysical Parameters: Shortwave and longwave radiant flux at the surface, multiple atmosphere levels, and TOA, scene identification, cloud parameters

Processing Level: 2

Product Type: Standard, post-launch

Maximum File Size: 354 MB

File Frequency: 1/hour

Primary Data Format: HDF

Browse Available: No

Additional Product Information: http://eosweb.larc.nasa.gov/PRODOCS/ceres/table_ceres.html

DAAC: NASA Langley Research Center

Science Team Contact: T. P. Charlock

CERES Monthly Gridded Radiative Fluxes and Clouds (FSW)

Product Description

The Monthly Gridded Radiative Fluxes and Clouds (FSW) product contains a month of space-and-time-averaged CERES data for a single scanner instrument. The FSW is also produced for combinations of scanner instruments. All instantaneous fluxes from the CERES CRS product for a month are sorted by 1° spatial regions, by day number, and by the Universal Time (UT) hour of observation. The mean of the instantaneous fluxes for a given region-hour bin is determined and recorded on the FSW along with other flux statistics and scene information. The mean adjusted fluxes at the four atmospheric levels defined by CRS are also included for both clear-sky and total-sky scenes. In addition, four cloud-height categories are defined by dividing the atmosphere into four intervals with boundaries at the surface, 700-, 500-, 300-hPa, and the top of the atmosphere (TOA). The cloud layers from CRS are put into one of the cloud-height categories and averaged over the region. The cloud properties are also column averaged and included on the FSW.

A complete listing of parameters for this data product can be found in the CERES Data Products Catalog at http://asd-www.larc.nasa.gov/DPC/DPC.html.

Research and Applications

This product is an interim step in the generation of regional and global radiation products from CERES footprint data. It contains the gridded data on radiation and cloud characteristics needed by the synoptic flux and clouds algorithm SYN. The contribution of this product is the averaging and gridding operations applied to both the radiative flux and cloud property data.

Data Set Evolution

The algorithm is based on ERBE algorithms and carries out aggregation of the high-resolution 20-km (nadir) data products to 1° (110 km) data cells using weighted averaging and linear interpolation to produce the flux and cloud data in this grid-cell format chosen for final products. This is an equal-angle grid consisting of regions that are 1° in latitude by 1° in longitude. The parameter list is essentially the same as for CRS.

The analysis algorithms are described in CERES ATBD Subsystem 6.0, which can be found at http://eospso.gsfc.nasa.gov/atbd/cerestables.html.

Suggested Reading

Stowe, L. *et al.*, 1993.

Wielicki, B. A. *et al.*, 1998.

CERES Monthly Gridded Radiative Fluxes and Clouds Product Summary

Coverage: Global

Spatial/Temporal Characteristics: 1° region/hour

Key Geophysical Parameters: Gridded surface, atmosphere layer, and TOA fluxes, clear-sky and total-sky cloud parameters in CRS, (e.g., cloud overlap, cloud pressure, cloud altitude, cloud temperature, ice-water properties, ice-particle properties, liquid-water properties)

Processing Level: 3

Product Type: Standard, post-launch

Maximum File Size: 1130 MB

File Frequency: 11/month

Primary Data Format: HDF

Browse Available: No

Additional Product Information: http://eosweb.larc.nasa.gov/PRODOCS/ceres/table_ceres.html

DAAC: NASA Langley Research Center

Science Team Contact: D. F. Young

CERES Synoptic Radiative Fluxes and Clouds (SYN)

Product Description

The Synoptic Radiative Fluxes and Clouds (SYN) product contains a day of space-and-time-averaged CERES data for a single scanner instrument. The SYN is also produced for combinations of scanner instruments. The 1° regional flux at the hour of observation from the CERES FSW product and concurrent diurnal data from geostationary satellites are used to estimate the regional flux at 3-hour intervals. Also at 3-hour intervals are estimates of the adjusted fluxes at the four atmospheric levels as defined by the CERES CRS product for both clear-sky and total-sky scenes, estimates of the average cloud parameters in four cloud-height categories, and column-averaged cloud parameters.

A complete listing of parameters for this data product can be found in the CERES Data Products Catalog at http://asd-www.larc.nasa.gov/DPC/DPC.html.

Research and Applications

The synoptic format of this product provides data which are global and simultaneous in time. This is preferred by climate modelers since the synoptic times ensure consistency with ground-truth meteorological observations from weather stations and radiosondes as well as with geostationary satellites, which provide images at synoptic hours. The production of a CERES synoptic data product is important because synoptic views provide a basis for studying the life cycle of cloud systems and for validating the CERES data processing, and it provides a regular data structure that simplifies the design of algorithms and operation of the data processing system. Synoptic fields of radiation and clouds are potentially valuable in developing and understanding the role of clouds in the generation and dissipation of available potential energy, since the calculation of this quantity requires integration over approximately horizontal layers within the atmosphere.

Data Set Evolution

The CERES time-space averaging and time-interpolation algorithm is based on techniques used in previous systems for deriving the Earth radiation budget, such as ERBE. The chief input to the time interpolation process is the gridded SW and LW TOA clear-sky and total-sky fluxes and cloud information provided by the FSW product. Data from the three possible systems which could carry CERES simultaneously in orbit (TRMM, Terra, and Aqua) provide up to six samples per day. This significantly reduces temporal sampling errors. Estimates of the cloud properties at synoptic times are also provided. The cloud-mask output defines clear-sky conditions for the 1° cells for the radiative fluxes, which are averaged over 3-hour periods. Interpolation to the synoptic times uses geostationary data to assist in modeling meteorological variations between times of observations.

The analysis algorithms are described in CERES ATBD Subsystem 7.0, which can be found at http://eospso.gsfc.nasa.gov/atbd/cerestables.html.

Suggested Reading

Breigleb, B. P., and V. Ramanathan, 1982.

Brooks, D.R. *et al.*, 1986.

Harrison, E. F. *et al.*, 1988.

Minnis, P., and E. F. Harrison, 1984.

Smith, G. L. *et al.*, 1995.

Wielicki, B. A. *et al.*, 1998.

Young, D. F. *et al.*, 1995a.

CERES Synoptic Radiative Fluxes and Clouds Summary

Coverage: Global

Spatial/Temporal Characteristics: 1° region/ 3-hour, monthly

Key Geophysical Parameters: Synoptic time-interval clear-sky, total-sky fluxes at surface, atmosphere levels, and TOA, cloud parameters including cloud overlap, cloud pressure, cloud altitude, cloud temperature, optical depth, ice-water properties, ice-particle properties, liquid-water properties, photosynthetically active radiation

Processing Level: 3

Product Type: Standard, post-launch

Maximum File Size: 240 MB

File Frequency: 1/3-hour (3-hour Level 3), 1/month (Monthly Level 3)

Primary Data Format: HDF

Browse Available: No

Additional Product Information: http://eosweb.larc.nasa.gov/PRODOCS/ceres/table_ceres.html

DAAC: NASA Langley Research Center

Science Team Contact: T. Wong

CERES Monthly Regional Radiative Fluxes and Clouds (AVG) and Monthly Zonal and Global Radiative Fluxes and Clouds (ZAVG)

Product Description

The Monthly Regional Radiative Fluxes and Clouds (AVG) product contains a month of space-and-time-averaged CERES data for a single scanner instrument. The AVG is also produced for combinations of scanner instruments. The 1° regional flux at the hour of observation from the CERES SYN product and concurrent diurnal data from geostationary satellites are used to estimate the daily regional flux, which is averaged to yield the monthly average flux. Adjusted fluxes at the four atmospheric levels defined by the CERES CRS product are also estimated for both clear-sky and total-sky scenes. In addition, four cloud-height categories are defined by dividing the atmosphere into four intervals with boundaries at the surface, 700-, 500-, 300-hPa, and the top of the atmosphere. The cloud layers from SYN are put into one of the cloud-height categories and diurnally averaged. The cloud properties are also column averaged. The AVG also contains, for each region, the hourly average fluxes for the month and an overall monthly average.

The Monthly Zonal and Global Radiative Fluxes and Clouds (ZAVG) product contains a month of space-and-time-averaged CERES data for a single scanner instrument. The ZAVG is also produced for combinations of scanner instruments. The space-and-time-averaged fluxes and cloud parameters on the CERES AVG product are spatially averaged from 1° regions to 1° zonal averages and a global monthly average.

A complete listing of parameters for these data products can be found in the CERES Data Products Catalog at http://asd-www.larc.nasa.gov/DPC/DPC.html.

Research and Applications

These products will be used by meteorological researchers to study climate and improve global climate models. Zonal quantities are needed for studying energy transport since averaging on large spatial scales minimizes the effects of regional-scale anomalies in studying climate change and global dynamics. Global averages can be compared with other historical data sets derived from different regional scales to detect climate temperature trends and evaluate large-scale

climate anomalies such as the effects of major volcanic eruptions.

Data Set Evolution

The product algorithm first calculates the means on a regional (1° equal-angle grid) basis from one month of synoptic maps from the SYN 3-hourly product. Regional means are then combined to obtain zonal and global averages. The main steps of the monthly averaging process are: 1) regionally sort the synoptically ordered data, 2) linearly average all flux data to produce monthly and monthly-hourly means, 3) average the cloud properties using the proper weighting schemes, and 4) combine and average the regional means into zonal and global means. Once regional means are computed for all parameters and all regions, these means are combined into zonal and global means. Area-weighting factors are used to correct for the variation of grid-box size with latitude.

The analysis algorithms are described in CERES ATBD Subsystem 8.0, which can be found at http://eospso.gsfc.nasa.gov/atbd/cerestables.html.

Suggested Reading

Harrison, E.F. *et al*., 1990b.

Li, Z., and H. Leighton, 1993.

Wielicki, B. A. *et al*., 1998.

Young, D. F. *et al*., 1995b.

CERES AVG and ZAVG Products Summary

Coverage: Global

Spatial/Temporal Characteristics: 1° region, 1° zone, global/month

Key Geophysical Parameters: Averaged clear-sky, total-sky surface, TOA, and standard CERES pressure-level fluxes; cloud parameters include: cloud overlap, pressure, temperature, optical depth, ice-particle properties, liquid-water properties, PAR

Processing Level: 3

Product Type: Standard, post-launch

Maximum File Size: 1188 MB

File Frequency: 1/month

Primary Data Format: HDF

Browse Available: No

Additional Product Information: http://eosweb.larc.nasa.gov/PRODOCS/ceres/table_ceres.html

DAAC: NASA Langley Research Center

Science Team Contact: T. Wong

CERES Monthly Gridded TOA/ Surface Fluxes and Clouds (SFC)

Product Description

The Monthly Gridded TOA/Surface Fluxes and Clouds (SFC) product contains a month of space-and-time averaged CERES data for a single scanner instrument. The SFC is also produced for combinations of scanner instruments. All instantaneous shortwave, longwave, and window fluxes at the top of the atmosphere (TOA) and surface from the CERES SSF product for a month are sorted by 1° spatial regions, by day number, and by the local hour of observation. The mean of the instantaneous fluxes for a given region-day-hour bin is determined and recorded in the SFC product along with other flux statistics and scene information. These average fluxes are given for both clear-sky and total-sky scenes. The regional cloud properties are column averaged and are included in the SFC product.

A complete listing of parameters for this data product can be found in the CERES Data Products Catalog at http://asd-www.larc.nasa.gov/DPC/DPC.html.

Research and Applications

This product is a necessary step in the transformation of raw CERES data to the radiation-budget outputs from product SRBAVG. The averaging and gridding operations performed on the footprint data serve to reduce variability by averaging to a 1-hour period and present the data in a uniform grid, which is required for temporal comparison of flux and cloud parameters.

Data Set Evolution

The parameters generated for this product are derived from the SSF product, which contains all the flux and cloud parameters. Each of the parameters from SSF is averaged to the 1° grid using equal weighting, which results in approximately 50 footprints being averaged for each geographic cell. These parameters are all inputs to the SRBAVG final radiation-budget product.

The analysis algorithms are described in CERES ATBD Subsystem 4.6, which can be found at http://eospso.gsfc.nasa.gov/atbd/cerestables.html.

Suggested Reading

Barkstrom, B. R., and B. A. Wielicki, 1995.

Cess, R. *et al.*, 1991.

Gupta, S. K. *et al.*, 1992.

Gupta, S. K. *et al.*, 1995.

Inamdar, A. K., and V. Ramanathan, 1994.

Inamdar, A. K., and V. Ramanathan, 1995.

Kratz, D. P., and Z. Li, 1995.

Li, Z. *et al.*, 1993.

Wielicki, B. A. *et al.*, 1998.

CERES Monthly Gridded TOA/Surface Fluxes and Clouds Summary

Coverage: Global

Spatial/Temporal Characteristics: 1° region/hour

Key Geophysical Parameters: Total-sky, clear-sky, and angular-model scene radiative fluxes (TOA and surface), cloud parameters, including cloud pressure, cloud altitude, cloud temperature, optical depth

Processing Level: 3

Product Type: Standard, post-launch

Maximum File Size: 615 MB

File Frequency: 18/month

Primary Data Format: HDF

Browse Available: No

Additional Product Information: http://eosweb.larc.nasa.gov/PRODOCS/ceres/table_ceres.html

DAAC: NASA Langley Research Center

Science Team Contacts:
D. F. Young
D. P. Kratz

CERES Monthly TOA/Surface Averages (SRBAVG)

Product Description

The Monthly TOA/Surface Averages (SRBAVG) product contains a month of space-and-time-averaged CERES data for a single scanner instrument. The SRBAVG is also produced for combinations of scanner instruments. The monthly average regional flux is estimated using diurnal models and the 1° regional fluxes at the hour of observation from the CERES SFC product. A second set of monthly average fluxes is estimated using concurrent diurnal information from geostationary satellites. These fluxes are given for both clear-sky and total-sky scenes and are spatially averaged from 1° regions to 1° zonal averages and a global average. For each region, the SRBAVG also contains hourly average fluxes for the month and an overall monthly average. The cloud properties from SFC are column averaged and are included on the SRBAVG.

A complete listing of parameters for this data product can be found in the CERES Data Products Catalog at http://asd-www.larc.nasa.gov/DPC/DPC.html.

Research and Applications

The cloud properties, as a function of LW and SW radiative fluxes at TOA and the surface, are critical to cloud-forcing issues, and cloud properties as a function of liquid-water and ice-water volume are critical to cloud dynamics modeling.

Data Set Evolution

This product is obtained from the chain of processes which start with the 1B radiances and flow through products BDS, SSF, SFC, and the CERES Instrument Earth Scans (IES), ultimately producing the final averaged radiative flux and surface-radiation-budget (SRB) product. The regional fluxes are calculated using two different methods, which will help produce very stable, accurate long-term data sets and averages for use in detailed regional studies of radiation and clouds and interdisciplinary studies. This is a post-launch product. Currently, there is no adopted method available for producing total-sky surface LW flux from TOA flux. Data required for parameterization must be obtained from either Meteorological Ozone and Aerosol (MOA) atmospheric data sets or from CERES and ISCCP cloud properties. In addition, data used in this product are limited to days in which there is at least one observation. The cloud parameters are also averaged monthly and monthly-daily. The surface radiation budget is the net radiative flux at the surface and is computed using the hourly gridded TOA and surface fluxes from SFC, parameterized models, atmospheric profiles, cloud parameters, and surface temperatures and emissivities to produce the downward and net shortwave and longwave fluxes at the surface. The LW algorithm is based on parameterized equations developed expressly for computing surface LW fluxes in terms of meteorological parameters obtained from satellite and/or other operational sources.

The analysis algorithms are described in CERES ATBD Subsystem 10.0, which can be found at http://eospso.gsfc.nasa.gov/atbd/cerestables.html.

Suggested Reading

Cess, R. *et al.*, 1991.

Gupta, S. K. *et al.*, 1992.

Harrison, E. F. *et al.*, 1995.

Li, Z. *et al.*, 1993.

Suttles, J. T., and G. Ohring, 1986.

Wielicki, B. A. *et al.*, 1998.

CERES Monthly TOA/Surface Averages Summary

Coverage: Global

Spatial/Temporal Characteristics: 1° region/month

Key Geophysical Parameters: Averaged total-sky, radiative fluxes (TOA and surface), net surface radiative fluxes (surface radiation budget), averaged cloud parameters

Processing Level: 3

Product Type: Standard, post-launch

Maximum File Size: 615 MB

File Frequency: 18/month

Primary Data Format: HDF

Browse Available: No

Additional Product Information: http://eosweb.larc.nasa.gov/PRODOCS/ceres/table_ceres.html

DAAC: NASA Langley Research Center

Science Team Contact: D. F. Young

MODIS Aerosol Product (MOD 04)

Product Description

The MODIS Aerosol Product (MOD 04) monitors the ambient aerosol optical thickness over the oceans globally and over a portion of the continents. Further, the aerosol size distribution is derived over the oceans, and the aerosol type is derived over the continents. Daily Level 2 (MOD 04) data are produced at the spatial resolution of a 10 × 10 1-km (at nadir)-pixel array.

Research and Applications

Aerosols are one of the greatest sources of uncertainty in climate modeling. Aerosols modify cloud microphysics by acting as cloud condensation nuclei (CCN), and, as a result, impact cloud radiative properties and climate. Aerosols scatter back to space and absorb solar radiation. The MODIS aerosol product will be used to study aerosol climatology, sources and sinks of specific aerosol types (e.g., sulfates and biomass-burning aerosol), interaction of aerosols with clouds, and atmospheric corrections of remotely sensed surface reflectance over the land.

Data Set Evolution

Prior to MODIS, satellite measurements were limited to reflectance measurements in one (GOES, METEOSAT) or two (AVHRR) channels. There was no real attempt to retrieve aerosol content over land on a global scale. Algorithms had been developed for use only over dark vegetation. The blue channel on MODIS, not present on AVHRR, offers the possibility to extend the derivation of optical thickness over land to additional surfaces. The algorithms will use MODIS bands 1 through 7 and 20 and require prior cloud screening using MODIS data. Over the land, the dynamic aerosol models will be derived from ground-based sky measurements and used in the net retrieval process.

Over the ocean, three parameters that describe the aerosol loading and size distribution will be retrieved. Pre-assumptions on the general structure of the size distribution are required in the inversion of MODIS data, and the volume-size distribution will be described with two log-normal modes: a single mode

to describe the accumulation mode particles (radius <0.5 μm) and a single coarse mode to describe dust and/or salt particles (radius >1.0 μm). The aerosol parameters we therefore expect to retrieve are: the ratio between the two modes, the spectral optical thickness, and the mean particle size.

The quality control of these products will be based on comparison with ground stations and climatology.

The related MODIS Cloud Product ATBD, *Algorithm for Remote Sensing of Tropospheric Aerosol from MODIS: Optical thickness over land and ocean and aerosol size distribution over the ocean*, can be found in PDF format at http://eospso.gsfc.nasa.gov/atbd/modistables.html.

Suggested Reading

Chu, D. A. *et al.*, 1998.

Dubovik, O. *et al.*, 2000.

Holben, B. N. *et al.*, 1992.

Holben, B. N. *et al.*, 1998.

Kaufman, Y. J., and C. Sendra, 1988.

Kaufman, Y. J., and L. A. Remer, 1994.

Kaufman, Y. J. *et al.*, 1997a,b.

King, M. D. *et al.*, 1992.

King, M. D. *et al.*, 1999.

Rao, C. R. N. *et al.*, 1989.

Remer, L. A. *et al.*, 1996.

Tanré, D. *et al.*, 1997.

MODIS Aerosol Product Summary

Coverage: Global over oceans, nearly global over land

Spatial/Temporal Characteristics: 10 km for Level 2

Key Science Applications: Aerosol climatology, biomass-burning aerosols, atmospheric corrections, cloud radiative properties, climate modeling

Key Geophysical Parameters: Atmospheric aerosol optical depth (global) and aerosol size distribution (oceans)

Processing Level: 2

Product Type: Standard, at-launch

Maximum File Size: 11 MB

File Frequency: 144/day

Primary Data Format: HDF-EOS

Browse Available: http://modis-atmos.gsfc.nasa.gov/MOD04_L2/sample.html

Additional Product Information: http://modis-atmos.gsfc.nasa.gov/MOD04_L2/index.html

Science Team Contacts:
Y. J. Kaufman
D. Tanré

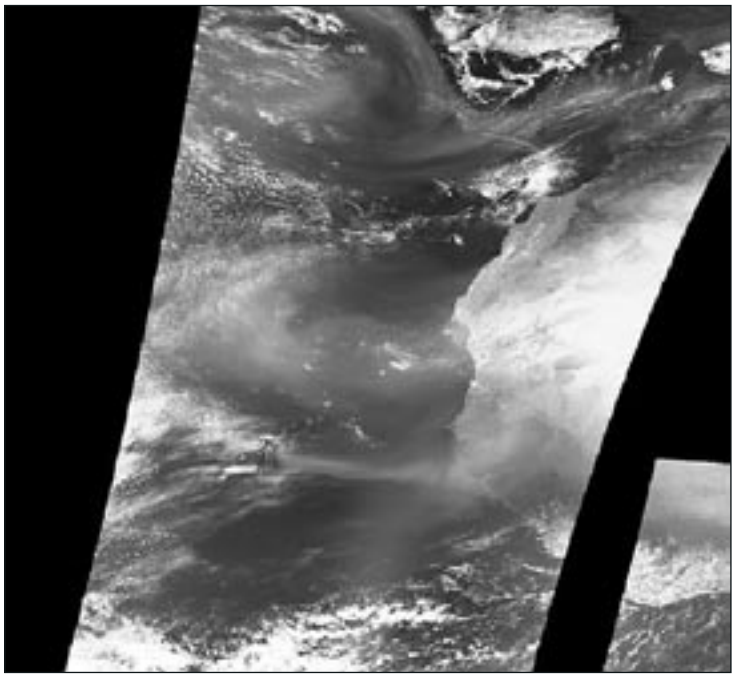

Terra MODIS Image of a Massive Sandstorm blowing off the northwest African desert. This sandstorm blanketed hundreds of thousands of square miles of the eastern Atlantic Ocean on February 29, 2000.

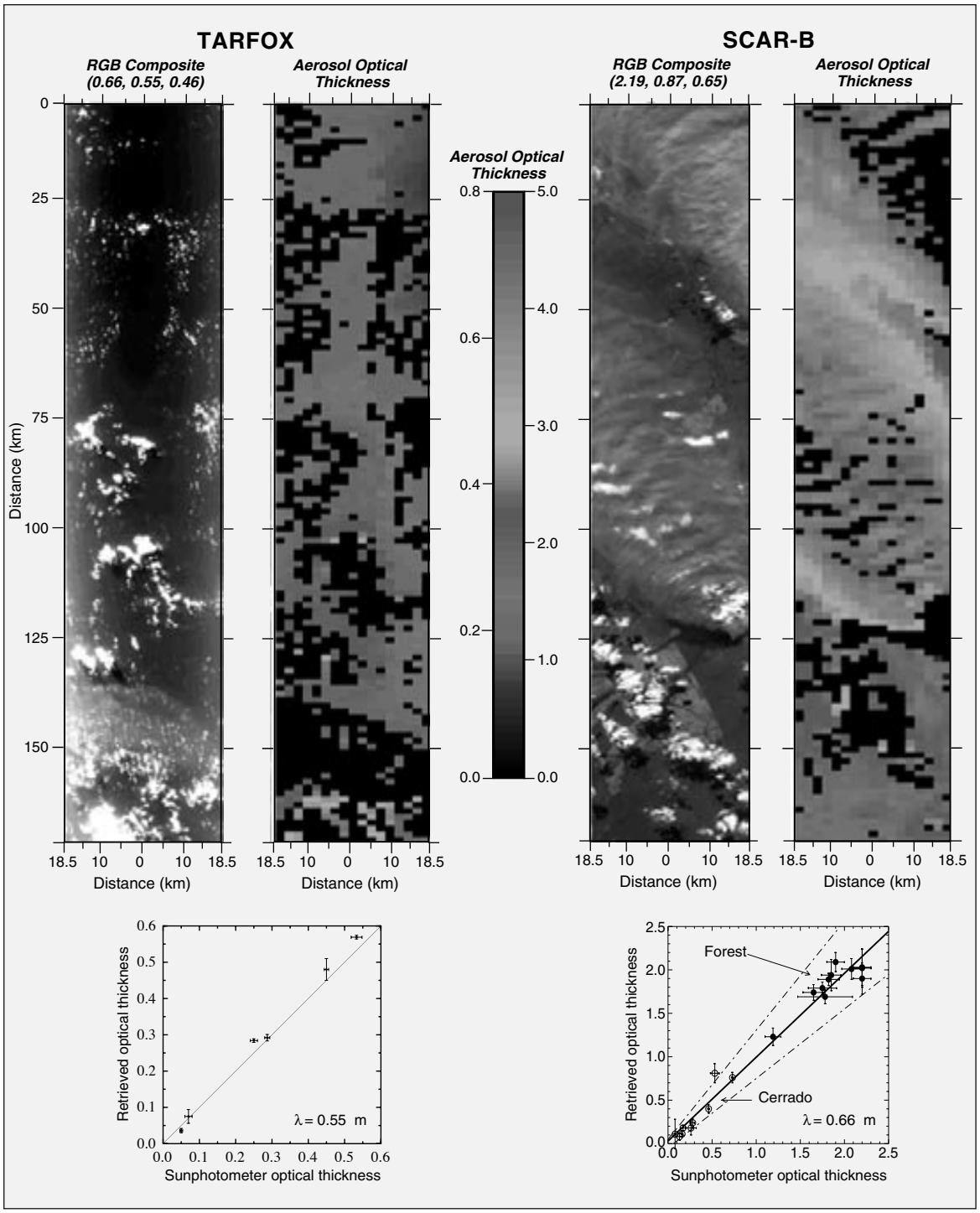

MODIS Airborne Simulator (MAS) Images and Corresponding Aerosol Thickness Retrievals for a 150 × 37-km section of flight during TARFOX (ocean scene) and SCAR-B (land scene). The bottom two panels are the validation of the retrieved aerosol optical thickness in comparison to sunphotometer observations at 0.55 μm (TARFOX; University of Washington C-131A measurements) and 0.66 μm (SCAR-B; ground-based AERONET measurements). (From King, M.D. *et al.*, 1999.)

MODIS Cloud Product (MOD 06)

Product Description

The MODIS Cloud Product (MOD 06) combines infrared and visible techniques to determine both physical and radiative cloud properties. Daily global Level 2 (MOD 06) data are provided. Cloud-particle phase (ice vs. water, clouds vs. snow), effective cloud-particle radius, and cloud optical thickness are derived using the MODIS visible and near-infrared channel radiances. An indication of cloud shadows affecting the scene is also provided. Cloud-top temperature, height, effective emissivity, phase (ice vs. water, opaque vs. non-opaque), and cloud fraction are produced by the infrared retrieval methods both day and night at 5 × 5 1-km-pixel resolution. Finally, the MODIS Cloud Product includes the cirrus reflectance in the visible at the 1-km-pixel resolution, which is useful for removing cirrus scattering effects from the land-surface reflectance product.

Research and Applications

A thorough description of global cloudiness and its associated properties is essential to the MODIS mission for two reasons. First, clouds play a critical role in the radiative balance of the Earth and must be accurately described in order to assess climate and potential climate change accurately. In addition, the presence or absence of cloudiness must be accurately determined in order to retrieve properly many atmospheric and surface parameters. For many of these retrievals, cloud cover, even thin cirrus, represents contamination. Key radiative properties of clouds such as phase, optical thickness, and temperature may be retrieved using MODIS instruments with unprecedented resolution.

Data Set Evolution

The determination of cloud-top properties will require the use of MODIS bands 29 and 31-36, along with the cloud-mask product (MOD 35), to screen for clouds. In addition, NCEP or DAO global model analyses of surface temperature and pressure, profiles of temperature and moisture, and blended SST analyses will be required in the calculation of cloud forcing as a function of atmospheric pressure and emissivity. The Menzel cloud-phase algorithm will require MODIS bands 29, 31, and 32 and analyses of surface emissivity.

The validation of cloud-top heights will be conducted through comparisons with stereo determinations of cloud heights from GOES and lidar estimates and aircraft observations of cirrus heights. Cloud emissivity will be compared to lidar-determined values. These interim products will be used in concert with field campaigns with the MAS instrument. The Menzel cloud-phase parameter will be validated using HIRS/AVHRR data and by comparison to the King cloud-phase parameter.

The King cloud-phase algorithm requires product MOD 02, calibrated multispectral radiances. Cloud-particle size and optical thickness require these radiances plus the cloud-top parameters within MOD 06

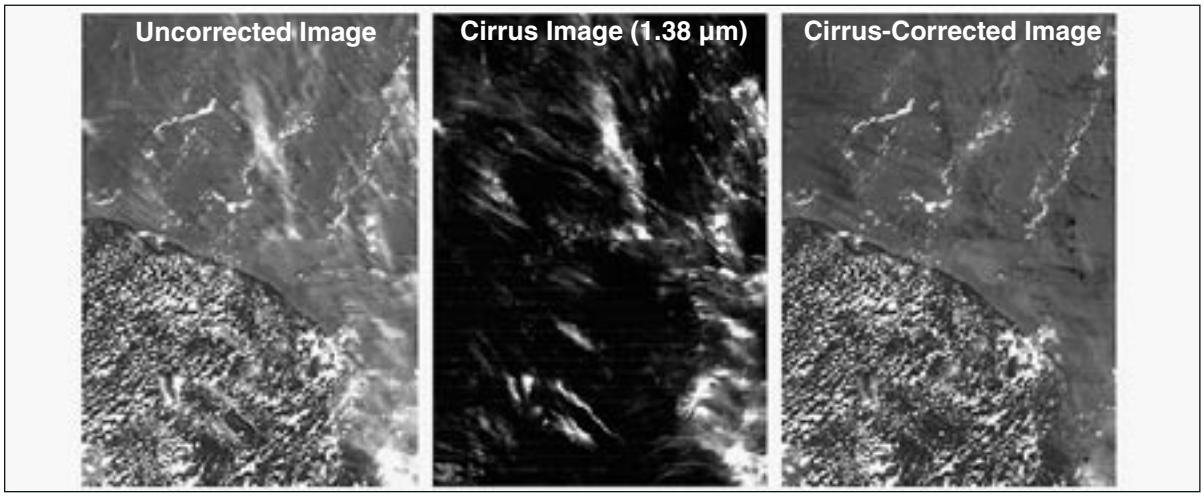

Sample Cloud Images from MODIS data on Terra, collected over South America on February 28, 2000. The left panel shows a 0.645 *µ*m image revealing both the upper level cirrus clouds and the lower level cumulus clouds. The middle panel shows the 1.38 *µ*m channel image. The upper level cirrus clouds are seen clearly in this image. The right panel is an image similar to the one in the left panel, except that the cirrus clouds shown in the middle panel have been removed.

and the Menzel cloud-phase parameter. In addition, these parameters require MODIS product MOD 43 (surface reflectance) and the NCEP or DAO analyses and profiles described above. The validation and quality control of these products will be performed primarily through the use of *in situ* measurements obtained during field campaigns and with the use of the MAS instrument.

The related MODIS Cloud Product ATBDs, *MODIS: Cloud Top Properties and Cloud Phase* and *Cloud Retrieval Algorithms for MODIS: Optical Thickness, Effective Particle Radius, and Thermodynamic Phase*, can be found in PDF format at http://eospso.gsfc.nasa.gov/atbd/modistables.html.

Suggested Reading

Gao, B. C. *et al*., 1998.

King, M. D. *et al*., 1992.

King, M.D. *et al*., 1996.

Nakajima, T. Y., and T. Nakajima, 1995.

Platnick, S. *et al*., 2000.

Strabala, K. I. *et al*., 1994.

Wylie, D. P., and W. P. Menzel, 1998.

MODIS Cloud Product Summary

Coverage: Global

Spatial/Temporal Characteristics: Resolutions of 1 km or 5 km/once or twice per day (varies with parameter)

Key Science Applications: Cloud parameterization, climate modeling, climate monitoring, increasing accuracy of other MODIS retrievals

Key Geophysical Parameters: Cloud-particle phase (two algorithms), cloud-particle size and optical thickness, cirrus reflectance at 1.375 µm, and cloud-top temperature, emissivity, and height

Processing Level: 2

Product Type: Standard, at-launch

Maximum File Size: 65 MB

File Frequency: 288/day

Primary Data Format: HDF-EOS

Browse Available:
http://modis-atmos.gsfc.nasa.gov/MOD06_L2/sample.html

Additional Product Information:
http://modis-atmos.gsfc.nasa.gov/MOD06_L2/index.html

Science Team Contacts:
M. D. King
W. P. Menzel
B. C. Gao

Cloud Optical Thickness

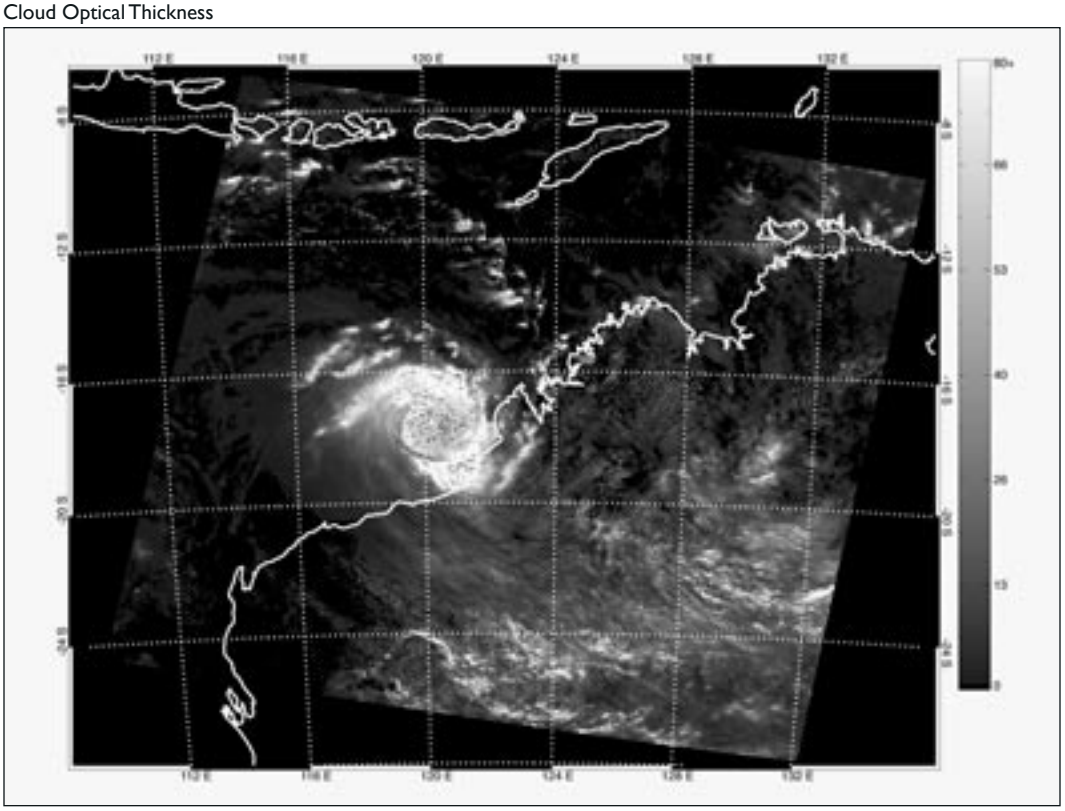

Effective Cloud-Particle Radius

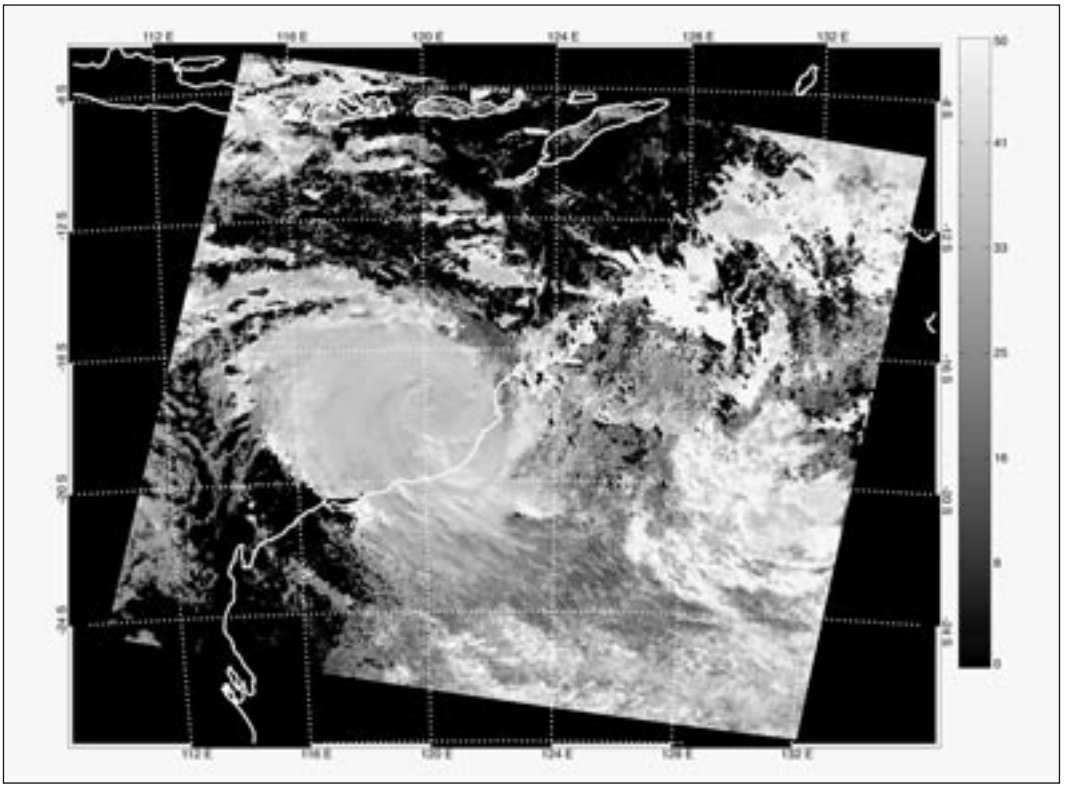

MODIS Retrieved Cloud Optical Thickness (unitless) and Effective Cloud-Particle Radius (in microns) for Tropical Cyclone Rosita shortly before it crossed the western Australian coastline at 0220 UTC on April 19, 2000. The images are derived from data from the visible and 2.1-μm channels on the Terra MODIS instrument.

MODIS Level 3 Atmosphere Products (MOD 08)

Product Description

There are three MODIS Level 3 Atmosphere Products, each covering a different temporal scale. The Earth Science Data Type names (and time spans) for each of the products are: MOD08_D3 (Daily), MOD08_E3 (8-Day), MOD08_M3 (Monthly).

Each of these Level 3 products contains statistics derived from over 50 science parameters from the Level 2 Atmosphere products: MOD04_L2, MOD05_L2, MOD06_L2, and MOD07_L2.

A range of statistical summaries is computed, depending on the Level 2 science parameter being considered. Statistics for a given Level 2 measurement might include:

- Simple (mean, minimum, maximum, standard deviation) statistics
- Parameters of normal and log-normal distributions
- Fraction of pixels that satisfy some condition (e.g., cloudy, clear)
- Histograms of the quantity within each grid box
- Histograms of the confidence placed in each measurement
- Histograms and/or regressions derived from comparing one science parameter to another; statistics may be computed for a subset that satisfies some condition
- Pixel counts

Statistics are sorted into 1° × 1° cells on an equal-angle grid and then summarized over the globe. The equal-angle grid has a fixed dimension of 360×180 pixels. It should be noted that three additional MOD 08 products, using the same temporal scales but summarized over an equal-area grid, will be available after launch.

The daily product contains nearly 400 statistical summary parameters. The 8-day and monthly products, which are identical in format, include over 600 statistical summary parameters.

Additional information on the MODIS Level 3 Atmosphere products can be obtained from the MODIS-Atmosphere web site at: http://modis-atmos.gsfc.nasa.gov.

Research and Applications

Users should refer to the research applications of Level 2 Atmosphere products from MOD 04, MOD 05, MOD 06, and MOD 07 listed in this handbook. Level 3 statistical products derived from Level 2 measurements lend themselves to longer-term time-series studies that help monitor variations in environmental conditions and aid research for assessing both natural and human-induced global change.

Data Set Evolution

Definition of Time Spans

For the daily product (MOD08_D3), Level 2 granules that overlap any part of the data day (0000 to 2400 UTC) are included in the computation of statistics. Therefore a particular Level 2 granule may be included in two consecutive MOD08_D3 products.

The 8-day product (MOD08_E3) is computed by manipulating and summarizing the daily product over eight consecutive days. The running 8-day interval begins with the first day of MODIS data on Terra (February 25, 2000). The 8-day intervals for MODIS on Aqua will be the same 8-day intervals as for MODIS on Terra for the period of data overlap. It should be noted that the starting day of the 8-day interval is not reset to the first, during the rollover of a calendar month or calendar year.

The monthly product (MOD08_M3) is computed by manipulating and summarizing the daily product over a calendar month.

Definition of Daily Statistics

For the daily product, assume that $x_1, x_2, \ldots, x_n$ represent the retrieved pixel values of a Level 2 parameter over a 1° × 1° grid box, Q_i is the quality flag for each retrieved pixel value, and w_i is the weighting factor (1 for the daily case), then the simple statistics are defined as:

$$\overline{X_d} = \frac{\Sigma_i^n w_i \cdot x_i}{\Sigma_i^n w_i} \qquad (1)$$

$$\overline{X_{dQ}} = \frac{\Sigma_i^n Q_i \cdot x_i}{\Sigma_i^n Q_i} \qquad (2)$$

$$X_{std} = \frac{\Sigma_1^n (w_i \cdot x_i - w_i \cdot \overline{X_d})^2}{\Sigma_i^n w_i^2} \qquad (3)$$

$$X_{stdQ} = \frac{\Sigma_1^n (Q_i \cdot x_i - Q_i \cdot \overline{X_{dQ}})^2}{\Sigma_i^n Q_i^2} \qquad (4)$$

$$X_{min} = min\ (x_1, x_2, \ldots, x_n) \qquad (5)$$

$$X_{max} = max\ (x_1, x_2, \ldots, x_n) \qquad (6)$$

In these equations, (1) will be referred to as the "regular" mean, (2) as the QA-weighted mean, (3) as the regular standard deviation, (4) as the QA-weighted

standard deviation, (5) as the minimum, and (6) as the maximum.

The simple statistics also include daily log regular mean, log standard deviation, log QA mean, and log QA standard deviation. These log quantities are calculated as shown in equations (1-4), except that x_1, x_2, …, x_n are replaced by their logarithms.

Regression statistics, based on the pixels within each 1° × 1° grid cell, include the slope, intercept, mean squared error (MSE), and the coefficient of determination (R^2).

The histograms and joint histograms report the counts of the pixels falling into predetermined numerical intervals.

The pixel counts are used to represent the number of pixels for the parameters that do not have QA flags, while the confidence-histograms-counts is used to represent the number of counts for each parameter that fall within each QA bin (e.g., good, very good, marginal, and total).

Definition of 8-day and Monthly Statistics

The 8-day and monthly statistics are based on the daily statistics with the assumption that the daily statistics from retrieved pixels can represent the statistics of the "populations" of each 1° × 1° grid cell. In other words, it is assumed that the samples composed of retrieved pixels can represent the "populations" composed of all the pixels within each grid cell.

The simple statistics for 8-day and monthly quantities include mean, standard deviation, and minimum and maximum values of the corresponding daily means (i.e., daily mean, daily QA mean, daily log mean, and daily log QA mean).

For example, if X_{d1}, X_{d2}, …,X_{dn} are the daily means for a Level 3 parameter, then their monthly simple statistics (i.e., mean, standard deviation, minimum, and maximum) are represented by equations (1, 3, 5, and 6) with X_i replaced by X_{di}. It should be noted that in the monthly case, the weights in equations (1) and (2) are taken either as unweighted (i.e., $w_i = 1$), pixel weighted (e.g., weighted by the number of pixels over the total pixels), or fraction weighted (e.g., weighted by the cloud fraction).

The fraction statistics represent the mean and standard deviation of the daily fraction values.

The regression statistics, which include four components (slope, intercept, mean-squared-error, and the coefficient of determination), are calculated by using the daily mean values of the first parameter versus the daily mean values of the second parameter. Therefore, two daily mean time series are used to calculate monthly regression attributes.

Histogram and joint-histogram statistics represent the number of times a parameter falls into each predefined interval.

The total counts are reported. This is simply the summation of all the counts from each interval for the parameter.

The 8-day and monthly product has an additional statistical parameter called "mean daily standard deviation." This parameter is used to represent the mean values of the daily standard deviations, such as the mean of daily standard deviation, mean of daily QA standard deviation, mean of log standard deviation, and mean of log QA standard deviation. The standard deviation of the mean is used to describe the variation of a parameter around its monthly mean, while the mean of the standard deviation is used to describe the average daily variation of a parameter. For example, a parameter may have a large daily standard devia-

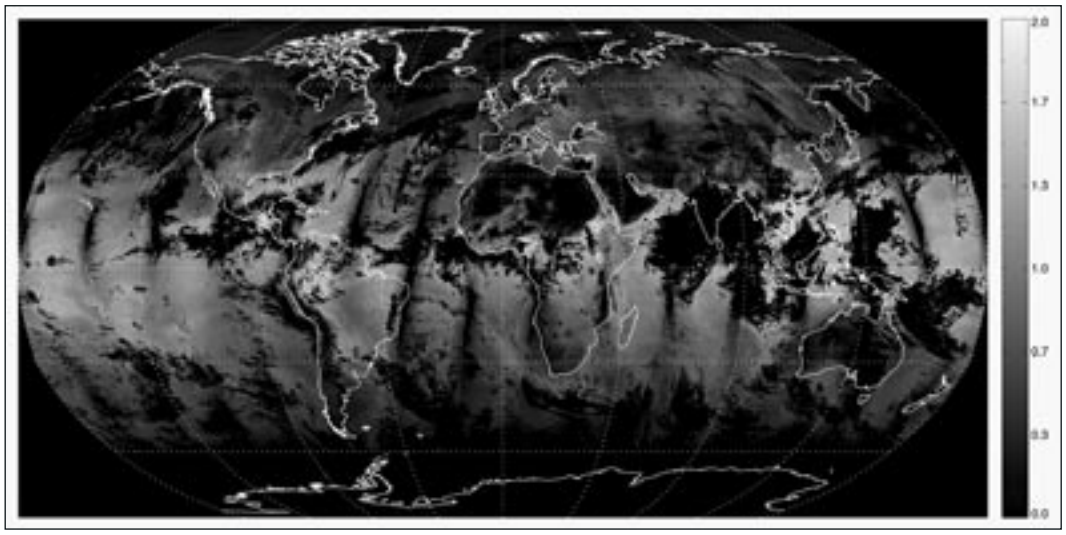

Level 3 MODIS Global Atmospheric Mean Water Vapor below 850 mb (in cm) for June 6, 2000, derived from data from the MODIS instrument on Terra.

tion on each day, but those variations may be similar to each other. In this case, the mean daily standard deviation will be large, but its standard deviation will be small.

The related MODIS data product ATBDs can be found in PDF format at http://eospso.gsfc.nasa.gov/atbd/modistables.html.

Suggested Reading

Ackerman, S. A. *et al.*, 1998.

Gao, B. C., and A.F. H. Goetz, 1990.

Gao, B. C. *et al.*, 1993a.

Gao, B. C. *et al.*, 1998.

Green, R. O., and J. E. Conel, 1995.

Gustafson, G. B. *et al.*, 1994.

Hayden, C. M., 1988.

Holben, B. N. *et al.*, 1992.

Houghton, J. T. *et al.*, 1984.

Jedlovec, G. J., 1987.

Kaufman, Y. J., and C. Sendra, 1988.

Kaufman, Y. J., and B. C. Gao, 1992.

Kaufman, Y.J., and L. A. Remer, 1994.

Kaufman, Y. J. *et al.*, 1997a,b.

King, M.D. *et al.*, 1992.

King, M. D. *et al.*, 1996.

King, M. D. *et al.*, 1998.

King, M. D. *et al.*, 1999.

Kleepsies, T. J., and L. M. McMillan, 1984.

Ma, X.L. *et al.*, 1984.

Nakajima, T. Y., and T. Nakajima, 1995.

Platnick, S. *et al.*, 2000.

Prabhakara, C. *et al.*, 1970.

Rao, C. R. N. *et al.*, 1989.

Remer, L.A. *et al.*, 1996.

Rossow, W. B., and L. C. Garder, 1993.

Saunders, R. W., and K. T. Kriebel, 1988.

Shapiro, M. A. *et al.*, 1982

Smith, W. L., and F. X. Zhou, 1982.

Smith, W. L. *et al.*, 1985.

Stowe, L. L. *et al.*, 1991.

Strabala, K. I. *et al.*, 1994.

Sullivan, J. *et al.*, 1993.

Tanré, D. *et al.*, 1997.

MODIS Level 3 Atmosphere Products Summary

Coverage: Global

Spatial/Temporal Characteristics: 1.0° latitude-longitude equal-angle grid/daily, 8-day, and monthly

Key Science Applications: Climate and ecosystem monitoring and modeling, cloud radiative properties, atmospheric properties, and atmospheric corrections

Key Geophysical Parameters: Aerosol properties, cloud radiative properties, atmospheric water vapor and temperature

Processing Level: 3

Product Type: Standard, at-launch

Maximum File Size: 411 MB (Daily Level 3), 713 MB (8-day and Monthly Level 3)

File Frequency: 1/day (Daily Level 3), 1/8-day (8-Day Level 3), 1/month (Monthly Level 3)

Primary Data Format: HDF-EOS

Browse Available: http://modis-atmos.gsfc.nasa.gov/MOD08_E3/browse_main.html

Additional Product Information: http://modis-atmos.gsfc.nasa.gov/MOD08_E3/index.html

Science Team Contact: M. D. King

MODIS Cloud Mask (MOD 35)

Product Description

The MODIS Cloud Mask product (MOD 35) is a daily, global Level 2 product generated at 1-km and 250-m (at nadir) spatial resolutions. The algorithm employs a series of visible and infrared threshold and consistency tests to specify confidence that an unobstructed view of the Earth's surface is observed. An indication of shadows affecting the scene is also provided. The 250-m cloud-mask flags are based on the visible channel data only. Radiometrically accurate radiances are required, so holes in the Cloud Mask will appear wherever the input radiances are incomplete or of poor quality.

Research and Applications

A determination of the presence of global cloudiness is essential to the MODIS mission for two reasons. First, clouds play a critical role in the radiative balance of the Earth and must be accurately described to assess climate and potential climate change. Second, the presence of cloudiness must be accurately determined to retrieve properly many atmospheric and surface parameters. For many of these retrieval algorithms even thin cirrus represents contamination.

Data Set Evolution

The MODIS cloud-mask algorithm employs a battery of spectral tests, which use methodology applied for the AVHRR Processing scheme Over cLoud Land

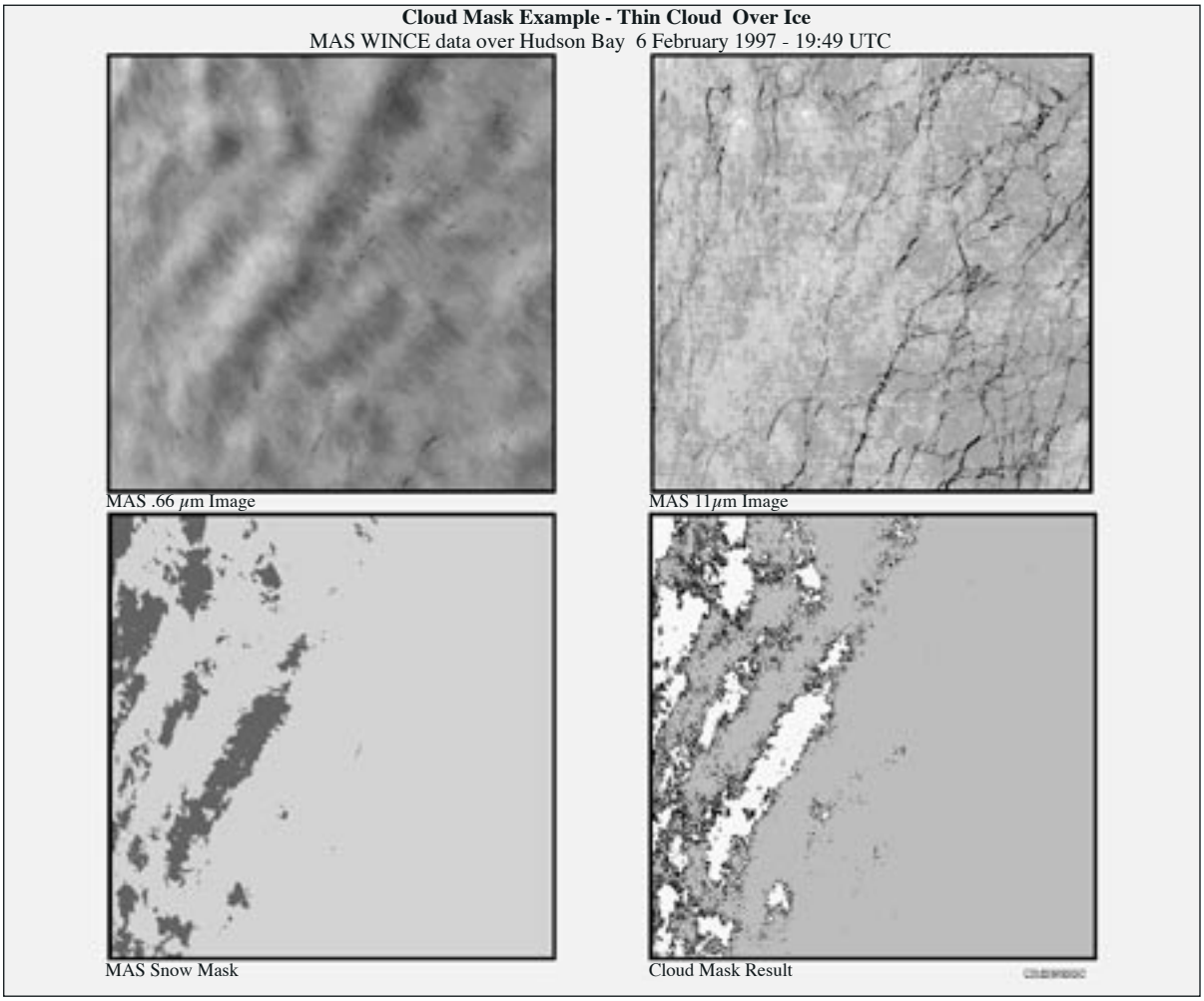

MODIS Cloud Mask for a difficult winter scene. The top two panels are MODIS Airborne Simulator (MAS) visible (0.66 μm) and infrared (11 μm) observations collected over Hudson Bay during the WINter Cloud Experiment (WINCE) on 6 February 1997. The cloud is very thin, nearly invisible in the infrared. Ice leads can be seen on the surface. The bottom left panel represents the results of a simple snow-mask algorithm that is applied as part of the cloud mask and aids in the final cloud-mask determination. The final product for this scene is shown in the bottom right panel, in which the lighter gray depicts clear conditions, white depicts clouds, and dark gray represents undecided conditions.

and Ocean (APOLLO), International Satellite Cloud Climatology Project (ISCCP), CLoud Advanced Very high resolution Radiometer (CLAVR), and Support of Environmental Requirements for Cloud Analysis and Archive (SERCAA) to identify cloudy FOVs. From these a clear-sky confidence level (high confident clear, probably clear, undecided, cloudy) is assigned to each FOV. For inconclusive results, spatial- and temporal-variability tests are applied. The spectral tests rely on radiance (temperature) thresholds in the infrared and reflectance thresholds in the visible and near-infrared. Thresholds vary with surface type, atmospheric conditions (moisture, aerosol, etc.), and viewing geometry. Along with MOD 02 calibrated radiances, a 1-km land/water mask, DEM, ecosystem analysis, snow/ice cover map, NCEP analysis of surface temperature and wind speed, and an estimate of precipitable water will be required as inputs.

Cloud-mask validation will be conducted using MAS data from several field campaigns, all-sky cameras, and comparison with NOAA operational instruments and, possibly, Terra instruments such as ASTER (see Volume 1).

The related MODIS Cloud Mask ATBD, *Discriminating Clear Sky from Cloud with MODIS*, can be found in PDF format at http://eospso.gsfc.nasa.gov/atbd/modistables.html.

Suggested Reading

Ackerman, S. A. *et al.*, 1998.

Gao, B. C. *et al.*, 1993a.

Gustafson, G. B. *et al.*, 1994.

King, M. D. *et al.*, 1992.

King, M. D. *et al.*, 1998.

Rossow, W. B., and L. C. Garder, 1993.

Saunders, R. W., and K. T. Kriebel, 1988.

Stowe, L. L. *et al.*, 1991.

MODIS Cloud Mask Summary

Coverage: Global

Spatial/Temporal Characteristics: 250 m and 1 km/daily

Key Science Applications: Cloud determination and screening, climate modeling, climate monitoring, increasing accuracy of other MODIS retrievals

Key Geophysical Parameters: Presence of cloud or shadow

Processing Level: 2

Product Type: Standard, at-launch

Maximum File Size: 48 MB

File Frequency: 288/day

Primary Data Format: HDF-EOS

Additional Product Information: http://modis-atmos.gsfc.nasa.gov/MOD35_L2/index.html

DAAC: NASA Goddard Space Flight Center

Science Team Contacts:
W. P. Menzel
S.A. Ackerman

SAGE III Aerosol and Cloud Data Products (SAGE III 01, 02)

Product Description

SAGE III Aerosol and Cloud Data Products (SAGE III 01 and 02 at Level 2) include aerosol extinction at eight wavelengths (385, 448, 521, 676, 754, 868, 1019, and 1537 nm) from the ground or opaque cloud tops to an altitude of approximately 40 km. Stratospheric optical depth is reported for each channel for which the profile base is at or below the tropopause. In addition, the presence of optically thin clouds is inferred based upon the wavelength dependence of aerosol extinction. These data are produced for each sunrise or sunset encountered by the spacecraft. Aerosol extinction profiles are determined as a residual following the clearing of previously determined contributions by molecular scattering and absorption by ozone and nitrogen dioxide.

Research and Applications

Aerosols play an essential role in the radiative and chemical processes that govern the Earth's climate. Since stratospheric aerosol loading has varied by a factor of 30 since 1979, long-term monitoring of tropospheric and stratospheric aerosols is crucial. SAGE III aerosol measurements will provide important contributions in the following areas:

- Research demonstrates that the long-term variability of aerosol abundance strongly modulates the rate of ozone destruction in the lower stratosphere (Solomon *et al.*, 1997).

- The impact of aircraft exhaust on ozone is strongly dependent on the abundance and properties of the ambient aerosol. The future of high-speed, stratospheric air travel is, in part, dependent on improved understanding of aerosol properties (Stolarski and Wesoky, 1993).

- Aerosol radiative forcing is the largest unknown in current climate models and, as a result, in predicting future climate. Accurate vertically resolved measurements of aerosol optical properties are an important element of improved climate prediction (IPCC, 1996).

- Observations from space of many geophysical properties like sea-surface temperature, vegetation, and atmospheric trace-gas species can be adversely affected by the presence of aerosols. Other EOS sensors like MODIS and MISR (on Terra) require SAGE III measurements of stratospheric aerosols to achieve optimal performance.

Clouds play a major role in determining the planet's solar and longwave energy balance and, thus, are important in governing the Earth's climate. SAGE III will provide measurements of mid- and high-level clouds including thin or "sub-visual" clouds that are not detectable by nadir-viewing passive remote sensors. These observations are important because:

- While low clouds primarily reflect incoming solar radiation back into space (acting to cool the planet), mid- and high-level clouds enhance the "greenhouse" effect by trapping infrared radiation (acting to warm the planet).

- Polar Stratospheric Clouds play a significant role in heterogeneous chemical processes that lead to stratospheric ozone destruction. The presence of thin clouds near the tropopause may also contribute to ozone loss in high and mid-latitudes.

Clouds play an important role in feedback processes (such as changes in altitude or amount of cloud) associated with climate change. Currently, neither the sign nor magnitude is known for the climatic impact of cloud response to changes in radiative processes brought about by human-caused increasing levels of greenhouse gases (like carbon dioxide) and aerosols.

Suggested Reading

IPCC, 1996.

Solomon, S. *et al.*, 1997.

Stolarski, R. S., and H. L. Wesoky, 1993.

SAGE III Aerosol and Cloud Data Products Summary

Coverage: 30 solar events per day, 15 northern high latitude, 15 southern high latitude

Spatial/Temporal Characteristics: 0.5 km vertical resolution

Key Science Applications: Aerosol trends, global change

Key Geophysical Parameters: Extinction (km^{-1})

Processing Level: 2

Product Type: Research, at-launch

Maximum File Size: 0.78 MB

File Frequency: 1/month

Primary Data Format: HDF-EOS, Big Endian IEEE Binary

Browse Available: Yes

Additional Product Information: http://eosweb.larc.nasa.gov/PRODOCS/sage3/table_sage3.html

DAAC: NASA Langley Research Center

Science Contact: L.W. Thomason

TOMS Aerosol Product

Product Description

The QuikTOMS aerosol index is formed directly from the measured radiances in two TOMS channels. Generally, positive values represent UV-absorbing aerosols while negative values represent non-absorbing aerosols. The two most important UV-absorbing aerosols are the silicate dust that originates in the Sahara each year and smoke from extensive agricultural burning in Africa and South America. Non-absorbing aerosols like sulfate particles from industrial pollution sources or from volcanoes are also seen. The identification is not perfect because of geophysical reasons (e.g., aerosol too low to the ground, or a mixture of absorbing and non-absorbing aerosols). Aerosol optical depths and single-scattering albedos can be calculated from the aerosol index, but the accuracy of the result is sensitive to the assumed parameters, particularly the height of the aerosol layer. Data coverage is the same as for the TOMS ozone product.

TOMS Aerosol Product Summary

Coverage: Global maps (90°S to 90°N)

Spatial/Temporal Characteristics: Gridded at 1° latitude × 1.25° longitude/daily

Wavelengths: Aerosol index derived from 331-nm and 360-nm backscattered radiances

Processing Level: 3

Product Type: Standard, at-launch

Maximum File Size: 0.16 MB

File Frequency: 1/day

Primary Data Format: ASCII

Browse Available: Yes

Additional Product Information: http://quiktoms.gsfc.nasa.gov

DAAC: NASA Goddard Space Flight Center

Science Team Contacts:
J. R. Herman
R. D. McPeters

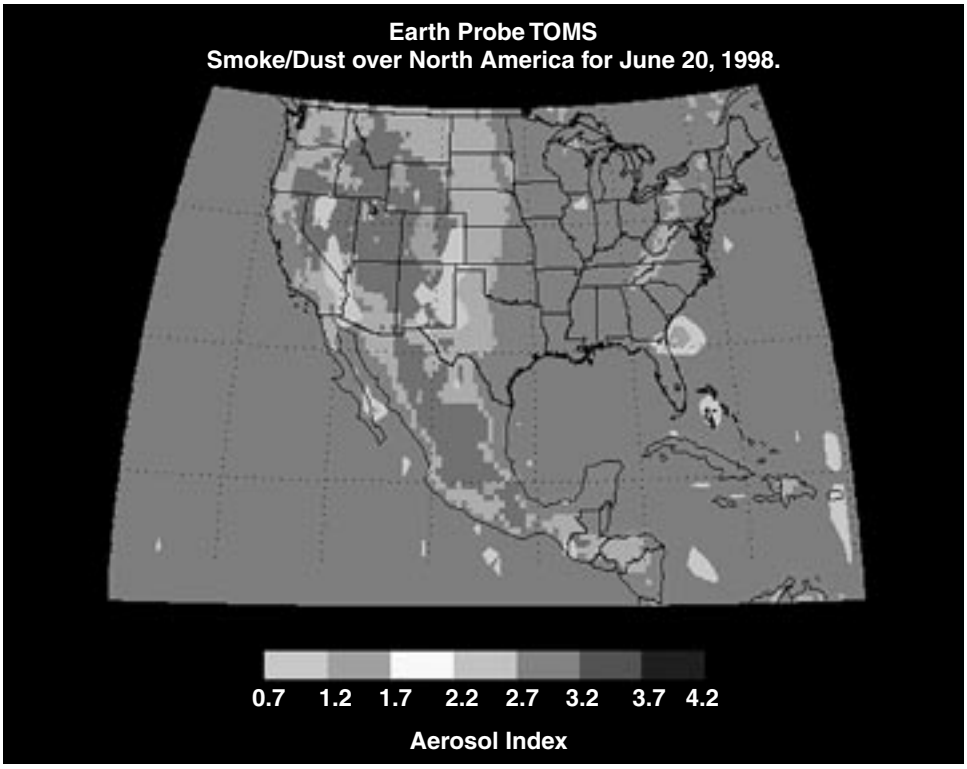

Smoke and Dust over North America on June 20, 1998, from Earth Probe TOMS data. Earth Probe TOMS detected smoke from the fires in Florida and desert dust from northern Africa advecting westward towards North America using the TOMS aerosol index. This image was created by compositing 2 days of data, with the majority of the data coming from June 20, 1998. The Aerosol data product containing measurements of UV-absorbing tropospheric aerosols from four NASA TOMS instruments (the TOMS on Nimbus-7 and Meteor 3M, using measured 340-nm and 380-nm radiances, and the TOMS on ADEOS and Earth Probe TOMS, using the 331-nm and 360-nm wavelength channels) can be used to generate daily global maps of these particles. See http://toms.gsfc.nasa.gov/ for more information.

Atmospheric Chemistry

Aqua
- AIRS
- AMSU-A
- HSB

Jason-1
- Poseidon-2

Meteor 3M
- SAGE III

QuikTOMS
- TOMS

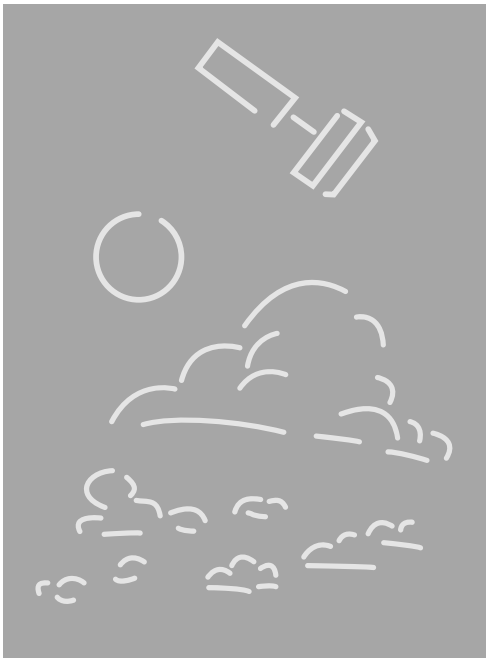

Atmospheric Chemistry – An Overview

Relationship to Global Change Issues

The distribution of chemical constituents in the atmosphere plays an important role in the radiative balance of the Earth-atmosphere system and in the long-term stability of our environment. Human activities involving combustion of fossil fuels and the use of chlorofluoromethane compounds (chlorofluorocarbons-CFCs) during the last century have led to drastic changes in the chemical composition of the Earth's atmosphere. Current estimates assuming continuous levels of human activities well into the 21st century indicate the potential for significant future global changes. It is well understood that the increases of greenhouse gases such as CO_2, N_2O, CH_4, H_2O, and others could lead to significant global warming. Similarly, the increased accumulation of CFCs has led to the formation of the northern and southern polar ozone "holes" with subsequent global ozone depletion.

Ozone is an important greenhouse gas and is at the same time critical to our environment. Stratospheric ozone, which accounts for 90% of the total atmospheric ozone, shields us from harmful solar UV radiation. Tropospheric ozone in the mid- and upper-troposphere is an important greenhouse gas. In addition, tropospheric ozone in high concentration near the Earth's surface is a health hazard. Studies of the Antarctic ozone hole have determined that ice clouds in the stratosphere (Polar Stratospheric Clouds, PSCs) are responsible for the rapid destruction of stratospheric ozone during Antarctic springtime. Similar types of ozone-destroying chemical reactions have also been found to occur with volcanic aerosols after major eruptions such as that of the Mount Pinatubo volcano in 1991.

The distribution of ozone in the atmosphere is determined by the concentration of the major reacting chemical families such as O_x, NO_x, CLO_x, and HO_x. Aerosols in the stratosphere, either in the form of PSCs or volcanic aerosols, also provide reacting surface areas for heterogeneous reactions to occur that affect the local ozone concentration. Finally, the ozone concentration also depends on the sources and sinks for ozone, the different reacting chemicals, and the dynamical circulation of the atmosphere, which continuously controls the redistribution of all the chemical species in the atmosphere. To understand fully the behavior of ozone in the atmosphere, long-term space-based observation of the different species involved in ozone chemistry, and the associated dynamical circulation of the atmosphere, will be required.

In the Aqua time frame, atmospheric chemistry measurements made by the different instruments will be focused on long-term global ozone behavior, with particular emphasis on the Arctic ozone. Latest data from the UARS instruments have indicated that atmospheric chlorine concentrations have leveled off from the continuous increases during the last few decades because of the Montreal Protocol's success in restricting the use of CFCs. Simple chemistry would indicate that the recovery of the ozone should be occurring. However, current model simulation studies have suggested that with the increase in the concentration of greenhouse gases, the recovery of the global ozone potentially could be delayed, with ozone depletion developing in the Arctic regions.

Global ozone data will be provided by the SAGE III, TOMS, and AIRS/AMSU-A/HSB instruments. SAGE III will provide additional measurements of stratospheric and upper tropospheric aerosols, PSCs, H_2O, NO_2, NO_3, and OClO. TOMS on QuikTOMS will also provide tropospheric aerosol data. AIRS/AMSU-A/HSB will additionally provide CO and CH_4 data. The above data sets will be used to monitor global ozone distribution, study Arctic ozone behavior, and provide global mapping of tropospheric ozone and aerosol distributions.

A more complete study of detailed ozone chemistry and the associated atmospheric dynamics will be possible using data sets to be acquired during the Aura (the former EOS Chemistry mission) time frame. Instruments such as HIRDLS, MLS, and OMI will provide detailed measurements of the various chemical species in the atmosphere and a detailed mapping of the dynamical circulation of the atmosphere. The TES instrument will provide measurements on most of the species involved in tropospheric ozone chemistry.

Product Overview

The data products described in this chapter are produced by the Meteor 3M/SAGE III mission, the QuikTOMS mission, the Poseidon-2 instrument on the Jason-1 spacecraft, and the AIRS/AMSU-A/HSB instrument triplet on the Aqua spacecraft. Ozone profile measurements will be provided by the SAGE III instrument on the Meteor 3M spacecraft, extending in altitude from the upper troposphere to the lower mesosphere. The SAGE III solar occultation measurements will be restricted to measurement sites near high latitudes in both northern and southern

hemispheres. SAGE III lunar measurements of ozone will have measurement sites at all latitudes.

QuikTOMS and AIRS/AMSU-A/HSB will provide total-ozone mapped products. The SAGE III ozone-profile data and the QuikTOMS and AIRS/AMSU-A/HSB total-ozone data will be used to continue the long-term global data base of ozone profiles and total burden.

For the Meteor 3M/SAGE III mission, half of the solar occultation measurements will be located in the Arctic region. The SAGE III OClO, NO_2, NO_3, and PSC measurements together with the total ozone measurements from QuikTOMS and AIRS/AMSU-A/HSB can be used to monitor the buildup of ozone destruction and recovery over the Arctic spring. The data can also be used to study the long-term changes of the Arctic ozone as the reversal of the buildup of atmospheric chlorine is in progress.

Higher in the atmosphere, the total electron content of the ionosphere will be derived from data of the Poseidon-2 radar altimeter. These data will provide a synoptic description of the ionosphere every 9.9 days and will be used to study the spatial and temporal variability of the ionosphere and its geomagnetic characteristics.

Product Interdependency and Continuity with Heritage Data

Both Meteor 3M/SAGE III and QuikTOMS are continuations of previous missions extending a heritage of ozone data products dating back more than two decades. SAGE III ozone-profile data products will be generated using algorithms similar to those used in the previous two SAGE missions, SAGE I and SAGE II. QuikTOMS ozone products will be produced using an algorithm similar to the one used for the long line of TOMS missions, beginning with the Nimbus 7 TOMS and extending to the Meteor 3 TOMS, ADEOS TOMS, and the current Earth Probe TOMS. The new ozone data sets produced by continuing past missions will be invaluable for long-term trend studies, and analysis of the long-term ozone trends will provide better understanding of the natural and human-induced changes occurring in atmospheric ozone levels.

Suggested Reading

Anderson, J. *et al.*, 2000.

Shinell, D. *et al.*, 1998.

Solomon, S. *et al.*, 1992.

Solomon, S. *et al.*, 1996.

World Meteorological Organization (WMO), 1992.

World Meteorological Organization (WMO), 1995.

AIRS/AMSU-A/HSB Trace Constituent Product (AIR 03)

Product Description

The Trace Constituent Product is included in the Level 2 retrieval data granules and is geolocated to an AMSU-A footprint.

A number of spectral features resolved by AIRS are due to strong absorption lines of trace constituents. The strength of these features depends on the vertical distribution of these gases and other factors. Examples of trace constituents that will be retrieved as research products are:

- CH_4 total burden (spatial resolution at the Earth's surface: 50-250 km)
- CO total burden (spatial resolution at the Earth's surface: approximately 50 km)

The accuracy of measuring these atmospheric constituents in the course of the retrieval of standard products will be evaluated during the first year of flight. The expected accuracy of the CO total burden, approximately 10%, is quite good compared to CO variability, whereas the expected accuracy of the CH_4 burden is not as good compared to its variability.

AIRS/AMSU-A/HSB Trace Constituent Product Summary

Coverage: Global

Spatial/Temporal Characteristics: 40.6 km FOV at nadir combined as required to coarser resolution to achieve greater signal to noise/ twice daily (daytime and nighttime)

Wavelengths: Infrared

Processing Level: 2

Product Type: Research, post-launch

Maximum File Size: 5 MB

File Frequency: 240/day

Primary Data Format: HDF-EOS

Browse Available: Yes

Additional Product Information: http://www-airs.jpl.nasa.gov/

DAAC: NASA Goddard Space Flight Center

Science Team Contact: L. L. Strow

AIRS/AMSU-A/HSB Ozone Product (AIR 08)

Product Description

The Ozone Product is included in the Level 2 retrieval data granules and is geolocated to an AMSU-A footprint.

Ozone profiles and burden are derived from AIRS infrared radiances within an AMSU-A footprint. The rms error of total ozone burden is expected to be ±10%.

Derived ozone product is:

- O_3 concentration profile (in Dobson Units for 3-5 layers)
- Total O_3 burden (Dobson Units)

AIRS/AMSU-A/HSB Ozone Product Summary

Coverage: Global

Spatial/Temporal Characteristics: 40.6 km FOV at nadir/twice daily (daytime and nighttime)

Wavelengths: Infrared

Processing Level: 2

Product Type: Research, at-launch

Maximum File Size: 5 MB

File Frequency: 240/day

Primary Data Format: HDF-EOS

Browse Available: Yes

Additional Product Information: http://www-airs.jpl.nasa.gov/

DAAC: NASA Goddard Space Flight Center

Science Team Contacts: L. L. Strow, J. Susskind

Poseidon-2 Total Electron Content

Product Description

This Level 2 product provides the measurement of the total electron content (TEC) of the ionosphere (in electrons/m^2) made by the Poseidon-2 radar altimeter on board Jason-1. The measurement is repeated every 9.9 days along a set of fixed ground tracks. The satellite makes 127 revolutions of the Earth every 9.9 days. The coverage of the measurement is limited from 66°S to 66°N due to the 66° inclination of the satellite's orbit plane. The longitudinal distance between the ground tracks is [315· cos(latitude)]km, i.e., 315 km at the equator, 223 km at 45°, and 128 km at 66°. Two kinds of product are available: The Interim Geophysical Data Record (IGDR) is available 3 days after the data collection, while the GDR, based on a more precisely determined orbit, is available 30 days after the data collection.

Research and Applications

The TEC measurements provide a synoptic description of the ionosphere on global scales (although restricted to 66°S - 66°N) every 9.9 days. This information is useful for the study of the spatial and temporal variability of the ionosphere and its geomagnetic characteristics. For example, studies based on the TOPEX/Poseidon data have been performed on the longitude structure of the ionosphere F region, including the quasi 2-day oscillation. Climatologies of the TEC have also been produced. TEC is also a useful indicator for the geomagnetic activities that influence telecommunication.

Data Set Evolution

The radar range between the spacecraft and sea surface is measured by the radar altimeter at two frequencies: 13.575 and 5.3 GHz. The differences in the measurements between the two channels are used to compute the range delay of the radar signals caused by the ionospheric free electrons as well as the TEC. The effects of other factors causing range errors, such as the sea-state biases, are corrected for before the computation of the TEC. The primary heritage for the Poseidon-2 TEC product is the corresponding product derived from the TOPEX/Poseidon dual-frequency altimeter, launched in 1992.

Suggested Readings

Codrescu, M. V. *et al.*, 1999.

Forbes, J. M. *et al.*, 1997.

Imel, D., 1994.

Vladimer, J. A. *et al.*, 1999.

Poseidon-2 Total Electron Content Summary

Coverage: Ocean areas from 66°S to 66°N

Spatial/Temporal Characteristics: 6.2-km resolution along-track every 9.9 days [315·cos (latitude) km longitudinal track spacing]

Key Science Applications: Variability and climatology of the ionosphere

Key Geophysical Parameters: Total electron content of the ionosphere

Processing Level: 2

Product Type: Standard, at-launch

Maximum File Size: 1.5 MB

File Frequency: 25/day

Primary Data Format: Binary

Browse Available: No

Additional Product Information: http://www-aviso.cnes.fr

DAAC: Jet Propulsion Laboratory

Science Team Contacts:
L.-L. Fu
Y. Menard

SAGE III NO_2, NO_3, O_3, and OClO Data Products (SAGE III 04, 05, 06, 07)

Product Description

The SAGE III reactive species profiles consist of the vertical density profiles of nitrogen dioxide (SAGE III 04), nitrogen trioxide (SAGE III 05), ozone (SAGE III 06), and the chlorine dioxide dimer (SAGE III 07). The ozone and nitrogen dioxide products are produced during both solar- and lunar- occultation events, while the nitrogen trioxide and chlorine dioxide species, which exist in measurable quantities only at night, are produced for lunar-occultation events only. Solar Level 2 products are produced with a 0.5-km vertical resolution, while lunar Level 2 products are produced with a 1-km vertical resolution. Ozone is retrieved in the altitude range from 6 km to 85 km, NO_2 from the tropopause to 50 km, NO_3 from 20 km to 55 km, and OClO in the lower stratosphere wherever it is sufficiently enhanced (winter polar vortex).

These products are measured using the Occultation Technique where the spectral extinction of the atmosphere is observed in the 290-1500 nm region. The unique spectral signature of each of these species is used to determine the slant-path-column abundance along the line of sight. This slant-column abundance profile is then inverted to obtain a vertical-density profile.

Research and Applications

The calibration insensitivity of the occultation technique allows SAGE III species measurements to be ideally suited for monitoring the atmosphere for long-term changes or trends. Like the predecessor SAGE I and II measurements, SAGE III results will be useful in measuring the recovery of stratospheric ozone levels as anthropogenic perturbations to the chemistry of the atmosphere recover to normal levels in response to action by the international community.

The high vertical resolution of the measurements will also be beneficial to the modeling community. In addition to ozone, SAGE III also measures water vapor, aerosol extinction, pressure, and temperature. Over suitable time scales these can be used as dynamical tracers in modern analyses using transformation to potential vorticity coordinates. This allows the relatively sparse direct coverage to be greatly expanded with the addition of dynamical observations.

SAGE III NO_2, NO_3, O_3, and OClO Data Products Summary

Coverage: 30 solar events per day, 15 northern high latitude, 15 southern high latitude; up to 30 lunar events per day ranging over all latitudes

Spatial/Temporal Characteristics: 0.5 km vertical resolution for species derived from solar occultation events and 1 km vertical resolution for species derived from lunar occultation events

Key Science Applications: Long-term trends and interannual variability in ozone, nitrogen dioxide; ozone-loss studies incorporating observations of reactive chlorine, reactive nitrogen, aerosols, and PSCs; chemical studies of reactive nitrogen in the middle stratosphere

Key Geophysical Parameters: Vertically resolved density profiles of ozone, nitrogen dioxide, nitrogen trioxide, and chlorine dioxide

Processing Level: 2

Product Type: Standard, at-launch

Maximum File Size: 0.05 MB

File Frequency: 196/week

Primary Data Format: HDF-EOS, Big Endian IEEE Binary Binary

Browse Available: Yes

Additional Product Information: http://eosweb.larc.nasa.gov/PRODOCS/sage3/table_sage3.html

DAAC: NASA Langley Research Center

Science Team Contact: J. M. Zawodny

TOMS Ozone Product

Product Description

QuikTOMS measurements of backscattered ultraviolet sunlight are used to derive total-column ozone. QuikTOMS is in a polar sun-synchronous orbit with approximately 10:30 AM local equator crossing time. TOMS scans to the left and right of the orbital track to give complete coverage of the sunlit Earth on a daily basis. The instrument FOV at nadir is approximately 40 km square. The data are averaged into a 1°-latitude by 1.25°-longitude uniform grid.

Total column ozone is derived using an algorithm identical to the one used for the Nimbus 7 and Earth Probe TOMS instruments. A radiative-transfer model is used to calculate backscattered radiances as a function of total ozone, latitude, viewing geometry, and reflecting surface conditions. Total column ozone can then be derived by comparing measured radiances with theoretical radiances calculated for the conditions of the measurement and finding the value of ozone that gives a computed radiance equal to the measured radiance.

TOMS Ozone Product Summary

Coverage: Global maps (90°S-90°N)

Spatial/Temporal Characteristics: Gridded at 1° latitude × 1.25° longitude/daily

Wavelengths: Ozone is derived by differential absorption from wavelength pairs: A 312 /331 nm, B 317/331 nm, C 323/331 nm

Processing Level: 3

Product Type: Standard, at-launch

Maximum File Size: 0.16 MB

File Frequency: 1/day

Primary Data Format: ASCII

Browse Available: Yes

Additional Product Information: http://quiktoms.gsfc.nasa.gov

DAAC: NASA Goddard Space Flight Center

Science Team Contact: P. K. Bhartia

Atmospheric Temperatures

Aqua
- AIRS
- AMSU-A
- HSB
- MODIS

Meteor 3M
- SAGE III

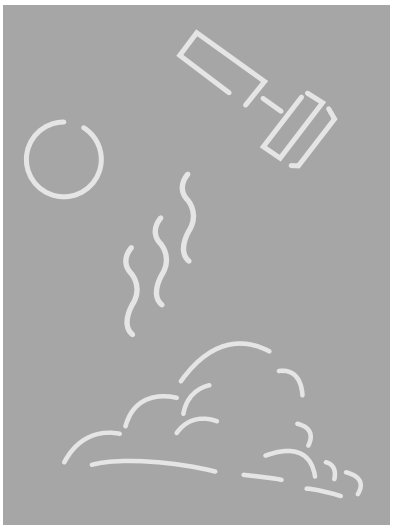

Atmospheric Temperatures – An Overview

Relationship to Global Change Issues

The atmosphere exhibits significant variations in temperature and pressure with altitude. In fact, the standard layers of the atmosphere are defined based on their vertical temperature profiles. The lowest 10-15 km of the atmosphere, where temperatures predominantly decrease with height, is called the troposphere, and the region from altitudes of about 15-50 km, where temperatures increase or stay steady with height, is called the stratosphere. The boundary between the troposphere and the stratosphere is the tropopause.

Upper-air temperature is an essential atmospheric parameter that plays a major role in determining the global circulation of the atmosphere and directly influences the hydrological cycle. Thus, upper-air temperature is a key input to global climate models. Tropospheric and stratospheric temperatures are central to the problem of climate warming both because tropospheric temperatures are the atmospheric temperatures of most immediate importance to life at the surface and because general circulation models (GCMs) predict that temperature changes with enhanced concentrations of greenhouse gases will have a characteristic profile, with warming in the troposphere and cooling in much of the stratosphere. Cooler stratospheric conditions are an expected consequence of the increased trapping of terrestrial radiation in the troposphere. Accurate knowledge of the fluctuations in stratospheric temperature on a global scale is also necessary to understand the recovery of the ozone layer, as most ozone depletion occurs in the lower portion of the stratosphere (15-25 km).

Three-dimensional wind and temperature fields are the highest priority data for understanding atmospheric dynamics and initializing forecast models. Prior to satellite observations, characterizing the global temperature distribution was greatly hindered by notable gaps over the oceans in the surface-based observation network. With satellites, those gaps are now filled, although a problem that remains even with satellites is the difficulty in inferring sharp temperature inversions.

Even in the absence of complete wind observations, model-based data-assimilation systems can provide dynamically consistent and statistically optimal global data sets at frequent time intervals. The data-assimilation system organizes the observations from many diverse instrument sources at different locations and times into a single consistent data product, complements the observations by propagating information from observed into unobserved regions and times, and supplements the observations by providing estimates of quantities that are difficult or impossible to measure directly.

Significant improvement in short-term weather forecasting skill is expected as the temperature profile data used as inputs to the weather forecast models improve well beyond the accuracy of present infrared sounders, which is about 2.5 K at a vertical resolution on the order of 5 km.

Product Overview

The AIRS/AMSU-A/HSB complement on the Aqua spacecraft will provide atmospheric temperature profiles, available globally, twice per day, under all cloud conditions in 50-km ground footprints. The anticipated accuracy of the temperature profiles is given as a global root-mean-square (rms) of 1 K per 1-km thick layers, matching that of radiosondes. This accuracy should lead to improved climate modeling and a substantial increase in the mid- and long-range weather forecast skill. AIRS/AMSU-A/HSB data will be assimilated operationally within 3 hours into the forecast GCM by the weather prediction centers in the U.S. (National Centers for Environmental Prediction, NCEP) and Europe (European Center for Medium-Range Weather Forecasts, ECMWF).

MODIS Atmospheric Profiles (MOD 07, 08) will provide atmospheric temperature information, as well as atmospheric stability, water vapor, and total ozone burden. Four assimilated products will be available in the Terra/Aqua timeframe. The SAGE III Temperature Products (SAGE III 08) will provide profiles of temperature and pressure derived from measurements of the oxygen A-band absorption feature near 762 nm.

Product Interdependency and Continuity with Heritage Data

Atmospheric temperature profiles have been obtained from several satellite instruments, most relevantly the Tiros Operational Vertical Sounder (TOVS) system on NOAA operational satellites since 1979 and the Geostationary Operational Environmental Satellite (GOES) VISSR Atmospheric Sounder since 1978. The TOVS system contains a High Resolution Infrared Radiation Sounder (HIRS and the follow-on HIRS2) and a microwave sounder, the latter originally as a 4-channel Microwave Sounding Unit (MSU) and subsequently as a 20-channel Advanced Microwave Sounding Unit (AMSU) on NOAA-K. The HIRS2/

MSU temperature data have been assimilated into numerical weather forecast models with significant improvements in forecast skill. Similar assimilation of the AIRS/AMSU-A/HSB temperature and humidity data into forecast models, along with surface winds from QuikScat, is critical to the full utilization of these data.

Suggested Reading

Daley, R., 1991.

Goldberg, M. D., and L. M. McMillin, 1999.

McMillin, L. M. *et al.*, 1995.

Pfaendtner, J. *et al.*, 1995.

Schubert, S. D. *et al.*, 1993.

Strow, L. L. *et al.*, 1998.

Suarez, M. *et al.*, 1994.

Susskind, J. *et al.*, 1998.

AIRS/AMSU-A/HSB Atmospheric Temperature Product (AIR 07)

Product Description

The AIRS Atmospheric Temperature Product is a vertical profile of temperature geolocated to an AMSU-A footprint and is included in the Level 2 retrieval data granules.

The product consists of temperatures at discrete pressures between the surface and 1 mb. Combined IR/MW temperature retrievals are expected to have an accuracy of better than l K in the rms sense for layer mean temperature in each 1-km layer between the surface and 200 mb, each 2-km layer between 200 mb and 100 mb, and each 4-km layer from 100 mb to 1 mb. The troposphere height is also to be reported.

Derived temperature products are:

- Atmospheric temperature profile for 30 levels
- Tropopause height
- Stratopause height

Research and Applications

The temperature profile is an important parameter for data assimilation to improve numerical weather prediction. Surface air temperatures are important for energy exchange between the Earth's surface and the atmosphere. All temperatures are important to monitor interannual variability and whether any significant global or regional temperature trends exist.

The AIRS Temperature Product is a significant improvement over what is achievable using current HIRS3/AMSU data or what can be expected from MODIS data.

Data Set Evolution

The AIRS Team algorithm comprises three sequential series of steps. The first series of steps creates the microwave product based exclusively on AMSU-A/HSB observations. This provides a first guess for surface skin temperature, microwave spectral surface emissivity, atmospheric temperature and moisture profiles, and atmospheric liquid-water profile to be used in subsequent steps. The liquid-water profile is not subsequently modified and is an AIRS team product on an AMSU-A footprint basis.

The next series of steps begins with a physically based cloud-clearing algorithm to give cloud-cleared AIRS radiances for all channels, that is, an estimate of what the radiances would have been if no clouds were present within the AMSU-A footprint. The cloud-cleared radiances are used to produce the first AIRS/AMSU-A product, which uses a statistical regression step followed by a linearly constrained physical retrieval step. These steps are rapid and can be used to produce reasonably accurate AIRS/AMSU-A products that are practical for operational numerical weather prediction use in a near-real-time mode.

The last sequence of steps produces the AIRS final product, based on a number of fully non-linear physical retrieval steps for surface skin temperature, spectral surface emissivity, temperature profile, water-vapor profile, and cloud parameters, and utilizing improved clear-column radiances computed iteratively.

Selected IR channels are used to produce the temperature profiles, primarily in the spectral regions 665 -750 cm^{-1} and 2378-2400 cm^{-1}.

The final product steps produce more-refined products, including product error estimates, and have improved rejection capability, compared to the first product. In the event a profile is rejected, a new retrieval is produced, starting from the microwave product initial guess and utilizing the AMSU-A/HSB channels together with those AIRS channels that are insensitive to cloud effects.

Data validation will be accomplished through comparison of the retrieved temperature profiles with simultaneous *in situ* measurements via radiosondes, dropsondes, lidars, and radio-acoustic sounding systems at selected DoE ARM/CART sites and other EOS-dedicated validation sites. Vicarious validation will be accomplished through comparison with MODIS, TOVS, and GPS retrievals.

Suggested Reading

Anyamba, E., and J. Susskind, 1998.

Aumann, H. H., and C. Miller, 1995.

Aumann, H. H. *et al.,* 1999.

Chahine, M. T. *et al.,* 1997a.

Fleming, H. F. *et al.*, 1986.

Haskins, R. D. *et al.*, 1997.

Hofstadter, M. *et al.*, 1999.

Janssen, M. A., 1993.

Lakshmi, V. *et al.*, 1998.

Lambrigtsen, B., 1996.

Rosenkranz, P. W., 1995.

Smith, W. L., and H. M. Woolf, 1976.

Susskind, J. *et al*., 1993.

Susskind, J. *et al*., 1998.

AIRS/AMSU-A/HSB Atmospheric Temperature Product Summary

Coverage: Global

Spatial/Temporal Characteristics: Resolution of AMSU-A FOV (40.6 km at nadir); 1-km vertical levels, surface-to-200- mb pressure level, coarser level separation above 200 mb/twice daily (daytime and nighttime)

Key Science Applications: Characterization of the atmosphere; atmospheric dynamics; climatology

Key Geophysical Parameters: Atmospheric temperature profile; tropopause height

Processing Level: 2

Product Type: Standard, at-launch

Maximum File Size: 5 MB

File Frequency: 240/day

Primary Data Format: HDF-EOS

Browse Available: Yes

Additional Product Information: http://www-airs.jpl.nasa.gov/

DAAC: NASA Goddard Space Flight Center

Science Team Contact: J. Susskind

MODIS Atmospheric Profiles (MOD 07)

Product Description

The MODIS Atmospheric Profiles product (MOD 07) consists of several parameters: total-ozone burden, atmospheric stability, temperature and moisture profiles, and atmospheric water vapor. All of these parameters are produced day and night for Level 2 at 5 × 5 1-km pixel resolution when at least 9 FOVs are cloud-free.

The MODIS total-ozone burden is an estimate of the total column tropospheric and stratospheric ozone content. The MODIS atmospheric stability consists of three daily Level 2 atmospheric stability indices. The Total Totals (TT), the Lifted Index (LI), and the K index (K) are each computed using the infrared temperature- and moisture-profile data, also derived as part of MOD 07. The MODIS temperature and moisture profiles are produced at 20 vertical levels for temperature and 15 levels for moisture. A simultaneous direct physical solution to the infrared radiative-transfer equation in a cloudless sky is used. The MODIS atmospheric water-vapor product is an estimate of the total tropospheric column water vapor made from integrated MODIS infrared retrievals of atmospheric moisture profiles in clear scenes.

Research and Applications

Total-column ozone estimates at MODIS resolution are required by MODIS investigators developing atmospheric correction algorithms. This information is crucial for accurate land- and ocean-surface-parameter retrievals. Furthermore, strong correlations have been found to exist between the meridional gradient of total ozone and the wind velocity at tropopause levels, providing the potential to predict the position and intensity of jet streams. Total-column ozone monitoring is also important due to the potential harm to the environment caused by anthropogenic ozone depletion.

Atmospheric instability measurements are predictors of convective-cloud formation and precipitation. The MODIS instrument offers an opportunity to characterize gradients of atmospheric stability at high resolution and greater coverage. Radiosonde-derived stability indices are limited by the coarse spacing of the point-source data, too coarse to pinpoint local regions of probable convection.

Atmospheric temperature and moisture sounding data at high spatial resolution from MODIS and high- spectral-resolution sounding data from AIRS will provide a wealth of new information on atmospheric structure in clear skies. The profiles will be used to correct for atmospheric effects for some of the MODIS products (e.g., sea-surface and land-surface temperatures, ocean aerosol properties, water-leaving radiances, and PAR) as well as to characterize the atmosphere for global greenhouse studies.

Total-column precipitable-water estimates at MODIS resolution are required by MODIS investigators developing atmospheric-correction algorithms. This information is crucial for accurate land and ocean surface-parameter retrievals. MODIS will also provide finer horizontal-scale atmospheric water-vapor gradient estimates than are currently available from the POES satellites.

Data Set Evolution

One of two ozone-retrieval methods developed using the HIRS will be chosen as best suited for application with MODIS data. Both use a first-guess perturbation method and radiances from MODIS channel 30 (9.6 μm) to solve the radiative-transfer equation. The perturbations are with respect to some *a priori* conditions that may be estimated from climatology, regression, or more commonly, from an analysis or forecast provided by a numerical model. The MODIS cloud-mask product (MOD 35) will also be used to screen for clouds.

Atmospheric-stability estimates will be derived from the MODIS temperature and moisture retrievals contained in this product. Layer temperature and moisture values may be used to estimate the temperature lapse rate of the lower troposphere and the low-level moisture concentration.

Temperature and moisture profile retrieval algorithms are adapted from the International TOVS Processing Package (ITPP), taking into account MODIS' lack of stratospheric channels and far higher horizontal resolution. The profile retrieval algorithm requires calibrated, navigated, and coregistered 1-km FOV radiances from MODIS channels 20, 22-25, 27-29, and 30-36. The MODIS cloud mask (MOD 35) is used for cloud screening. The algorithm also requires NCEP model analyses of temperature and moisture profiles as a first guess and an NCEP analysis of surface temperature and pressure.

Several algorithms for determining atmospheric water vapor, or precipitable water, exist. The most direct calculations are done by integrating the moisture profile through the atmospheric column. Other, split-window methods also exist. This class of tech-

niques uses the difference in water-vapor absorption between channel 31 (11 μm) and channel 32 (12 μm).

Data validation will be conducted by comparing results to *in situ* radiosonde measurements, NOAA HIRS operational retrievals, GOES sounder operational retrievals, NCEP analyses, and retrievals from the AIRS/AMSU-A/HSB instrument package on the Aqua platform. A field campaign using a profiler network in the central U.S. and the MAS-equipped aircraft will be initiated in the first year after launch. Quality control will consist of manual and automatic inspections, with regional and global mean temperatures at 300, 500, and 700 hPa monitored weekly, along with 700 hPa dew-point temperatures. For total ozone, data validation will consist of comparing the TOMS, as well as operational NOAA ozone, estimates from HIRS to the MODIS retrievals.

Suggested Reading

Hayden, C. M., 1988.

Houghton, J. T. *et al*., 1984.

Jedlovec, G. J. 1987.

Kleepsies, T. J., and L. M. McMillan, 1984.

Ma, X. L. *et al*., 1984.

Prabhakara, C. *et al*., 1970.

Shapiro, M. A. *et al*., 1982.

Smith, W. L., and F. X. Zhou, 1982.

Smith, W. L. *et al*., 1985.

Sullivan, J. *et al*., 1993.

(See figure on pg. 84.)

MODIS Atmospheric Profiles Summary

Coverage: Global, clear-sky only

Spatial/Temporal Characteristics: 5 km

Key Science Applications:
- Ozone: atmospheric correction, prediction of cyclogenesis, anthropogenic ozone depletion
- Atmospheric stability: atmospheric correction, prediction of convective cloudiness and precipitation, characterization of the atmosphere
- Soundings: atmospheric-correction- algorithm development and use, characterization of the atmosphere
- Total-column water vapor: atmospheric-correction algorithm development and use, characterization of the atmosphere

Key Geophysical Parameters: Total-column ozone, atmospheric stability (Total Totals, Lifted Index, and K index), atmospheric profiles of temperature and moisture, atmospheric total-column water vapor

Processing Level: 2

Product Type: Standard, at-launch

Maximum File Size: 28 MB

File Frequency: 288/day

Primary Data Format: HDF-EOS

Browse Available:
http://modis-atmos.gsfc.nasa.gov/MOD08_E3/browse_main.html

Additional Product Information:
http://modis-atmos.gsfc.nasa.gov/MOD07_L2/index.html

DAAC: NASA Goddard Space Flight Center

Science Team Contact:
W. P. Menzel

SAGE III Temperature and Pressure Data Products (SAGE III 08)

Product Description

The SAGE III Temperature and Pressure Data Products (SAGE III 08 at Level 2) consist of profiles of temperature and pressure derived from measurements of the oxygen A-band absorption feature near 762 nm. The profiles extend from an altitude of 0.5 km (or cloud top) up to an altitude of 85 km in 0.5-km increments. In addition, the temperature profiles are also reported on pressure surfaces from 1000 hPa to 0.004 hPa. Associated temperature and pressure uncertainty profiles are also produced.

Research and Applications

SAGE III temperature measurements will provide a unique data set for monitoring and understanding atmospheric temperature changes. In particular, the long-term stability and self-calibration capabilities of SAGE III may permit the detection of trends in stratospheric and mesospheric temperature that would be important diagnostics of climate change. SAGE III temperature and pressure measurements will provide important contributions in the following areas:

- SAGE III temperature measurements in the upper stratosphere and mesosphere will be the only source of long-term temperature measurements in this region of the atmosphere.
- Short-term temperature variations are important in understanding the photochemical interactions and feedback in the formation and destruction of stratospheric ozone.
- SAGE III temperature measurements will allow the monitoring of periodic temperature changes, such as those associated with the solar cycle and quasi-biennial oscillation, and the effects of radiative forcing by aerosols.
- An improved temperature climatology will lead to better radiative-dynamical-chemical general circulation models and enhance the understanding of the interactions between temperature and pressure and the state of the climate system.
- Temperature and pressure measurements are essential to SAGE III for computing molecular scattering and the retrieval of mass mixing ratios of gaseous species on pressure surfaces.

SAGE III Temperature and Pressure Data Products Summary

Coverage: 30 solar events per day, 15 northern high latitude, 15 southern high latitude

Spatial/Temporal Characteristics: 0.5 km vertical resolution/weekly

Key Science Applications: Monitoring and understanding atmospheric temperature changes

Key Geophysical Parameters: Profiles of temperature and pressure

Processing Level: 2

Product Type: Standard, at-launch

Maximum File Size: 0.05 MB

File Frequency: 196/week

Primary Data Format: Binary

Browse Available: Yes

Additional Product Information: http://eosweb.larc.nasa.gov/PRODOCS/sage3/table_sage3.html

DAAC: NASA Langley Research Center

Science Team Contact: M. C. Pitts

Winds

Aqua
- AMSR-E

Jason-1
- Poseidon-2

QuikScat
- SeaWinds

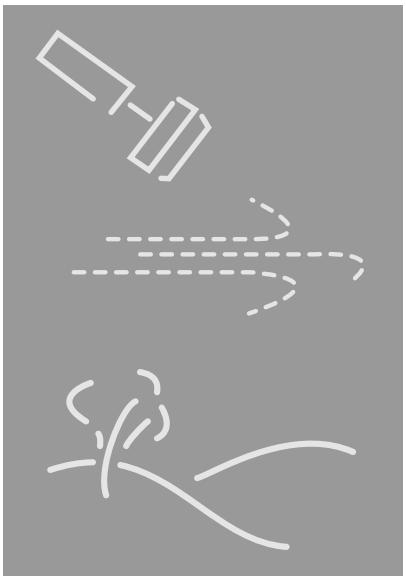

Winds – An Overview

Relationship to Global Change Issues

Winds are critical to transports of heat and chemical constituents within the atmosphere and thus are critical to understanding atmospheric dynamics and climate change. For example, stratospheric wind estimates provide information about the sources, sinks, and transport mechanisms of stratospheric trace gases important to resolving global warming issues. Winds are also a vehicle for addressing various multidisciplinary questions involving the global biogeochemical and hydrologic cycles. The 1991-1992 El Niño was the first El Niño to be predicted in advance, based on winds as the driving force of a global circulation model. Because wind field profiles have been primarily measured by land-based rawinsondes, measurements have been too irregularly distributed to provide adequate data for global climate studies.

Areas largely devoid of data, especially prior to satellites, include, importantly, oceanic areas (covering 70% of the Earth's surface), and some less-developed southern hemisphere land areas. Wind measurements historically have been inferred from satellite cloud-tracking imagery or computed from pressure gradients. Tracking of clouds by satellites provides estimates of low- and high-level winds over portions of the Earth, but uncertainties in heights introduce errors, and there are many gaps in the data. The desired accuracy is ±10%, which corresponds to about 1 m/s in the lower troposphere and 5 m/s in the upper troposphere. Even with these data, however, there are significant gaps in global coverage.

Knowledge of wind velocity over the ocean is of critical importance for understanding and predicting many oceanographic, meteorological, and climate phenomena. Wind stress is the single largest source of momentum to the upper ocean, and winds drive oceanic motions on scales ranging from surface waves to basin-wide current systems. Winds over the oceans regulate the crucial coupling between the air and the sea that maintains global and regional climate, by modulating air-sea fluxes of heat, moisture, and chemical substances. Measurements of surface-wind velocity can be assimilated into regional and global numerical weather prediction systems, thereby extending and improving our ability to predict future weather patterns on many scales.

Until the advent of satellite-borne measurements, available ocean-wind-velocity data sets have been severely deficient in coverage and accuracy. Ship reports are geographically and phenomenologically biased and are inaccurate owing to untrained observers, poor instrumentation, badly placed anemometers, inadequate correction for ship's velocity, and data transcription and transmission errors (Pierson, 1990). Measurements from moored meteorological buoys are highly accurate, but they are few in number and tend to be concentrated in near-coastal regions in the northern hemisphere.

Only satellite-borne instruments can acquire wind data with global coverage, high spatial resolution, and frequent sampling. Wind speeds over ocean areas can be derived from both passive-microwave and active-microwave instruments. However, satellite-borne radar scatterometers are the only remote sensing systems presently capable of providing accurate, frequent, high-resolution measurements of ocean near-surface wind speed and direction in both clear-sky and cloudy conditions. The scatterometer measurements, however, are highly indirect, and significant processing is required to estimate near-surface wind velocity from the backscattered power measured directly by the scatterometer.

A Ku-band scatterometer, "SeaWinds," is now flying on the QuikScat platform, and another version of SeaWinds will be flying on the ADEOS II Japanese spacecraft during the EOS era. These two instruments will provide accurate multiple measurements of the radar cross-section of the ocean surface, leading to estimates of near-surface oceanic wind velocity and related quantities such as the horizontal component of wind stress.

Product Overview

The AMSR-E surface wind product provides wind speeds over the oceans in terms of a neutral stability wind at 10 m above the surface, doing so with a spatial resolution of 20 km. The Poseidon-2 product provides wind speeds between 66°N and 66°S, at a resolution of 6.2 km. SeaWinds provides vector winds, not simply wind speeds, over the ice-free portions of the global oceans, at a 25-km resolution.

Product Interdependency and Continuity with Heritage Data

The AMSR-E wind-speed retrieval algorithm builds on earlier research using SMMR, SSM/I, and TMI data. The AMSR-E retrievals should be more accurate than those from SSM/I because of the AMSR-E having two additional sets of dual-polarization channels at 6.9 and 10.7 GHz.

The primary heritage sequence for SeaWinds dates back to the SEASAT-A Satellite Scatterometer (SASS) instrument, which was the first dedicated spaceborne

microwave scatterometer. It flew on the SEASAT mission from June to October, 1978, and operated at a frequency of 14.6 GHz. The SASS instrument used four fan-beam antennas to illuminate measurement swaths on each side of the spacecraft ground track, with ground footprints oriented at angles of ±45° and ±135° with respect to the subsatellite track. As only two azimuthal measurements were obtained at each location in the swaths, it was not possible to determine a unique wind direction based on scatterometer data alone.

Although there were many difficulties associated with the processing and interpretation of SASS data, the SASS instrument represented a milestone in scatterometer development and a positive scientific contribution to oceanographic and meteorological research. The SASS measurements proved to be an invaluable set of realistic data for the development and testing of wind-retrieval and ambiguity-removal algorithms. Although the SEASAT data set was temporally short by oceanographic standards, a wide range of scientific studies has been conducted using vector wind information calculated from SASS measurements.

The European Space Agency (ESA) ERS-1 mission was launched in July 1991, carrying a C-band (5.3 GHz) Active Microwave Instrument (AMI), which operates both as a synthetic aperture radar (SAR) and as a scatterometer. In scatterometer mode, the ERS-1 AMI illuminates a 500-km-wide swath on the starboard side of the spacecraft. Although fan-beam antennas are used to achieve the broad swath illumination for the AMI as with SASS, the AMI utilizes range gating, rather than Doppler filtering, to achieve along-beam spatial resolution. Within the measurement swath, the ERS-1 AMI illuminates footprints oriented at 45°, 90°, and 135° with respect to the satellite ground track; each location in the swath is therefore imaged from three separate viewing geometries. This "3-look" imaging strategy successfully reduces the 4-fold directional ambiguity to a 2-fold ambiguity for most measurements, with directions approximately 180° apart. This reduction in directional ambiguity greatly simplifies the processing required to select a single, unique direction.

The ERS-1 AMI has operated nearly continuously since early 1992 and has provided the longest record of global scatterometer data yet obtained. Although its coverage is limited by its single-swath design and narrow swath width, and there appears to be a lack of wind-velocity sensitivity at C-band (especially at low wind speeds and small incidence angles), the ERS-1 AMI vector wind data are being actively studied by the oceanographic, meteorological, and air-sea-interaction research communities.

Both C- and Ku-band scatterometers flew in the mid-1990s before the launch of the EOS SeaWinds instrument on QuikScat. The ERS-2 mission began in early 1995 and carries a 3-look, single-swath, C-band AMI identical to that on ERS-1. The planned overlap between the ERS-1 and ERS-2 missions should allow on-orbit cross-calibration of the two instruments, resulting in a 5-7-year data set of consistent winds from C-band scatterometers.

The NASA Scatterometer (NSCAT) instrument was implemented as a follow-on to SASS. While based heavily on SASS heritage, NSCAT had significant design enhancements that allowed it to obtain more-accurate and extensive vector wind measurements. Like SASS, NSCAT operated at Ku-band and used fan-beam antennas to allow measurements to be obtained in two, ~600-km-wide swaths. NSCAT flew in a polar orbit as a NASA contribution to the Japanese ADEOS mission, which launched in early 1996.

Suggested Reading

Naderi, F. M. *et al.*, 1991.

Pierson, W. J., 1990.

AMSR-E Sea Surface Wind Speed

Product Description

The Sea Surface Wind Speed derived from the AMSR-E microwave radiances is in terms of a neutral stability wind at 10 m above the surface. The spatial resolution of this product is 24 km, and its expected rms accuracy at this resolution is 1.0 m/s. Only the scalar wind speed is retrievable, not wind direction. This product is available for both clear and cloudy conditions, but not for areas containing rain. The higher AMSR-E frequencies are used to identify those cells that contain rain, for which the wind speed will not be reported. The product will be produced for individual pixels across the AMSR-E swath (Level 2) as well as an Earth-gridded product (0.25° in latitude and longitude) averaged daily, weekly, and monthly (Level 3).

Research and Applications

Surface winds drive ocean currents by transferring momentum from the atmosphere to the surface and strongly influence the surface evaporative flux of water vapor and consequent thermal coupling between the atmosphere and the ocean. They are a critical component in the redistribution of water vapor and cloud water, facilitating the poleward transport of energy and contributing to patterns of precipitation. Equatorial trade winds are also intimately tied to the El Niño cycle, in which slackening of these winds presages the migration of the west Pacific warm pool toward South America, with dramatic consequences for global weather.

Data Set Evolution

The wind-speed retrieval algorithm is based on experience gained from previous microwave radiometers, including SMMR, SSM/I, and TMI. In particular, the SSM/I has demonstrated the ability of a microwave radiometer to measure wind speed to an accuracy of about 1 m/s. For 250,000 SSM/I overflights of buoys (1987-1999), the root-mean-squared (rms) difference between the SSM/I and buoy wind is 1.3 m/s. About half this difference (in a root sum squared [rss] sense) is due to the spatial-temporal mismatch between the point buoy observation and the 25-km SSM/I footprint. The AMSR-E wind speed retrievals should be more accurate than those from SSM/I because AMSR-E has two additional sets of dual-polarization channels at 6.9 and 10.7 GHz, which help separate the cloud signal from the wind signal and remove crosstalk due to varying sea surface temperature.

Suggested Reading

Goodberlet, M. A. *et al.*, 1989.

Halpern, D. *et al.*, 1994.

Hollinger, J. P., 1971.

Nordberg,W. *et al.*, 1971.

Schluessel, P., and H. Luthardt, 1991.

Wentz, F. J., 1975.

Wentz, F. J., 1992.

Wentz, F. J., 1997.

Wilheit T. T., and M. G. Fowler, 1977.

Wilheit, T. T., and A. T. C. Chang, 1980.

AMSR-E Sea Surface Wind Speed Summary

Coverage: Ocean surface, clear and cloudy skies except in the presence of rainfall

Spatial/Temporal Characteristics:
Level 2: swath pixels at 24-km resolution
Level 3: 0.25° latitude-longitude grid/daily, weekly, and monthly

Key Science Applications: Climate variability, air-sea interaction, hydrological cycle, ocean circulation

Key Geophysical Parameters: Sea surface wind speed

Processing Level: 2, 3

Product Type: Standard, post-launch

Maximum File Size: 10 MB

File Frequency: 29/day

Primary Data Format: HDF-EOS

Browse Available: Accompanies data product

Additional Product Information:
http://wwwghcc.msfc.nasa.gov/AMSR/html/amsr_products.html

DAAC: National Snow and Ice Data Center

Science Team Contact:
F. J. Wentz

Poseidon-2 Normalized Radar Backscatter Coefficient and Wind Speed

Product Description

This Level 2 product provides the measurement of the normalized radar backscatter coefficient and its associated wind speed at a resolution of 6.2 km along the ground tracks of the satellite. The measurement is repeated every 9.9 days along a set of fixed ground tracks. The satellite makes 127 revolutions of the Earth every 9.9 days. The coverage of the measurement is limited from 66° S to 66° N due to the 66° inclination of the satellite's orbit plane. The longitudinal distance between the ground tracks is [315·cos(latitude)] km, i.e., 315 km at the equator, 223 km at 45°, and 128 km at 66°. The normalized radar backscatter coefficient is measured at two frequencies (Ku band at 13.6 GHz and C band at 5.3 GHz). Three kinds of product are available: 1) the Operational Sensor Data Record (OSDR), which is available three hours after data collection; 2) the Interim Geophysical Data Record (IGDR), which is available three days after the data collection; and 3) the GDR, which is available 30 days after the data collection. The accuracy of the normalized radar backscatter coefficient is 0.7 dB for absolute value and 0.2 dB for relative value. The accuracy of wind speed is 2 m/s for OSDR and 1.7 m/s for IGDR and GDR.

Research and Applications

The global distribution and variability of wind speed is used to study the dynamics of ocean waves and monitor the sea state for ship routing and other maritime applications. The normalized radar backscatter coefficient is related to the air-sea gas-transfer coefficient through its relation with the sea-surface mean- square slope. The Jason-1 dual-frequency measurement of the backscatter makes this relation robust for estimation of the gas-transfer coefficient. The global distribution and variability of the gas-transfer coefficient is used to study the global CO_2 flux and the carbon cycle.

Data Set Evolution

The power of the radar return signal is controlled by an automatic gain control (AGC) loop to ensure that the radar altimeter electronics operate properly. This AGC reading is used to calculate the normalized radar backscatter coefficient. This coefficient is corrected for radar pointing angle as well as sea-state effects based on information obtained from the radar-return waveform. Further correction is made for the effects of atmospheric attenuation caused by liquid water and water vapor, which are obtained from the on-board microwave radiometer. The normalized radar backscatter coefficient is then used to compute wind speed using empirically derived algorithms.

Suggested Reading

Brown, G. S., 1979.

Chelton, D. B., and P. J. McCabe, 1985.

Freilich, M. H., and P. G. Challenor, 1994.

Hara, T. *et al*., 1995.

Poseidon-2 Normalized Radar Backscatter Coefficient and Wind Speed Summary

Coverage: Ocean areas from 66°S to 66°N

Spatial/Temporal Characteristics: 6.2-km resolution along-track every 9.9 days; [315 ·cos(latitude)]-km longitudinal track spacing

Key Science Applications: Ocean-wave dynamics (wind speed); air-sea gas transfer and CO_2 flux

Key Geophysical Parameters: Wind speed; normalized radar backscatter coefficient

Processing Level: 2

Product Type: Standard, at-launch

Maximum File Size: 1.5 MB

File Frequency: 25/day

Primary Data Format: Binary

Browse Available: Yes

Additional Product Information: http://www-aviso.cnes.fr

DAAC: Jet Propulsion Laboratory

Science Team Contact: L.-L. Fu

SeaWinds – Normalized Radar Cross-Section and Ancillary Data

Product Description

This Level 1B data set contains Earth-located, time-ordered SeaWinds normalized radar cross-section measurements and ancillary data from a single orbit, corresponding to all SeaWinds measurements acquired during the orbital period known as a "rev." By convention "revs" start at the southernmost orbital latitude and contain only the data from a single orbit.

Data include instrument state; spacecraft position, attitude, and velocity; pulse locations on Earth, complete pulse backscatter cross-section, uncertainty and quality, as well as dynamic data for individual terms in the radar equation; antenna azimuth; 13.4 GHz brightness temperatures calculated from SeaWinds noise estimates for each complete pulse; backscatter cross-section, uncertainty, quality, and Earth location for each of the central eight, high-resolution (~4 × 25 km) slices generated from the Linear Frequency Modulation Chirp.

The data are sorted in time order by telemetry frame. Each telemetry frame contains data from 100 scatterometer pulses. For nominal SeaWinds operating parameters, each Level 1B rev file contains information on more than 1-million full backscatter measurements (pulses) and more than 8-million high-resolution-slice backscatter measurements. Internal calibration data are recorded in flag-indicated calibration pulses.

SeaWinds Normalized Radar Cross-Section and Ancillary Data Summary

Coverage: Global (land, ocean, ice) for each rev 1800-km-wide swath (v-pol); 1400-km-wide swath (h-pol)

Spatial/Temporal Characteristics: ~25 × 35 km resolution for pulse IFOV; ~4 × 25 km resolution for slices

Wavelength: 13.4 GHz

Processing Level: 1B

Product Type: Standard, at-launch

Maximum File Size: 175 MB

File Frequency: 14.25/day

Primary Data Format: NCSA HDF

Browse Available: No

Additional Product Information: http://podaac.jpl.nasa.gov/quikscat/

DAAC: Jet Propulsion Laboratory

Science Team Contact: D. G. Long

SeaWinds – Grouped and Surface-Flagged Backscatter and Attenuations in 25 km Swath Grid

Product Description

This Level 2A data set contains Earth-located and grouped SeaWinds normalized radar cross-section measurements, quality and uncertainty flags, and autonomous rain flags and atmospheric corrections from a single orbital period known as a "rev", corresponding to all SeaWinds backscatter measurements acquired during that period. By convention, revs start and end at the southernmost orbital latitude.

Each composite backscatter measurement combines all of the high-resolution slices from a single scatterometer pulse that are located within a given wind vector cell. All ancillary values required for rain flagging, atmospheric absorption correction (including processed AMSR measurements from ADEOS II), and surface flagging are included.

Wind vector cells are defined as 25 × 25-km areas in a locally rectangular along-track, across-track coordinate system aligned with the satellite subtrack.

SeaWinds Backscatter and Attenuations Summary

Coverage: Global (land, ocean, ice) for each rev 1800-km-wide swath

Spatial/Temporal Characteristics: Slice composites in 25-km wind vector cells

Wavelength: 13.4 GHz

Processing Level: 2A

Product Type: Standard, at-launch

Maximum File Size: 14.4 MB (compressed), 40 MB (uncompressed)

File Frequency: 14.25/day

Primary Data Format: NCSA HDF

Browse Available: No

Additional Product Information: http://podaac.jpl.nasa.gov/quikscat/

DAAC: Jet Propulsion Laboratory

Science Team Contact: M. H. Freilich

SeaWinds – Ocean Wind Vectors in 25 km Swath Grid (Level 2B) and Ocean Wind Vectors in 25 km Grid (Level 3)

Product Description

The Level 2B SeaWinds Ocean Wind Vectors in 25 km Swath Grid data set contains Earth-located, open-ocean near-surface vector wind solutions and ancillary quality flags and values from a single SeaWinds rev, organized by wind vector cell. By convention, revs are orbital periods that start and end at the southernmost orbital latitude.

Wind vector cells are defined as 25 × 25-km areas in a locally rectangular along-track, across-track coordinate system aligned with the satellite subtrack.

Vector wind solutions are given as (speed, direction) pairs. The wind-speed value corresponds to equivalent neutral stability winds at a height of 10 m above the mean sea surface. Wind directions are provided in the oceanographic convention: winds flowing toward the North have direction 0°, with positive angles increasing clockwise.

Each wind vector cell may contain up to 4 potential wind vector solutions resulting from the maximum likelihood wind-retrieval algorithm applied to the Level 2A backscatter data from that wind vector cell. Multiple solutions are provided in order of decreasing likelihood. A flag in the Level 2B product indicates the specific wind vector solution chosen by the standard median filter ambiguity removal algorithm. A rain flag is provided to indicate wind vector cells for which atmospheric effects may significantly degrade the accuracy of the wind solution.

The Level 3 Ocean Wind Vectors in 25 km Grid data set consists of gridded values of scalar wind speed, meridional and zonal components of wind velocity, wind speed squared, and time given in fractions of a day. Rain probability determined using the Multidimensional Histogram (MUDH) Rain Flagging technique is also included as an indicator of wind values that may have degraded accuracy due to the presence of rain. Data are currently available in Hierarchical Data Format (HDF) and exist from 19 July 1999 to the present.

The Level 3 data are obtained from the Direction Interval Retrieval with Threshold Nudging (DIRTH) wind vector solutions contained in the QuikScat Level 2B data and are provided on an approximately 0.25° × 0.25° global grid. Separate maps are provided for both the ascending pass (6 a.m. equator crossing) and descending pass (6 p.m. equator crossing). By maintaining the data at nearly the original Level 2B sampling resolution and separating the ascending and

descending passes, very little overlap occurs in one day. However, when overlap between subsequent swaths does occur, the values are over-written, not averaged. Therefore, a QuikScat SeaWinds Level 3 file contains only the latest measurement for each day.

In addition to the above mentioned Level 3 Product, which was created by the SeaWinds on QuikScat Project, several additional Level 3 products have been produced by members of the SeaWinds on QuikScat Science Working Team. Many of these products provide the QuikScat data on coarser grids (0.5° or 1°) and at smaller time intervals (6 or 12 hour maps) and use advanced interpolation techniques to fill gaps in the wind fields. A list of the publicly available QuikScat Level 3 products produced by members of the SeaWinds on QuikScat Science Working Team can be found on the PO.DAAC SeaWinds on QuikScat web site, http://podaac.jpl.nasa.gov/quikscat.

Suggested Reading

Freilich, M. H., and R. S. Dunbar, 1999.

Naderi, F. M. *et al.*, 1991.

Wentz, F. J., and D. K. Smith, 1999.

SeaWinds Ocean Wind Vectors Summary

Coverage: Global ice-free open ocean for each rev 1800-km-wide swath (Level 2B); Global ice-free open ocean (Level 3)

Spatial/Temporal Characteristics: 25-km wind vector cells within the swath (Level 2B); 0.25° × 0.25° grid/daily (Level 3)

Wavelength: 13.4 GHz

Processing Level: 2B, 3

Product Type: Standard, at-launch

Maximum File Size: 8.25 MB (compressed Level 2B), 32.66 MB (uncompressed Level 2B); 35 MB (Level 3)

File Frequency: 14.25/day (Level 2B); 1/day (Level 3)

Primary Data Format: NCSA HDF

Browse Available: Daily ascending and descending images available at http://podaac.jpl.nasa.gov/quikscat/ (Level 3)

Additional Product Information: http://podaac.jpl.nasa.gov/quikscat/

DAAC: Jet Propulsion Laboratory

Science Team Contact: M. H. Freilich

Sea Surface Height and Ocean Wave Dynamics

Jason-1
- DORIS
- JMR
- Poseidon-2

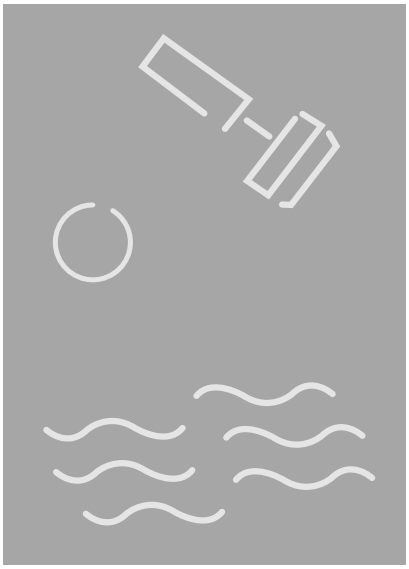

Sea Surface Height and Ocean Wave Dynamics – An Overview

Relationship to Global Change Issues

The ocean covers 70% of the Earth's surface and is responsible for regulating the Earth's climate and sustaining life. The upper three meters of the ocean stores the same amount of heat as resides in the entire atmosphere. The circulation of the ocean's water mass carries half of the poleward transport of the heat gained in the Earth's tropics. The ocean and its circulation patterns thus play a key role in determining the state of the Earth's climate and its evolution. However, observing the global oceans from surface level is difficult, to say the least. It takes months for a research ship to cross an ocean basin to make measurements, and during the course of the cruise the ocean will have already changed in many ways, thereby greatly hindering the attempt to make global and systematic ocean observations to comprehend its totality and variability.

The development of satellite radar altimetry in the 1970s for measuring sea surface height from space has opened the door to global observation of a key aspect of the dynamics of the ocean. The deviation of the sea surface from the equilibrium sea surface in balance with the Earth's gravity, the geoid, is a measure of the surface dynamic pressure of the ocean caused by ocean currents. This height relative to the geoid is called ocean topography. The gradient of ocean topography allows scientists to calculate the speed and direction of the surface geostrophic current velocity; and the temporal change of the topography allows the determination of the current variability. Due to the thermal expansion of sea water, the ocean topography is also related to the heat content of the ocean. Satellite altimetric observation of the global ocean topography thus provides important information about ocean circulation and its heat transport. This information has been used to constrain ocean circulation models for making prediction of the state of the deep ocean, where direct global observations are difficult and expensive. Altimetry data have also been used to initialize coupled ocean-atmosphere models for improved forecasting of seasonal-to-interannual climate variability phenomena such as El Niño and La Niña. Long-term measurement of the ocean topography is thus a key element of a global observing system for building a record of long-term climate change and its prediction.

In addition to sea surface height, the radar return waveform from the Poseidon-2 instrument is also used to produce measurements of the ocean wave height and radar backscatter cross-section, which are then used to determine ocean wind speed. The global wave-height field undergoes changes due to changes in the wind field. In addition to responding to atmospheric storms, the wave-height field also reflects seasonal-to-interannual changes of the wind field in relation to climate change.

The radar backscatter cross-section can be used to estimate the air-sea gas-exchange rate, which is important for the study of the global CO_2 flux and thus the carbon cycle. The wind speed measurements can be used to complement scatterometer observations for studying global ocean dynamics.

Product Overview

The Jason-1 Poseidon-2/JMR/DORIS sea surface height data and Poseidon-2 significant wave height data are organized as sequential records along the ground track of the satellite. Each record contains all the information regarding the instrument's measurements averaged over a period close to one second of flight time, including the measurements of sea-surface height, wave height, radar backscatter cross-section, and wind speed, along with a host of auxiliary data, including the atmospheric, geophysical, and instrumental corrections, plus other relevant information such as ocean-tide-model products and atmospheric pressure products.

Product Interdependency and Continuity with Heritage Data

The heritage of satellite-based altimetric data products traces back to the short-lived SeaSat project in June-October 1978. The European Space Agency's Remote Sensing Satellite (ERS-1), launched in 1991, carried a radar altimeter amongst its complement of five instruments, to obtain further data on sea surface height. The following year saw the launch of the joint U.S.-French TOPEX/Poseidon mission, with a central goal of accurate sea surface height measurement. The Jason-1 Poseidon-2 is a follow-on to the highly successful TOPEX/Poseidon mission.

Suggested Reading

Fu, L.-L. *et al.,* 1994.

Ménard, Y. *et al*., 2000.

Wunsch, C., and E. M. Gaposchkin, 1980.

Wunsch, C., and D. Stammer, 1998.

Poseidon-2/JMR/DORIS Sea Surface Height (SSH)

Product Description

This Level 2 product provides the measurement of the sea surface height relative to a model of the ellipsoidal Earth (the ellipsoid) at a resolution of 6.2 km along the ground tracks of the satellite. The measurement is repeated every 9.9 days along a set of fixed ground tracks. The Jason-1 satellite makes 127 revolutions of the Earth every 9.9 days. The coverage of the measurement is limited to the latitude range 66° S to 66° N due to the 66° inclination of the satellite's orbit plane. The longitudinal distance between the ground tracks is [315· cos(latitude)] km, i.e., 315 km at the equator, 223 km at 45°, and 128 km at 66°. This product is used to generate gridded Level 3 products by various Jason-1 Science Working Team members. Two kinds of product are available. The Interim Geophysical Data Record (IGDR) is available three days after the data collection, while the GDR, based on a more precisely determined orbit, is available 30 days after the data collection. The root-mean-square error is 5 cm for the IGDR and 4.2 cm for the GDR.

Poseidon-2 is the key instrument for measuring sea surface heights, with DORIS providing precise orbit determinations for these measurements and JMR providing range corrections.

Research and Applications

The global distribution and variability of sea surface height provides key inputs to the study of the ocean circulation and its heat transport and hence the ocean's role in climate change such as El Niño. Sea surface height is a dynamic upper boundary condition of the ocean and hence a powerful constraint for the simulation of the interior of the ocean by numerical models via data assimilation. In addition, sea surface height data are also useful for studying the ocean tides, monitoring the global mean sea level change, and providing information for marine navigation, fisheries, and offshore operations, e.g., oil drilling.

Data Set Evolution

Sea surface height is determined from the difference between the range measurement made by a nadir-looking radar altimeter and the altitude (relative to the ellipsoid) of the spacecraft determined by the precision orbit determination technique. The radar range measurement is corrected for the path delay of the radar signals caused by the ionospheric free electrons (via simultaneous radar measurements in the Ku and C bands), the tropospheric water vapor (via an on-board 3-frequency microwave radiometer), and the dry air mass in the atmosphere (via the products from operational meteorological centers). The range measurement is further corrected for the effects of ocean gravity waves that create a bias in the measurement depending on the sea state (wave height, wind speed, etc.) The sea surface height determined from the corrected radar range is then subject to further corrections for geophysical effects other than ocean circulation dynamics and thermodynamics such as ocean tides, and atmospheric pressure loading.

Suggested Reading

Fu, L.-L. *et al.,* 1994.

Ménard, Y. *et al*., 2000.

Wunsch, C., and E. M. Gaposchkin, 1980.

Wunsch, C., and D. Stammer, 1998.

Poseidon-2/JMR/DORIS Sea Surface Height Summary

Coverage: Ocean areas from 66° S to 66° N.

Spatial/Temporal Characteristics: 6.2-km resolution along-track every 9.9 days; [315 ·cos(latitude)] km longitudinal track spacing

Key Science Applications: Ocean circulation and heat transport, ocean data assimilation

Key Geophysical Parameters: Sea surface height

Processing Level: 2

Product Type: Standard, at-launch

Maximum File Size: 1.5 MB

File Frequency: 25/day

Primary Data Format: Binary

Browse Available: Yes

Additional Product Information: http://www-aviso.cnes.fr

DAAC: Jet Propulsion Laboratory

Science Team Contacts:
L.-L. Fu
Y. Ménard

Poseidon-2 Significant Wave Height

Product Description

This Level 2 product provides the measurement of the significant wave height at a resolution of 6.2 km along the ground tracks of the satellite. The measurement is repeated every 9.9 days along a set of fixed ground tracks. The satellite makes 127 revolutions of the Earth every 9.9 days. The coverage of the measurement is limited from 66º S to 66º N due to the 66º inclination of the satellite's orbit plane. The longitudinal distance between the ground tracks is [315· cos(latitude)] km, i.e., 315 km at the equator, 223 km at 45º and 128 km at 66º. This product is used to generate gridded Level 3 products by various Jason-1 Science Working Team members. Three kinds of product are available. The Operational Sensor Data Record (OSDR) is available three hours after data collection. The accuracy of the measurement is the greater of the following: 0.5 m or 10% of the truth. The Interim Geophysical Data Record (IGDR) is available three days after data collection; and the GDR is available 30 days after data collection.

Research and Applications

The global distribution and variability of significant wave height are used to study the dynamics of ocean-surface waves and global change in the marine environment. The data are also used to describe and predict the sea state condition for applications to ship routing, offshore operations and structure design, and coastal monitoring and prediction.

Data Set Evolution

Significant wave height is determined from the slope of the leading edge of the radar return waveform. The value is determined from the onboard waveform tracking algorithm and corrected on the ground using an algorithm based on parameters of the sea state and the off-nadir pointing angle of the radar. Both parameters are obtained from the altimeter data processing stream.

Suggested Reading

Carter, D. J. T. *et al*., 1992.

Cotton, P. D., and D. J. T. Carter, 1994.

Mognard, N. M., 1984.

Mognard, N. M., and B. Lago, 1988.

Rufenach, C. L., and W. R. Alpers, 1978.

Poseidon-2 Significant Wave Height Summary

Coverage: Ocean areas from 66° S to 66° N.

Spatial/Temporal Characteristics: 6.2-km resolution along-track every 9.9 days; [315 ·cos(latitude)] km longitudinal track spacing

Key Science Applications: Ocean wave dynamics and prediction

Key Geophysical Parameters: Significant wave height

Processing Level: 2

Product Type: Standard, at-launch

Maximum File Size: 1.5 MB

File Frequency: 25/day

Primary Data Format: Binary

Browse Available: Yes

Additional Product Information: http://www-aviso.cnes.fr

DAAC: Jet Propulsion Laboratory

Science Team Contacts:
L.-L. Fu
Y. Ménard

Surface Temperatures of Land and Oceans, Fire Occurrence, and Volcanic Effects

Aqua
- AIRS
- AMSR-E
- AMSU-A
- HSB
- MODIS

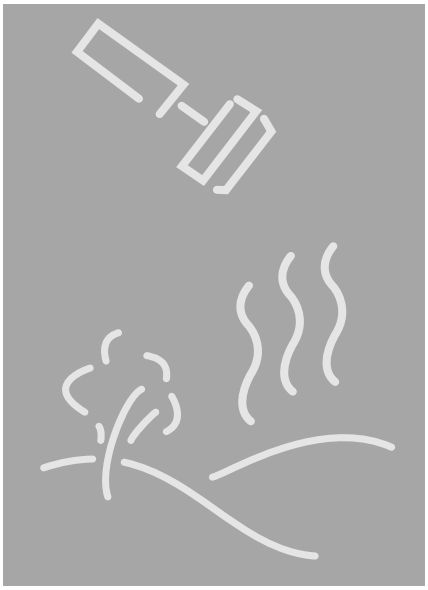

Surface Temperatures of Land and Oceans, Fire Occurrence, and Volcanic Effects – An Overview

Relationship to Global Change Issues

Land and ocean surface temperatures have a multitude of impacts on the Earth system. On land, soil and canopy temperature are among the main determinants of the rate of growth of vegetation, and they govern seasonal initiation and termination of growth. Hydrologic processes such as evapotranspiration and snow and ice melt are highly sensitive to surface temperature fluctuations, as are the rates of heat flow and water transport between the surface and the atmosphere. In addition, surface temperature is an important discriminating factor in the classification of land surface types. For the oceans, the surface temperature influences the rate of growth of phytoplankton, the rate of absorption of carbon dioxide and other gases by sea water, and the rate of flow of heat to and from the atmosphere. Thus, temperature products are key not only for global temperature mapping and change determination but also as inputs to many additional product algorithms.

Fire changes the surface-cover type and releases gases and particulate matter into the atmosphere, affecting ecosystems and atmospheric chemistry on a rapid and intense scale. Similarly, the burning of oil slicks on water is another significant and intense, but infrequent, input into the land and atmosphere systems.

Volcanic eruptions can have short- and long-term consequences on both the local land surface and the regional and global atmosphere, including destruction of local crops and, for some eruptions, lowering of the global tropospheric temperatures. Higher in the atmosphere, in the middle and upper stratosphere, the effect of volcanic emissions can be cooling instead, from increased reflection of solar radiation caused by volcanic aerosols and reduced absorption of ultraviolet light brought on by reduced ozone. Both the cooling of the troposphere and the warming of the middle and upper stratosphere can impact climate change.

Product Overview

Land- and ocean-surface temperatures will be obtained by five instruments on Aqua, the MODIS, AMSR-E, and AIRS/AMSU-A/HSB, each with complementary advantages. Fire products will be obtained from MODIS.

Regarding the surface temperatures, temperature algorithms require calibrated radiances as a basic input. Since the radiation received by satellites has passed through the atmosphere, corrections must be made for atmospheric attenuation and scattering. Hence meteorological data on temperature and water-vapor profiles, as well as chemical constituents, are needed. Also, the radiation emitted by the surface depends on surface emissivity as well as temperature. Further complicating the situation, land-surface pixels generally contain a mixture of materials having different emissivities, geometric characteristics, and topographic characteristics that must be known prior to computing the temperature. Land-material emissivities also can vary significantly as a function of wavelength, and, for the mid-wavelength IR bands, sufficient reflectance can exist that solar reflected energy must be predicted and removed from the measured radiance. At microwave wavelengths, the surface emissivity can vary significantly as a function of the soil moisture and vegetation biomass. Estimates of these parameters can be obtained using multichannel microwave data, e.g., from AMSR-E, and ancillary data, e.g., from external sources and precomputed databases keyed on surface material provided by the MODIS land-cover-type product and the global ocean masks.

At microwave frequencies, the emissivity of the sea surface depends not only on sea surface temperature (SST) but also on roughness, the angle of incidence, and polarization. Surface waves mix the horizontal and vertical polarizations and change local incidence angles. Capillary waves result in diffraction of the radiation. Sea foam increases emissivity for both horizontal and vertical polarizations. Relationships between these effects and wind vectors have been determined by previous studies. The wind-vector relationships in conjunction with a tilt+foam+diffraction model provide the means to compute the sea surface emissivity. At infrared frequencies, the sea surface emissivity is usually assumed to be unity.

The AIRS/AMSU-A/HSB surface temperature measurements are retrieved iteratively, with updated cloud-cleared radiances and temperature-moisture profiles. Both microwave and infrared channels are used except in those cases where cloud cover prevents the successful use of the infrared channels, in which cases a microwave-only retrieval is made. SSTs for the combined microwave/infrared retrievals are expected to have an rms accuracy of better than 0.3 K under conditions of ≤80% cloud cover. AIRS/AMSU-A/HSB land surface temperatures are expected to have an accuracy of about 1 K.

AMSR-E will provide SST measurements through clouds at a spatial resolution of 50 km. The primary

AMSR-E channels for sensing SST are the 6.9 and 10.7 GHz channels. At these frequencies, non-raining clouds are nearly transparent, with 97% of the surface radiation reaching the top of the atmosphere. In addition, the micrometer-sized atmospheric aerosols have no effect in the microwave spectrum. The microwave radiation penetrates about 1 cm into the sea water. Thus the skin temperature sensed by microwaves is considerably deeper than that for the infrared measurements (1 cm compared to several micrometers). A physically based algorithm is used to retrieve the surface temperature. Computer simulations and comparisons of TRMM microwave retrievals (see Volume 1) with buoy measurements indicate that the accuracy of the retrievals is about 0.5 K at a spatial resolution of 50 km. Retrievals will not be possible for a limited number of pixels due to contamination by sun glitter or significant rain. These are relatively rare occurrences (5% of all observations), and almost complete global coverage will be available on a daily basis.

AMSR-E land-surface temperature measurements are retrieved as part of the AMSR-E surface soil-moisture product. Soil moisture and vegetation water content are retrieved simultaneously with surface temperature in a multi-channel retrieval algorithm. The retrieved surface temperature is a spatial average over the heterogeneous land cover within the footprint and represents the temperature within a skin depth of a few centimeters below the surface. (The skin depth varies with the moisture content of the soil and vegetation.) The accuracy of the surface temperature measurements, taking into account the variability in emissivity and other complications, is estimated as approximately 2-3 K.

The MODIS land-surface temperature product (MOD 11) provides the composite temperature of each pixel and the estimated emissivity from database information plus adjustments made possible by the multi-window algorithm. The temperature accuracy is better than 1 K for materials with known emissivities. MODIS SST (MOD 28), derived from radiance measurements, is an estimate of the skin temperature (top micrometers) of the 1-km pixel viewed by MODIS. The algorithm is similar to the land-surface temperature algorithm in that it uses multiple atmospheric window techniques to estimate the atmospheric parameters required to compensate for absorption and scattering. The bulk temperature of the near-surface ocean is the temperature of the upper 10-20 cm to one meter as measured by conventional thermometers on buoys and ships. Extensive analysis has been done of satellite and *in situ* data to enable the algorithm to estimate bulk temperature as well as skin temperature.

The MODIS thermal anomaly product (MOD 14) contains information unique to understanding the characteristics of fires, including energy emitted, size, temperature, and the ratio of smoldering to flaming area, and is available for both day and night periods. The composites produced include a monthly day-and-night fire-occurrence aggregation and a summary of the number of fires in classes related to the strength of the fire. The fire product also includes monitoring of the burning of oil slicks. Separately, MOD 40 detects burn scars.

Product Interdependency and Continuity with Heritage Data

The AIRS/AMSU-A/HSB surface temperatures build on the heritage of the HIRS3/AMSU-A, although should obtain improved accuracies because of the much higher spectral resolution of the AIRS. The AIRS/AMSU-A/HSB retrievals will take advantage of both infrared and microwave channels, then be compared with the infrared-only retrievals of the MODIS and the microwave-only retrievals of the AMSR-E.

The AMSR-E SST is a stand-alone product, not requiring inputs from other sensors or ancillary data. However, blending of the AMSR-E microwave retrievals with the infrared retrievals from AIRS and MODIS offers the potential for a significant synergism in that the microwave retrievals are not affected by clouds or aerosols while the infrared retrievals offer superior spatial resolution.

The MODIS land-surface temperature product requires MODIS calibrated radiances and the cloud-mask product as inputs. Also, atmospheric temperature and water-vapor profiles are needed along with a database of emissivities, the use of which is driven by the land-cover-classification products, which enable surface material to be specified for each pixel. The land-surface temperature product is an input to other land products including vegetation indices, evapotranspiration, and net primary production, and as a background temperature estimate for the MODIS fire product.

Similarly, the MODIS SST product uses MODIS calibrated radiances and the cloud-mask product, but does not require the complex emissivity estimation databases and algorithms that the MODIS land-surface temperature product requires. Sun glint is a significant source of error in the mid-wavelength IR bands, so the mask product is critical for identifying glint pixels as are sea surface wind ancillary data, which are used to estimate the magnitude of the glint-area radiance.

The MODIS fire product uses calibrated MODIS radiances, the MODIS cloud mask, vegetation indices, land surface temperature, and land cover type.

In situ surface temperatures are measured at numerous locations around the world. These locations include meteorological stations on land and ship- and buoy-based instruments at sea. However, these measurements are not adequate in terms of the radiative phenomena or spatial coverage. Land- and sea-surface temperature data taken by instruments on Aqua will add to the valuable input already provided by AVHRR, HIRS, Landsat, CZCS, and the Terra instruments, contributing to a large, long-term global land- and sea-surface temperature data set that should lead to a more complete understanding of the effects of the various Earth system cycles on surface temperature.

Suggested Reading

Becker, F., 1987.

Chahine, M. T., 1980.

Deepak, A., 1980.

Justice, C. *et al*., 1998.

Kaufman, Y. J. *et al*., 1998a,b.

Njoku, E., 1994.

Njoku, E. G., and O. B. Brown, 1993.

Parker, D. E. *et al*., 1995.

Price, J. C., 1983.

Price, J. C., 1984.

Reynolds, R. W., and T. M. Smith, 1994.

Robinson, J. M., 1991.

Smith, W. L. *et al*., 1996.

Susskind, J. *et al*., 1998.

AIRS/AMSU-A/HSB Surface Analysis Product (AIR 06)

Product Description

The AIRS Surface Analysis Product consists of sea- and land-surface skin temperature and infrared and microwave spectral surface emissivity. One sounding of each parameter is produced in a given AMSU-A footprint.

The skin temperature is representative of the temperature in the clear portion of the scene. Objective rejection criteria indicate those cases in which a successful AIRS/AMSU-A/HSB retrieval cannot be produced, generally because of excessive cloud cover in the field of view. No infrared spectral surface emissivity is produced under these conditions.

All retrieved values are given an error estimate and a flag indicative of whether they are combined microwave/infrared (MW/IR) retrievals or primarily MW retrievals. Successful MW/IR retrievals are expected about two thirds of the time.

Sea surface temperatures for the combined MW/IR retrieval are expected to have an rms accuracy of better than 0.3 K for a single spot retrieval under conditions of up to 80% cloudiness. Land surface temperatures are expected to have an accuracy of about 1 K. The degradation compared to sea surface temperature is due to non-homogeneity in the scene with regard to both surface skin temperature and spectral emissivity.

Research and Applications

Sea- and land-surface temperatures play a strong role in the exchange of energy from the surface to the atmosphere and also strongly affect longwave radiation lost to space. They are very important for studying interannual variability and the effects of phenomena such as El Niño on the global circulation.

The surface temperatures and emissivities are considerably better than what is achievable from HIRS3/AMSU-A data because the high spectral resolution of AIRS allows for very clean windows in the 8-12- μm and 4.0-3.7-μm regions, which better discriminate surface from atmospheric emission and allow for the determination of surface spectral emissivity.

Data Set Evolution

The surface parameters are retrieved iteratively in a number of passes. Each pass is a fully non-linear retrieval using the latest set of cloud-cleared radiances and temperature-moisture profiles determined from the sounding channels. Selected AIRS channels are used in the surface parameter retrieval in the spectral ranges 758-980 cm^{-1}, 1072-1234 cm^{-1}, 2170 cm^{-1}-2177 cm^{-1}, and 2393-2668 cm^{-1}.

The surface skin temperature is determined as well as coefficients of eight spectral-emissivity functions and three functions of the spectral bi-directional reflectance of solar radiation. The surface-parameter retrieval step also uses six microwave channels between 23.8 GHz and 150 GHz that provide information about the microwave spectral emissivity and determine the surface skin temperature in those cases when a successful combined MW/IR retrieval could not be produced.

The AMSU-A data are critical for accounting for cloud effects on the AIRS observations. Successful AIRS/AMSU-A soundings of all atmospheric parameters can generally be produced in cases of multilayer clouds with up to 80% fractional cloud cover in the AMSU-A footprint.

Data validation will be accomplished through comparison of the retrieved surface temperatures and emissivities with simultaneous *in situ* measurements at DoE ARM/CART sites and MODIS and ASTER dedicated validation sites. Vicarious validation will be accomplished through comparisons with MODIS and ASTER-retrieved land surface temperatures and AVHRR-retrieved sea surface temperatures.

Suggested Reading

Anyamba, E., and J. Susskind, 1998.

Aumann, H. H., and C. Miller, 1995.

Chahine, M. T. *et al.*, 1987.

Chahine, M. T. *et al.*, 1997.

Janssen, M. A., 1993.

Lakshmi, V. *et al.*, 1998.

Lambrigtsen, B., 1996.

Rosenkranz, P. W., 1995.

Smith, W. L., and H. M. Woolf, 1976.

Susskind, J., and D. Reuter, 1985.

Susskind, J. *et al.*, 1993.

Susskind, J. *et al.*, 1998.

AIRS/AMSU-A/HSB Surface Analysis Product Summary

Coverage: Global

Spatial/Temporal Characteristics: Resolution of AMSU-A FOV (40.6 km at nadir)/twice daily (daytime and nighttime)

Key Science Applications: Exchange of energy from surface to atmosphere, interannual variability, TOA longwave radiation

Key Geophysical Parameters: Land and sea surface skin temperature, infrared spectral surface emissivity, microwave spectral surface emissivity

Processing Level: 2

Product Type: Standard, at-launch

Maximum File Size: 5 MB

File Frequency: 240/day

Primary Data Format: HDF-EOS

Browse Available: Yes

Additional Product Information:
http://www-airs.jpl.nasa.gov/

DAAC: NASA Goddard Space Flight Center

Science Team Contacts:
J. Susskind
H. Revercomb
L. L. Strow

AMSR-E Sea Surface Temperature

Product Description

The sea surface temperature (T_S) derived from the AMSR-E microwave radiances is indicative of the water temperature at a depth of about one millimeter. The spatial resolutions of this product are 38 km and 56 km, and its expected rms accuracy at these resolutions is 0.5 K. At microwave frequencies below 11 GHz, non-raining clouds are nearly transparent, and hence this product is available even when clouds are present. However, retrievals in rainy areas, which can be identified using higher AMSR-E frequencies, are not reliable and will not be reported. The product will be produced for individual pixels across the AMSR-E swath (Level 2) as well as an Earth-gridded product (0.25° in latitude and longitude) averaged daily, weekly, and monthly (Level 3).

Research and Applications

Sea surface temperature reflects the storage of thermal energy in the upper mixed layer of the oceans. It is relevant as a potential indicator of global climate change, responding to long-term variations in total heat flux. Shorter term variability, particularly that associated with the onset of El Niño and La Niña phases, also has significant ramifications. For example, the normally productive fisheries in the upwelling zones of the eastern Pacific experience dramatic declines in stocks during the warm El Niño phase. Furthermore, this cycle strongly influences global precipitation and weather patterns, leading to severe flooding in some areas and severe droughts and associated fires in others. The value of improvements in the ability to anticipate the occurrence and magnitude of El Niño events based on combined analysis of remote sensing data and general circulation models was clearly demonstrated before and during the 1997/98 El Niño and the 1998/99 La Niña. By having advance warning of impending shifts in weather patterns, regions that are most strongly affected by these phenomena were able to act to mitigate those effects. Accurate SST measurements are also a principal component of atmospheric general circulation models, defining the surface boundary conditions, and serve as a validation reference for more-sophisticated coupled models, which attempt to calculate both atmospheric and oceanic state self-consistently. Other areas of interest which benefit from accurate measurements of sea surface temperature include studies of coastal flow and boundary-current dynamics, which are relevant both to the research community and to users such as those in the shipping and fishing industries, as well as to navies, all of which rely heavily on the ability to effect safe and efficient ocean transit.

Data Set Evolution

The T_S retrieval algorithm is based on experience gained from previous microwave radiometers, including SMMR, SSM/I, and the TRMM microwave imager (TMI). In particular, recent analysis of the TMI data has provided the means to characterize the sea-surface emission precisely as a function of T_S and wind speed. In preparation for AMSR-E, a T_S algorithm was developed for TMI. The performance of the TMI algorithm was assessed by comparison with the Reynolds' Optimum Interpolation (OI) SST product, which is a blend of AVHRR retrievals and buoy/ship reports. The rms difference between the TMI and OI T_S retrievals is 0.8°C. Some of this difference is due to the spatial-temporal mismatch between the two types of observations as well as errors in the OI product. The AMSR-E T_S retrievals should be more accurate than the TMI retrievals because AMSR-E has an additional set of dual-polarization channels at 6.9 GHz, which is ideally suited for T_S retrievals. Also, TMI is experiencing some calibration problems due to the heating and cooling of the radiometer over the course of an orbit. This problem should be less severe for AMSR-E, which will be in a sun-synchronous orbit.

Suggested Reading

Hofer, R. E. *et al.*, 1981.

Lipes, R. G. *et al.*, 1979.

Parker, D. E. *et al.*, 1995.

Reynolds, R. W., and T. M. Smith, 1994.

Wentz, F. J., 1983.

(AMSR-E Sea Surface Temperature, continued)

AMSR-E Sea Surface Temperature Summary

Coverage: Global ocean surface, clear and cloudy skies except in the presence of rainfall

Spatial/Temporal Characteristics:
Level 2: Swath pixels at 38-km and 56-km resolution
Level 3: 0.25° latitude-longitude grid/daily, weekly, and monthly

Key Science Applications: Climate variability, air-sea interaction, radiation balance, hydrological cycle, ocean circulation

Key Geophysical Parameters: Sea surface temperature

Processing Level: 2, 3

Product Type: Standard, post-launch

Maximum File Size: 10 MB

File Frequency: 29/day

Primary Data Format: HDF-EOS

Browse Available: Accompanies data product

Additional Product Information:
http://wwwghcc.msfc.nasa.gov/AMSR/html/amsr_products.html

DAAC: National Snow and Ice Data Center

Science Team Contact:
F. J. Wentz

MODIS Land Surface Temperature (LST) and Emissivity (MOD 11, MOD 11comb, MOD 11adv)

Product Description

The Aqua MOD11 product is similar to the Terra MOD11 product (see p. 191 in Volume 1). It contains Level 2 and 3 LST and emissivity retrieved from Aqua MODIS data at spatial resolutions of 1 km and 5 km over global land surfaces under clear-sky conditions. The generalized split-window LST algorithm will be used to retrieve LST for MODIS pixels with known emissivities in bands 31 and 32. The physics-based day/night LST algorithm will be used to simultaneously retrieve surface band emissivities and temperatures from a pair of daytime and nighttime MODIS observations in bands 20, 22, 23, 29, and 31-33 over all types of land cover.

The MOD11comb (combination) product contains Level 2 and 3 land-surface emissivities and temperatures retrieved through the combination of Aqua and Terra MODIS data. The MOD11comb surface temperature, with an enhanced diurnal feature, will be more suitable for various applications than an Aqua or Terra product alone.

In the early post-launch period, the Aqua MOD11adv (advanced) product will include Level 2 and 3 land surface emissivities and temperatures retrieved by an advanced LST algorithm that also corrects the effects of thin cirrus clouds and aerosols with inputs from MODIS atmospheric products.

Research and Applications

Land-surface temperature is a good indicator of both the energy balance at the Earth's surface and the greenhouse effect because it is one of the key parameters in the physics of the land-surface processes. It is required for a wide variety of climate, hydrological, ecological, and biogeochemical studies. This product will be used in generating other MODIS products and in a variety of EOS interdisciplinary studies.

Data Set Evolution

The Aqua MODIS LST products build and improve upon the experience of LST retrieval from MODIS Airborne Simulator (MAS) data and Terra MODIS data.

Suggested Reading

Justice, C. *et al*., 1998.

Running, S. W. *et al*., 1994.

Salisbury, J. W., and D. M. D'Aria, 1992.

Snyder, W., and Z. Wan, 1996.

Wan, Z., and J. Dozier, 1996.

Wan, Z., and Z.-L. Li, 1997.

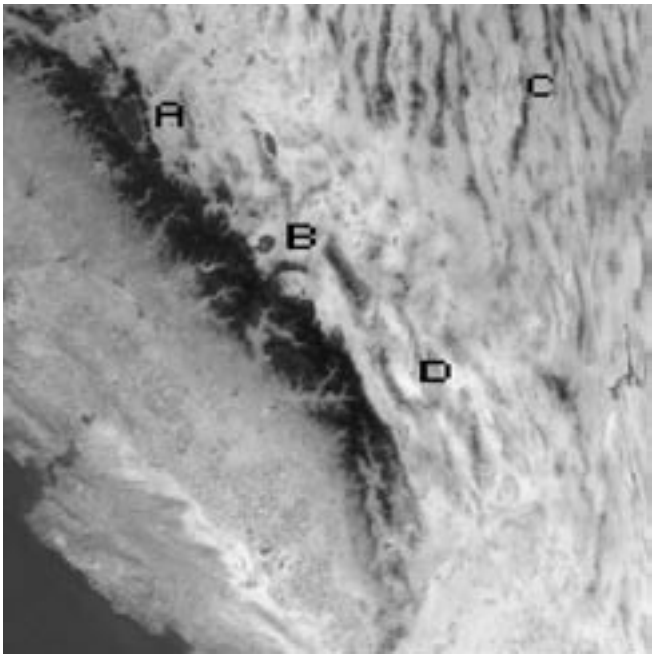

Sample MOD 11 Level-2 LST Image generated from Terra MODIS data in bands 31 and 32 on April 4, 2000 (19:15 UTC) in California and Nevada. The dark area in the lower left corner is the Pacific Ocean. The sites to the left of symbols A, B, C, and D are Lake Tahoe, Mono Lake, Railroad Valley, and Death Valley. The coincident IR radiometer measurement data over Mono Lake agree with the MODIS LST value within 1.2K. (Image developer: MODIS Science Team / MODLAND / Z. Wan, UCSB).

MODIS Land Surface Temperature and Emissivity Summary

Coverage: Global land surface

Spatial/Temporal Characteristics: 1 km, 5 km, and 0.5°/8-day and monthly

Key Science Applications: Inputs to climate, hydrological, ecological modeling

Key Geophysical Parameters: Land surface temperature, land surface emissivity

Processing Level: 2, 3

Product Type: Standard, at-launch and post-launch

Maximum File Size: 24 MB

File Frequency: 288 /day

Primary Data Format: HDF-EOS

Additional Product Information: http://modis-land.gsfc.nasa.gov/products/products.asp?ProdFamID=8

DAAC: EROS Data Center

Science Team Contact: Z. Wan

MODIS Thermal Anomalies – Fires (MOD 14); MODIS Burn Scars (MOD 40)

Product Description

The MODIS Thermal Anomalies product includes fire occurrence (day/night), fire location, the logical criteria used for the fire selection, and an energy calculation for each fire. The product also includes composite 8-day-and-night fire occurrence (full resolution), composite monthly day-and-night fire occurrence (full resolution), gridded 10-km summary per fire class (daily/8-day/monthly), and a gridded 0.5° summary of fire counts per class (daily/8-day/monthly). The Level 2 product includes various fire-related parameters including the occurrence of day and nighttime thermal anomalies, flagged and grouped into different temperature classes with emitted energy from the fire. These parameters are retrieved daily at 1-km resolution. The fire product uses the special fire channel at 3.9 μm that saturates at 500 K and the high-saturation level of the 11-μm channel. During the night, the fire product will also use the 1.65- and 2.15-μm channels. The standard products will include the area burned.

Research and Applications

Fire is an important process within a significant number of terrestrial biomes, and the release of gases and particulate matter during biomass burning is an important contributor to the chemical reactions and physical processes taking place in the atmosphere. Fire is a significant and continuous factor in the ecology of savannas, boreal forests, and tundra, and plays a central role in deforestation. Fire information will be used to drive regional emissions models, trace-gas transport models, and mesoscale models of atmospheric chemistry. Important impacts of fires include:

- changes of physical state of vegetation and release of greenhouse gases;
- release of chemically reactive gases during biomass burning;
- release of soot and other particulate matter during fires;
- changes in the exchange of energy and water between land surfaces and the atmosphere; and
- changes in plant community development and soil nutrient, temperature, and moisture, and cloud development and reflectivity.

Data Set Evolution

The MODIS fire products build and improve upon the experience of fire assessment primarily using the NOAA AVHRR and GOES systems. Currently, no one sensing system provides the instrument characteristics needed for an effective global fire-monitoring program. The MODIS sensor has been designed to include characteristics specifically for fire detection and will provide a unique capability over existing sensors in terms of fire monitoring. The locational accuracy and improved instrument characterization and calibration will enable unprecedented fire-monitoring data sets. The combination of Terra and Aqua data will provide four observations per day, giving

NOAA/AVHRR-Detected High-Temperature Sources for June 25, 1992, derived from the IGBP-DIS global 1-km set provided by the USGS Eros Data Center.

(MODIS Thermal Anomalies, continued)

a good sampling of the diurnal cycle of fire activity. MODIS will also offer unique spatial and radiometric capabilities for burn-scar detection. Automatic procedures for burn-scar detection will be developed to provide a standard burn-scar product.

Suggested Reading

Andreae, M. O. *et al*., 1994.

Justice C. O. *et al*., 1993.

Justice C. O. *et al*., 1998.

Kaufman, Y. J. *et al*., 1990.

Kaufman, Y. J. *et al*., 1998a.

Levine, J. S., 1991.

Penner, J. E. *et al*., 1992.

MODIS Thermal Anomalies – Fires and Burn Scars Summary

Coverage: Global, daytime/nighttime

Spatial/Temporal Characteristics: 1 km, 10 km, and 0.5°/1-day (MOD 14 only), 8-day, 16-day (MOD 40 only), monthly

Key Geophysical Parameters: Fire occurrence and class, fire selection criteria, fire location, smoldering and flaming ratio, burned area

Processing Level: 2, 3 for MOD 14; 4 for MOD 40

Product Type: Standard, at-launch and post-launch

Maximum File Size: 81 MB (MOD 14), 92 MB (MOD 40)

File Frequency: 1/day (Daily, MOD 14 only), 1/8-day (8-day), 1/16-day (16-day, MOD 40 only), 1/month (Monthly)

Primary Data Format: HDF-EOS

Additional Product Information: http://modis-land.gsfc.nasa.gov/products/products.asp?ProdFamID=1

DAAC: EROS Data Center

Science Team Contacts:
Y. J. Kaufman
C. O. Justice

MODIS Sea Surface Temperature (SST) (MOD 28)

Product Description

This Level 2 and 3 product provides sea surface temperature at 1-km (Level 2) and 4.6 km, 36 km, and 1° (Level 3) resolutions over the global oceans. In addition, a quality-assessment parameter is included for each pixel. The Level 2 product is produced daily and consists of global day and night coverage every 24 hours. It is used to generate the gridded Level 3 products daily, 8-day weekly, monthly, and yearly for day and night conditions. A quality parameter is provided for each data set.

Research and Applications

The global distribution and variability of sea surface temperature are key inputs to Earth energy and hydrological balance studies and long-term climate-change studies. In addition, sea surface temperature is required by a number of MODIS algorithms including those for precipitable water, lifted index, water-leaving radiance, productivity, oceanic aerosol properties, and temperature and water-vapor profiles. MODIS sea surface temperature retrievals will be incorporated into a match-up database with radiance and buoy sea surface temperature observations (see MOD 32).

Data Set Evolution

Sea surface temperature determination is based on MODIS-calibrated mid- and far-IR radiances (Bands 20, 22, 23, 31, and 32 from MOD 02), using an algorithm that exploits the differences in atmospheric transmissivity in the different IR bands to enable highly accurate estimation of the atmospheric effects, thereby enabling ancillary input to the algorithm along with a land mask, which is used to mark non-water pixels while an ice-extent mask limits polar sea coverage. A sequence of spatial and temporal homogeneity tests is applied to validate the quality of the cloud-free observations. The AIRS SST estimate will be used as a near-real-time quality assessment of skin temperature. Visible and near-IR radiances (Bands 3, 4, 5, 6) will be used as a secondary cloud flag in the event that the cloud-screening product is not available.

Suggested Reading

Abbott, M. R., and D. B. Chelton, 1991.

Barton, I. J. *et al*., 1989.

Brown, O. B., and R. E. Cheney, 1983.

Deschamps, P., and T. Phulpin, 1980.

Edwards, T. *et al*., 1990.

Llewellyn-Jones, D. T. *et al*., 1984.

McClain, E. P. *et al*., 1985.

Minnett, P. J., 1991.

Minnett, P. J., 1995.

Schluessel, P. *et al*., 1990.

Smith, A. H. *et al*., 1994.

Smith, W. L. *et al*., 1996.

Strong, A. E., and E. P. McClain, 1984.

MODIS Sea Surface Temperature Summary

Coverage: Global ocean surface, clear-sky only

Spatial/Temporal Characteristics: 1 km/daily (Level 2); 4.6 km, 36 km, 1°/daily, 8-day, monthly, yearly (Level 3)

Key Science Applications: Energy and hydrological balance, climate-change models

Key Geophysical Parameters: Sea surface temperature

Processing Level: 2, 3

Product Type: Standard, at-launch

Maximum File Size: 33 MB (Level 2); 640 MB binned, 134 MB mapped (Level 3)

File Frequency: 288/day (Daily Level 2), 4/day (Daily Level 3), 4/8-day (8-day Level 3), 4/month (Monthly Level 3), 4/year (Yearly Level 3)

Primary Data Format: HDF-EOS

Browse Available: 36 km sample imagery available at the Goddard DAAC (Level 3 only)

Additional Product Information: http://modis-ocean.gsfc.nasa.gov/dataprod.html

DAAC: NASA Goddard Space Flight Center

Science Team Contact: O. Brown

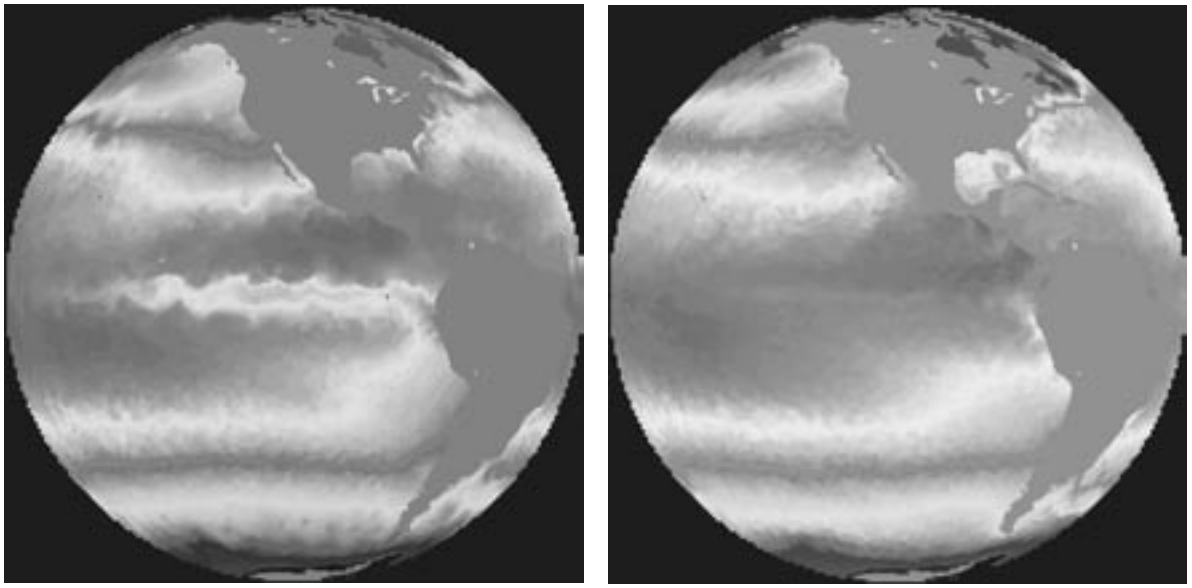

Changes in Pacific Sea Surface Temperature (SST) due to El Niño. SST from the NOAA AVHRR, showing patterns before (left) and during (right) the major 1992 El Niño. The improved accuracy of IR SST products expected from MODIS will enable investigation of the relatively small changes in SST hypothesized to be responsible for triggering El Niño cycles in the Pacific and their ramifications globally. (Note: temperatures range from 20° to 30°C.) (From Brown, O., and G. Feldman, "Reports to the Nation: El Niño and Climate Prediction," Spring 1994, No. 3, University Corporation for Atmospheric Research, Boulder, CO.)

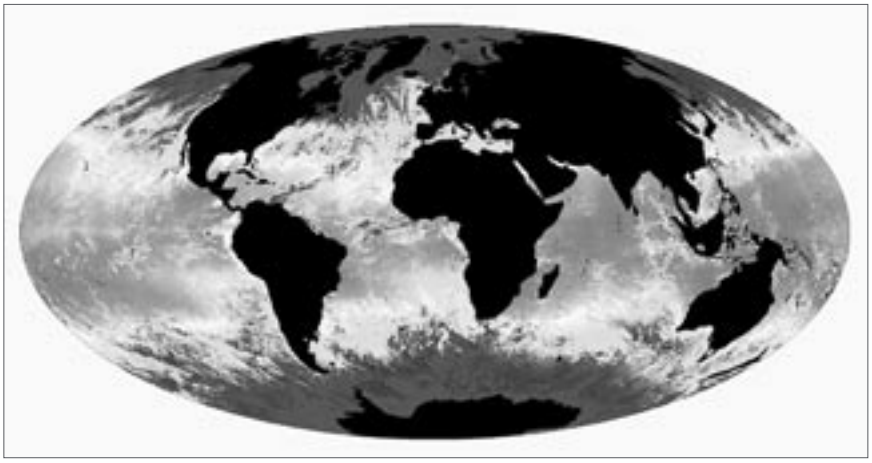

An Example of an 8-day Global Sea Surface Temperature Map generated using data acquired in March 2000 from the MODIS instrument on Terra.

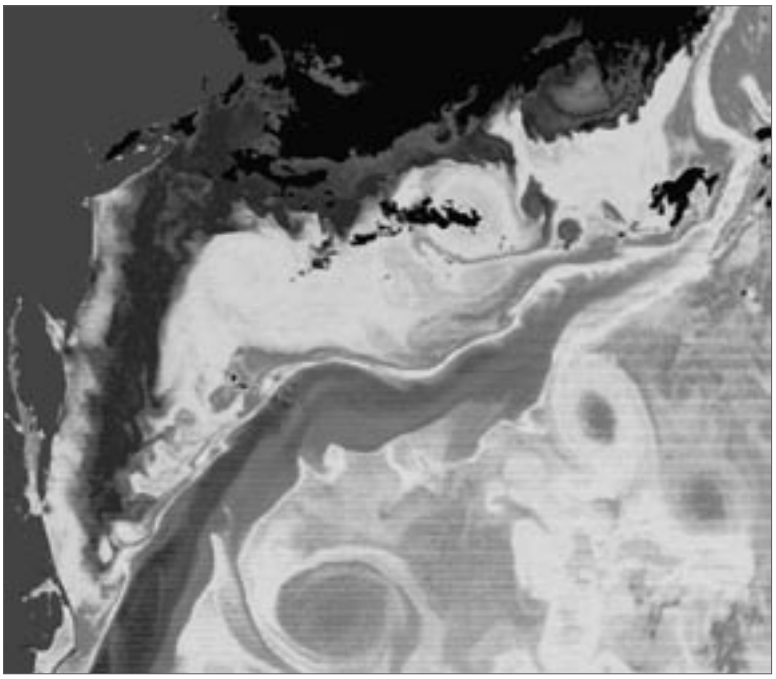

Sea Surface Temperature off the East Coast of North America, May 8, 2000, derived from data of the MODIS instrument on Terra. This is a Level 2, 1-km resolution product and shows entrainment of Gulf Stream, shelf, and Sargasso Sea waters into cold and warm core rings.

Vegetation Dynamics, Land Cover, and Land Cover Change

Aqua
- AMSR-E
- MODIS

Landsat 7*
- ETM+

VCL
- MBLA

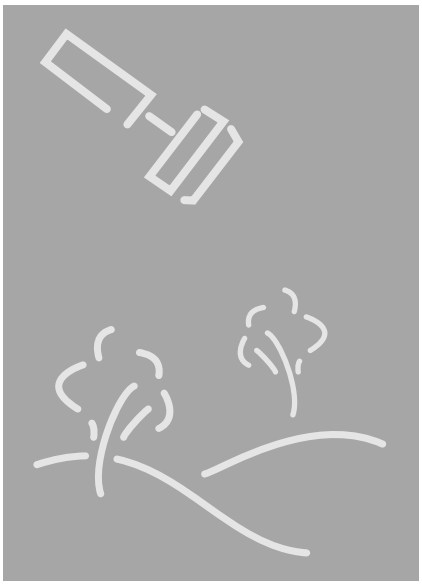

* See Overview Product Description immediately following, and also see chapter on Radiance/Reflectance and Irradiance Products.

Vegetation Dynamics, Land Cover, and Land Cover Change – An Overview

Relationship to Global Change Issues

In spite of the severe inroads of human constructions, much of the Earth's land surface remains vegetated, and this vegetation remains critical to the life-support systems of humans and all other land-based terrestrial animals. Knowledge of vegetation, land cover and land-use change provides the basis for understanding land and water resource management and a range of research and global monitoring objectives, including global carbon modeling, greenhouse gas emission inventories, regional environment and development assessments, and forest resource management. Ecologists and climatologists have developed models that describe the matter and energy exchanges, but lack of long-term global data limits their use in Earth system models. Additionally, we lack good global data on land-surface albedos, on the distribution of soils and important properties of vegetation morphology and physiology, and on water storage in soils and snow cover and its relationship to runoff. Incorporation of this information in the land-surface component of climate models will improve estimates of exchanges of water and energy with the atmosphere and lead to more realistic climate simulations.

Product Overview – Vegetation

The MODIS land-vegetation products provide information on terrestrial systems that have important links to climate and atmospheric composition. These links are needed for development and application of fully coupled models of the Earth's system. They involve exchanges of energy and moisture, radiatively active trace gases such as carbon dioxide and methane, and photochemically active species such as nitric oxide and non-methane hydrocarbons, released by soils, plants, and biomass burning.

The MODIS products provide the basic measurements of the photosynthetic engines that drive carbon transport on land. For land areas, vegetation density and vegetation-canopy factors are produced, and these are used to generate land primary productivity, the amount of carbon fixed by vegetation growth per day or per a longer unit of time such as a year. The MODIS vegetation measurements are provided by the Vegetation Indices (MOD 13), Leaf Area Index (LAI) and Fraction of Photosynthetically Active Radiation (FPAR)(MOD 15), and Vegetation Cover Conversion (MOD 44) products.

Vegetation indices are radiometric measures of the amount of vegetation present on the ground in a particular pixel. The MODIS indices are obtained from measurements of reflected visible and near-infrared energy from vegetation and are called normalized difference vegetation indices (NDVIs). These indices have values between -1 and 1 and increase with increasing amounts of vegetation. Several new indices have been developed which compensate for soil and atmospheric effects, and these are combined into the modified vegetation index (MVI), also to be produced by MODIS. The indices will be produced at different resolutions and time-averaging intervals to provide measures of vegetation density and productivity required by global-change models.

The LAI product provides information on the structural property of a plant canopy such as the number of equivalent layers of leaves the vegetation displays relative to a unit ground area. It is derived from the vegetation index. This parameter is an input to the Photosynthesis and Net Primary Production algorithms that produce the global model inputs for land. The FPAR product provides another key input to the production algorithm. It measures the proportion of available radiation in the specific photosynthetically active wavelengths of the spectrum that a canopy absorbs. It is also derived from the vegetation index. These two products provide the vegetation measurements that are combined with surface temperature and radiation inputs in the vegetation-production algorithm.

The two primary vegetation products from the VCL mission and its MBLA instrument are geolocated canopy-top height and geolocated vertical distribution of intercepted surfaces (VDIS). These are both Level 2 products obtained with a spatial resolution of approximately 25 km. The canopy-top height provides a unique measure of vegetative heights at global scales and also an indication of above-ground biomass. The VDIS provides a new means to classify vegetation architecture and functions as a predictor of the successional state of a forest.

The ETM+ instrument on Landsat 7 does not directly provide vegetation products in the sense that the MODIS instrument on Aqua or the MBLA on VCL do. Rather, calibrated radiances from ETM+ are made widely available to the scientific community concerned with the global distribution and characterization of vegetation at higher resolution than provided by MODIS. It is left to the scientific community to develop specific ETM+ products, which will include maps that quantify land use, land cover, deforestation, plant biomass, urban sprawl, and ice-sheet dynamics.

Product Overview – Land Cover and Land Cover Change

The AMSR-E, MODIS, MBLA, and ETM+ instruments will all obtain information of value to studies of land cover and land cover change, AMSR-E for soil moisture, MBLA for ground elevations, and MODIS and ETM+ for land cover types.

The AMSR-E soil moisture product obtains a measure of the mean volumetric moisture content in the top few millimeters of soil, at a 56-km spatial resolution. The product is restricted to non-mountainous regions with no snow, low vegetation, and no ongoing precipitation. However, in spite of the limitations, AMSR-E is considered the best instrument to date for satellite sensing of soil moisture. The anticipated accuracy of the AMSR-E soil moisture estimates in the restricted regions of soil moisture retrievals is about 0.06 g cm^{-3}.

The MBLA ground-elevation measurements will obtain billions of sub-canopy surface elevation points, determined by assuming that the laser waveform's last return exceeding a set threshold level is the ground return. These measurements will provide a significant advance over current remote sensing topographic techniques, none of which is able reliably to penetrate a canopy-covered surface to obtain accurate surface heights.

The MODIS Land Cover Type product (MOD 12) maps global terrestrial land cover at 1-km resolution. The land cover change product will detect areas of change and identify types of change processes as they occur. Land cover, as well as both human and natural alteration of land cover, plays a major role in global-scale patterns of climate and biogeochemistry.

The MODIS land cover product will recognize 18 basic classes of land cover types, independent of climate. Vegetation classes will separate needleleaf, broadleaf, and graminoid leaf structures; annually deciduous and evergreen canopy habitats; and sparse-to-dense-cover fractions following the International Geosphere-Biosphere Programme (IGBP) scheme. Also, major classes of agricultural activities will be recognized as well as several categories of land surfaces with little or no plant cover, such as bare sand, soil, or rock.

The MODIS land cover product will detect and categorize changes in terrestrial features and processes on a global scale. Independent of the land cover product, the land-cover-change algorithm will compare, pixel-by-pixel, the temporal development curve of a set of biophysical and spatial indicators derived from MODIS data.

As indicated above, the ETM+ instrument on Landsat 7 will not directly be the source of land-cover and land-cover-change products, but rather will be the source of calibrated radiances at 30-m resolution and at seven spectral bands that will make it possible for members of the scientific community worldwide to apply their own algorithms to develop products that define land cover and land cover change on a global basis.

Product Interdependency and Continuity with Heritage Data

The MODIS land products flow in a chain from the Level 2 reflectance and land cover type parameters to biophysical- and biochemical-derived products used as inputs to Earth system models. Specific product dependencies for the land vegetation indices are MODIS radiance and imagery products, including Level 1B calibrated radiance, surface-leaving radiance, and aerosol optical depth. The vegetation index is the key input to Leaf Area Index and FPAR products, which are the key inputs along with land cover type into the biomass-product algorithm.

Each MODIS product has its own science requirements and objectives and builds on the heritage of products produced for many years from AVHRR and other data sets. MODIS will produce a "continuity" NDVI to maintain the AVHRR NDVI time series using an algorithm that closely approximates the heritage index. A worldwide database has been created with the AVHRR data, and EOS will continue this series.

The products that will come into being as a result of analysis of the calibrated radiances from ETM+ will continue the long heritage of measurements that extend back to the Landsat 1 satellite, launched in 1972. Despite improvements in Landsat through the development of ETM+, continuity has been maintained with the original measurements from Landsat 1 and with the spectral enhancements added to Landsats 4 and 5. Improvements incorporated in the Landsat 7 sensor include a 15-m panchromatic band, superior spatial resolution for the thermal band (60 versus 120 m), and two solar calibrators.

Landsats 2 and 3, launched in 1975 and 1978 respectively, were configured similarly. In 1984, Landsat 4 was launched with the MSS and a new instrument called the Thematic Mapper (TM). Instrument upgrades included improved ground resolution (30 m) and 3 new channels, or bands. In addition to using an updated instrument, Landsat 4 made use of the multimission modular spacecraft (MMS),

which replaced the Nimbus-based spacecraft design employed for Landsats 1-3. Landsat 5, a duplicate of Landsat 4, was launched in 1984 and continued returning useful data in the late 1990s, far beyond its 5-year design life. Landsat 6, equipped with a 15-m panchromatic band, was lost immediately after launch in 1993.

Suggested Reading

Asrar, G., 1989.

Lambin, E. F., and A. H. Strahler, 1994a,b.

Los, S. O. *et al*., 1994.

Moody, A., and C. E. Woodcock, 1995.

Nemani, R. R., and S. W. Running, 1995.

Nyoku, E., and L. Li, 1999.

Oliver, C. D., and B. C. Larson, 1990.

Rencz, A., 1999.

Running, S. W. *et al*., 1994.

Sellers, P. J., 1987.

Ustin, S. L. *et al*., 1993.

van Leeuwen, W. J. D. *et al*., 1999.

Vonder, O. W., and J. P. G. W. Clevers, 1998.

Vorosmarty, C. *et al*., 1991.

AMSR-E Surface Soil Moisture

Product Description

This Level 2 and 3 product provides surface soil moisture at 56-km resolution on a nominal 25-km Earth-registered grid. Gridded brightness temperatures are also provided at Level 3. Quality-control indices and surface-type classification are included. The product spatial resolution is determined by the sensor resolution at the lowest frequency used in the retrievals (6.9 GHz). Surface soil moisture is defined as the mean volumetric moisture content (g cm^{-3}) in the top few millimeters of soil, or skin depth, averaged over the retrieval resolution. In regions of moderate-to-dense vegetation cover, snow, frozen ground, precipitation, open water, or mountainous terrain, soil moisture retrievals are not made. The accuracy of the soil-moisture retrievals is best for bare soils, and worsens as the vegetation cover increases. Surface temperature and vegetation water content are retrieved simultaneously with the soil moisture and are included in the product. The Level 2 product is provided in ascending and descending swath segments. The Level 3 product is generated by compositing the ascending and descending Level 2 products into daily global maps.

Research and Applications

Water and energy fluxes at the land-atmosphere interface are influenced to a large extent by the surface soil moisture. Satellite-derived information on soil moisture and its variability is thus important for modeling surface hydrologic processes, for enabling improved weather and climate prediction, and for monitoring floods, droughts, and vegetation status on a global basis.

Data Set Evolution

Soil-moisture remote sensing requires measurements at long wavelengths to penetrate vegetation cover, and large antennas to provide adequate spatial resolution. The AMSR-E is the best instrument to date for this purpose, with a lowest frequency of 6.9 GHz and a spatial resolution of 56 km at this frequency. The AMSR-E goal is to obtain soil-moisture estimates with an accuracy of ~0.06 g cm^{-3} in regions with vegetation water content of less than ~1.5 kg m^{-2}. No adequate satellite soil-moisture data sets currently exist. The AMSR-E soil-moisture data set is produced using algorithms developed from field-experiment data using airborne and ground-based instrumentation and from historical Nimbus 7 SMMR data analysis.

Suggested Reading

Njoku, E. G., and D. Entekhabi, 1996.

Njoku, E., and L. Li, 1999.

Wang, J. R., and B. J. Choudhury, 1995.

AMSR-E Surface Soil Moisture Summary

Coverage: Global land surface, although only under snow-free and low-vegetation conditions

Spatial/Temporal Characteristics: 56-km spatial resolution on a nominal 25-km Earth-fixed grid; swath (Level 2) and daily (Level 3) ascending and descending

Key Science Applications: Hydrological processes, climate modeling and monitoring

Key Geophysical Parameters: Surface soil moisture

Processing Level: 2, 3

Product Type: Standard, at-launch

Maximum File Size: 0.5 MB

File Frequency: 29/day

Primary Data Format: HDF-EOS

Browse Available: Accompanies data product

Additional Product Information: http://wwwghcc.msfc.nasa.gov/AMSR/html/amsr_products.html

DAAC: National Snow and Ice Data Center

Science Team Contact: E. G. Njoku

MODIS Surface Reflectance; Atmospheric Correction Algorithm Products (also called Spectral Reflectance) (MOD 09)

Product Description

The MODIS Surface-Reflectance Product (MOD 09) is computed from the MODIS Level 1B land bands 1, 2, 3, 4, 5, 6, and 7 (centered at 648 nm, 858 nm, 470 nm, 555 nm, 1240 nm, 1640 nm, and 2130 nm, respectively). The product is an estimate of the surface spectral reflectance for each band as it would have been measured at ground level if there were no atmospheric scattering or absorption.

The correction scheme includes corrections for the effect of atmospheric gases, aerosols, and thin cirrus clouds; it is applied to all noncloudy MOD 35 Level 1B pixels that pass the Level 1B quality control. The correction uses band 26 to detect cirrus cloud, water vapor from MOD 05, aerosol from MOD 04, and ozone from MOD 07; best-available climatology is used if the MODIS water vapor, aerosol, or ozone products are unavailable. Also, the correction uses MOD 43, BRDF without topography, from the previous 16-day time period for the atmosphere-BRDF coupling term.

Research and Applications

The surface-reflectance product is the input for product generation for several land products: Vegetation Indices (VIs), BRDF, thermal anomaly, snow/ice, and Fraction of Photosynthetically Active Radiation/Leaf Area Index (FPAR/LAI). It is, therefore, an important and essential product. The at-launch version will be fully operational.

Data Set Evolution

The Aqua MODIS product will be based upon the latest version of the Terra MODIS product.

Suggested Reading

Vermote, E. F. *et al*., 1997.

MODIS Surface Reflectance; Atmospheric Correction Algorithm Products Summary

Coverage: Global land surface (Level 2)

Spatial/Temporal Characteristics: Bands 1 and 2, 250 m; bands 3-7, 500 m; daylight data only

Key Science Applications: Global climate modeling, regional climate modeling, surface-energy-balance modeling, land cover characterization

Key Geophysical Parameters: Surface reflectance

Processing Level: 2

Product Type: Standard, at-launch

Maximum File Size: 424 MB

File Frequency: 288/day

Primary Data Format: HDF-EOS

Additional Product Information: http://modis-land.gsfc.nasa.gov/mod09/

DAAC: EROS Data Center

Science Team Contact: E.Vermote

MODIS Land Cover Type (MOD 12)

Product Description

This Level 3 product contains land cover type and land cover change parameters, which will be produced at 1-km resolution on a quarterly basis beginning 18 months following launch of the Terra and Aqua platforms. In the period 6-18 months after launch, prototype products will be made available. The land cover parameter identifies 17 categories of land cover following the IGBP global vegetation database, which defines nine classes of natural vegetation, three classes of developed lands, two classes of mosaic lands, and three classes of nonvegetated lands (snow/ice, bare soil/rocks, water). The land cover change parameter quantifies subtle and progressive land-surface transformations as well as major rapid changes. As such, it is not a conventional change product that only compares changes in land cover type at two times but combines analyses of change in multispectral-multitemporal data vectors with models of vegetation-change mechanisms to recognize both the type of change and its intensity. It will highlight interannual variability in particular. In addition to the basic 1-km product, summary products containing proportions of land covers and change characteristics will be available at one-quarter, one-half, and 1-degree resolutions. These products are prepared independently from the 250-m Land Cover Change Product and use a different algorithm.

Research and Applications

This product is used for biophysical and biogeochemical parameterization of land cover for input to global- and regional-scale models of climate, hydrologic processes, and biogeochemical cycling. Examples of biogeophysical parameters keyed to land cover include leaf-area index, vegetation density, and FPAR. Other parameters are biomass permanence and energy-transfer characteristics of the land surface.

Data Set Evolution

Recent attempts to produce regional-scale land cover datasets use coarse spatial resolution and high-temporal-frequency data from the AVHRR instrument aboard the NOAA series of meteorological satellites. Most of these efforts have used the Normalized Difference Vegetation Index (NDVI) parameter derived from these data. The NDVI generally quantifies the biophysical activity of the land surface and as such does not provide land cover directly. The MODIS land cover algorithm draws from information domains well beyond those used in these efforts including directional surface reflectance, texture, vegetation index, acquisition geometry, land-surface temperature, and snow/ice cover derived from the MODIS instruments on both Terra and Aqua. The algorithm will use a hybrid decision-tree neural-network classifier. Product validation will be based on a network of about 400 test sites. High-resolution imagery (e.g., Landsat) will be used to establish truth for the sites,

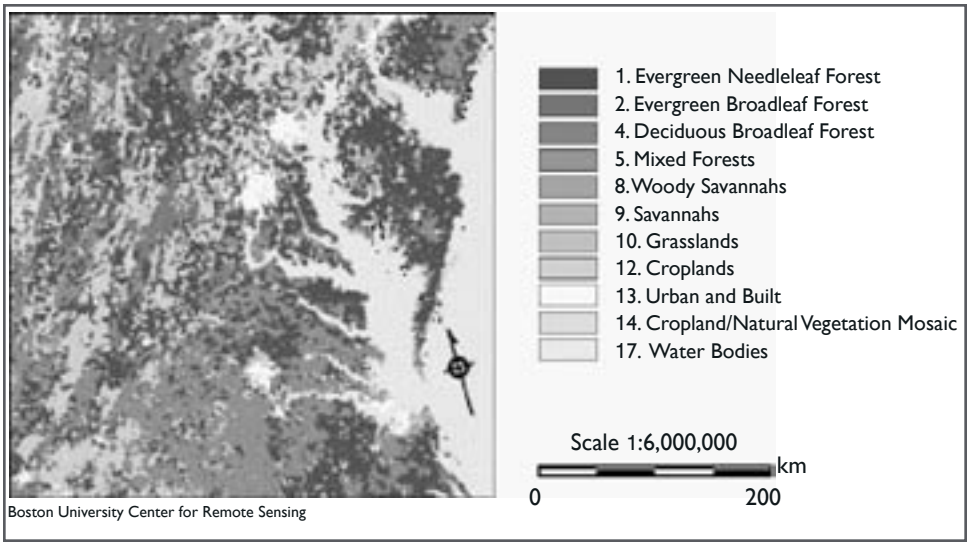

Land Cover Classes in a Mid-Atlantic Subset of the North American Prototype of the MODIS Land Cover Product, September 1999.

which will be used to train the land-cover classifier and validate the products. The validation procedure will characterize the accuracy of the product as well as provide information that can be used in spatial aggregation to provide land cover data and land cover change data at coarser resolutions.

Suggested Reading

Justice, C. *et al*., 1998.

Running, S. W. *et al*., 1994.

Running, S. W. *et al*., 1995.

Salisbury, J. W., and D. M. D'Aria, 1992.

Snyder, W., and Z. Wan, 1996.

Strahler, A. *et al*., 1995.

Wan, Z., and J. Dozier, 1996.

Wan, Z., and Z.-L. Li, 1997.

MODIS Land Cover Type Summary

Coverage: Global, clear-sky only

Spatial/Temporal Characteristics: 1 km, 1/4°, 1/2°, 1°/seasonal (96-day)

Key Science Applications: Biogeochemical cycles, land cover change

Key Geophysical Parameters: Land cover type, land cover change

Processing Level: 3

Product Type: Standard, post-launch

Maximum File Size: 16 MB

File Frequency: 289/96-day

Primary Data Format: HDF-EOS

Additional Product Information: http://modis-land.gsfc.nasa.gov/products/products.asp?ProdFamID=10

DAAC: EROS Data Center

Science Team Contact
A. H. Strahler

MODIS Vegetation Indices (MOD 13)

Product Description

The MODIS Vegetation-Index (VI) products will provide consistent spatial and temporal comparisons of global vegetation conditions that will be used to monitor the Earth's terrestrial photosynthetic vegetation activity in support of change detection and phenologic and biophysical interpretations. Gridded vegetation-index maps depicting spatial and temporal variations in vegetation activity are derived at 8-day, 16-day, and monthly intervals for precise seasonal and interannual monitoring of the Earth's vegetation. The MODIS VI products will improve upon currently available indices and will more accurately monitor and detect changes in the state and condition of the Earth's vegetative cover. The vegetation-index products are made globally robust with enhanced vegetation sensitivity and minimal variations associated with external influences (atmosphere, view and sun angles, clouds) and inherent, non-vegetation influences (canopy background, litter), in order to serve more effectively as a "precise" measure of spatial and temporal vegetation change.

Two vegetation-index (VI) products are to be produced globally for land at launch. One is the standard normalized difference vegetation index (NDVI), which is referred to as the "continuity index" to the existing NOAA-AVHRR-derived NDVI. The other is an enhanced vegetation index (EVI) with improved sensitivity in high biomass regions and improved vegetation monitoring through a decoupling of the canopy background signal and a reduction in atmosphere influences. The two VIs complement each other in global vegetation studies and improve upon the extraction of canopy biophysical parameters. A new compositing scheme that reduces angular, sun-target-sensor variations is also utilized. The gridded vegetation-index maps will use as input MODIS Terra and Aqua surface reflectances, corrected for molecular scattering, ozone absorption, and aerosols, and adjusted to nadir and standard sun angles with use of BRDF models. The gridded vegetation indices will include quality-assurance (QA) flags with statistical data, indicating the quality of the VI product and input data. The MODIS vegetation-index products will include:

- 250-m NDVI and QA as 8-day, 16-day, and monthly products (high resolution)
- 1-km NDVI, EVI, and QA as 8-day, 16-day, and monthly products (standard resolution)
- 25-km NDVI, EVI, and QA as 8-day, 16-day, and monthly products (coarse resolution)

Research and Applications

Due to their simplicity, ease of application, and widespread familiarity, vegetation indices are widely used by the broader user community from global circulation climate modelers and EOS instrument teams and interdisciplinary projects in hydrology, ecology, and biogeochemistry to those making regional- and global-based applications involving natural-resource inventories, land-use planning, agricultural monitoring and forecasting, and drought forecasting. Some of the more common applications of the vegetation index concern:

- Global warming/climate
- Global biogeochemical and hydrologic modeling
- Agriculture; precision agriculture; crop stress, crop mapping
- Rangelands; water supply forecasting; grazing capacities; fuel supply
- Forestry, deforestation, and net primary production studies
- Pollution/health issues (Rift valley fever, mosquito-producing rice fields)
- Desertification
- Anthropogenic-change detection and landscape disturbances.

Data Set Evolution

At the time of the launch of Aqua, there will be a 20-year NDVI global data set (1981-2000) from the NOAA- AVHRR series, which could be extended by MODIS Terra and Aqua data to provide a long-term data record for use in operational monitoring studies. The MODIS Terra and Aqua data set can readily be composited to provide 16-day, cloud-free time-series maps of vegetation activity. When both Terra and Aqua data are combined, higher frequency, 8-day, cloud-free time-series data will be readily made available.

Suggested Reading

Cihlar, J. C. *et al.*, 1997.

Huete, A. R. *et al.*, 1994.

Huete, A. R. *et al.*, 1997.

Huete, A. R. *et al.*, 1999.

Myneni, R. B. *et al.*, 1997a,b.

van Leeuwen, W. J. D. *et al.*, 1999.

MODIS Vegetation Indices Summary

Coverage: Global land surface

Spatial/Temporal Characteristics: 250 m, 1 km, and 0.25° resolutions/16-day and monthly products for Terra and Aqua data separately, plus an 8-day product for combined Terra and Aqua data.

Key Science Applications: Global vegetation monitoring, biogeochemical and hydrologic modeling, health and food security, range and forestry monitoring, agriculture management

Key Geophysical Parameters: Vegetation indices (NDVI & EVI)

Processing Level: 3

Product Type: Standard, at-launch

Maximum File Size: 277 MB

File Frequency: 289/16-day (16-day), 289/month (Monthly)

Primary Data Format: HDF-EOS

Additional Product Information: http://modis-land.gsfc.nasa.gov/products/products.asp?ProdFamID=6

DAAC: EROS Data Center

Science Team Contact: A. R. Huete

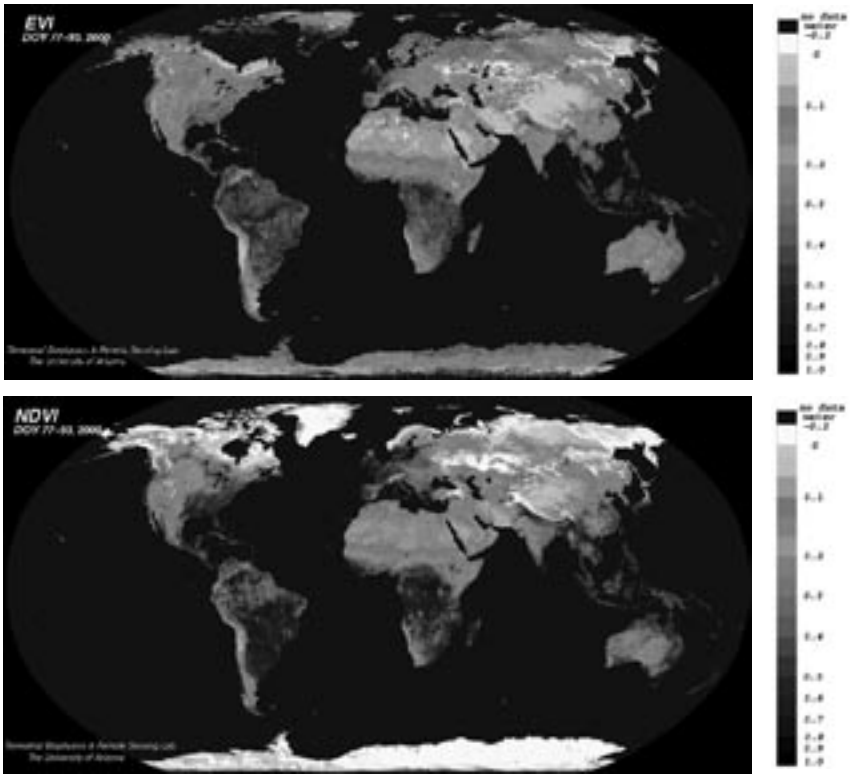

Global Composite of MODIS Enhanced Vegetation Index (top) and Normalized Difference Vegetation Index (bottom), both from data of the Terra MODIS for March 17 - April 2, 2000.

High Resolution (500 m) Composite of the Normalized Difference Vegetation Index for North and South America, from data of the Terra MODIS instrument for April 22 - May 7, 2000.

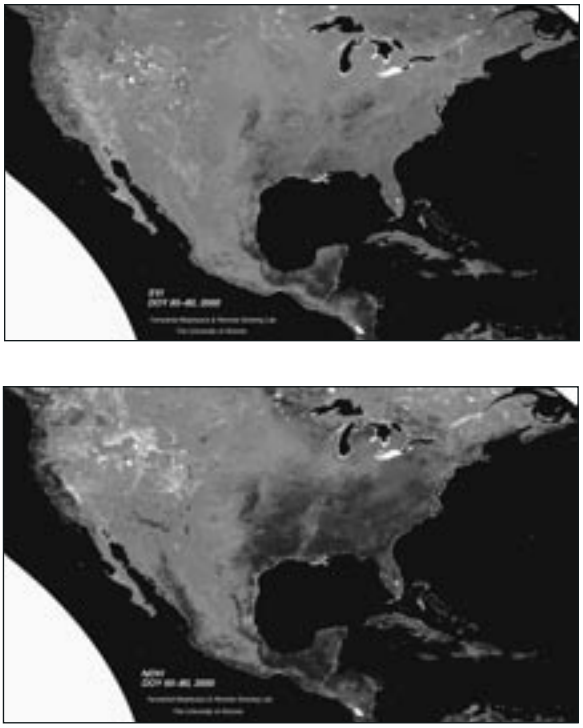

High Resolution (1 km) Composite of MODIS Enhanced Vegetation Index (top) and Normalized Difference Vegetation Index (bottom) for North America, from data of the Terra MODIS instrument for March 5 - March 20, 2000.

MODIS Leaf Area Index (LAI) and Fraction of Photosynthetically Active Radiation (FPAR) – Moderate Resolution (MOD 15)

Product Description

The MOD 15 Leaf Area Index (LAI) and Fraction of Photosynthetically Active Radiation absorbed by vegetation (FPAR) are 1-km at-launch products provided on a daily and 8-day basis. LAI defines an important structural property of a plant canopy, namely the one-sided leaf area per unit ground area. FPAR measures the proportion of available radiation in the photosynthetically active wavelengths (400 to 700 nm) that a canopy absorbs. The LAI product will be a LAI value between 0 and 8 of the global gridded database at the corresponding modified vegetation index (MVI) compositing interval. The FPAR product will be an FPAR value between 0.0 and 1.0 assigned to each 1-km cell of the global gridded database at the corresponding MVI compositing interval.

Research and Applications

LAI and FPAR are biophysical variables that describe canopy structure and are related to functional process rates of energy and mass exchange. Both LAI and FPAR have been used extensively as satellite- derived parameters for calculation of surface photosynthesis, evapotranspiration, and NPP. These products are essential in calculating terrestrial energy, carbon, water-cycle processes, and biogeochemistry of vegetation. The LAI product is an input to Biome-BGC (Biogeochemical) models to produce conversion-efficiency coefficients, which are combined with the FPAR product to produce daily terrestrial PSN (photosynthesis) and annual NPP.

Data Set Evolution

This product is derived from the Surface Reflectance Product (MOD 09), the Land Cover Type product (MOD 12), and ancillary information on surface characteristics such as land cover type and background. The retrievals are performed by comparing observed and modeled surface reflectances for a suite of canopy structures and soil patterns that covers a range of expected natural conditions. All canopy/soil patterns for which the magnitude of the residuals in the comparison does not exceed uncertainties in observed and modeled surface reflectances are treated as acceptable solutions. For each acceptable solution, a value of FPAR is also evaluated. The mean and dispersion values of the LAI solution distribution function are taken as the retrieved LAI accuracy; likewise for FPAR. A three-dimensional formulation of the radiative transfer is used to derive spectral and angular biome-specific signatures of vegetation canopies. Should this main algorithm fail, a back-up algorithm is triggered to estimate LAI and FPAR using a Normalized Difference Vegetation Index (NDVI).

Suggested Reading

Knyazikhin, Y. *et al*., 1998a,b.

Myneni, R. B. *et al*., 1997b.

Tian, Y. *et al*., 2000.

Zhang, Y. *et al*., 2000.

MODIS LAI and FPAR – Moderate Resolution Summary

Coverage: Global

Spatial/Temporal Characteristics: 1 km/daily, 8-day

Key Science Applications: Biogeochemical cycle modeling, NPP estimation

Key Geophysical Parameters: Leaf area index, fraction of photosynthetically active radiation absorbed by vegetation

Processing Level: 4

Product Type: Standard, at-launch

Maximum File Size: 5.8 MB

File Frequency: 289/day (Daily Level 4), 289/8-day (8-day Level 4)

Primary Data Format: HDF-EOS

Additional Product Information: http://modis-land.gsfc.nasa.gov/products/products.asp?ProdFamID=5

DAAC: EROS Data Center

Science Team Contacts:
R. B. Myneni
S.W. Running

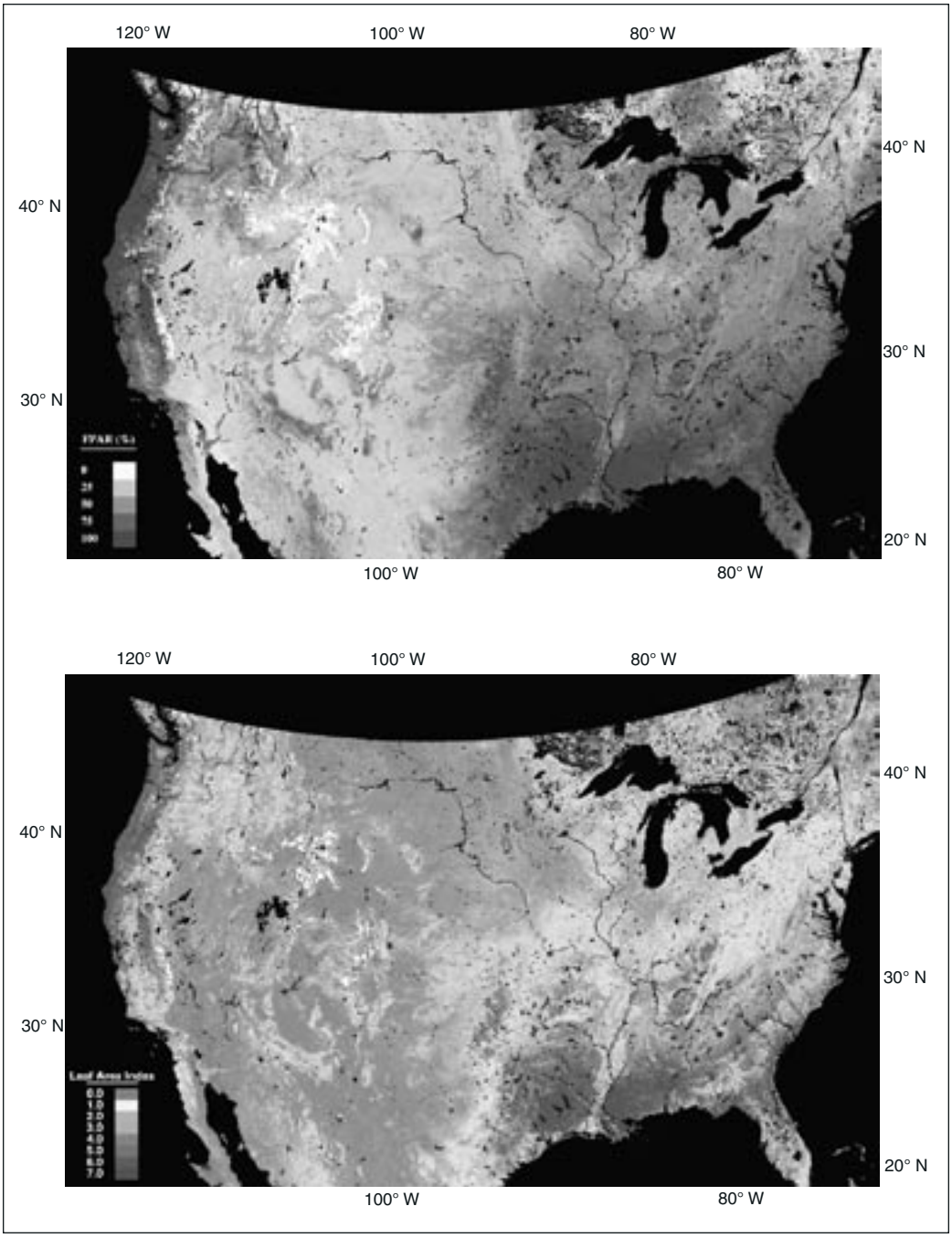

The First Complete Continental Computation of Two MODIS Land Products, Leaf Area Index (LAI) and Fraction of Absorbed Photosynthetically Active Radiation (FPAR). Both of these variables quantify green vegetation but in different ways. LAI defines canopy leaf area, while FPAR defines the amount of incoming solar radiation absorbed by the plant canopies. These variables are used to parameterize terrestrial vegetation for global carbon, hydrologic, and climate models, and also are used for a number of land management applications. This image is a time composite from March 24 to April 9, 2000, using MODIS Spectral Channels 1 and 2 at 250 m rescaled to 1 km spatial resolution. The image shows that in this early spring time period, most agricultural land and deciduous forest does not yet show spring leaf growth. Continental greening will occur rapidly over the next 4-6 weeks.

MODIS Surface Resistance and Evapotranspiration (MOD 16)

Product Description

This Level 4 product consists of Surface Resistance and Evapotranspiration (ET) parameters and has a temporal resolution of eight days at a spatial resolution of 1 km over the land surface only. The land Surface Resistance is an Aqua product that captures sub-optimum conditions produced by soil/atmospheric moisture deficits for vegetation photosynthesis and transpiration. The spatial resolution of these products is 1 km.

Research and Applications

These two parameters are essential to global modeling of climate, water balance, and trace gases. In addition, they are required in estimating photosynthesis, respiration, and net primary production. The surface-resistance product is an Aqua (post-launch) research data product intended for real-time implementations. Practical applications of this product are for monitoring wildfire danger and crop/range drought.

Data Set Evolution

The Surface Resistance product will be calculated using the MODIS Land Surface Temperature (MOD 11) and the MODIS modified vegetation index (MOD 13), and will be used along with incident radiation for computing the ET.

Suggested Reading

Dickinson, R. E., 1987.

Goward, S. N., and A. S. Hope, 1989.

Nemani, R. R., and S. W. Running, 1989.

Nemani, R. R. *et al.*, 1993.

Running, S. W. *et al.*, 1989.

Running, S. W. *et al.*, 1994.

MODIS Surface Resistance and Evapotranspiration Summary

Coverage: Global

Spatial/Temporal Characteristics: 1 km/8-day, yearly

Key Science Applications: Global water balance, net primary production

Key Geophysical Parameters: Surface resistance, evapotranspiration

Processing Level: 4

Product Type: Research, post-launch

Maximum File Size: 5.8 MB

File Frequency: 289/8-day

Primary Data Format: HDF-EOS

Additional Product Information: http://modis-land.gsfc.nasa.gov/products/products.asp?ProdFamID=3

DAAC: EROS Data Center

Science Team Contact: S.W. Running

MODIS Vegetation Production and Net Primary Production (MOD 17)

Product Description

MOD 17 is a Level 4 product consisting of 8-day Net Photosynthesis (PSN) and Net Primary Production (NPP). Annual NPP is the time integral of the PSN product over a year.

Research and Applications

This product provides an accurate measure of terrestrial vegetation growth and production activity. The theoretical use is to define the seasonally dynamic flux of terrestrial-surface carbon dioxide for climate modeling. Fluxes will be computed specific to each vegetation type. The practical utility is to measure crop yield and forest production and any other socially significant products of vegetation growth. As this global NPP product becomes regularly available, a wide variety of derived products is expected to be developed making regionally specific estimates of crop production. The value of an unbiased, regular source of crop and forest production estimates for global political and economic decision making is immense.

Data Set Evolution

The NPP parameter is the yearly integral of the PSN which is obtained from the product of PAR (Photosynthetically Active Radiation), FPAR (Fraction of Photosynthetically Active Radiation) and conversion-efficiency coefficients obtained from other MODIS products and other sensors and ancillary data. The algorithms for these products are based on the original logic of Monteith (1972), which relates PSN and NPP to the amount of Absorbed Photosynthetically Active Radiation (APAR). The MODIS modified vegetation indices (MVI) along with climate variables and the land cover product are used to estimate APAR.

Suggested Reading

Field, C. B. *et al*., 1995.

Monteith, J. L., 1972.

Prince, S. D., and S. N. Goward, 1995.

Ruimy, A. *et al*., 1994.

Running, S. W., 1990.

Running, S. W. *et al*., 1994.

MODIS Vegetation Production and Net Primary Production Summary

Coverage: Global

Spatial/Temporal Characteristics: 0.5, 1, 10 km/8-day, yearly

Key Science Applications: Interannual variability of vegetation

Key Geophysical Parameters: NPP, photosynthesis, respiration

Processing Level: 4

Product Type: Standard, at-launch

Maximum File Size: 4.3 MB

File Frequency: 289/8-day

Primary Data Format: HDF-EOS

Additional Product Information: http://modis-land.gsfc.nasa.gov/products/products.asp?ProdFamID=3

DAAC: EROS Data Center

Science Team Contact: S.W. Running

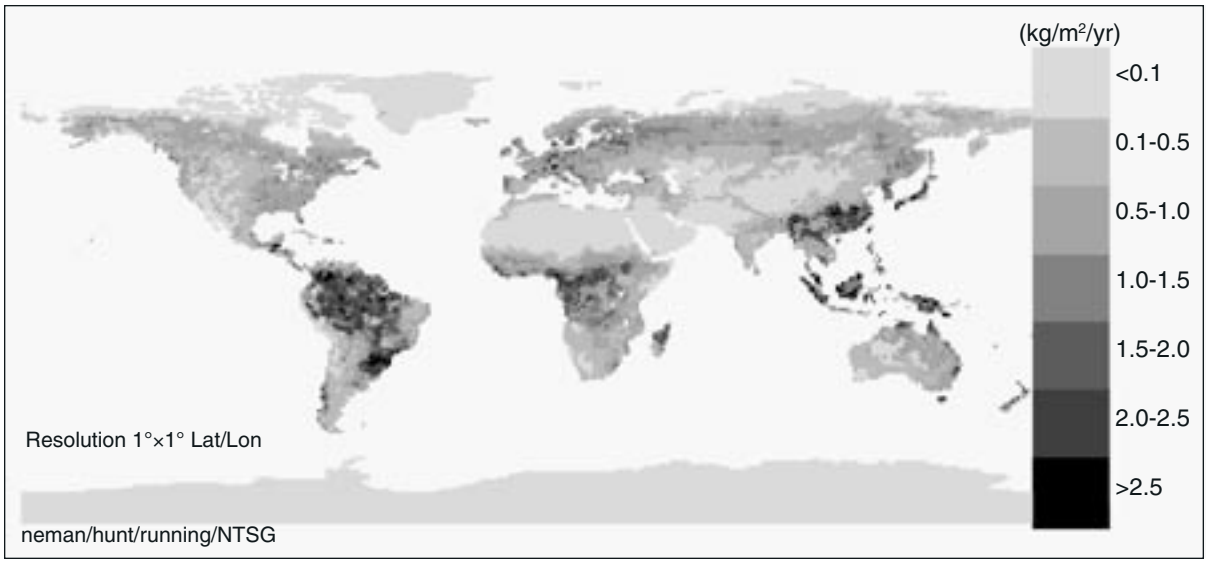

Global Net Primary Production (NPP) during 1987. This data set is produced using 1° × 1° gridded climate data from 7000 weather stations distributed globally, Mathews land cover classes collapsed into six classes, biome-specific NDVI-LAI relations used to estimate LAI from NOAA/NASA Pathfinder data, and an ecosystem simulation model, BIOME-BGC.

MODIS Surface Reflectance BRDF/Albedo Parameter (MOD 43)

Product Description

The Bidirectional Reflectance Distribution Function (BRDF)/Albedo parameter provides: 1) coefficients for mathematical functions that describe the BRDF of each pixel in the seven MODIS "Land" bands (1-7); and 2) albedo measures derived simultaneously from the BRDF for bands 1-7 as well as three broad bands (0.4-0.7, 0.7-3.0, and 0.4-3.0 micrometers).

Because deriving BRDF and albedo requires merging multiple looks at each pixel, the BRDF/Albedo parameter is provided every 16 days. Its spatial resolution is 1 km, gridded to Level 3. A 32-day summary albedo product at 0.25° spatial resolution is also provided. Both Terra and Aqua data are merged as available.

Research and Applications

The BRDF functions provided by the BRDF/Albedo parameter: 1) allow normalization of MODIS data to standard viewing and illumination angles, thus removing geometric effects from multidate images; 2) quantify the directional information in the remotely-sensed signal, which is related to ground-cover type; and 3) provide a surface-radiation-scattering model for boundary-layer parameterization in regional and global climate modeling. The BRDF can also be used in extraction of surface reflectances at Level 2. Two albedo measures are provided: "black-sky" albedo (directional-hemispherical reflectance) and "white-sky" albedo (bihemispherical reflectance). These are intrinsic surface properties, independent of atmospheric state. They describe the upward scattering of the solar beam and of uniform diffuse irradiance, respectively, and may be used as input to global and regional climate models.

Data Set Evolution

The BRDF/Albedo algorithm combines gridded, multidate, multiband surface-reflectance data from EOS MODIS and MISR (on Terra) instruments to produce BRDF functions and derived albedo measures. For each grid cell, all cloud-free observations in a 16-day period are assembled and fit to the Ross-Thick/Li-Sparse semiempirical model that describes the BRDF as a linear function of two basic BRDF shapes. In addition, a single empirical model (modified Walthall) is currently also fitted. The algorithm outputs include: 1) Ross-Thick/Li-Sparse BRDF parameters that best fit

the observations, 2) modified Walthall parameters, 3) black-sky and white-sky albedos in three broad bands, and 4) nadir BRDF-adjusted reflectances (NBARs).

Suggested Reading

Barnsley, M. J., and J.-P. Muller, 1991.

d'Entremont, R. E. *et al.*, 1999.

Hu, B. *et al.*, 1997.

Hu, B. *et al.*, 1999.

Hu, B. *et al.*, 2000.

Justice, C. *et al.*, 1998.

Li, X. *et al.*, 1995.

Liang, S. *et al.*, 1999

Lucht, W., 1998.

Lucht, W., and P. Lewis, 2000.

Lucht, W. *et al.*, 2000.

Wanner, W. *et al.*, 1995.

Wanner, W. *et al.*, 1997.

MODIS Surface Reflectance BRDF/Albedo Parameter Summary

Coverage: Global land surface

Spatial/Temporal Characteristics: 1 km, 16 km, 0.5°/16-day; 0.25°/32-day

Key Science Applications: Biogeochemical-cycle modeling, net primary productivity estimation, global climate models

Key Geophysical Parameters: Bidirectional reflectance, spectral albedo

Processing Level: 3

Product Type: Standard, at-launch

Maximum File Size: 329 MB (16-day), 946 MB (32-day)

File Frequency: 289/16-day (16-day), 1/month (32-day)

Primary Data Format: HDF-EOS

Additional Product Information: http://modis-land.gsfc.nasa.gov/products/products.asp?ProdFamID=2

DAAC: EROS Data Center

Science Team Contacts:
A. H. Strahler
J.-P. Muller

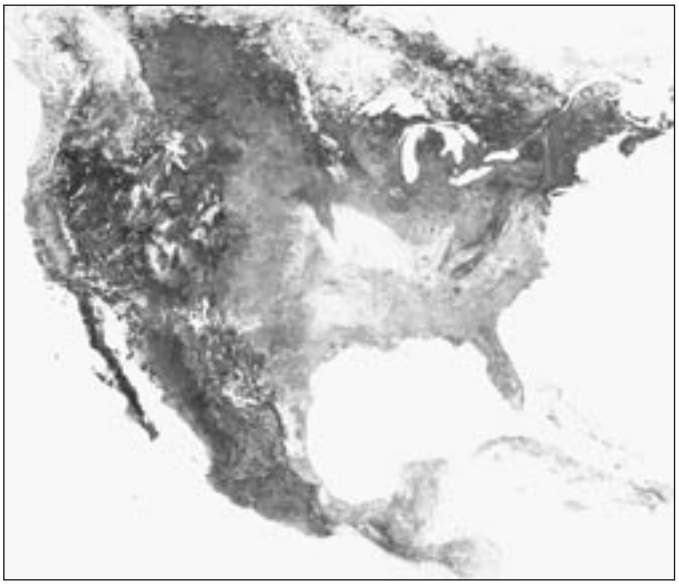

Bihemispherical Albedo (White-Sky Albedo) for North America for the period April 22 - May 7, 2000, calculated from the MODIS BRDF/Albedo product algorithm using data from the Terra MODIS near-infrared channel (Band 2). In this image, cloud cover has obscured some regions in the central U.S. as well as other smaller areas shown in white. Light tones in the southeastern U.S. indicate strong reflectance from leaf cover, while much of the more northern regions remains leafless.

MODIS Vegetation Cover Conversion (MOD 44)

Product Description

Using MODIS data from the two 250-m bands, the vegetation cover conversion product will show the global distribution of the occurrence of vegetation cover change. Where there is sufficient evidence, the type of change will be labeled (e.g., forest conversion to agricultural fields or grassland or bare surface). The distribution of these changes will be represented at a resolution of 250 meters and as gridded 10-km summaries. These will be generated at 3-month intervals. An interannual product is also being produced, displaying the global distribution of vegetation-cover change during the previous year.

Research and Applications

Vegetation-cover change is an important driver of many important biogeochemical, hydrological, and climate processes. It also represents the integrated response to several biophysical and anthropogenic impacts. Among the important influences of vegetation-cover change are the following:

- It strongly affects changes in many biophysical factors such as surface roughness and albedo;
- It has a major effect on changes in sensible heat flux, because it affects global albedo and surface roughness, which in turn affects atmospheric drag;
- It is of crucial importance for determining the biogeochemical cycling of carbon, nitrogen, and other elements at regional-to-global scales;
- It has a major impact on the runoff characteristics of catchments through its effects on evapotranspiration and partitioning of precipitation into overland flow, interflow, and groundwater accretion;
- It gives a direct insight into ecosystem response related to climate change and anthropogenic influences;
- It affects biodiversity through direct impacts on habitat;
- It provides increasingly important information for natural-resource managers.

This product will be combined with data obtained from finer spatial resolution data from sensors such as ETM+ on Landsat 7 and ASTER on Terra (see Volume 1) to assist in the identification of the types of vegetation conversion occurring. The product also provides information to assist the acquisition strategy of finer resolution systems since it helps flag areas where significant changes are likely to be occurring.

Data Set Evolution

Previous work has shown that data with a resolution of 1 km and coarser are sufficient for the mapping of the distribution of vegetation cover and for the monitoring of those changes in vegetation cover caused by seasonal-to-interannual climate change. However, such relatively coarse resolution data are often inadequate to detect changes caused by anthropogenic factors. Analyses of many types of vegetation-cover change indicate that they are relatively small in size largely due to the inherently local nature of anthropogenic vegetation-cover conversions. Consequently a very large proportion of changes is only detectable at fine spatial resolutions. For this reason it was decided to use the two 250-m bands for the identification and mapping of this type of conversion.

Suggested Reading

Townshend, J. R. G., and C. O. Justice, 1988.

Townshend, J. R. G. *et al.*, 1991.

Zhan, X. *et al.*, 1999.

MODIS Vegetation Cover Conversion Summary

Coverage: Global, daytime

Spatial/Temporal Characteristics: 250 m, 10 km/3-month, yearly

Key Geophysical Parameters: Vegetation-cover change occurrence and type

Processing Level: 4

Product Type: Research, at-launch and post-launch

Maximum File Size: 1 GB/tile (land tiles only)

File Frequency: 1/month (Monthly Level 4), 1/year (Yearly Level 4)

Primary Data Format: HDF

Browse Available: http://www.geog.umd.edu/landcover/modis

Additional Product Information: http://modis-land.gsfc.nasa.gov/products/products.asp?ProdFamID=2

DAAC: EROS Data Center

Science Team Contact: J. R. G. Townshend

VCL (MBLA): Geolocated Ground Elevations

Product Description

The strong scientific need for accurate, global topographic databases has led to recent progress in limited release of portions of the Defense Mapping Agency Digital Terrain Elevation Data (DTED) Level 1 data that have 90-m horizontal pixel resolution and 16-m vertical accuracy. Despite this progress the scientific benefit for global studies is not nearly realized. The existing DTED Level 1 data will not be released for the entire Earth, and space-based imaging sensors now in orbit and planned in the EOS Terra/Aqua era (1999-2005) require global topography at DTED Level 2 resolution (30 m spatial, 16 m vertical) for full realization of their science potential in land-cover/global productivity, short-term climate modeling, and natural hazard studies. The Shuttle Radar Topography Mission (SRTM) has flown to address these needs. Since Interferometric Synthetic Aperture Radar (IfSAR) data, or the conventional photogrammetric data sets, are only relative in their measurement of surface elevation, direct measurements are needed to "control" the vertical dimension of the topographic image. Estimates of topographic control points (TCPs) needed for a global DTED Level 2 are well in excess of 100,000,000. Only a limited number of these TCPs can be provided by ground-based radar targets and GPS receivers; the remainder will have to be estimated from existing maps and digital elevation models that do not routinely achieve the 1-meter level of vertical accuracy and do not have a common reference frame. Of equal importance, none of the existing remote sensing techniques listed above has the ability to reliably penetrate a canopy-covered surface to provide accurate measurements of surface topographic height. Such measurements are needed for a variety of geophysical, hydrological, and land-use purposes.

The VCL surface-elevation measurements using the MBLA instrument will have a common, global reference frame and are "direct" rather than inferred. Furthermore, only VCL will address the vegetation-cover issues that limit all present mapping techniques to tens-of-meters rms in forested areas. The VCL mission, by virtue of its primary vegetation-canopy measurements, will provide billions of sub-canopy surface elevation points. The surface-height measurement is obtained when processing the returned laser waveform. The last return that is captured that exceeds a given threshold is the ground return. Calibration and validation experiments using the aircraft simulator of the VCL instrument, LVIS, have demonstrated that even within the densest canopies, a majority of laser pulses return waveforms with valid ground reflections.

VCL Geolocated Ground Elevations Summary

Coverage: 67°N - 67°S

Spatial/Temporal Characteristics: ~25 m resolution along track, ~2 km across track

Key Science Applications: Global data set of topographic elevations in consistent reference frame, topographic control points for other applications

Key Geophysical Parameters: Topographic elevations

Processing Level: 2

Product Type: Standard, at-launch

Science Team Contact:
R. O. Dubayah

VCL (MBLA): Geolocated Canopy-Top Heights

Product Description

Within the returned waveform from the MBLA instrument, the first return above a threshold represents the top of the canopy, and the last return in the waveform represents the ground return. Canopy height is calculated by subtracting the elevations of the first and last returns. Vegetation height is a function of species composition, climate, and site quality, and can be used for land cover classification alone or in conjunction with vegetation indices, e.g., NDVI. Leaf-on versus leaf-off conditions will also affect this measurement for certain species. Along-track measurements, i.e., footprint-to-footprint, of VCL-derived height variation provides additional information such as fractal (Palmer, 1988) or autocorrelative (Cohen *et al.,* 1990) properties of the canopy that further may be used to differentiate among natural and anthropogenically disturbed land cover patterns (Krummel *et al.,* 1987). When coupled with species composition and site-quality information (e.g., edaphic and climatic variables), height serves as an estimate of stand age or successional state, which can be correlated to carbon flux rates (Ustin *et al.,* 1993).

In addition to providing a unique metric, i.e., the vertical dimension, to classify vegetative cover at global scales, height is highly correlated with above-ground biomass (Oliver and Larson, 1990; Avery and Burkhart, 1994; Nilsson, 1996). Biomass in forests represents the major reservoir of carbon in terrestrial ecosystems that can be quickly mobilized by disturbance or land-use change (e.g., Houghton *et al.,* 1987; Dixon *et al.,* 1994).

Suggested Reading

Avery, T. E., and H. E. Burkhart, 1994.

Cohen, W. B. *et al.,* 1990.

Dixon, R. K. *et al.,* 1994.

Houghton, R. A. *et al.,* 1987.

Krummel, J. R. *et al.,* 1987.

Nilsson, M., 1996.

Oliver, C. D., and B. C. Larson, 1990.

Palmer, M. W., 1988.

Ustin, S. L. *et al.,* 1993.

VCL Geolocated Canopy-Top Heights Product Summary

Coverage: 67°N - 67°S

Spatial/Temporal Characteristics: ~25 m resolution along track, ~2 km across track

Key Science Applications: Global climate modeling, terrestrial ecosystem modeling, above-ground biomass estimation, biodiversity studies, aerodynamic roughness.

Key Geophysical Parameters: Canopy height

Processing Level: 2

Product Type: Standard, at-launch

Science Team Contact:
R. O. Dubayah

VCL (MBLA): Geolocated Vertical Distribution of Intercepted Surfaces (VDIS)

Product Description

By recording the complete time-varying amplitude of the return signal of the laser pulse from the MBLA instrument between the first and last returns (representing the canopy top and the ground), VCL captures a waveform that is related to canopy architecture. This architecture is specifically related to the nadir-projected vertical distribution of the surface area of canopy components (foliage, trunk, twigs, and branches) that reflect the incoming laser pulse. Like the simple height estimate, the vertical distribution of laser return provides a new means to classify vegetation and functions as a predictor of the successional state of a forest. Trees in younger stands tend to exhibit a more leptokurtic vertical distribution of phytomass concentrated near the ground. As a stand ages and grows, the vertical distribution of canopy components becomes more platykurtic. Bimodal distributions are associated with the presence of an understory that may occur in more mature stands. Older stands characterized by canopy gaps and trees of multiple ages and sizes exhibit a more even distribution of canopy components (e.g., Aber, 1979; Brown and Parker, 1994).

When combined with greenness measures from other sensors, such as ETM+, MODIS, or AVHRR, VCL observations may be used to determine whether the greenness signal is the result solely of low-lying vegetation (via the height distribution). Many areas of the world have ground covers with greenness indices comparable to those of forests, making land cover discrimination based on greenness measures alone difficult. Measures of the vertical organization of canopy components are also critical for modeling factors that relate to biophysical and micrometeorological processes at the atmospheric-vegetation boundary layer such as radiative transfer, evapotranspiration, and trace gas flux.

Suggested Reading

Aber, J. D., 1979.

Brown, M. J., and G. G. Parker, 1994.

VCL (MBLA) Level 2: Geolocated Vertical Distribution of Intercepted Surfaces (VDIS) Summary

Coverage: 67°N - 67°S

Spatial/Temporal Characteristics: ~25 m resolution along track, ~2 km across track

Key Science Applications: Global climate modeling, terrestrial ecosystem modeling, above-ground biomass estimation, biodiversity studies, aerodynamic roughness.

Key Geophysical Parameters: Above-ground vertical distribution of intercepted surfaces

Processing Level: 2

Product Type: Standard, at-launch

Science Team Contact:
R. O. Dubayah

Phytoplankton and Dissolved Organic Matter

Aqua
• MODIS

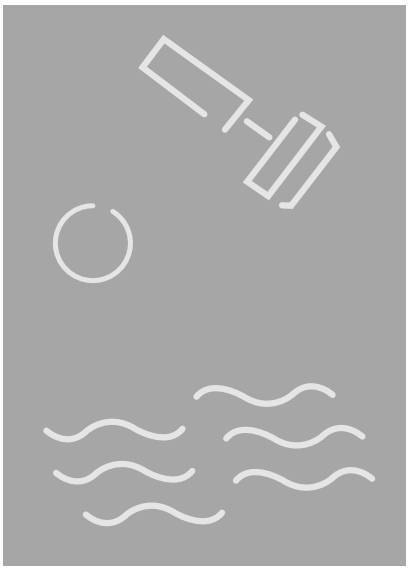

Phytoplankton and Dissolved Organic Matter – An Overview

Relationship to Global Change Issues

The global oceans, covering 70% of the Earth's surface and extending in some locations to depths exceeding 10 km, contain a varied abundance of life forms; and central to the ocean ecosystem are the unicellular plants called phytoplankton. Phytoplankton take dissolved carbon dioxide from sea water and use it for phytoplankton photosynthesis, enabling phytoplankton growth and releasing oxygen. This process captures approximately the same amount of carbon as does photosynthesis by land vegetation.

Phytoplankton photosynthesis has been a primary sink for the increased carbon dioxide injected into the atmosphere over the past century through human activities such as biomass burning and fossil-fuel burning. The amount and distribution of carbon dioxide consumed by the phytoplankton depends heavily on ocean circulation, which supplies nutrients to the upper layers of the ocean where sunlight is abundant. Some fraction of carbon produced by the phytoplankton sinks to the ocean floor—a long-term sink for atmospheric carbon dioxide. The fraction is not well known and is a source of a large uncertainty in the global carbon budget.

Changes in the amount of phytoplankton indicate changes in productivity of the oceans and provide a key ocean link for the monitoring of global climate change. Ocean and land biological productivity, heat-exchange processes, and water-exchange processes are tightly coupled, and it is important for global-change models to take such interactions into account in global climate-change prediction. The hope is that the phytoplankton and dissolved organic matter data products will help scientists to determine whether ocean productivity is changing and, if so, how such changes relate to the global carbon cycle and other global changes.

Product Overview

The ten products discussed in this chapter are all from the MODIS instrument, on both the Terra and Aqua satellites. They are all related, in one way or another, to oceanic life forms.

The Ocean Primary Productivity product (MOD 27) provides the time rate of change of phytoplankton biomass, which governs the fixing of carbon and influences CO_2 in the atmosphere and ultimately global climate. MOD 27 is a Level 4 product that provides an estimate of the ocean primary productivity on a weekly and an annual basis. It is analogous to the Net Primary Production (NPP) product over land (MOD 04). The Pigment Concentration product (MOD 19) and three associated products, Suspended Solids Concentration (MOD 23), Organic Matter Concentration (MOD 24), and Ocean Water Attenuation Coefficient (MOD 26), are used to support development and validation of the algorithms for primary productivity.

The Coccolith Concentration product (MOD 25) provides five parameters describing the concentration of coccoliths, calcium carbonate scales produced by the phytoplankton group named coccolithophores. These scales eventually sink to the ocean floor, accounting for about 75% of the deposition of carbon on the sea floor. Similarly, the Phycoerythrin Concentration product (MOD 31) provides three parameters regarding phycoerythrin, one of the major algal pigment groups in ocean water. Experimental evidence suggests that water-leaving radiance includes backscattering and absorption effects of phycoerythrin pigments that should be taken into account in space-based estimations of primary productivity.

The primary phytoplankton indicator product used as input to the primary ocean productivity algorithm is Chlorophyll *a* Pigment Concentration (MOD 21). This product uses the Normalized Water-leaving Radiance (MOD 18) and Match-up Database (MOD 32) to calibrate semi-analytical models using the remote-sensing reflectances in the MODIS ocean bands and has a companion, intermediate product termed Absorption Coefficients (MOD 36). The second phytoplankton indicator used as input to the productivity algorithm is the Chlorophyll Fluorescence product (MOD 20), which provides another measure of chlorophyll concentration and hence phytoplankton concentration.

Product Interdependency and Continuity with Heritage Data

The phytoplankton and dissolved organic matter products require water-leaving radiances (MOD 18) and the MODIS match-up data base (MOD 32), which provides remote sensing and *in situ* sea-surface-radiance measurements. Some individual products require additional parameters, such as Chlorophyll *a* Case I for Fluorescence and downwelling sea-surface radiance for Chlorophyll *a*. The MODIS pigment algorithms were developed from existing CZCS pigment algorithms to provide a direct link to the series of measurements made by CZCS over a period of about 7.5 years. The MODIS measurements will continue the ocean color data sets from the CZCS

and SeaWiFS, overlapping with the latter, and will benefit from other simultaneous data sets and the further global context that they can provide.

Suggested Reading

Esaias, W. E. *et al*., 1999.

Gordon, H. R., 1978.

Gordon, H. R., 1997.

Goyet, C., and P. G. Brewer, 1993.

Iverson, R. L. *et al*., 2000.

Letelier, R. M. *et al*., 1997.

Sikes, S., and V. Fabry, 1994.

Yoder, J. A. *et al*., 1993.

MODIS Pigment Concentration (MOD19), Suspended Solids Concentration (MOD 23), Organic Matter Concentration (MOD 24), and Ocean Water Attenuation Coefficient (MOD 26)

Product Description

This set of products provides particle concentrations in Case 1 sea water, which have optical properties dominated by chlorophyll and associated covarying detrital pigments. (Case 2 waters contain substances that affect optical properties that may not covary with chlorophyll, such as gelbstoff, suspended sediments, coccolithophores, detritus, and bacteria.) Product MOD 19 is total Pigment Concentration; Product MOD 23 is Suspended Solids Concentration; Product MOD 24 is Organic Matter Concentration in two parameters, Particulate and Dissolved; and Product 26 gives the Ocean Water Attenuation Coefficient at two wavelengths, 490 nm and 530 nm. The products are available at Level 2 daily and at Level 3 daily, 8-day weekly, monthly, and yearly.

Research and Applications

This set of ocean-substance concentrations is needed for input to the ocean productivity algorithm, which is a key element in global biogeochemical models and ultimately global climate models. The pigment parameter is the sum of the chlorophyll *a* and phaeopigment concentration in Case 1 waters. The suspended-solids parameter is a measure of ocean-suspended sediments, which is used in the analysis of complex bio-optical properties of coastal and estuarine regions/environments and helps to map the extent of terrestrial changes. The organic-matter concentration relates to the composite of carbon and nitrogen substances. The ocean water attenuation coefficient is derived using MODIS bands 10 and 11 and describes penetration of sunlight in the sea.

Data Set Evolution

The algorithm is based primarily on methods and algorithms developed for the CZCS program described by Gordon and Clark (1980) and refined and adapted to the MODIS bands. The recasting of the CZCS forms of the phytoplankton pigment algorithms in terms that are more representative for MODIS has resulted in minor changes. Of particular significance is the fact that the multiple band ratios will provide a robustness not possible with the CZCS's limited spectral coverage.

Suggested Reading

Gordon, H. R., and D. K. Clark, 1980.

Gordon, H. R. *et al.*, 1980.

Gordon, H. R., and A. Y. Morel, 1983.

Lorenzen, C. J., and S. W. Jeffrey, 1980.

Smith, R. C., and K. S. Baker, 1977.

MOD 19, MOD 23, MOD 24, and MOD 26 Data Product Summary

Coverage: Global ocean surface, clear-sky only

Spatial/Temporal Characteristics: 1 km/daily (Level 2); 4.6 km, 36 km, 1°/daily, 8-day, monthly, yearly (Level 3)

Key Science Applications: Ocean productivity, biogeochemical models

Key Geophysical Parameters: Total ocean pigment, suspended solids, organic-matter concentration, attenuation coefficient

Processing Level: 2, 3

Product Type: Standard, at-launch

Maximum File Size:
MOD 19: 102 MB (Level 2); 620 MB (Level 3)

MOD 23: 102 MB (Level 2); 640 MB binned, 134 MB mapped (Level 3)

MOD 24: 83 MB (Level 2); 640 MB binned, 134 MB mapped (Level 3)

MOD 26: 102 MB (Level 2); 640 MB binned, 134 MB mapped (Level 3)

File Frequency:
MOD 19: 144/day (Daily Level 2); 3/day (Daily Level 3), 3/8-day (8-day Level 3), 3/month (Monthly Level 3), 3/year (Yearly Level 3)

MOD 23, MOD 24, MOD 26: 144/day (Daily Level 2); 1/day (Daily Level 3), 1/8-day (8-day Level 3), 1/month (Monthly Level 3), 1/year (Yearly Level 3)

Primary Data Format: HDF-EOS

Browse Available: 36 km sample imagery available at the Goddard DAAC (Level 3 only)

Additional Product Information:
http://modis-ocean.gsfc.nasa.gov/dataprod.html

DAAC: NASA Goddard Space Flight Center

Science Team Contact:
D. Clark

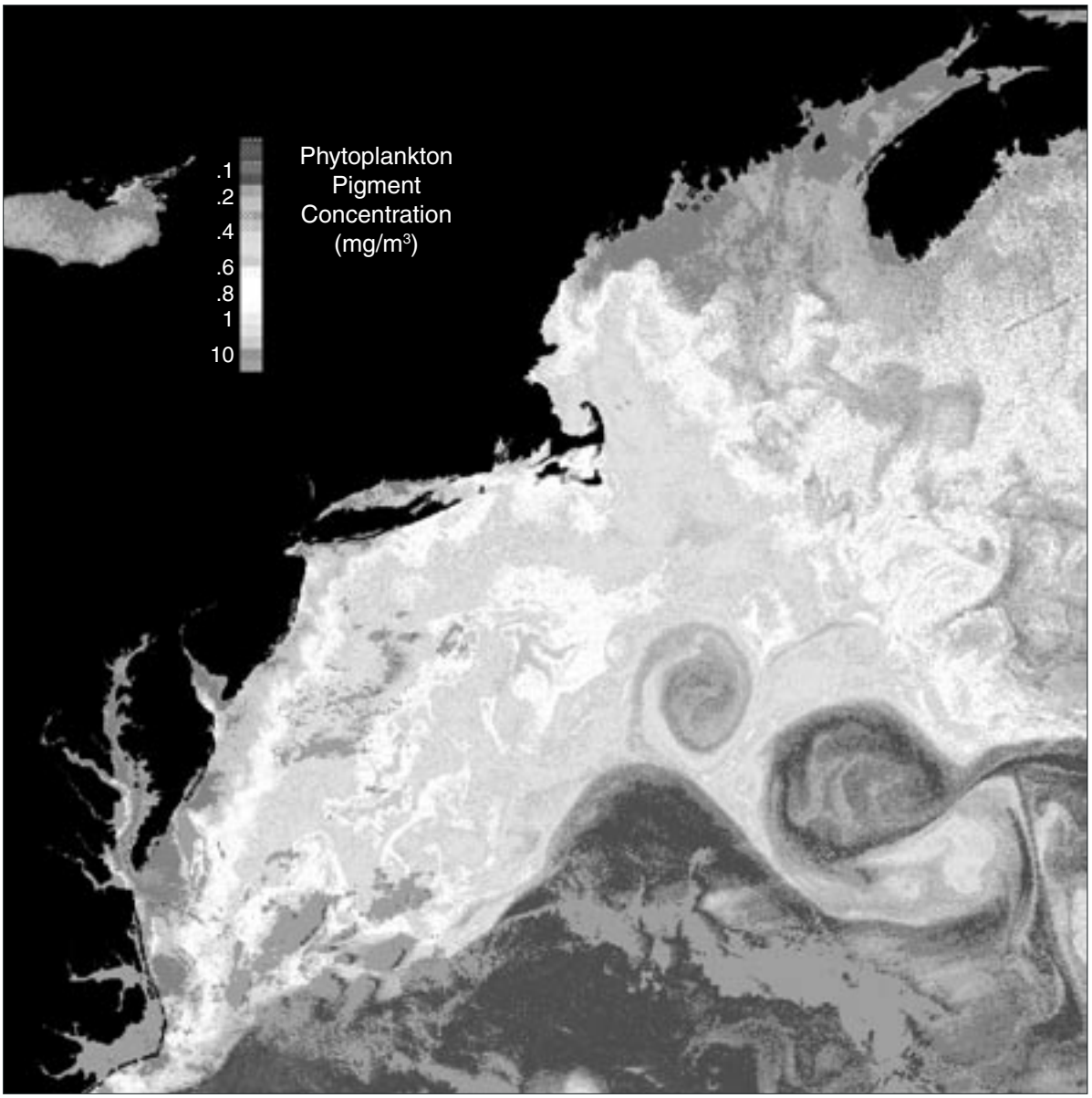

U.S. East Coast Ocean-Color Image. This daily Coastal Zone Color Scanner (CZCS) product for the northeastern coast of the United States reveals the high pigment concentrations along the coast and the influence of the Gulf Stream. Phytoplankton concentrations, and additional ocean-carbon-system parameters from MODIS, will be considerably more accurate than was possible with the CZCS because of improvements in spectral bands, calibration, and algorithms. (From NASA GSFC.)

MODIS Chlorophyll Fluorescence (MOD 20)

Product Description

This Level 2 product contains several parameters describing ocean chlorophyll fluorescence properties. Fluorescence line height is a relative measure of the amount of radiance leaving the sea surface at the fluorescence wavelength of 683 nm. Fluorescence Efficiency provides a relative measure of the absorption of PAR and its emission as chlorophyll fluorescence. The third parameter is Fluorescence Line Curvature. The spatial resolution will be 1 km for chlorophyll levels greater than 1.5 mg/m^3 and 5 × 5 km for values less than 1.5. The Level 2 product is produced daily, and Level 3 is gridded and produced daily, 8-day weekly, monthly, and yearly.

Research and Applications

Solar-stimulated chlorophyll fluorescence is a measure of the current photophysiology of phytoplankton, in contrast to the biomass estimate provided by chlorophyll. The product quantifies the level of photosynthesis by phytoplankton in the ocean. Historically, the coupling between fluorescence and chlorophyll has been studied extensively, and recent research has focused on the use of Sun-stimulated fluorescence to estimate primary productivity (Kiefer and Reynolds, 1992). Basic fluorometric measurements are made using an instrument described by Holm-Hansen *et al*. (1965) that uses blue-light stimulation; this method has been used unchanged for 30 years. Gower and Borstad (1990) was among the first to attempt to use sun-stimulated radiance at 683 nm to estimate chlorophyll concentrations from aircraft and satellites.

Data Set Evolution

Inputs to the algorithm are chlorophyll concentration (within MOD 19), Absorbed Radiation by Phytoplankton (ARP) (within MOD 22), and Water-Leaving Radiance (MOD 18). Water-leaving radiance for MODIS bands 13 (667 nm), 14 (678 nm), and 15 (748 nm) are used in the algorithm. The algorithm is applied to the daily input standard-product data sets and is remapped into standard Level 3 grids. The validation approach will be to compare the fluorescence results with other MODIS data products (e.g., Chlorophyll *a*), with surface measurements, and with other satellite-based estimates of the same products. The products are produced only for non-cloud, glint-free ocean pixels during daylight hours.

Suggested Reading

Abbott, M. R. *et al*., 1982.

Abbott, M. R., and R. M. Letelier, 1998.

Chamberlin, W. S., and J. Marra, 1992.

Gower, F. J. R., and G. A. Borstad, 1990.

Holm-Hansen, O. *et al*., 1965.

Kiefer, D. A., and R. A. Reynolds, 1992.

Letelier, R. M. *et al*., 1997.

Topliss, B. J., and T. Platt, 1986.

MODIS Chlorophyll Fluorescence Summary

Coverage: Global ocean surface, clear-sky only

Spatial/Temporal Characteristics: 1 km for chlorophyll levels greater than 2.0 mg/m^3/daily, (Level 2); 4.6 km, 36 km, 1°/8-day, monthly, yearly (Level 3)

Key Science Applications: Ocean chlorophyll, ocean productivity

Key Geophysical Parameters: Chlorophyll fluorescence (fluorescence line height, fluorescence efficiency, fluorescence line curvature)

Processing Level: 2, 3

Product Type: Standard, at-launch

Maximum File Size: 102 MB (Level 2); 640 MB binned, 134 MB mapped (Level 3)

File Frequency: 144/day (Daily Level 2); 3/day (Daily Level 3), 3/week (Weekly Level 3), 3/month (Monthly Level 3), 3/year (Yearly Level 3)

Primary Data Format: HDF-EOS

Additional Product Information: http://modis-ocean.gsfc.nasa.gov/dataprod.html

DAAC: NASA Goddard Space Flight Center

Science Team Contact: M. Abbott

Chlorophyll *a* (Chl)

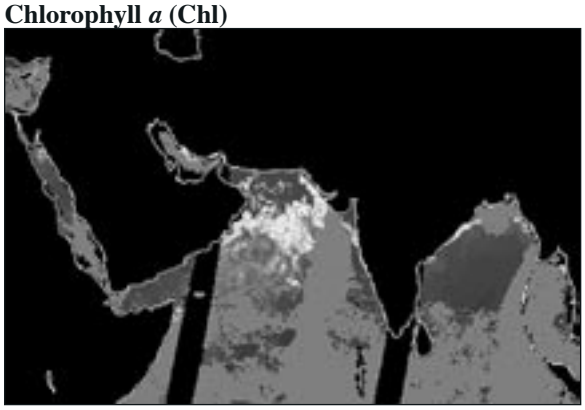

Chlorophyll *a* Concentrations (MOD 21) as measured by MODIS in the Indian Ocean on March 1, 2000. Chlorophyll, the green pigment in plants and phytoplankton, absorbs sunlight for use in photosynthesis. Note the high concentrations (light grays) in the Arabian Sea and relatively low concentrations (dark grays) in the Bay of Bengal. The black color in the image represents land areas and gaps between successive satellite orbits, and the gray "stripes" indicate where clouds or sun glint prevented accurate measurements.

Fluorescence Line Height (FLH)

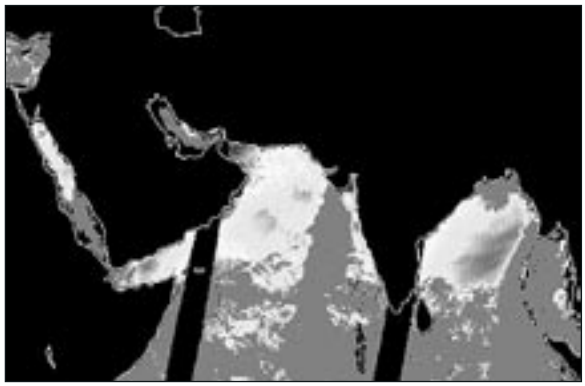

Chlorophyll Fluorescence (MOD 20) as measured from the Terra MODIS instrument on March 1, 2000. Phytoplankton re-emit some of the light that is captured by chlorophyll as fluorescence. The amount of fluorescence is roughly proportional to the amount of chlorophyll, so in this image, for example, high fluorescence can be found in the Arabian Sea.

FLH/Chl Ratio

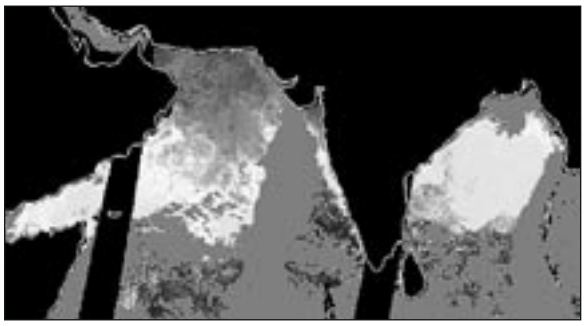

Ratio of Chlorophyll Fluorescence (MOD 20) to Chlorophyll *a* Concentration (MOD 21), illustrating the considerable variability in the amount of fluorescence per unit of chlorophyll. This variability is largely a function of the health of the phytoplankton. A high ratio implies lower growth rates, as the light captured by phytoplankton is being re-emitted as fluorescence rather than being used for photosynthesis. Phytoplankton in the Arabian Sea are probably growing more rapidly than elsewhere, perhaps in response to dust inputs (which are rich in iron) from the Arabian Peninsula.

MODIS Chlorophyll a Pigment Concentration (MOD 21) and Absorption Coefficients (MOD 36)

Product Description

This is a Level 2 and 3 product which contains ocean chlorophyll *a* pigment concentration for Case 1 and Case 2 waters at 1-km resolution. It is produced daily at Level 2 and daily, 8-day weekly, monthly, and yearly at Level 3. Absorption parameters generated by the chlorophyll algorithm are also provided as the intermediate product MOD 36, Absorption Coefficients, which includes absorption due to water, phytoplankton, detritus, and gelbstoff, and gelbstoff absorption only. Valid data exist only for ocean cloud-free pixels and the weekly composite will be an average of cloud-free acquisitions for each ocean pixel.

Research and Applications

Chlorophyll *a* concentration is a key input to the Ocean Primary Productivity product (MOD 27) and is used to trace oceanographic currents, jets, and plumes. The product provides the concentration of chlorophyll in Case 1 sea water (water that has optical properties that are dominated by chlorophyll and associated covarying detrital pigments) and in Case 2 waters (waters that contain substances that affect optical properties but do not covary with chlorophyll, such as gelbstoff (marine chromomorphic dissolved organic matter [CDOM] substance that absorbs at 400 nm), suspended sediments, coccolithophores, detritus, and bacteria). The algorithm derives from extensive research using CZCS data in which good performance was obtained for Case 1 waters and has evolved to perform successfully for the Case 2 waters for the MODIS algorithm. The 1-km resolution and nearly daily coverage will allow the observation of mesoscale oceanographic features in coastal and estuarine environments, which are of increasing importance in marine science studies.

Data Set Evolution

The product algorithm is based on a semi-analytical, bio-optical model of remote sensing reflectance which uses Water-Leaving Radiance (MOD 18), PAR (MOD 22), and Absorption Coefficients (MOD 36). The model is inverted to obtain the absorption coefficient due to phytoplankton at 675 nm, and chlorophyll *a* concentration is derived from this coefficient. The algorithm will be thoroughly tested during the SeaWiFS project, and post-launch validation will be conducted using data from instrumented collection cruises through ocean test sites including the nine used for algorithm development. Also, hyperspectral data will be used to simulate the 10-nm bands and produce comparison results.

Suggested Reading

Austin, R. W., 1974.

Carder, K. L. *et al*., 1986.

Carder, K. L. *et al*., 1991a,b.

Holm-Hansen, O., and B. Riemann, 1978.

Lee, Z. P. *et al*., 1996.

Smith, R. C., and K. S. Baker, 1982.

(MODIS Chlorophyll a Pigment Concentration and Absorption Coefficients, continued)

MODIS Chlorophyll *a* Pigment Concentration and Absorption Coefficients Summary

Coverage: Global ocean surface, clear-sky only

Spatial/Temporal Characteristics: 1 km/daily (Level 2); 4.6 km, 36 km, 1°/daily, 8-day, monthly, yearly (Level 3)

Key Science Applications: Ocean productivity, bio-optical properties

Key Geophysical Parameters: Case 1 and 2 chlorophyll *a* concentration, absorption coefficients

Processing Level: 2, 3

Product Type: Standard, at-launch

Maximum File Size:
MOD 21: 83 MB (Level 2); 640 MB binned, 134 MB mapped (Level 3)

MOD 36: 102 MB (Level 2); 865 MB binned, 134 MB mapped (Level 3)

File Frequency: 144/day (Daily Level 2); 2/day (Daily Level 3), 2/8-day (8-day Level 3), 2/month (Monthly Level 3), 2/year (Yearly Level 3)

Primary Data Format: HDF-EOS

Browse Available: 36 km sample imagery available at the Goddard DAAC (Level 3 only)

Additional Product Information:
http://modis-ocean.gsfc.nasa.gov/dataprod.html

DAAC: NASA Goddard Space Flight Center

Science Team Contact:
K. Carder

MODIS Coccolith Concentration (MOD 25)

Product Description

This Level 2 and 3 product provides five parameters describing the concentration of coccoliths in sea water: the detached coccolith concentration in number/m^3; the estimated calcite concentration due to the coccoliths in mg-$CaCO_3$/m^3; the pigment concentration in the coccolithophore biomass; a descriptor for the particular look-up table used; and a quality measure. The product is produced at 1-km spatial resolution daily for Level 2 and at 4.6-km, 36-km, and 1° resolution daily, 8-day weekly, monthly, and yearly for Level 3.

Research and Applications

Coccolithophores are small marine phytoplankton which form external calcium carbonate ($CaCO_3$) scales (called coccoliths) having diameters of a few mm and a thickness of 250 to 750 nm. Coccolithophores are the largest source of calcium carbonate on Earth. Thus, coccolith production is an important part of the biogenic carbon cycle. The observed characteristics of coccolithophores, including their ubiquitous nature, possible role in climate, and intense scattering property, make a global-scale study of their distribution an important application for MODIS imagery. Specifically, it is important to estimate the rate at which $CaCO_3$ is formed by phytoplankton and to look for long-term changes in that rate.

Data Set Evolution

The algorithm for extracting the detached coccolith concentration from surface waters is based on the semianalytic model of ocean color of Gordon (1988). The model relates the normalized water-leaving radiance to the absorption and scattering properties of the constituents of the water using radiative-transfer theory. The absorption and scattering properties are then related to the constituent concentrations through statistical analysis of direct measurements. The model is validated by comparison with a set of water-leaving radiances independent of the measurements used to establish the statistical relationships between constituents and optical properties.

Suggested Reading

Balch, W. M. *et al.*, 1991.

Gordon, H. R. *et al.*, 1988.

Groom, S. B., and P. M. Holligan, 1987.

Holligan, P. M. *et al.*, 1983.

Sarmiento, J. L. *et al.*, 1988.

Sikes, S., and V. Fabry, 1994.

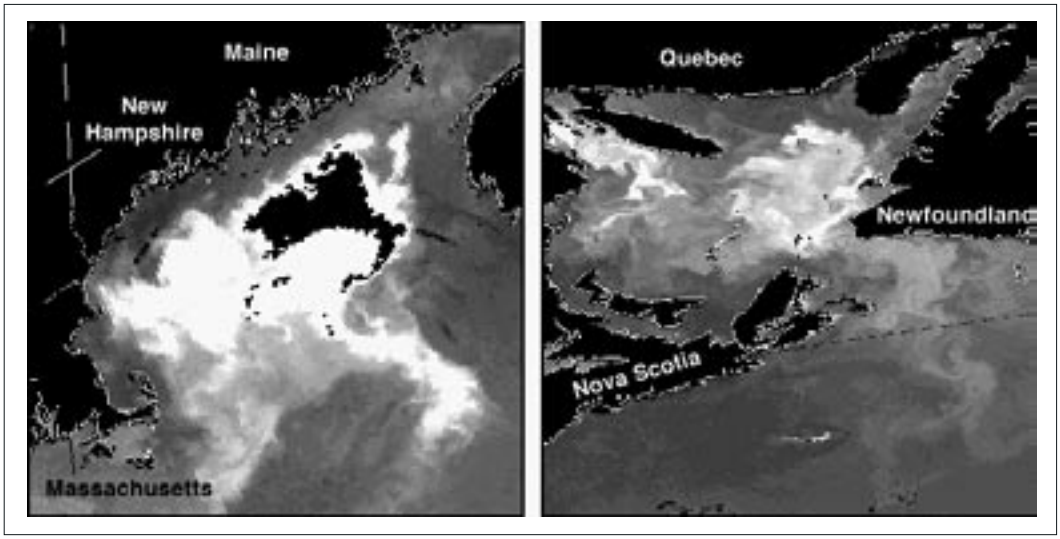

Coastal Zone Color Scanner Images of the Gulf of Maine and the Gulf of St. Lawrence. Satellite ocean-color imagery, in addition to allowing the concentration of single-celled plants to be measured remotely, permits the detection and identification of certain algal blooms. The white-to-light-grey waters in both regions are blooms of a single type of algae (called coccolithophores), that affects regional climate and fisheries.

(MODIS Coccolith Concentration, continued)

MODIS Coccolith Concentration Summary

Coverage: Global ocean surface, clear-sky only

Spatial/Temporal Characteristics: 1 km/daily (Level 2); 4.6 km, 36 km, 1°/daily, 8-day, monthly, yearly (Level 3)

Key Science Applications: Input to global biogeochemical cycle models

Key Geophysical Parameters: Coccolith and calcite concentration, pigment concentration in coccolithophore blooms

Processing Level: 2, 3

Product Type: Standard, at-launch

Maximum File Size: 102 MB (Level 2); 640 MB binned, 134 MB mapped (Level 3)

File Frequency: 144/day (Daily Level 2); 3/day (Daily Level 3), 3/8-day (8-day Level 3), 3/month (Monthly Level 3), 3/year (Yearly Level 3)

Primary Data Format: HDF-EOS

Browse Available: 36 km sample imagery available at the Goddard DAAC (Level 3 only)

Additional Product Information: http://modis-ocean.gsfc.nasa.gov/dataprod.html

DAAC: NASA Goddard Space Flight Center

Science Team Contacts:
H. R. Gordon
W. B. Balch

MODIS Ocean Primary Productivity (MOD 27)

Product Description

This Level 4 product provides an estimate of the Ocean Primary Productivity on an 8-day and an annual basis at spatial resolutions of 4.6 km and 36 km.

Research and Applications

The objective of the product is to quantify the magnitude and interannual variability (for decadal trends) in the oceanic primary productivity and phytoplankton carbon fixation. Primary productivity is the time rate of change of phytoplankton biomass, and, with allowance for excreted soluble carbon compounds, reflects the daily integrated photosynthesis within the water column. The integral of the values over the year is the annual primary productivity. The annual productivity product will be used for global- and regional-scale studies of interannual variability of ocean productivity, for comparisons with annual summations of short-term analytic estimates, and for comparison with global biogeochemical models.

Data Set Evolution

Ocean primary-productivity algorithms fall into two general classes, termed empirical and analytic algorithms. The empirical approach is based on simple correlation between time-averaged *in situ* estimates of productivity and satellite-derived estimates of surface chlorophyll concentration. The analytic approach is based on models of the general photosynthetic response of the algal biomass as a function of major environmental variables such as light, temperature, and nutrient concentration. The overall methodologies differ significantly in the way various parameters are estimated and in the way they are assigned spatially and temporally across ocean basins. The approach taken for the MODIS algorithm is to begin implementation of an annual, global, empirical algorithm for at-launch product generation, while pursuing a vigorous research program within the SeaWiFS Science Team, to develop a consensus analytic algorithm for short-term (daily to weekly) global productivity. Cloudiness prevents deriving chlorophyll *a* concentrations over about 60% of the ocean on daily basis, excluding that already lost due to high sun glint. Chlorophyll *a* concentrations derived from all available sensors, including the Terra and

Aqua MODIS instruments, will be used to increase sampling frequency since these plankton processes vary rapidly over time and space.

Suggested Reading

Eppley, R. W. *et al*., 1985.

Esaias, W. E. *et al*., 1999.

Fitzwater, S.E. *et al*., 1982.

Iverson, R.L. *et al*., 2000.

Morel, A., and J. M. Andre, 1991.

Platt, T. C. *et al*., 1991.

MODIS Ocean Primary Productivity Summary

Coverage: Global ocean surface, clear-sky only

Spatial/Temporal Characteristics: 4.6 km and 36 km/8-day and a running annual average

Key Science Applications: Ocean productivity, biogeochemical models

Key Geophysical Parameters: Annual and weekly ocean productivity

Processing Level: 4

Product Type: Standard, at-launch

Maximum File Size: 1200 MB binned (8-day), 1360 MB binned (Yearly); 32 MB mapped (8-day and Yearly)

File Frequency: 4/8-day

Primary Data Format: HDF-EOS

Additional Product Information: http://modis-ocean.gsfc.nasa.gov/dataprod.html

DAAC: NASA Goddard Space Flight Center

Science Team Contact: W. Esaias

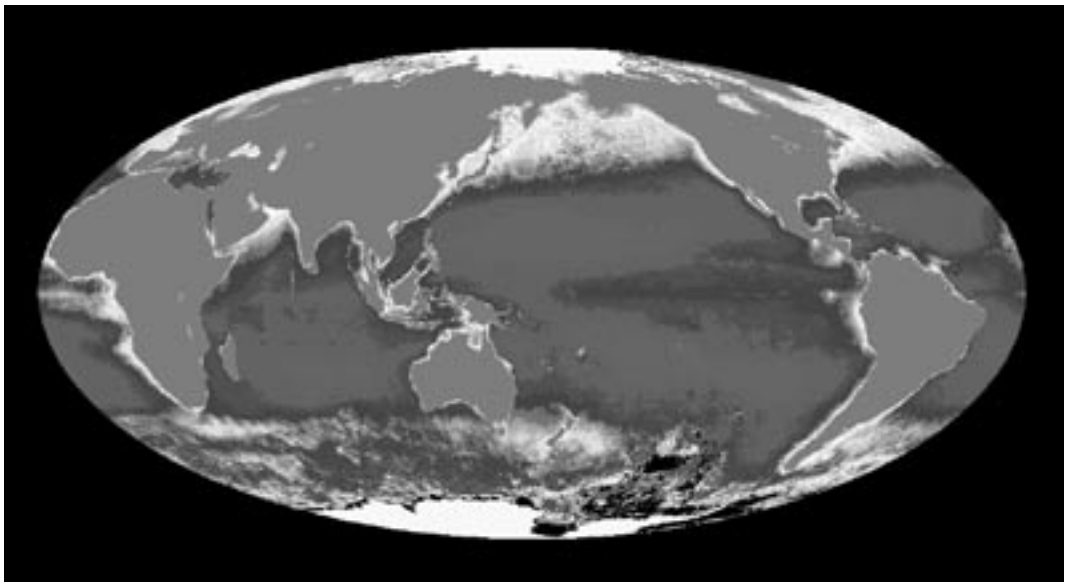

Global Ocean Phytoplankton Biomass. A pre-MODIS, global ocean-color product from the Coastal Zone Color Scanner shows the algal pigment concentrations within the upper layers of the ocean and indicates the biomass and productivity distribution within the oceans. While this is an annual product, MODIS will provide comparable global coverage on a weekly-to-monthly basis to enable scientists to study large-scale changes in marine ecosystems over weeks to decades. (From NASA GSFC.)

MODIS Phycoerythrin Concentration (MOD 31)

Product Description

This product consists of three parameters which give the concentration of one of the major algal pigment groups in ocean water, Phycoerythrin. The three parameters are Phycoerythrobilin Concentration, Phycourobilin Concentration, and Constituent Inherent Optical Properties (CDOM absorption, chlorophyllous absorption, and particulate backscatter). These quantities are provided for Level 2 at 1-km spatial resolution daily and for Level 3 daily, 8-day weekly, monthly, and yearly at 4.6-km, 36-km, and 1° resolution. The product is valid only for clear-sky ocean pixels.

Phycoerythrin is one of three major algal pigment groups found in marine phytoplankton and bacteria (Bidigare, 1990). The phycoerythrins are further subdivided into phycourobilin-rich (PUB) and phycoerythrobilin-rich (PEB) phycoerythrins. This algorithm retrieves both PUB- and PEB- rich cases. Phycoerythrin is a chlorophyll accessory pigment and serves to receive photosynthetically usable light in the 480-505-nm and 540-560-nm ranges. It is used to infer the global extent of phycoerythrin-bearing phytoplankton such as cyanobacteria, which are nitrogen-fixing and thus provide information on the nitrogen cycle. Used in conjunction with phytoplankton chlorophyllous pigment, the apparent species diversity of the oceans can be inferred.

Research and Applications

One of the intended uses of the phycoerythrin data product is to allow scientific investigators to study the global distributions of the phycoerythrin pigment and, in so doing, to allow definition of the diversity of phycoerythrin-bearing species such as cyanobacteria. When used in conjunction with chlorophyll distribution, phycoerythrin determination allows global phytoplankton species variability studies.

Data Set Evolution

The phycoerythrin retrieval algorithm requires water-leaving radiances generated from the incident solar irradiance, the total backscatter, and the total absorption of sea water. The PUB and PEB parameters are retrieved by a sequential-convergent-iteration method (Gordon *et al*., 1988) that uses five independent bands. MODIS band 10 (488 nm) and band 12 (551 nm) correspond to the peaks of the PUB and PEB phycoerythrins. The major assumption for the algorithm is that the pigment-specific absorption-coefficient spectral model used is applicable for the oceanic province where the satellite image was acquired. The algorithm will be validated by ship and airborne laser-induced and water Raman-normalized fluorescence measurements.

Suggested Reading

Bidigare, R. R. *et al*., 1990.

Culver, M. E., and M. J. Perry, 1994.

Gordon, H. R. *et al*., 1988.

Hoge, F. E., and R. N. Swift, 1986.

Hoge, F. E., and R. N. Swift, 1990.

Hoge, F. E. *et al*., 1999a.

Hoge, F. E. *et al*., 1999b.

MODIS Phycoerythrin Concentration Summary

Coverage: Global ocean surface, clear-sky only

Spatial/Temporal Characteristics: 1 km/daily (Level 2); 4.6 km, 36 km, 1°/daily, 8-day, monthly, yearly (Level 3)

Key Science Applications: Global phytoplankton species studies, ocean productivity models

Key Geophysical Parameters: Phycoerythrobilin-rich (PEB) and phycourobulin-rich (PUB) phycoerythrins

Processing Level: 2, 3

Product Type: Research, at-launch

Maximum File Size: 102 MB (Level 2); 640 MB binned, 134 MB mapped (Level 3)

File Frequency: 144/day (Daily Level 2); 2/day (Daily Level 3), 2/8-day (8-day Level 3), 2/month (Monthly Level 3), 2/year (Yearly Level 3)

Primary Data Format: HDF-EOS

Browse Available: 36 km sample imagery available at the Goddard DAAC (Level 3 only)

Additional Product Information: http://modis-ocean.gsfc.nasa.gov/dataprod.html

DAAC: NASA Goddard Space Flight Center

Science Team Contact: F. E. Hoge

Snow and Ice Cover

Aqua
- AMSR-E
- MODIS

Snow and Ice Cover – An Overview

Relationship to Global Change Issues

Snow and ice cover dramatically influence surface albedo, hydrologic properties, the interactions between the atmosphere and the underlying surface, and regulation of ecosystem biological activity. For instance, when sea ice is formed in the ocean or snow is deposited on land, these processes can double the degree to which the surface reflects incoming solar energy, hence affecting the Earth's radiation balance and, in turn, its climate. Furthermore, both snow and ice are highly variable components of the climate system, changing dramatically from summer to winter, and, to a lesser extent, from year to year. The combination of high variability and impacts on critical climate processes insures the importance of monitoring snow and ice to the understanding of global change.

Two key sensors on board Aqua that will provide enhanced global sea ice and snow measurements to supplement existing data sets are the AMSR-E and MODIS. Both will provide information to be used in the development of more accurate models to help understand and predict Earth's climate and the role of snow and ice in it.

AMSR-E data will provide daily, global coverage of sea ice and snow regardless of cloud conditions or darkness. The derived sea ice and snow parameters will be used both operationally and for climate research. By extending the existing time series of sea ice and snow parameters, which currently span over 20 years, scientists expect to obtain a better understanding of global, hemispheric, and regional variabilities on seasonal, interannual, and decadal time scales. The improved spatial resolution possible from the AMSR-E sensor, relative to previous satellite passive-microwave instruments, will also allow greater insight into the processes which define the role of the cryosphere in the climate system.

MODIS data will be used to monitor the dynamics of large-area (greater than 10 square kilometers) snow and ice cover using daily and 8-day products. Information about snow and ice cover, including surface temperature, is important for a number of agricultural, industrial, social, and environmental reasons. For example, in some regions snow cover data can be critical in successfully predicting water supply, planning for agricultural and industrial developments, anticipating flooding, forecasting crop yield, and estimating freeze damage.

Product Overview

Global snow-water equivalent and snow depth will be mapped daily and every five days over the Earth's land surfaces at 25-km resolution using the AMSR-E snow-water equivalent and snow-depth algorithm. A global, daily snow-storage map will be an at-launch AMSR-E product. Snow-water equivalent values will be inferred based on the resampled brightness data. After one day, a daily map will be generated by compositing all the data within that day. The MODIS snow cover product will be mapped daily and as 8-day composites at 500-m resolution over the Earth's land surfaces, using an algorithm based on the normalized difference of a visible and a shortwave-infrared band.

The sea ice products derived from AMSR-E include sea ice concentration, ice temperature, and snow depth over sea ice. Daily sea ice concentrations and ice temperatures will be mapped on the standard SSM/I grid. Ascending data will also be separated from descending data for day/night discrimination. Sea ice concentrations will be mapped at both 25-km and 12.5-km resolutions while sea ice temperatures will be mapped on the 25-km-resolution grid only. Snow depth on sea ice will be a five-day product and mapped at a grid resolution of 12.5 km. A daily sea ice product will also be obtained from MODIS at a much finer, 1 km, resolution than the AMSR-E product but with use limited largely to cloud-free conditions. The MODIS sea ice product is based on the normalized difference between a visible and a shortwave-infrared band signal.

Product Interdependency and Continuity with Heritage Data

There have been several satellite missions that have collected snow and ice data for many years. Snow and ice are among the variables included in NASA's Pathfinder Program, which is providing research-quality data sets on global change from past and current satellite instruments. The heritage of both the AMSR-E and MODIS sensors is strong. Data sets from these sensors will extend those from historical and current sensors and provide the continuity needed for long-term global climate-change studies.

The first detailed data sets of sea ice distributions regardless of cloud cover or solar illumination came from the data of the Electrically Scanning Microwave Radiometer (ESMR) on the Nimbus 5 satellite launched in December 1972. ESMR and its successor, the Scanning Multichannel Microwave Radiometer

(SMMR), launched on Nimbus 7 in October 1978, provided the data for three major sea ice atlases describing the seasonal cycles and interannual variability of the Arctic and Antarctic sea ice covers for the years 1973-76 and 1978-87. The SMMR has been superseded by the Special Sensor Microwave/Imager (SSM/I), which has flown as part of the Defense Meteorological Satellite Program (DMSP) since 1987. The SSM/I is similar to SMMR, and its data also have been analyzed to determine snow cover and sea ice conditions. Most recently, time-series analyses of the combined SMMR and SSM/I data sets have yielded information on global sea ice trends and on regional and hemispheric variabilities spanning a 20-year period. The AMSR-E data will help to extend this 20-year sea ice record.

Other sources of historical satellite data for ice and snow are Landsat, which started operation (as the Earth Resources Technology Satellite) in 1972, the Advanced Very High Resolution Radiometer (AVHRR) on the NOAA satellites, which started operation in 1978, Seasat, Geosat, and many Japanese, European, and Russian satellite sensors. Landsat provides very high resolution (15-80 m in the visible and near-infrared bands, and 60-120 m in the thermal-infrared bands), while AVHRR provides moderate resolution (1 km) in the visible and infrared channels. Because of higher spatial resolution, broader spectral range, and extensive calibration and validation programs, both AMSR-E and MODIS are expected to provide more accurate data products than is currently possible with their primary precursors, the SSM/I and AVHRR, respectively.

Suggested Reading

Chang, A. T. C. *et al.*, 1987.

Chang, A. T. C. *et al.*, 1997.

Comiso, J. C. *et al.*, 1997.

Comiso, J. C., 2000.

Foster, J. L. *et al.*, 1984.

Gloersen, P. *et al.*, 1992.

Hall, D. K. *et al.*, 1995.

Klein, A. G. *et al.*, 1998.

Markus, T., and D. J. Cavalieri, 1998.

Markus, T., and D. J. Cavalieri, 2000.

Parkinson, C. L., 1997.

Parkinson, C. L. *et al.*, 1987.

Weeks, W. F., 1981.

Zwally, H. J. *et al.*, 1983.

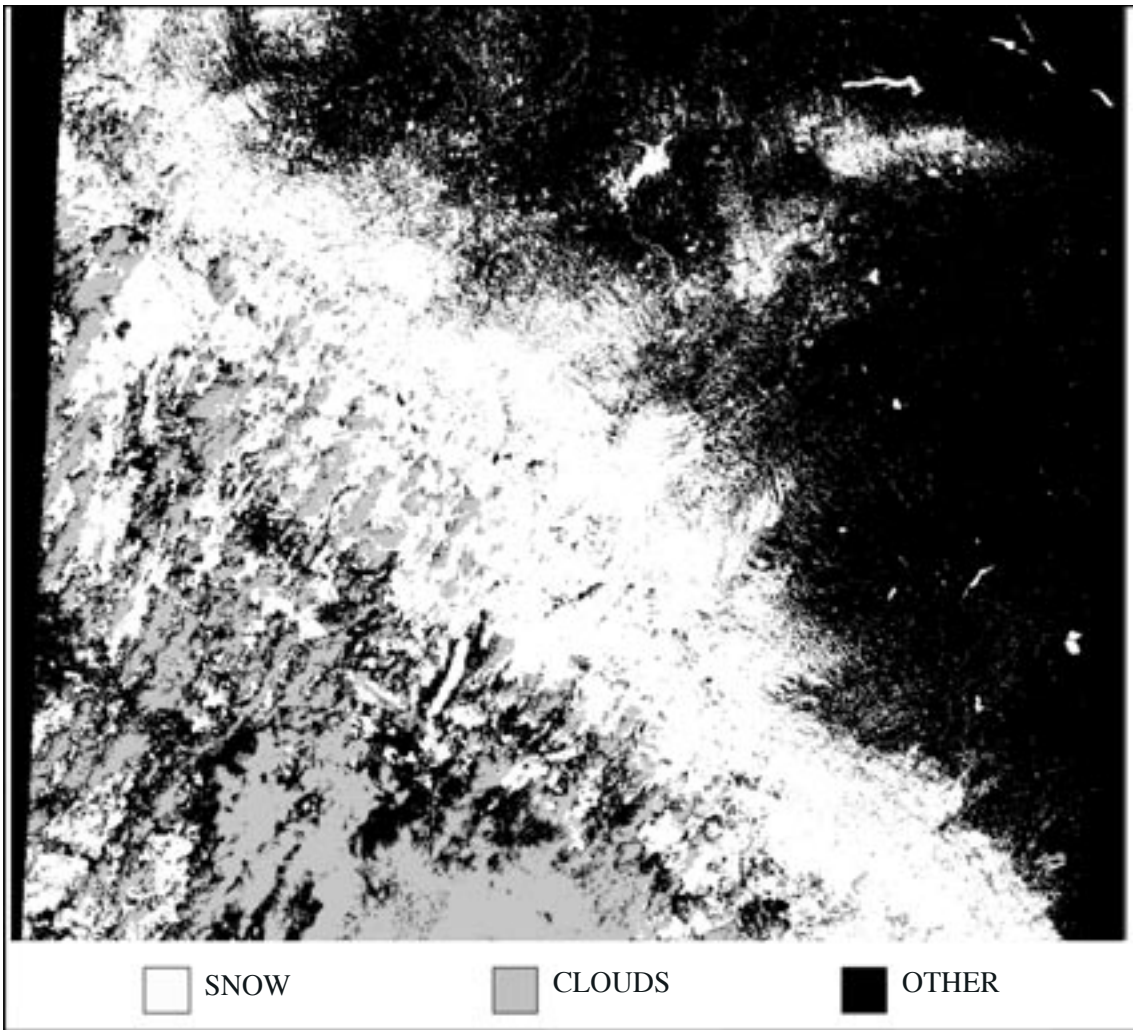

Landsat TM Scene of Northern Montana including Glacier National Park, after the application of the SNOMAP algorithm (Hall *et al*., 1995). The TM Scene was acquired on March 14, 1991 (scene i.d. #5256917454). (Note: Snow and non-snow features were classified automatically by the SNOMAP algorithm, but cloud features were classified by supervised classification.)

AMSR-E Sea Ice Concentration

Product Description

Sea ice concentrations will be produced from modified versions of the NASA Team algorithm (Markus and Cavalieri, 2000) and the Bootstrap algorithm (Comiso and Zwally, 1997). The NASA Team algorithm will be used as the standard algorithm to process Arctic data, while the Bootstrap algorithm will be used as the standard algorithm to process Antarctic data. Ice-concentration-difference maps derived from the two algorithms for both hemispheres will also be archived for comparison. Sea ice concentrations from both algorithms and their differences will be produced as gridded products (Level 3) and mapped onto a 25-km grid, enabling ready continuation of a twenty-year historical data set derived from SMMR and SSM/I. The ice-concentration products will also be gridded at 12.5 km to take advantage of the higher spatial resolution of the sensor. The grids at both resolutions use a polar stereographic projection defined for the SMMR and SSM/I data sets (NSIDC, 1996).

Research and Applications

Polar sea ice is an important component of the global climate system. It insulates the atmosphere from the oceanic heat below in winter and keeps the ocean from absorbing heat from the sun in the spring and summer. Because of the high albedo of sea ice and its snow cover, it also plays an important role in the regional and global energy balance. The most important measure of the polar sea ice cover is its concentration. This product enables quantification of ice-free water in the leads and polynyas within the ice pack as well as the extent of the sea ice cover itself. Over twenty years of satellite passive-microwave sea ice data exist and have been used to study seasonal, regional, and interannual sea ice variabilities of the Arctic and Antarctic (e.g., Gloersen *et al.*, 1992; Jacobs and Comiso, 1997; Cavalieri *et al.*, 1997).

Data Set Evolution

The modified NASA Team and Bootstrap sea ice algorithms have considerable heritage. The NASA Team algorithm is based on the use of radiance ratios called the polarization and the spectral gradient ratio. The technique has been used since the launch of the Nimbus 7 SMMR in 1978 (Cavalieri *et al.*, 1984; Gloersen and Cavalieri, 1986) and continued with modifications (Cavalieri *et al.*, 1991) with the series of SSM/I sensors first launched in 1987. The Bootstrap algorithm makes use of the multifrequency capabilities of the sensor to reduce errors due to variations in emissivity and temperature, and, like the NASA Team algorithm, has been applied to both the SMMR and SSM/I data sets (Comiso, 1986; Comiso, 1995). The theoretical foundation and details of the two original algorithms and a comparative analysis of results from a year of SSM/I data are presented in Comiso *et al.* (1997).

Suggested Reading

Cavalieri, D. J. *et al.*, 1984.

Cavalieri, D. J. *et al.*, 1991.

Cavalieri, D. J. *et al.*, 1997.

Comiso, J. C., 1986.

Comiso, J. C., 1995.

Comiso, J. C., and H. J. Zwally, 1997.

Comiso, J. C. *et al.*, 1997.

Gloersen P., and D. J. Cavalieri, 1986.

Gloersen, P. *et al.*, 1992.

Jacobs, S. S., and J. C. Comiso, 1997.

Markus, T., and D. J. Cavalieri, 2000.

NSIDC, 1996.

(AMSR-E Sea Ice Concentration, continued)

AMSR-E Sea Ice Concentration Summary

Coverage: Global

Spatial/Temporal Characteristics: 12.5 km and 25 km/ascending, descending, and daily averages

Key Geophysical Parameters: Sea ice concentration and difference

Processing Level: 3

Product Type: Standard, at-launch

Maximum File Size: 53 MB

File Frequency: 1/day

Primary Data Format: HDF-EOS

Browse Available: Accompanies data product

Additional Product Information: http://wwwghcc.msfc.nasa.gov/AMSR/html/amsr_products.html

DAAC: National Snow and Ice Data Center

Science Team Contacts:
D. J. Cavalieri
J. C. Comiso

AMSR-E Snow Depth on Sea Ice

Product Description

Snow depth on sea ice will be mapped every five days at a 12.5-km grid resolution. The algorithm, described in detail by Markus and Cavalieri (1998), makes use of the spectral-gradient ratio, defined using the 18- and 37-GHz vertically polarized radiances, and the total sea ice concentration measured with the modified NASA Team sea ice algorithm (Markus and Cavalieri, 2000). Currently, the algorithm is limited to the Southern Ocean and to the Arctic seasonal sea ice zones. Snow depth is measured in centimeters with a precision of 1 cm and an estimated accuracy of 5 cm.

Research and Applications

The overall importance of snow depth on sea ice to the climate system is well documented (e.g., Ledley, 1991; Eicken *et al*., 1995). Snow cover on sea ice primarily affects the climate through its effect on surface albedo and the thermal insulation between ocean and atmosphere. Given that the change in sea ice coverage from summer to winter is over 15 million km^2 in the Southern Ocean and 5 million km^2 in the Arctic, the effect of snow cover can be substantial. Snow depth and accumulation rate are important variables in the fresh-water budget of the polar oceans. A quantitative knowledge of snow-depth variability could provide a useful estimate of precipitation minus evaporation (P-E), which is critically needed in state-of-the-art coupled ice-ocean models (Häkkinen, 1995). Current applications of the retrieved snow depths over the Southern Ocean include the study of interannual and regional variabilities of snow depth on sea ice (Markus and Cavalieri, 1998) and a study of mixed-layer ocean properties using an ECMWF-SSM/I forced mixed-layer model (Markus, 1999).

Data Set Evolution

The snow-depth-on-sea-ice algorithm has considerable heritage in Nimbus 7 SMMR and the DMSP SSM/I snow-depth algorithms derived for land applications (e.g., Chang *et al*., 1987). The instrument channels used are similar (18/19 GHz and 37 GHz), but the functional form is different, making use of ratios of radiances in the snow-depth-on-sea-ice algorithm instead of linear differences for the land algorithm. In contrast to the Equal-Area Scalable

Earth (EASE) grid used for snow cover on land, the Level 3 grid used for snow depth on sea ice will be the so-called SSM/I polar stereographic grid, from NSIDC, with a grid size of 12.5 km. It matches the 12.5-km grid used for sea ice concentration.

Suggested Reading

Chang, A. T. C. *et al*., 1997.

Eicken, H. *et al*., 1995.

Häkkinen, S., 1995.

Ledley, T. S., 1991.

Markus, T., and D. J. Cavalieri, 1998.

Markus, T., and D. J. Cavalieri, 2000.

Markus, T., 1999.

NSIDC, 1996.

AMSR-E Snow Depth on Sea Ice Summary

Coverage: Southern Ocean and the Arctic seasonal sea ice zones

Spatial/Temporal Characteristics: 12.5 km/ 5-day average

Key Geophysical Parameters: Snow depth on sea ice

Processing Level: 3

Product Type: Standard, at-launch

Maximum File Size: 53 MB

File Frequency: 1/day

Primary Data Format: HDF-EOS

Browse Available: Accompanies data product

Additional Product Information: http://wwwghcc.msfc.nasa.gov/AMSR/html/amsr_products.html

DAAC: National Snow and Ice Data Center

Science Team Contacts:
D. J. Cavalieri
J. C. Comiso

AMSR-E Sea Ice Temperatures

Product Description

Sea ice temperatures will be produced from a modified version of the Bootstrap algorithm and from a simple relationship among ice temperature, ice emissivity, and ice concentration. Sea ice temperatures will be produced as gridded products (Level 3) and mapped onto a 25-km grid defined for the SMMR and SSM/I data sets by NSIDC. It is based on a polar stereographic projection.

Research and Applications

Satellite data provide a quantification of the polar sea ice cover in only two dimensions. Thickness, the third dimension, is not currently observable with satellite systems. While changes in ice temperature are closely linked with the temperatures of the ocean and atmosphere, these changes may also reflect changes in ice thickness and snow cover. For example, a warming of the mixed layer of the Arctic Ocean may lead to a thinning of the ice cover, which in turn may result in a warming of the ice. Thus, by monitoring the ice temperature, the snow depth, and the surface temperature derived, for example, from MODIS and AVHRR data (e.g., Comiso, 1999), it may be possible to detect changes in ice thickness.

Data Set Evolution

Microwave observations of sea ice at 6 GHz represent emissions primarily from the snow/ice interface and below. Since the emissivity for sea ice is relatively stable at this frequency, SMMR data have been used by Gloersen *et al*. (1992) to obtain maps of ice temperatures from 1979 through 1987. This time series was discontinued in 1987 because the lowest frequency for SSM/I is 19 GHz, which is not suitable for the purpose. The AMSR-E will have a 6-GHz channel and will provide the opportunity to obtain sea ice temperatures once again. The AMSR-E algorithm for ice temperature will be part of the revised Bootstrap Algorithm (Comiso and Zwally, 1997) that makes use of 6-GHz information to reduce spatial variations in ice temperatures. The algorithm is different from that of Gloersen *et al*. in that the initial ice concentration used to calculate the effective emissivity at 6 GHz is derived from a combination of the 6- and 37-GHz data, using the Bootstrap

technique. Also, a threshold of 80% ice concentration used by Gloersen *et al*., below which the temperature is set to 271 K, is not used.

Suggesting Reading

Comiso, J. C., 2000.

Comiso, J. C., and H. J. Zwally, 1997.

Gloersen, P. *et al*., 1992.

NSIDC, 1996.

AMSR-E Sea Ice Temperatures Summary

Coverage: Global

Spatial/Temporal Characteristics: 25 km/ ascending, descending, and daily averages

Key Geophysical Parameters: Sea ice temperature

Processing Level: 3

Product Type: Standard, at-launch

Maximum File Size: 19.5 MB

File Frequency: 1/day

Primary Data Format: HDF-EOS

Browse Available: Accompanies data product

Additional Product Information: http://wwwghcc.msfc.nasa.gov/AMSR/html/amsr_products.html

DAAC: National Snow and Ice Data Center

Science Team Contacts:
D. J. Cavalieri
J. C. Comiso

AMSR-E Snow-Water Equivalent and Snow Depth

Product Description

Snow-water equivalent (SWE) and snow depth will be mapped daily and every five days over the Earth's land surfaces at 25-km resolution using an AMSR-E snow-water-equivalent and snow-depth algorithm. A global, daily snow-storage map will be an at-launch AMSR-E product. Snow-water-equivalent values will be inferred, based on the resampled brightness data. After one day, a daily map will be generated by compositing all the data within one day.

Snow storage is a key parameter of the global energy and water balance. Snow-water-equivalent values for the U.S. are currently mapped by NOAA/NWS/NOHRSC based on gamma radiation data. An NOHRSC low-flying aircraft collects data over selected flight lines a couple of times per year during the winter season. Snow-water-equivalent values between the flight lines are generated by optimum interpolation. Qualities of these data are difficult to assess.

Research and Applications

The objective of this product is to quantify the amount and interannual variability of snow storage during the winter season. Snow is one of the most important renewable resources, for instance providing over 70% of the water supply in the western U.S. Information on the amount of snow storage and timing of discharge is critical for resource managers. Untimely melting of the snowpack could cause enormous damage to properties and loss of human lives.

Data Set Evolution

The algorithm to retrieve the snow-water equivalent from AMSR-E data has a considerable heritage. It is based on the observations from multi-frequency radiometers. The current algorithm is built on the algorithm developed for the SMMR data. Due to the effects of grain size, density, stratigraphy, and wetness on microwave signals, a statistical retrieval approach has been adopted.

Global snow cover will be mapped using a visible sensor at a resolution of 500 m (MOD 10). These data could provide snow mapping at basin scale for hydrological model applications. The persistent cloud

cover over some parts of the world restricts this technique. With a combination of microwave and visible data, a better snow cover product can be expected.

AMSR-E Snow-Water Equivalent and Snow Depth Summary

Coverage: Global

Spatial/Temporal Characteristics: EASE grid 25-km resolution/daily, 5-day, monthly

Key Geophysical Parameters: Snow-water equivalent, snow depth

Processing Level: 3

Product Type:
Snow-water equivalent: Standard, at-launch
Snow depth: Research, post-launch

Maximum File Size: 3.2 MB

File Frequency: 1/day (Daily Level 3), 1/5-day (5-day Level 3), 1/month (Monthly Level 3)

Primary Data Format: HDF-EOS

Browse Available: Accompanies data product

Additional Product Information:
http://wwwghcc.msfc.nasa.gov/AMSR/html/amsr_products.html

DAAC: National Snow and Ice Data Center

Science Team Contact:
A.T. Chang

MODIS Snow Cover (MOD 10)

Product Description

Global snow cover (including over ice on large, inland water bodies) will be mapped daily and as 8-day composites over the Earth's land surfaces at 500-m resolution using an algorithm called SNOMAP (Hall *et al.*, 1995, Klein *et al.,* 1998). A global, daily snow cover map will be an at-launch MODIS product. Snow cover, with its high albedo, is a key parameter of the global energy balance, reflecting much of the incident solar radiation back to space. Snow cover of the Northern Hemisphere is currently mapped by NOAA on a daily basis, but the accuracy of the maps has been difficult to determine, in part because a variety of techniques has been used to map snow cover over the 34-year period during which the maps have been produced.

Additionally, snow/cloud discrimination is difficult and often impossible using the current NOAA sensors because of the available bands. MODIS bands will allow automatic snow/cloud discrimination, and, in conjunction with the MODIS cloud mask (MOD 35), will allow automated snow mapping. The MODIS 8-day-composite snow cover product is designed to provide snow-cover persistence statistics for each pixel so that users can determine how long the snow has been on the ground during the compositing period. This is especially important during the transition seasons.

Research and Applications

Large, inland water bodies such as the Great Lakes, are often ice-covered during the winter months, and navigation during part of the winter is a significant problem. NOAA data are currently used to map ice cover on the Great Lakes, but discrimination between snow/ice and cloud is a problem. Additionally, ice cover on lakes can be an important climate indicator, as the dates of freeze-up and break-up are influenced by meteorological conditions. A trend toward earlier break-up, for example, could signify a warming as has been observed in some areas (e.g., Comb, 1990). Thus, it is important to measure ice conditions on large lakes over an extended period of time in order to detect trends as well as for operational uses over the short term.

Data Set Evolution

SNOMAP has a considerable heritage. It is based on the normalized difference of a visible and a short-wave-infrared band. This technique has been used, since at least 1978, to map snow from aircraft (Kyle *et al.*, 1978). Since the mid-1980s, it has been used to map snow using Landsat data on the drainage-basin scale (Dozier, 1989). The SNOMAP algorithm has been enhanced by incorporating the normalized difference vegetation index (NDVI), to map the snow cover in denser forests than was possible with the original algorithm (Klein *et al.*, 1998).

Global snow cover has also been mapped using passive-microwave data at a resolution of about 50 km (Foster and Chang, 1993). While these data allow snow mapping through cloud cover, passive-microwave data do not provide a resolution that is suitable for detailed snow mapping. Basin-scale mapping is required for hydrological modeling, and, in particular for snowmelt-runoff calculations, which are essential for hydroelectric-power generation and for water-supply forecasts in the western U.S. and in many other parts of the world. The expected use of passive-microwave and MODIS snow cover data together should yield information on snow extent and snow-water equivalent (Salomonson *et al.*, 1995). Snow cover data are also needed for general circulation modeling.

MODIS Snow Cover Summary

Coverage: Global, daytime

Spatial/Temporal Characteristics: 500 m/daily; 500 m/8-day composite; 1/4°/daily and 8-day composite

Key Geophysical Parameters: Snow cover, lake-ice cover

Processing Level: 2, 3 (mapped)

Product Type: Standard, at-launch

Maximum File Size: 23 MB (Level 2), 12 MB (Level 3)

File Frequency: 288/day (Daily Level 2); 333/day (Daily Level 3), 333/8-day (8-day Level 3)

Primary Data Format: HDF-EOS

Additional Product Information: http://snowmelt.gsfc.nasa.gov/MODIS_Snow/modis.html

DAAC: National Snow and Ice Data Center

Science Team Contact: D. Hall

Suggested Reading

Comb, D. G., 1990.

Dozier, J., 1989.

Foster, J. L., and A. T.C. Chang, 1993.

Hall, D.K. *et al.*, 1995.

Klein *et al.*, 1998.

Kyle, H. L. *et al.*, 1978.

Salomonson, V. V. *et al.*, 1995.

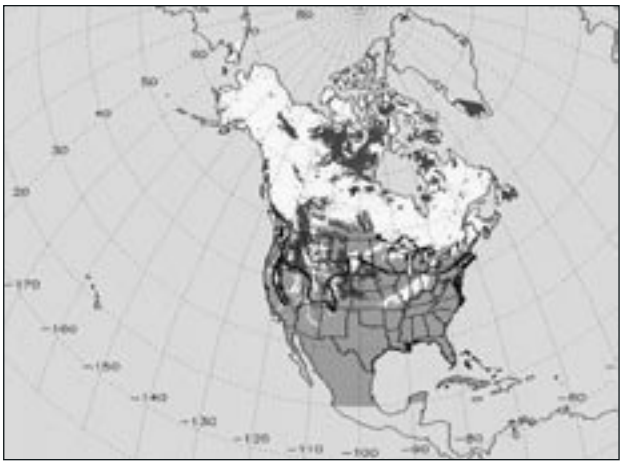

MODIS "Browse" Product (5-km resolution) showing the Maximum Snow Cover (white) in North America composited for the 8-day period March 5-12, 2000. Dark gray indicates clouds, and the black line represents the average March snowline as determined from NOAA/NESDIS snow cover maps for the years 1966-1998.

MODIS Sea Ice Cover (MOD 29)

Product Description

Global sea ice cover will be mapped daily and every eight days at 1-km resolution using an algorithm called ICEMAP. Global sea ice cover will be an at-launch MODIS product. Sea ice is present over approximately 7% of the Earth's ocean surface (Parkinson, 1997). Snow-covered sea ice, with its high albedo, is a key parameter of the global energy balance, reflecting much of the incident solar radiation back to space. Additionally, the sea ice cover is an insulating layer between the ocean and atmosphere; heat loss through open water is up to 100 times greater than heat loss through thick ice. As a consequence, leads and polynyas (linear and nonlinear openings in the sea ice, respectively) are significant to the energy budget of the ice-covered ocean and to local and regional climatology. Such open-water areas and areas of reduced ice concentration are also important for shipping in ice-covered seas.

Research and Applications

Sea ice cover is currently mapped by NOAA visible and near-infrared sensors, and by microwave sensors, both passive and active. Using the NOAA sensors, snow/cloud discrimination is a major hindrance in identifying sea ice. The passive-microwave sensors map sea ice through cloud cover, but at a resolution of only about 30 km. Active microwave sensors have good spatial resolution, up to about 25 m, but currently do not map sea ice cover globally on a daily basis. MODIS will be able to map sea ice globally, but with the significant limitation that cloud cover will obscure the view of the surface for much of the time. Together, the MODIS and microwave sensors will provide important information on the presence and concentration of sea ice. MODIS data, when available, will provide the higher resolution view of sea ice that is not obtainable using passive-microwave data.

Data Set Evolution

ICEMAP has a considerable heritage. It is based on the normalized difference of a visible and a shortwave infrared band. This technique has been used to map snow from aircraft and satellites (Kyle *et al*., 1978; Dozier, 1984; and Hall *et al*., 1995) and has been shown to be effective for mapping sea ice as well. The 8-day composited sea-ice-cover product is designed to provide sea-ice-cover persistence statistics for each pixel so that users can determine how long sea ice has been present during the previous 10 days in any given location. A cloud mask (MOD 35) will be provided by another MODIS investigator.

Suggested Reading

Dozier, J., 1984.

Hall, D. K. *et al*., 1995.

Kyle, H. L. *et al*., 1978.

Parkinson, C. L., 1997.

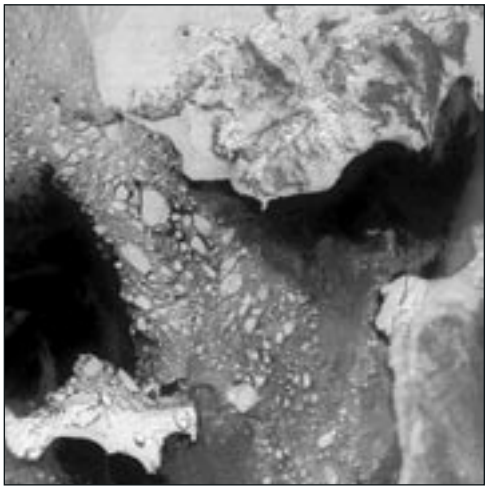

Sea Ice Image of the Bering Sea for May 7, 2000, generated from Terra MODIS band 2 (0.85 μm) data at 250 m spatial resolution. The Seward Peninsula is visible at the top of the image, and St. Lawrence Island can be seen in the lower left. Black areas are either clouds or open water. Individual snow-covered ice floes are visible, as is newly-formed sea ice, which has a lower reflectance and can sometimes be difficult to distinguish from the surrounding water. The ice flow direction is predominantly southward from the Bering Strait (upper left).

(MODIS Snow and Sea Ice Albedo, continued)

MODIS Sea Ice Cover Summary

Coverage: Global, daytime over nonequatorial ocean

Spatial/Temporal Characteristics: 1 km/daily; 1 km/8-day composite; 1/4°/daily and 8-day composite

Key Geophysical Parameters: Sea ice cover

Processing Level: 2, 3 (mapped)

Product Type: Standard, at-launch

Maximum File Size: 19 MB (Level 2); 6 MB (Daily Level 3), 12 MB (8-day Level 3)

File Frequency: 288/day (Daily Level 2); 626/day (Daily Level 3), 626/8-day (8-day Level 3)

Primary Data Format: HDF-EOS

Browse Available: No

Additional Product Information: http://snowmelt.gsfc.nasa.gov/MODIS_Snow/modis.html

DAAC: National Snow and Ice Data Center

Science Team Contact: D. Hall

MODIS Snow and Sea Ice Albedo (MODISALB)

Product Description

As currently envisioned, the MODIS snow and sea ice albedo product will provide daily albedo estimates of the seasonally snow-covered areas of the Earth with a spatial resolution of 1 km, and, for the climate-modeling grid product, 1/4° × 1/4° resolution. Once a surface has been identified as covered by either snow (MOD 10) or sea ice (MOD 29), the snow- albedo algorithm will be used to estimate the albedo of these surfaces under clear-sky conditions (Klein and Hall, 2000).

In addition to relying on other MODIS snow products to determine whether an area is snow or sea-ice covered, the planned MODIS snow-albedo product will utilize the MODIS cloud mask and the MODIS surface reflectance and global land cover products.

Research and Applications

The albedo of snow and sea ice is among the highest of all naturally occurring land surface albedos. The high albedo and large areal extent enable snow and sea ice to influence strongly the Earth's radiation budget. At a local scale, the high albedo of these surfaces affects energy exchange between the surface and the atmosphere.

Snow and ice albedos will be used in general circulation models to improve the parameterization of the Earth's albedo on a daily basis. This will enable more accurate forecasts of the Earth's climate. In addition, for sea ice, the differences in sea ice albedo will help to classify sea ice type. Determination of sea ice type is important for calculating the energy exchange between the ocean and the atmosphere.

Data Set Evolution

The MODIS snow albedo product builds on a heritage of snow and sea ice albedo algorithms (De Abreu *et al*., 1994; Knap and Oerlemans, 1996; Stroeve *et al*., 1997) developed for use with sensors on other environmental satellites, primarily NOAA AVHRR.

Suggested Reading

De Abreu, R. A. *et al*., 1994.

Klein, A. G., and D. K. Hall, 2000.

Knap, W.H., and J. Oerlemans, 1996.

Stroeve, J. *et al*., 1997.

MODIS Snow and Sea Ice Albedo Summary

Coverage: Global

Spatial/Temporal Characteristics: 1 km and 1/4°/daily and 8-day composite

Key Science Applications: Input to hydrological and GCM models

Key Geophysical Parameters: Snow/ice albedo

Processing Level: 3

Product Type: Standard, post-launch

Maximum File Size: 17 MB

File Frequency: 128/day

Primary Data Format: HDF-EOS

Browse Available: No

Additional Product Information: http://snowmelt.gsfc.nasa.gov/MODIS_Snow/modis.html

DAAC: National Snow and Ice Data Center

Science Team Contact: D. Hall

Appendix A: EOS Distributed Active Archive Centers (DAACs) Contact Information

DAAC & Discipline	Address	User Support Office Contact Information
Alaska SAR Facility (ASF) Sea Ice, Polar Processes, Synthetic Aperture Radar (SAR) Imagery	Alaska SAR Facility, User Services PO Box 757320 University of Alaska Fairbanks, AK 99775-7320	*Email:* asf@eos.nasa.gov, uso@asf.alaska.edu *Phone:* 907-474-6166 *Fax:* 907-474-5195 *URL:* www.asf.alaska.edu/
Land Processes (LP) DAAC Land Processes	United States Geological Survey EROS Data Center Sioux Falls, SD 57198	*Email:* edc@eos.nasa.gov *Phone:* 605-594-6116 *Fax:* 605-594-6963 *URL:* edcdaac.usgs.gov
GSFC Earth Sciences (GES) DAAC Upper Atmosphere, Global Biosphere, Atmospheric Dynamics	NASA/Goddard Space Flight Center Code 902.2 Greenbelt, MD 20771	*Email:* gsfc@eos.nasa.gov *Phone:* 301-614-5224 *Fax:* 301-614-5268 *URL:* daac.gsfc.nasa.gov/
Physical Oceanography (PO) DAAC Physical Oceanography	Physical Oceanography DAAC M/S Raytheon-299 4800 Oak Grove Drive Pasadena, CA 91109	*Email:* jpl@eos.nasa.gov, podaac@podaac.jpl.nasa.gov *Phone:* 626-744-5508 *Fax:* 626-744-5506 *URL:* podaac.jpl.nasa.gov/
Langley Research Center (LaRC) Radiation Budget, Clouds, Aerosols, Tropospheric Chemistry	NASA/Langley Research Center Mail Stop 157D 2 South Wright Street Hampton, VA 23681-2199	*Email:* larc@eos.nasa.gov *Phone:* 757-864-8656 *Fax:* 757-864-8807 *URL:* eosweb.larc.nasa.gov/
Natoinal Snow and Ice Data Center (NSIDC) Snow and Ice, Cryosphere and Climate	University of Colorado Campus Box 449 Boulder, CO 80309-0449	*Email:* nsidc@eos.nasa.gov, nsidc@kryos.colorado.edu *Phone:* 303-492-6199 *Fax:* 303-492-2468 *URL:* www-nsidc.colorado.edu
Oak Ridge National Laboratory (ORNL) Biogeochemical Dynamics	Oak Ridge National Laboratory Environmental Sciences Division PO Box 2008, MS 6407, Bldg. 1507 Oak Ridge, TN 37831-6407	*Email:* ornl@eos.nasa.gov, ornldaac@ornl.gov *Phone:* 423-241-3952 *Fax:* 423-574-4665 *URL:* www-eosdis.ornl.gov
Socioeconomic Data and Applications Center (EDAC) Human Impact on Global Change	Socioeconomic Data and Applications Center Columbia Univ./Lamont-Doherty Earth Observatory P.O. Box 1000, 61 Rt. 9W Palisades, NY 10964	*Email:* ciesin.info@ceisin.columbia.edu *Phone:* 845-365-8920 *Fax:* 845-365-8922 *URL:* sedac.ciesin.org, www.ciesin.org
Global Hydrology Resource Center (GHRC) Lightning, Hydrologic Processes	National Space Science and Technology Center 320 Sparkman Drive Huntsville, AL 35805	*Email:* ghrc@eos.nasa.gov *Phone:* 256-961-7932 *Fax:* 256-961-7859 *URL:* ghrc.msfc.nasa.gov/

Appendix B: Points of Contact

ACRIM III

Richard C. Willson
Columbia University
1001 B Avenue, Suite 200
Coronado, CA 92118
Phone: 619-522-2945 or 619-628-8507
Fax: 619-522-2967 or 619-522-2967
Email: acrim@acrim.com

AIRS/AMSU-A/HSB

Hartmut H. Aumann
Mail Stop 230-300
Jet Propulsion Laboratory
4800 Oak Grove Drive
Pasadena, CA 91109-8099
Phone: 818-354-6865
Fax: 818-393-4918
Email: hha@airs1.jpl.nasa.gov

Moustafa T. Chahine
Mail Stop 180-904
Jet Propulsion Laboratory
4800 Oak Grove Drive
Pasadena, CA 91109-8099
Phone: 818-354-6057
Fax: 818-393-4218
Email: moustafa.t.chahine@jpl.nasa.gov

Catherine Gautier
ICESS
University of California Santa Barbara
Santa Barbara, CA 93106
Phone: 805-893-8095
Fax: 805-893-2578
Email: gautier@icess.ucsb.edu

Henry E. Revercomb
Space Science and Engineering Center
University of Wisconsin Madison
1225 W. Dayton Street
Madison, WI 53706
Phone: 608-263-6758
Fax: 608-263-6738
Email: hankr@ssec.wisc.edu

Philip W. Rosenkranz
Massachusetts Institute of Technology
77 Massachusetts Avenue, Room 26-343
Cambridge, MA 02139
Phone: 617-253-3073
Fax: 617-258-7864
Email: pwr@mit.edu

David H. Staelin
Massachusetts Institute of Technology
77 Massachusetts Avenue,
Room 26-341
Cambridge, MA 02139
Phone: 617-253-3711
Fax: 617-258-7864
Email: staelin@ll.mit.edu

L. Larrabee Strow
Department of Physics
University of Maryland Baltimore County
1000 Hilltop Circle
Baltimore, MD 21250
Phone: 410-455-2528
Fax: 410-455-1072
Email: strow@umbc.edu

Joel Susskind
Code 910.4
NASA/Goddard Space Flight Center
Greenbelt, MD 20771
Phone: 301-286-7210
Fax: 301-286-1761
Email: f41js@charney.gsfc.nasa.gov

AMSR-E

Peter Ashcroft
Remote Sensing Systems
438 First St., Suite 220
Santa Rosa, CA 95404
Phone: 707-545-2904
Fax: 707-545-2906
Email: ashcroft@remss.com

Donald J. Cavalieri
Code 971
NASA/Goddard Space Flight Center
Greenbelt, MD 20771
Phone: 301-614-5901
Fax: 301-614-5644
Email: don@cavalieri.gsfc.nasa.gov

Alfred T. Chang
Code 974
NASA/Goddard Space Flight Center
Greenbelt, MD 20771
Phone: 301-614-5766
Fax: 301-614-5808
Email: achang@rainfall.gsfc.nasa.gov

Josefino C. Comiso
Code 971
NASA/Goddard Space Flight Center
Greenbelt, MD 20771
Phone: 301-614-5708
Fax: 301-614-5644
Email: comiso@joey.gsfc.nasa.gov

Ralph Ferraro
Code E/RA2, Room 601, WWBG
NOAA/NESDIS/ORA
Atmospheric Research & Applications Division
5200 Auth Road
Camp Springs, MD 20746-4304
Phone: 301-763-8251 x147
Fax: 301-763-8580
Email: ralph.r.ferraro@noaa.gov

Christian Kummerow
Department of Atmospheric Sciences
Colorado State University
Ft. Collins, CO 80524
Phone: 970-491-7473
Fax: 970-491-8449
Email: kummerow@atmos.colostate.edu

Elena Lobl
Code SD60
NASA/Marshall Space Flight Center
NSSTC 320 Sparkman Drive
Huntsville, AL 35805
Phone: 256-961-7912
Fax: 256-922-5788
Email: Elena.Lobl@msfc.nasa.gov

Eni G. Njoku
Mail Stop 300-233
Jet Propulsion Laboratory
4800 Oak Grove Drive
Pasadena, CA 91109-8099
Phone: 818-354-3693
Fax: 818-354-9476
Email: eni.g.njoku@jpl.nasa.gov

Akira Shibata
National Space Development Agency of Japan
Earth Observing Research Center
1-9-9, Roppongi
Minato-ku, Tokyo, 106
Japan
Phone: 81-33-224-7040
Fax: 81-33-224-7051
Email: Ashibata@eorc.nasda.go.jp

Roy W. Spencer
Code SD60
NASA/Marshall Space Flight Center
NSSTC 320 Sparkman Drive
Huntsville, AL 35805
Phone: 256-961-7960
Fax: 256-922-5788
Email: roy.spencer@msfc.nasa.gov

Frank J. Wentz
Remote Sensing Systems
1101 College Avenue, Suite 220
Santa Rosa, CA 95404
Phone: 707-545-2904
Fax: 704-545-2906
Email: wentz@remss.com

Thomas T. Wilheit
Department of Meteorology
Texas A&M University
Eller O&M Building, Room 1204
College Station, TX 77843-3150
Phone: 979-845-0176
Fax: 979-862-4466
Email: wilheit@tamu.edu

CERES

Bruce R. Barkstrom
Mail Stop 420
NASA/Langley Research Center
Hampton, VA 23681
Phone: 757-864-5676
Fax: 757-864-7996
Email: b.r.barkstrom@larc.nasa.gov

Thomas P. Charlock
Mail Stop 420
NASA/Langley Research Center
Hampton, VA 23681
Phone: 757-864-5687
Fax: 757-864-7996
Email: t.p.charlock@larc.nasa.gov

Richard N. Green
Mail Stop 420
NASA/Langley Research Center
Hampton, VA 23681
Phone: 757-864-5684
Fax: 757-864-7996
Email: r.n.green@larc.nasa.gov

David P. Kratz
Mail Stop 420
NASA/Langley Research Center
Hampton, VA 23681
Phone: 757-864-5669
Fax: 757-864-7996
Email: d.p.kratz@larc.nasa.gov

Robert B. Lee III
Mail Stop 420
NASA/Langley Research Center
Hampton, VA 23681
Phone: 757-864-5679
Fax: 757-864-7996
Email: r.b.lee@larc.nasa.gov

Norman G. Loeb
Mail Stop 420
NASA/Langley Research Center
Hampton, VA 23681
Phone: 757-864-5688
Fax: 757-864-7996
Email: n.g.loeb@larc.nasa.gov

Patrick Minnis
Mail Stop 420
NASA/Langley Research Center
Hampton, VA 23681
Phone: 757-864-5671
Fax: 757-864-7996
Email: p.minnis@larc.nasa.gov

Kory J. Priestley
Mail Stop 420
NASA/Langley Research Center
Hampton, VA 23681
Phone: 757-864-8147
Fax: 757-864-7996
Email: k.j.priestley@larc.nasa.gov

David F. Young
Mail Stop 420
NASA/Langley Research Center
Hampton, VA 23681
Phone: 757-864-5740
Fax: 757-864-7996
Email: d.f.young@larc.nasa.gov

Bruce A. Wielicki
Mail Stop 420
NASA/Langley Research Center
Hampton, VA 23681
Phone: 757-864-5683
Fax: 757-864-7996
Email: b.a.wielicki@larc.nasa.gov

Takmeng Wong
Mail Stop 420
NASA/Langley Research Center
Hampton, VA 23681
Phone: 757-864-5607
Fax: 757-864-7996
Email: takmeng.wong@larc.nasa.gov

MODIS

Mark Abbott
College of Oceanic & Atmospheric Sciences
Oceanography Administration Building 104
Oregon State University
Corvallis, OR 97331-5503
Phone: 541-737-4045
Fax: 541-737-2064
Email: mark@oce.orst.edu

Steven A. Ackerman
Department of Atmospheric & Oceanic Sciences
University of Wisconsin Madison
1225 W. Dayton Street
Madison, WI 53706
Phone: 608-263-3647
Fax: 608-262-5974
Email: stevea@ssec.wisc.edu

William B. Balch
Bigelow Laboratory
McKown Point
W. Boothbay Harbor, ME 04575
Phone: 207-633-9600
Fax: 207-633-9641
Email: bbalch@bigelow.org

William L. Barnes
Code 970
NASA/Goddard Space Flight Center
Greenbelt, MD 20771
Phone: 301-614-5675
Fax: 301-614-5666
Email: wbarnes@neptune.gsfc.nasa.gov

Otis Brown
RSMAS/MPO
University of Miami
4600 Rickenbacker Causeway
Miami, FL 33149-1098
Phone: 305-361-4018
Fax: 305-361-4622
Email: obrown@rsmas.miami.edu

Kendall Carder
Department of Marine Science
University of South Florida
140 Seventh Avenue South
St. Petersburg, FL 33701-5016
Phone: 727-553-3952
Fax: 727-553-3918
Email: kcarder@monty.marine.usf.edu

Dennis Clark
Code E/RA28
NOAA/NESDIS
5200 Auth Road, Room 105
Camp Springs, MD 20746-4304
Phone: 301-763-8102
Fax: 301-763-8108
Email: dclark1@nesdis.noaa.gov

Wayne Esaias
Code 971
NASA/Goddard Space Flight Center
Greenbelt, MD 20771
Phone: 301-614-5709
Fax: 301-614-5644
Email: wayne.e.esaias.1@gsfc.nasa.gov

Robert H. Evans
RSMAS/MPO
University of Miami
Meteorology & Physical Oceanography
4600 Rickenbacker Causeway
Miami, FL 33149-1098
Phone: 305-361-4799
Fax: 305-361-4622
Email: bob@miami.rsmas.miami.edu

Bo-Cai Gao
Remote Sensing Division, Code 7212
Naval Research Laboratory
4555 Overlook Drive, SW
Washington, DC 20375-5320
Phone: 202-767-8252
Fax: 202-404-8894
Email: gao@rsd.nrl.navy.mil

Howard R. Gordon
Department of Physics
University of Miami
Coral Cables, FL 33124
Phone: 305-284-2323
Fax: 305-284-4222
Email: gordon@phyvax.ir.miami.edu

Bruce W. Guenther
Code 920.1
NASA/Goddard Space Flight Center
Greenbelt, MD 20771
Phone: 301-614-5940
Fax: 301-614-5970
Email: bruce.w.guenther.1@gsfc.nasa.gov

Dorothy Hall
Code 974
NASA/Goddard Space Flight Center
Greenbelt, MD 20771
Phone: 301-614-5771
Fax: 301-614-5808
Email: dhall@glacier.gsfc.nasa.gov

Frank E. Hoge
Building N-159 (West)
NASA/Wallops Flight Facility
Wallops Island, VA 23337
Phone: 804-824-1567
Fax: 804-824-1036
Email: hoge@osb1.wff.nasa.gov

Alfredo R. Huete
Department of Soil, Water, and Environmental Sciences
University of Arizona
1200 E South Campus Drive
Shantz Building #38
Tuscon, AZ 85721-0038
Phone: 520-621-3228
Fax: 520-621-1647
Email: ahuete@ag.arizona.edu

Christopher O. Justice
Department of Environmental Sciences
University of Virginia
Clark Hall
Charlottesville, VA 22903
Phone: 804-924-3197
Fax: 804-924-4761
Email: justice@virginia.edu

Yoram J. Kaufman
Code 913
NASA/Goddard Space Flight Center
Greenbelt, MD 20771
Phone: 301-614-6189
Fax: 301-614-6307
Email: kaufman@climate.gsfc.nasa.gov

Michael D. King
Code 900
NASA/Goddard Space Flight Center
Greenbelt, MD 20771
Phone: 301-614-5636
Fax: 301-614-5620
Email: king@climate.gsfc.nasa.gov

Edward J. Masuoka
Code 922
NASA/Goddard Space Flight Center
Greenbelt, MD 20771
Phone: 301-614-5515
Fax: 301-614-5269
Email: emasuoka@ltpmail.gsfc.nasa.gov

W. Paul Menzel
NOAA/NESDIS
University of Wisconsin Madison
1225 W. Dayton Street
Madison, WI 53706
Phone: 608-264-5325
Fax: 608-262-5974
Email: paulm@ssec.wisc.edu

Harry E. Montgomery
Code 920.1
NASA/Goddard Space Flight Center
Greenbelt, MD 20771
Phone: 301-614-5941
Fax: 301-614-5970
Email: hmontgom@mcst.gsfc.nasa.gov

Jan-Peter Muller
Department of Geomatic Engineering
University College London
Gower Street
London WC1E 6BT
United Kingdom
Phone: 44-20-7679-7227
Fax: 44-20-7679-0453
Email: jpmuller@ge.ucl.ac.uk

Ranga B. Myneni
Department of Geography
Boston University
Center for Remote Sensing
675 Commonwealth Avenue
Boston, MA 02215
Phone: 617-353-5742
Fax: 617-353-8399
Email: rmyneni@crsa.bu.edu

Steven W. Running
University of Montana
School of Forestry
Missoula, MT 59812
Phone: 406-243-6311
Fax: 406-243-4510
Email: swr@ntsg.umt.edu

Vincent V. Salomonson
Code 900
NASA/Goddard Space Flight Center
Greenbelt, MD 20771
Phone: 301-614-5634
Fax: 301-614-5620
Email: vsalomon@pop900.gsfc.nasa.gov

Alan H. Strahler
Department of Geography
Center for Remote Sensing
Boston University
725 Commonwealth Avenue
Boston, MA 02215
Phone: 617-353-5984
Fax: 617-353-8399
Email: alan@bu.edu

Didier Tanré
Laboratoire d' Optique Atmosphérique
Université des Sciences et Techniques de Lille
Bat P5
F-59655 Villeneuve d'Ascq Cedex
France
Phone: 33-3-20-33-70-33
Fax: 33-3-20-43-43-42
Email: tanre@loa.univ-lille1.fr

Kurtis Thome
Remote Sensing Group/OCS
University of Arizona
1630 E. University Blvd
Tucson, AZ 85721-0094
Phone: 520-621-4535
Fax: 520-621-8292
Email: kurt.thome@opt-sci.arizona.edu

John R.G. Townshend
Department of Geography
University of Maryland at College Park
2181 LeFrak Hall
College Park, MD 20742-8225
Phone: 301-405-4050
Fax: 301-314-9299
Email: jt59@umail.umd.edu

Eric Vermote
Code 923
NASA/Goddard Space Flight Center
Greenbelt, MD 20771
Phone: 301-614-5521
Fax: 301-614-5269
Email: eric@kratmos.gsfc.nasa.gov

Zhengming Wan
Institute for Computational Earth Systems Science
University of California
Santa Barbara, CA 93106-3060
Phone: 805-893-4541
Fax: 805-893-2578
Email: wan@icess.ucsb.edu

ETM+

Samuel N. Goward
Department of Geography
University of Maryland College Park
1113 LeFrak Hall
College Park, MD 20742
Phone: 301-405-4055
Fax: 301-314-9299
Email: sg21@umail.umd.edu

Ralph J. Thompson
EROS Data Center
U.S. Geological Survey
Sioux Falls, SD 57198
Phone: 605-594-6162
Fax: 605-594-6963
Email: rjthompson@edcmail.cr.usgs.gov

Darrel L. Williams
Code 923
NASA/Goddard Space Flight Center
Greenbelt, MD 20771
Phone: 301-614-6692
Fax: 301-614-6695
Email: darrel@ltpmail.gsfc.nasa.gov

SAGE III

William P. Chu
Mail Stop 475
NASA/Langley Research Center
Hampton, VA 23681-2199
Phone: 757-864-2675
Fax: 757-864-2671
Email: W.P.Chu@larc.nasa.gov

Er-Woon Chiou
Mail Stop 475
NASA/Langley Research Center
Hampton, VA 23681-2199
Phone: 757-864-6810
Fax: 757-864-2671
Email: E.Chiou@larc.nasa.gov

M. Patrick McCormick
Hampton University
Center for Atmospheric Sciences
23 Tyler Street
Hampton, VA 23668
Phone: 757-728-6867
Fax: 757-727-5090
Email: mcc@hamptonu.edu

Michael C. Pitts
Mail Stop 475
NASA/Langley Research Center
Hampton, VA 23681-2199
Phone: 757-864-2693
Fax: 757-864-2671
Email: M.C.Pitts@larc.nasa.gov

Larry W. Thomason
Mail Stop 475
NASA/Langley Research Center
Hampton, VA 23681-2199
Phone: 757-864-6842
Fax: 757-864-2671
Email: l.w.thomason@larc.nasa.gov

Charles Trepte
Mail Stop 475
NASA/Langley Research Center
Hampton, VA 23681-2199
Phone: 757-864-5836
Fax: 757-864-2671
Email: c.r.trepte@larc.nasa.gov

Joseph M. Zawodny
Mail Stop 475
NASA/Langley Research Center
Hampton, VA 23681-2199
Phone: 757-864-2681
Fax: 757-864-2671
Email: j.m.zawodny@larc.nasa.gov

QuikTOMS

Pawan K. Bhartia
Code 916
NASA/Goddard Space Flight Center
Greenbelt, MD 20771
Phone: 301-614-5736
Fax: 301-614-5903
Email: bhartia@chapman.gsfc.nasa.gov

Jay R. Herman
Code 916
NASA/Goddard Space Flight Center
Greenbelt, MD 20771
Phone: 301-614-6039
Fax: 301-614-5903
Email: jay.herman@gsfc.nasa.gov

Richard D. McPeters
Code 916
NASA/Goddard Space Flight Center
Greenbelt, MD 20771
Phone: 301-614-6038
Fax: 301-614-5903
Email: mcpeters@wrabbit.gsfc.nasa.gov

Jason-1

Lee-Lueng Fu
Mail Stop 300-323
Jet Propulsion Laboratory
4800 Oak Grove Drive
Pasadena, CA 91109-8099
Phone: 818-354-8167
Fax: 818-393-6720
Email: llf@pacific.jpl.nasa.gov

Yves Ménard
Centre National d'Etudes Spatiales
DSO/ED/AL
bpi 2002
18 Ave. Edouard Belin
31401 Toulouse, Cedex
France
Phone: 33-56-127-4872
Fax: 33-56-128-2595
*Email:*Yves.Menard@cnes.fr

SeaWinds

Michael H. Freilich
College of Oceanic & Atmospheric Sciences
Oregon State University
104 Oceanographic Administration Building
Corvallis, OR 97331-5503
Phone: 541-737-2748
Fax: 541-737-2064
Email: mhf@oce.orst.edu

David G. Long
Electrical & Computer Engineering Department
Brigham Young University
459 Clyde Building
Provo, UT 84602-4099
Phone: 801-378-4383
Fax: 801-378-6586
Email: long@ee.byu.edu

VCL

Ralph O. Dubayah
Department of Geography
University of Maryland College Park
1113 Lefrak Hall
College Park, MD 20742
Phone: 301-405-4069
Fax: 301-314-9299
Email: rdubayah@geog.umd.edu

Appendix C: References

Abbott, M.R., and D.B. Chelton, 1991: Advances in passive remote sensing of the ocean, U.S. National Report to IUGG. *Reviews of Geophysics*, Supplement, 571-583.

Abbott, M.R., and R.M. Letelier, 1998: Decorrelation scales of chlorophyll as observed from bio-optical drifters in the California Current. *Deep-Sea Res.*, **45**, 1639-1668.

Abbott, M.R., P.J. Richerson, and T.M. Powell, 1982: In situ response of phytoplankton fluorescence to rapid variations in light. *Limn. Oceanog.*, **27**, 218-225.

Aber, J.D., 1979: A method for estimating foliage-height profiles in broadleaved forests. *J. Ecology*, **67**, 35-40.

Ackerman, S.A., K.I. Strabala, W.P. Menzel, R.A. Frey, C.C. Moeller, and L.E. Gumley, 1998: Discriminating clear sky from clouds with MODIS. *J. Geophys. Res.*, **103**, 32,141-32,157.

Alishouse, J.C., S. Synder, J. Vongsathorn, and R.R. Ferraro, 1990: Determination of oceanic total precipitable water from the SSM/I. *IEEE Trans. Geosci. Remote Sens.*, **28**, 811-816.

Anderson, J., J.M. Russell III, S. Solomon, and L.E. Deaver, 2000: Halogen occultation experiment confirmation of stratospheric chlorine decrease in accordance with the Montreal Protocol. *J. Geophys. Res.*, **105**, 4483.

Andreae, M.O., J. Fishman, M. Garstang, J.G. Goldammer, C.O. Justice, J.S. Levine, R.J. Sholes, B.J. Stocke, A.M. Thompson, B. VanWilgen, and STARE/TRACE-A SAFARI-92 Science Team, 1994: Biomass burning in the global environment. *Global Atmospheric-Biospheric Chemistry*, ed. by R.G. Prinn, Plenum Press, New York, 83-101.

Anyamba, E., and J. Susskind, 1998: A comparison of TOVS surface skin and air temperature with other data sets. *J. Geophys. Res.*, **103** (C5), 10,489-10,511.

Asrar, G., 1989: *Theory and Applications of Optical Remote Sensing*, John Wiley & Sons, New York, 734 pp.

Asrar, G., and J. Dozier, 1994: *Science Strategy for the Earth Observing System.* American Institute of Physics Press, Woodbury, NY., 119 pp.

Asrar, G., and R. Greenstone, eds., 1995: *MTPE/EOS Reference Handbook.* NASA Pub. NP-215, National Aeronautics and Space Administration, Washington, D.C., 276 pp.

Aumann, H.H., and C. Miller, 1995: Atmospheric Infrared Sounder (AIRS) on the Earth Observing System. *Advanced and Next Generation Satellites. Europt/SPIE.*

Aumann, H., D. Gregorich, S. Gaiser, D. Hagan, T. Pagano, and D. Ting, 1999: AIRS Algorithm Theoretical Basis Document Level 1B Part 1: Infrared Spectrometer, version 2.1, available at http://eospso.gsfc.nasa.gov/atbd/airstables.html.

Austin, R.W., 1974: Inherent spectral radiance signals of the ocean surface. In *Ocean Color Analysis*, SIO ref. 74-10, Scripps Inst. Oceanog., La Jolla, CA, 2.1-2.20.

Avery, T.E., and H.E. Burkhart, 1994: Forest Measurements. McGraw-Hill, New York, 416 pp.

Avis, L.M., R.N. Green, J.T. Suttles, and S.K. Gupta, 1984: A robust pseudoinverse spectral filter applied to the Earth Radiation Budget Experiment (ERBE) scanning channels. *NASA Tech. Memo.* TM-85781, 33 pp.

Balch, W.M., P.M. Holligan, S.G. Ackleson, and K.J. Voss, 1991: Biological and optical properties of mesoscale coccolithophore blooms in the Gulf of Maine. *Limn. Oceanog.*, **34**, 629-643.

Barkstrom, B.R., 1984: The Earth Radiation Budget Experiment (ERBE). *Bull. Amer. Meteor. Soc.*, **65**, 1170-1185.

Barkstrom, B.R., and G.L. Smith, 1986: The Earth radiation budget experiment: Science and implementation. *Rev. Geophys.*, **24**, 379-390.

Barkstrom, B.R., and B.A. Wielicki, 1995: Clouds and the Earth's Radiant Energy System (CERES) Algorithm Theoretical Basis Document. Volume I - Overviews, Subsystem 0 - CERES Data Processing System Objectives and Architecture, NASA Ref. Pub. 1376, vol. I, 21-97.

Barnsley, M.J., and J.-P. Muller, 1991: Measurement, simulation and analysis of directional reflectance properties of Earth surface materials. ESA SP-319, 375-382.

Barton, I.J., M. Zavody, D.M. O'Brien, D.R. Cutten, R.W. Saunders, and D.T. Llewellyn-Jones, 1989: Theoretical algorithms for satellite-derived sea surface temperatures. *J. Geophys. Res.*, **94**, 3365.

Baum, B.A., R.M. Welch, P. Minnis, L.L. Stowe, J.A. Coakley, Jr., Q. Trepte, P. Heck, X. Dong, D. Doelling, S. Sun-Mack, T. Murray, T. Berendes, K.-S. Kuo, and P. Davis, 1995a: Imager clear-sky determination and cloud detection (Subsystem 4.1). *Clouds and the Earth's Radiant Energy System (CERES) Algorithm Theoretical Basis Document, Volume III: Cloud Analyses and Radiance Inversions (Subsystem 4)*, NASA Ref. Pub. 1376, 3, ed. by the CERES Science Team, 43-82.

Baum, B.A., P. Minnis, J.A. Coakley, Jr., B.A. Wielicki, P. Heck, V. Tovinkere, Q. Trepte, S. Mayor, T. Murray, and S. Sun-Mack, 1995b: Imager cloud height determination (Subsystem 4.2). *Clouds and the Earth's Radiant Energy System (CERES) Algorithm Theoretical Basis Document, Volume III: Cloud Analyses and Radiance Inversions (Subsystem 4)*, NASA Ref. Pub. 1376, 3, ed. by the CERES Science Team, 83-134.

Becker, F., 1987: The impact of spectral emissivity on the measurement of land surface temperature from a satellite. *Int. J. Remote Sens.*, **8** (10), 1509-1522.

Beer, J., G.M. Raisbeck, and F. Yiou, 1991: The variation of ^{10}Be and solar activity. In *The Sun in Time*, ed. by C.P. Sonnet, M.S. Giampapa, and M.S. Mathews, U. Arizona Press, 343-359.

Bidigare, R.R., M.E. Ondrusek, J.H. Morrow, D.A. Kiefer, 1990: In vivo absorption properties of algal pigments. SPIE Vol. 1302, Ocean Optics X, 290-302.

Breigleb, B.P., and V. Ramanathan, 1982: Spectral and diurnal variations in clear-sky planetary albedo. *J. Climate Appl. Meteor.*, **21**, 1168-1171.

Brest, C.L., and S.N. Goward, 1987: Deriving surface albedo measurements from narrow band satellite data. *Int. J. Remote Sens.*, **8**, 351-367.

Brooks, D.R., E.F. Harrison, P. Minnis, J.T. Suttles, and R.S. Kandel, 1986: Development of algorithms for understanding the temporal and spatial variability of the Earth's radiation balance. *Rev. Geophys.*, **24**, 422-438.

Brown, G.S., 1979: Estimation of surface winds using satellite-borne radar measurements at normal incidence. *J. Geophys. Res.*, **84**, 3974-3978.

Brown, M.J., and G.G. Parker, 1994: Canopy light transmittance in a chronosequence of mixed-species deciduous forests. *Canadian J. Forest Res.*, **24**, 1694-1703.

Brown, O.B., and R.E. Cheney, 1983: Advances in satellite oceanography. *Rev. Geophys. Space Phys.*, **21**, 1216-1230.

Carder, K.L., R.G. Steward, J.H. Paul, and G.A. Vargo, 1986: Relationship between chlorophyll and ocean color constituents as they affect remote-sensing reflectance models. *Limn. Oceanog.*, **31**, 403-413.

Carder, K.L., S.K. Hawes, K.A. Baker, R.C. Smith, R.G. Steward, and B.G. Mitchell, 1991a: Reflectance model for quantifying chlorophyll *a* in the presence of productivity degradation products. *J. Geophys. Res.*, **96**, 599-611.

Carder, K.L., W.W. Greg, D.K. Costello, K. Haddad, and J.M. Prospero, 1991b: Determination of Saharan dust radiance and chlorophyll from CZCS imagery. *J. Geophys. Res.*, **96**, 5369-5378.

Carter, D.J.T., P.G. Challenor, and M.A. Srokosz, 1992: An assessment of Geosat wave height and wind speed measurements. *J. Geophys. Res.*, **97**, 11,383-11,392.

Cavalieri, D.J., P. Gloersen, and W.J. Campbell, 1984: Determination of sea ice parameters with the Nimbus-7 SMMR. *J. Geophys. Res.*, **89**, 5355-5369.

Cavalieri, D.J., J. Crawford, M.R. Drinkwater, D. Eppler, L.D. Farmer, R.R. Jentz, and C.C. Wackerman, 1991: Aircraft active and passive microwave validation of sea ice concentration from the DMSP SSM/I. *J. Geophys. Res.*, **96**, 21,989-22,008.

Cavalieri, D.J., P. Gloersen, C.L. Parkinson, J.C. Comiso, and H.J. Zwally, 1997: Observed hemispheric asymmetry in global sea ice changes. *Science*, **272**, 1104-1106.

Cess, R., E. Dutton, J. DeLuisi, and F. Jiang, 1991: Determining surface solar absorption from broadband satellite measurements for clear skies: Comparisons with surface measurements. *J. Climatol.*, **4**, 236-247.

Chahine, M.T., 1980: Infrared remote sensing of sea surface temperature. In *Remote Sensing of Atmospheres and Oceans*, ed. by A. Deepak, Academic Press, New York, 411-435.

Chahine, M.T., 1977: Remote sounding cloudy atmospheres. II. Multiple cloud formations. *J. Atmos. Sci.*, **34**, 744-757.

Chahine, M.T., 1982: Remote sounding of cloud parameters. *J. Atmos. Sci.*, **39**, 159-170.

Chahine, M.T., 1992: The hydrological cycle and its influence on climate. *Nature*, **359**, 373-380.

Chahine, M.T., H.H. Aumann, and F.S. Taylor, 1977: Remote sounding of cloudy atmospheres. III. Experimental verifications. *J. Atmos. Sci.*, **34** (5), 758-765.

Chahine, M.T., R. Haskins, J. Susskind, and D. Reuter, 1987: Satellite observations of atmospheric and surface interaction parameters. *Adv. Space Res.*, **7**, 111-119.

Chahine, M.T., H. Aumann, M. Goldberg, R. Haskins, E. Kalnay, L. McMillin, P. Rosenkranz, W. Smith, D. Staelin, L. Strow, and J. Susskind, 1997a: AIRS Team Unified Retrieval for Core Products–Level 2, version 1.6; updated at http://eospso.gsfc.nasa.gov/atbd/airstables.html.

Chahine, M.T., H. Aumann, E. Kalnay, H. Revercomb, L. McMillin, W. Smith, L. Strow, R. Haskins, E. Fetzer, E. Fishbein, S. Granger, M. Hofstadter, B. Lambrigtsen, T. Li, E. Olsen, C. Thompson, R. Knuteson, P. vanDelst, and W. McMillan, 1997b: AIRS Team Science Data Validation Plan—Core Products, version 1.2; updated at http://eospso.gsfc.nasa.gov/atbd/airstables.html.

Chahine, M.T., R. Haskins, and E. Fetzer, 1997c: Observation of the recycling rate of moisture in the atmosphere: 1988-1994. *GEWEX News,* **7** (3), 1.

Chamberlin, W.S., and J. Marra, 1992: Estimation of photosynthetic rate from measurements of natural fluorescence: Analysis of the effects of light and temperature. *Deep-Sea Res.*, **39**, 1695-1706.

Chang A.T.C., and T.T. Wilheit, 1979: Remote sensing of atmospheric water vapor, liquid water and wind speed at the ocean surface by passive microwave techniques from the Nimbus-5 satellite. *Radio Sci.*, **14**, 793-802.

Chang, A.T.C., J.L. Foster, and D.K. Hall, 1987: Nimbus 7 SMMR derived global snow cover parameters. *Ann. Glaciol.*, **9,** 39-44.

Chang, A.T.C, L.S. Chiu, and T.T. Wilheit, 1993: Oceanic monthly rainfall derived from SSM/I. *Eos Trans. Amer. Geophys. Union*, **74**, 505-513.

Chang, A.T.C., J.L. Foster, D.K. Hall, B.E. Goodison, A.E. Walker, J.R. Metcalfe, and A. Harby, 1997: Snow parameters derived from microwave measurements during the BOREAS winter field campaign. *J. Geophys. Res.*, **102**, 29,663-29,671.

Chang, A.T.C., L.S. Chiu, C. Kummerow, J. Meng, and T.T. Wilheit, 1999: First results of the TRMM monthly oceanic rain rate: Comparison with SSM/I. *Geophys. Res. Lett.*, **26**, 2379-2382.

Chang, H.D., P.H. Hwang, T.T. Wilheit, A.T.C. Chang, D.H. Staelin, and P.W. Rosenkranz, 1984: Monthly distributions of precipitable water from the Nimbus 7 SMMR data. *J. Geophys. Res.*, **89**, 5328-5334.

Charlock, T.P., and T.L. Alberta, 1996: The CERES/ARM/GEWEX Experiment (CAGEX) for the retrieval of radiative fluxes with satellite data. *Bull. Amer. Meteor. Soc.*, **77**, 2673-2683.

Charlock, T.P., F. Rose, S.-K Yang, T. Alberta, and G. Smith, 1993: An observation study of the interaction of clouds, radiation, and the general circulation. *Proceedings of the IRS '92: Current Problems in Atmospheric Radiation.* Tallinn (3-8 August 1992), A. Deepak Publishing, 151-154.

Charlock, T.P., D. Rutan, G.L. Smith, F.G. Rose, T.L. Alberta, N. Manalo-Smith, L.H. Coleman, D.P. Kratz, T.D. Bess, and K.A. Bush, 1995: Clouds and the Earth's Radiant Energy System (CERES) Algorithm Theoretical Basis Document. Volume IV - Determination of Surface and Atmosphere Fluxes and Temporally and Spatially Averaged Products (Subsystems 5-12), Subsystem 5.0 - Compute Surface and Atmospheric Fluxes, NASA Ref. Pub. 1376, Vol. IV, 1-52.

Chelton, D.B., and P.J. McCabe, 1985: A review of satellite altimeter measurement of sea surface wind speed: with a proposed new algorithm. *J. Geophys. Res.*, **90**, 4707-4720.

Chomko, R., and H.R. Gordon, 1998: Atmospheric correction of ocean color imagery: Use of the Junge power-law aerosol size distribution with variable refractive index to handle aerosol absorption. *Appl. Opt.*, **37**, 5560-5572.

Chu, D.A., Y.J. Kaufman, L.A. Remer, and B.N. Holben, 1998: Remote sensing of smoke from MODIS airborne simulator during the SCAR-B experiment. *J. Geophys. Res.*, **103** (D24), 31,979-31,987.

Cihlar, J.C., H. Ly, Z. Li, J. Chen, H. Pokrant, and F. Huang, 1997: Mult-temporal, multichannel AVHRR data sets for land biosphere studies—Artifacts and corrections. *Remote Sens. Environ.*, **60**, 35-57.

Coakley, J., R.D. Cess, and F.B. Yurevich, 1983: The effect of tropospheric aerosol on the Earth's radiation budget: A parameterization for climate models. *J. Atmos. Sci.*, **40**, 116-138.

Codrescu, M.V., S.E. Palo, X. Zhang, T.J. Fuller-Rowell, and C. Poppe, 1999: TEC climatology derived from TOPEX/POSEIDON measurements. *J. Atmos. Solar-Terrest. Phys.*, **61** (3-4), 281-298.

Cohen, W.B., T.A. Spies, and G.A. Bradshaw, 1990: Semivariograms of digital imagery for analysis of conifer canopy structure. *Remote Sens. Environ.*, **57**, 167-178.

Comb, D.G., 1990: Ice-out in Maine. *Nature*, **347**, 510.

Comiso, J.C., 1986: Characteristics of winter sea ice from satellite multispectral microwave observations. *J. Geophys. Rev.*, **91**, 975-994.

Comiso, J.C., 1995: SSM/I sea ice concentrations using the bootstrap algorithm, NASA Ref. Pub. 1380, December 1995, 49 pp.

Comiso, J.C., 2000: Variability and trends in Antarctic surface temperatures from in situ and satellite infrared measurements. *J. Climate*, **13** (10), 1674-1696.

Comiso, J.C., and H.J. Zwally, 1997: Temperature corrected bootstrap algorithm. *IEEE IGARSS'97 Digest*, **3**, 857-861.

Comiso, J.C., D.J. Cavalieri, C.P. Parkinson, and P. Gloersen, 1997: Passive microwave algorithms for sea ice concentration: A comparison of two techniques. *Remote Sens. Environ.*, **60**, 357-384.

Cotton, P.D., and D.J.T. Carter, 1994: Cross calibration of TOPEX, ERS-1 and Geosat wave heights. *J. Geophys. Res.*, **99**, 25,025-25,033.

Culver, M.E., and M.J. Perry, 1994: Detection of phycoerythrin fluorescence in upwelling irradiance spectra. *Eos, Trans. Amer. Geophys. Union*, **75**, 233.

Daley, R., 1991: *Atmospheric Data Analysis,* Cambridge University Press, 457 pp.

De Abreu, R.A., J. Key, J.A. Maslanik, M.C. Serreze, and E.F. LeDrew, 1994: Comparison of in situ and AVHRR-derived broadband albedo over Arctic sea ice. *Arctic*, **47** (3), 288-297.

Deepak, A., ed., 1980: *Remote Sensing of Atmospheres and Oceans*, Academic Press, New York, 641 pp.

d'Entremont, R.E., C.L. Barker Schaaf, W. Lucht, and A.H. Strahler, 1999: Retrieval of red spectral albedo and bidirectional reflectance using AVHRR HRPT and GOES satellite observations of the New England region. *J. Geophys. Res.*, **D-104**, 6229-6239.

Deschamps, P., and T. Phulpin, 1980: Atmospheric correction of infrared measurements of sea surface temperature using channels at 3.7, 11, and 12 mm. *Boundary-Layer Meteor.*, **18**, 131-143.

Deschamps, P.Y., M. Herman, and D. Tanré, 1983: Modeling of the atmospheric effects and its application to the remote sensing of ocean color. *Appl. Opt.*, **33**, 7096-7116.

Dickinson, R.E., 1987: Evapotranspiration in global climate models. *Adv. Space Res.*, **7**, 17-26.

Di Girolamo, L., and R. Davies, 1994: A band-differenced angular signature technique for cirrus cloud detection. *IEEE Trans. Geosci. Remote Sens.*, **32**, 890-896.

Diner, D.J., C.J. Bruegge, J.V. Martonchik, G.W. Bothwell, E.D. Danielson, V.G. Ford, L.E. Hovland, K.L. Jones, and M.L. White, 1991: A Multi-angle Imaging Spectroradiometer for terrestrial remote sensing from the Earth Observing System. *Int. J. Imaging Sys. Technol.*, **3**, 92-107.

Dixon, R. K., S. Brown, R.A. Houghton, A.M. Solomon, M.C. Trexler, and J. Wisniewski, 1994: Carbon pools and flux of global forest ecosystems. *Science*, **263**, 185-190.

Dong, X., P. Minnis, G.G. Mace, E.E. Clothiaux, C. Long, and S. Sun-Mack, 1999: Validation of CERES/VIRS cloud properties using ground-based measurements obtained at the DOE ARM sites. *Proc. AMS 10th Conf. Atmos. Rad.*, Madison, WI, June 28-July 2, 29-32.

Dozier, J., 1984: Snow reflectance from Landsat-4 thematic mapper. *IEEE Trans. Geosci. Remote Sens.*, **22**, 323-328.

Dozier, J., 1989: Spectral signature of alpine snow cover from the Landsat Thematic Mapper. *Remote Sens. Environ.*, **28**, 9-22.

Dubovik, O., A. Smirnov, B.N. Holben, M.D. King, Y.J. Kaufman, T.F. Eck, and I. Slutsker, 2000: Accuracy assessments of aerosol optical properties retrieved from Aerosol Robotic Network (AERONET) sun and sky radiance measurements. *J. Geophys. Res.*, **105** (D8), 9791-9806.

Eddy, J.A., 1976: The Maunder Minimum. *Science*, **192**, 1189-1202.

Edwards, T., R. Browining, J. Delderfield, D.J. Lee, K.A. Lidiard, R.S. Milborrow, P.H. McPherson, S.C. Peskett, G.M. Toplis, H.S. Taylor, I. Mason, G. Mason, A. Smith, and S. Stringer, 1990: The along track scanning radiometer–measurement of sea-surface temperature from ERS-1. *J. British Interplanetary Soc.*, **43**, 160.

Eicken, H., H. Fischer, and P. Lemke, 1995: Effects of the snow cover on Antarctic sea ice and potential modulation of its response to climate change. *Ann. Glaciol.*, **21**, 369-376.

Eppley, R.W., E. Stewart, M.R. Abbott, and U. Heyman, 1985: Estimating ocean primary production from satellite chlorophyll: Introduction to regional differences and statistics for the Southern California Bight. *J. Plank. Res.*, **7**, 57-70.

Esaias, W.E., R.L. Iverson, and K. Turpie, 1999: Ocean province classification using ocean colour data: Observing biological signatures of variations in physical dynamics. *Global Change Biology*, **5**, 1-17.

Evans, R.H., and H.R. Gordon, 1994: CZCS System Calibration: A retrospective examination. J. *Geophys. Res.*, **99C**, 7293-7307.

Farrar, M.R., and E.A. Smith, 1992: Spatial resolution enhancement of terrestrial features using deconvolved SSM/I microwave brightness temperatures. *IEEE Trans. Geosci. Remote Sens.*, **30**, 349-355.

Farrar, M.R., E.A. Smith, and X. Xiang, 1994: The impact of spatial resolution enhancement of SSM/I microwave brightness temperatures on rainfall retrieval algorithms. *J. Appl. Meteor.*, **33**, 313-333.

Ferraro, R.R, 1997: SSM/I derived global rainfall estimates for climatological applications. *J. Geophys. Res.*, **102**, 16,715-16,735.

Field, C.B., J.T. Randerson, and C.M. Malstrom, 1995: Global net primary production: Combining ecology and remote sensing. *Remote Sens. Environ.*, **51**, 74-88.

Fitzwater, S.E., G.A. Knauer, and J.H. Martin, 1982: Metal contamination and its effect on primary production measurements. *Limn. Oceanog.*, **27**, 544-551.

Fleming, H.F., M.D. Goldberg, and D.S. Crosby, 1986: Minimum variance simultaneous retrieval of temperature and water vapor from radiance measurements. *Proc. Second Conference on Satellite Meteorology,* Williamsburg, Amer. Meteor. Soc., 20-23.

Forbes, J.M., D. Revelle, X. Zhang, and R.E. Markin, 1997: Longitude structure of the ionosphere F region from TOPEX/Poseidon and ground-based data during January 20-30, 1993, including the quasi 2-day oscillation. *J. Geophys. Res.-Space Phys.*, **102** (A4), 7293-7299.

Foster, J.L., and A.T.C. Chang, 1993: Snow cover. In *Atlas of Satellite Observations Related to Global Change*, ed. by R.J. Gurney, J.L. Foster, and C.L. Parkinson, Cambridge University Press, Cambridge, U.K., 361-370.

Foster, J.L., D.K. Hall, A.T.C. Chang, and A. Rango, 1984: An overview of passive microwave snow research and results. *Rev. Geophys.*, **22**, 165-178.

Foukal, P.A., and J.L. Lean, 1988: Magnetic modulation of solar luminosity by photospheric activity. *Astrophys. J.*, **328**, 347.

Foukal, P.A., and J.L. Lean, 1990: An empirical model of total solar irradiance variation between 1874 and 1988. *J. Science*, **246**, 556-558.

Freilich, M.H., and P.G. Challenor, 1994: A new approach for determining fully empirical altimeter wind speed model functions. *J. Geophys. Res.*, **99**, 25,051-25,062.

Freilich, M.H., and R.S. Dunbar, 1999: The accuracy of the NSCAT 1 vector winds: Comparisons with National Data Buoy Center buoys. *J. Geophys. Res.*, **104**, 11,231-11,246.

Fu, L.-L., E.J. Christensen, C.A. Yamarone, M. Lefebvre, Y. Menard, M. Dorrer, and P. Escudier, 1994: TOPEX/Poseidon Mission Overview. J. *Geophys. Res.*, **99**, 24,369-24,381.

Fu, Q., and K. Liou, 1993: Parameterization of the radiative properties of cirrus clouds. *J. Atmos. Sci.*, **50**, 2008-2025.

Gao, B.C., and A.F.H. Goetz, 1990: Column atmospheric water vapor and vegetation liquid water retrievals from airborne imaging spectrometer data. *J. Geophys. Res.*, **95**, 3549-3564.

Gao, B.C., A.F.H. Goetz, and W.J. Wiscombe, 1993a: Cirrus cloud detection from airborne imaging spectrometer data using the 1.38 micron water vapor band. *Geophys. Res. Lett.*, **4**, 301-304.

Gao, B.C., K.D. Heidebrecht, and A.F.H. Goetz, 1993b: Derivation of scaled surface reflectances from AVIRIS data. *Remote Sens. Environ.*, **44**, 165-178.

Gao, B.C., Y.J. Kaufman, W. Han, and W.J. Wiscombe, 1998: Correction of thin cirrus path radiance in the 0.4 - 1.0 μm spectral region using the sensitive 1.375-μm cirrus detecting channel. *J. Geophys. Res.*, **103**, 32,169-32,176.

Gautier, C., and M. Landsfeld, 1997: Surface solar radiation flux and cloud radiative forcing for the Atmospheric Radiation Measurement (ARM) Southern Great Plain (SGP): A satellite, surface observations and radiative transfer model study. *Science*, **54**, 1289-1307.

Gillespie, A.R., A.B. Kahle, and R.E. Walker, 1986: Color enhancement of highly correlated images. I. Decorrelation and HSI contrast stretches. *Remote Sens. Environ.*, **20**, 209-235.

Gloersen P., and D.J. Cavalieri, 1986: Reduction of weather effects in the calculation of sea ice concentration from microwave radiances. *J. Geophys. Res.*, **91**, 3913-3919.

Gloersen, P., W.J. Campbell, D.J. Cavalieri, J.C. Comiso, C.L. Parkinson, and H.J. Zwally, 1992: *Arctic and Antarctic Sea Ice, 1978-1987: Satellite Passive Microwave Observations and Analysis*, NASA Spec. Pub. 511, National Aeronautics and Space Administration, Washington, D.C., 290 pp.

Goldberg, M.D., and L.M. McMillin, 1999: Methodology for deriving deep-layer temperatures from combined satellite infrared and microwave observations. *J. Climate*, **12**, 5-20.

Goodberlet, M.A., C.T. Swift, and J.C. Wilkerson, 1989: Remote sensing of ocean surface winds with the SSM/I. *J. Geophys. Res.*, **94**, 14,547-14,555.

Goodman, A.H., and A. Henderson-Sellers, 1988: Cloud detection analysis: A review of recent progress. *Atmos. Res.*, **21**, 203.

Gordon, H.R., 1978: Removal of atmospheric effects from satellite imagery of the oceans. *Appl. Opt.*, **17**, 1631-1636.

Gordon, H.R., 1987: Calibration requirements and methodology for remote sensors viewing the oceans in the visible. *Remote Sens. Environ.*, **22**, 103-126.

Gordon, H.R., 1997: Atmospheric correction of ocean color imagery in the Earth Observing System era. *J. Geophys. Res.*, **102D**, 17,081-17,106.

Gordon, H.R., and D.K. Clark, 1980: Atmospheric effects in the remote sensing of phytoplankton pigments. *Boundary-Layer Meteor.*, **18**, 300-313.

Gordon, H.R., and D.K. Clark, 1981: Clear water radiances for atmospheric correction of coastal zone color scanner imagery. *Appl. Opt.*, **20** (24), 4175-4180.

Gordon, H.R. and A.Y. Morel, 1983: *Remote Assessment of Ocean Color for Interpretation of Satellite Visible Imagery: A Review*, Springer-Verlag, New York, 114 pp.

Gordon, H.R., and M. Wang, 1994: Retrieval of water-leaving radiance and aerosol optical thickness over the oceans with SeaWiFS: A preliminary algorithm. *Appl. Opt.*, **33**, 443-452.

Gordon, H.R., D.K. Clark, J.L. Mueller, and W.A. Hovis, 1980: Phytoplankton pigments derived from the Nimbus-7 CZCS: Initial comparisons with surface measurements. *Science*, **210**, 63-66.

Gordon, H.R., O.B. Brown, R.H. Evans, J.W. Brown, R.C. Smith, K.S. Baker, and D.K. Clark, 1988: A semi-analytic radiance model of ocean color. *J. Geophys. Res.*, **93**, 10,909-10,924.

Gordon, H.R., T. Du, and T. Zhang, 1997: Remote sensing ocean color and aerosol properties: Resolving the issue of aerosol absorption. *Appl. Opt.*, **36**, 8670-8684.

Goward, S.N., and A.S. Hope., 1989: Evapotranspiration from combined reflected solar and emitted terrestrial radiation: Preliminary FIFE results from AVHRR data. *Adv. Space Res.*, **9** (7), 239-249.

Gower, F.J.R., and G.A. Borstad, 1990: Mapping of phytoplankton by solar-stimulated fluorescence using an imaging spectrometer. *Int. J. Remote Sens.*, **11**, 313-320.

Goyet, C., and P.G. Brewer, 1993: Biochemical properties of the oceanic cycle. In *Modeling Oceanic Climate Interactions*, ed. by J. Willebrand, NATO Advanced Study Institute, **I11**, 271-297.

Green, R.N., and B.A. Wielicki, 1995: Convolution of imager cloud properties with CERES footprint point spread function (Subsystem 4.4). *Clouds and the Earth's Radiant Energy System (CERES) Algorithm Theoretical Basis Document, Volume III: Cloud Analyses and Radiance Inversions (Subsystem 4)*, NASA Ref. Pub. 1376, Vol. III, ed. by the CERES Science Team, 177-194.

Green, R.N., B.A. Wielicki, J.A. Coakley, L.L. Stowe, and P.O'R. Hinton, 1995: CERES inversion to instantaneous TOA fluxes (Subsystem 4.5). *Clouds and the Earth's Radiant Energy System (CERES) Algorithm Theoretical Basis Document, Volume III: Cloud Analyses and Radiance Inversions (Subsystem 4)*, NASA Ref. Pub. 1376, Vol. III, ed. by the CERES Science Team, 195-206.

Green, R.O., and J.E. Conel, 1995: Movement of water vapor in the atmosphere measured by an imaging spectrometer at Rogers Dry Lake, CA. *Proc. Summaries of the Fifth Annual JPL Airborne Earth Science Workshop*, JPL Pub. 95-1, 1, 79–83.

Greenstone, R., and M.D. King, 1999: *EOS Science Plan Executive Summary: The State of Science in the EOS Program*, NASA Goddard Space Flight Center, Greenbelt, MD, 64 pp.

Gregg, W.W., and K.L. Carder, 1990: A simple solar irradiance model for cloudless maritime atmospheres. *Limn. Oceanog.*, **35** (8), 1657-1675.

Grody, N.C., 1976: Remote sensing of atmospheric water content from satellites using microwave radiometry. *IEEE Trans. Antennas Propagat.*, **AP-24**, 155-162.

Grody, N.C., A. Gruber, and W.C. Shen, 1980: Atmospheric water content over the tropical Pacific derived from the Nimbus 6 scanning microwave spectrometer. *J. Appl. Meteor.*, **19**, 986-996.

Groom, S.B., and P.M. Holligan, 1987: Remote sensing of coccolithophore blooms. *Adv. Space Res.*, **7**, 73-78.

Gupta, S.K., W.L. Darnell, and A.C. Wilber, 1992: A parameterization for longwave surface radiation from satellite data: Recent improvements. *J. Appl. Meteor.*, **31**, 1361-1367.

Gupta, S.K., W.L. Darnell, N.A. Ritchey, and A.C. Wilber, 1995: Clouds and the Earth's Radiant Energy System (CERES) Algorithm Theoretical Basis Document. Volume III - Cloud Analyses and Determination of Improved Top of Atmosphere Fluxes (Subsystem 4), Subsystem 4.6.3 - An Algorithm for Longwave Surface Radiation Budget for Total Skies, NASA Ref. Pub. 1376, Vol. III, 235-242.

Gustafson, G.B., R.G. Isaacs, R.P. d'Entremont, J.M. Sparrow, T.M. Hamill, C. Grassotti, D.W. Johnson, C.P. Sarkisian, D.C. Peduzzi, B.T. Pearson, V.D. Jakabhazy, J.S. Belfiore, and A.S. Lisa, 1994: Support of Environmental Requirements for Cloud Analysis and Archive (SERCAA): Algorithm descriptions. Phillips Laboratory Scientific Report No. 2, Hanscom Air Force Base, MA, 100 pp.

Haines, B.J., and Y.E. Bar-Sever, 1998: Monitoring the TOPEX microwave radiometer with GPS: Stability of columnar water vapor measurements. *Geophys. Res. Lett.*, **25**, 3563-3566.

Häkkinen, S., 1995: Seasonal simulation of the Southern Ocean coupled ice-ocean system. *J. Geophys. Res.*, **100**, 22,733-22,748.

Hall, D.K., G.A. Riggs, and V.V. Salomonson, 1995: Development of methods for mapping global snow cover using Moderate Resolution Imaging Spectroradiometer (MODIS) data. *Remote Sens. Environ.,* **54**, 127-140.

Halpern, D., A. Hollingsworth, and F.J. Wentz, 1994: ECMWF and SSM/I global surface wind speeds. *J. Atmos. Oceanic Techno.*, **11**, 779-788.

Hansen, J., A. Lacis, R. Ruedy, M. Sato, and H. Wilson, 1993: How sensitive is the world's climate? *Research and Exploration*, **9**, 143-158.

Hara, T., E.J. Bock, N.M. Frew, and W.R. McGillis, 1995: Relationship between air-sea gas transfer velocity and surface roughness. In *Air-Water Gas Transfer*, ed. by B. Jahne and E.C. Monahan, AEON Verlag & Studio, Hanau, 611-616.

Harrison, E.F., D.R. Brooks, P. Minnis, B.A. Wielicki, W.F. Staylor, G.G. Gibson, D.F. Young, F.M. Denn, and the ERBE Science Team, 1988: First estimates of the diurnal variation of longwave radiation from the multiple-satellite Earth Radiation Budget Experiment (ERBE). *Bull. Amer. Meteor. Soc.*, **69**, 1144-1151.

Harrison, E.F., P. Minnis, B.R. Barkstrom, B.A., Wielicki, G.G. Gibson, F.M. Denn, and D.F. Young, 1990a: Seasonal variation of the diurnal cycles of Earth's radiation budget determined from ERBE. *AMS 7th Conf. on Atmos. Radiation*, San Francisco, CA, July 23-27, 87-91.

Harrison, E.F., P. Minnis, B.R. Barkstrom, V. Ramanathan, R.D. Cess, and G.G. Gibson, 1990b: Seasonal variation of cloud radiative forcing derived from the Earth Radiation Budget Experiment. *J. Geophys. Res.*, **95**, 18,687-18,703.

Harrison, E.F., D.F. Young, P. Minnis, G.G. Gibson, R.D. Cess, V. Ramanathan, T.D. Murray, and D.J. Travers, 1995: Clouds and the Earth's Radiant Energy System (CERES) Algorithm Theoretical Basis Document. Volume IV - Determination of Surface and Atmosphere Fluxes and Temporally and Spatially Averaged Products (Subsystems 5-12), Subsystem 10.0 - Monthly Regional TOA and Surface Radiation Budget, NASA Ref. Pub. 1376, Vol. IV, 139-156.

Haskins, R.D., R.M. Goody, and L. Chen, 1997: A statistical method for testing a GCM with spectrally-resolved satellite data. *J. Geophys. Res.*, **102** (D14), 16,563-16,581.

Hayden, C.M., 1988: GOES-VAS simultaneous temperature-moisture retrieval algorithm. *J. Appl. Meteor.*, **27**, 705-733.

Hays, J.D., J. Imbrie, and N.J. Shackleton, 1976: Variations in the Earth's orbit: Pacemaker of the ice ages. *Science*, **194**, 1121-1132.

Hickey, J.R., L.L. Stowe, H. Jacobowitz, P. Pellegrino, R.H. Maschoff, F. House, and T.H. Vonder Haar, 1980: Initial determinations from Nimbus 7 cavity radiometer measurements. *Science*, **208**, 281.

Hofer, R.E., E.G. Njoku, and J.W. Waters, 1981: Microwave radiometric measurements of sea surface temperature from the SeaSat satellite: First results. *Science*, **212**, 1385-1387.

Hoffman, L.H., W.L. Weaver, and J.F. Kibler, 1987: Calculation and accuracy of ERBE scanner measurement locations. NASA Tech. Paper 2670.

Hofstadter, M., H. Aumann, E. Manning, S. Gaiser, C. Gautier, and S. Yang, 1999: AIRS Algorithm Theoretical Basis Document Level 1B Part 2: Visible/Near-Infrared Channels, version 2.1, available at http://eospso.gsfc.nasa.gov/atbd/airstables.html.

Hoge, F.E., and R.N. Swift, 1986: Chlorophyll pigment concentration using spectral curvature algorithms: An evaluation of present and proposed satellite ocean color sensor bands. *Appl. Opt.*, **25**, 3677-3682.

Hoge, F.E., and R.N. Swift, 1990: Photosynthetic accessory pigments: Evidence for the influence of phycoerythrin on the submarine light field. *Remote Sens. Environ.*, **34**, 19-35.

Hoge, F.E., C.W. Wright, P.E. Lyon, R.N. Swift, and J.K. Yungel, 1999a: Satellite retrieval of inherent optical properties by inversion of an oceanic radiance model: A preliminary algorithm. *Applied Optics*, **38**, 495-504.

Hoge, F.E., C.W. Wright, P.E. Lyon, R.N. Swift, and J.K. Yungel, 1999b: Satellite retrieval of the absorption coefficient of phytoplankton phycoerythrin pigment: Theory and feasibility status. *Applied Optics*, **38**, 7431-7441.

Holben, B.N., E. Vermote, Y.J. Kaufman, D. Tanré, and V. Kalb, 1992: Aerosol retrieval over land from AVHRR data-application for atmospheric correction. *IEEE Trans. Geosci. Remote Sens.*, **30**, 212-222.

Holben, B.N., T.F. Eck, I. Slutsker, D. Tanré, J.P. Buis, A. Setzer, E. Vermote, J.A. Reagan, Y.J. Kaufman, T. Nakajima, F. Lavenu, I. Jankowiak, and A. Smirnov, 1998: AERONET-A federated instrument network and data archive for aerosol characterization. *Remote Sens. Environ.*, **66** (1), 1-16.

Holligan, P.M., M. Viollier, D.S. Harbour, P. Camus, and M. Champagne-Philippe, 1983: Satellite and ship studies of coccolithophore production along the continental shelf edge. *Nature*, **304**, 339-342.

Hollinger, J.P., 1971: Passive microwave measurements of sea surface roughness. *IEEE Trans. Geosci. Electron.*, **GE-9**, 165-169.

Holm-Hansen, O. and B. Riemann, 1978: Chlorophyll *a* determination: Improvements in methodology. *Oikos*, **30**, 438-477.

Holm-Hansen, O., C.J. Lorenzen, R.W. Holmes, and J.D.H. Strickland, 1965: Fluorometric determination of chlorophyll. *J. Cons. Int. Explor. Mer.*, **30**, 3-15.

Hong, Y., C. Kummerow, and W.S. Olson, 1999: Separation of convective/stratiform precipitation using microwave brightness temperature. *J. Appl. Meteor.*, **38**, 1195-1213.

Houghton, J.T., F.W. Taylor, and C.D. Rodgers, 1984: *Remote Sounding of Atmospheres*. Cambridge University Press, Cambridge, UK, 343 pp.

Houghton, R.A., R.D. Boone, J.R. Fruci, J.E. Hobbie, J.M. Melillio, C.A. Palm, B.J. Peterson, G.R. Shaver, G.M. Woodwell, B. Moore, D.L. Skole, and N. Myers, 1987: The flux of carbon from terrestrial ecosystems to the atmosphere in 1980 due to changes in land use: Geographic distribution of the global flux. *Tellus*, **39B**, 122-139.

Hu, B., W. Lucht, X. Li, and A.H. Strahler, 1997: Validation of kernel-driven models for global modeling of bidirectional reflectance. *Remote Sens. Environ.*, **62**, 201-214.

Hu, B., W. Lucht, and A.H. Strahler, 1999: The interrelationship of atmospheric correction of reflectances and surface BRDF retrieval: A sensitivity study. *IEEE Trans. Geosci. Remote Sens.*, **37**, 724-738.

Hu, B., W. Lucht, A. Strahler, C. Schaaf, and M. Smith, 2000: Surface albedos and angle-corrected NDVI from AVHRR observations over South America. *Remote Sens. Env.*, **71**, 119-132.

Huete, A., C. Justice, and H. Liu, 1994: Development of vegetation and soil indices for MODIS-EOS. *Remote Sens. Environ.*, **49**, 224- 234.

Huete, A.R., H.Q. Liu, K. Batchily, and W. van Leeuwen, 1997: A comparison of vegetation indices over a global set of TM images for EOS-MODIS. *Remote Sens. Environ.*, **59**, 440-451.

Huete, A.R., C.O. Justice, and W. van Leeuwen, 1999: MODIS Vegetation Index (MOD 13) Algorithm Theoretical Basis Document (ATBD-MOD-13), version 3, available at http://eospso.gsfc.nasa.gov/atbd/modistables.html.

Imel, D., 1994: Evaluation of the TOPEX/POSEIDON dual-frequency ionosphere correction. *J. Geophys. Res.*, **99**, 24,895-24,906.

Inamdar, A.K., and V. Ramanathan, 1994: Physics of greenhouse effect and convection in warm oceans. *J. Climate*, **7**, 715-731.

Inamdar, A.K., and V. Ramanathan, 1995: Clouds and the Earth's Radiant Energy System (CERES) Algorithm Theoretical Basis Document. Volume III - Cloud Analyses and Determination of Improved Top of Atmosphere Fluxes (Subsystem 4), Subsystem 4.6.2 - Estimation of Longwave Surface Radiation Budget From CERES, NASA Ref. Pub. 1376, Vol. III, 217-234.

IPCC, 1996: Summary for policymakers. In *Climate Change 1995: The Science of Climate Change*, ed. by J.T. Houghton, L.G. Meira Filho, B.A. Callander, N. Harris, A. Kattenberg, and K. Maskell, Cambridge University Press, Cambridge, UK, 1-7.

Iqbal, M., 1983: *An Introduction to Solar Radiation*. Academic Press, Toronto and New York, 390 pp.

Iverson, R.L., W.E. Esaias, and K. Turpie, 2000: Ocean annual phytoplankton carbon and new production, and annual export production estimated with empirical equations and CZCS data. *Global Change Biology*, **6**, 57-72.

Jacobs, S.S., and J.C. Comiso, 1997: A climate anomaly in the Amundsen and Bellingshausen Seas. *J. Climate*, **10**, 697-709.

Janssen, M.A., ed., 1993: *Atmospheric Remote Sensing by Microwave Radiometry*, Chap. 1, John Wiley & Sons, New York, 572 pp.

Jarecke, P.J., M.A. Folkman, and L.A. Darnton, 1991: Radiometric calibration plan for the clouds and the Earth's radiant energy system instruments. *Proc. SPIE*, **1493**, 244-254.

Jedlovec, G.J., 1987: Determination of atmospheric moisture structure from high resolution MAMS radiance data. Ph.D. Thesis, University of Wisconsin, Madison, WI, 157 leaves.

Justice, C.O., J.P. Malingreau, and A. Setzer 1993: Satellite remote sensing of fires: potential and limitation. In *Fire in the Environment: The ecological, atmospheric, and climatic importance of vegetation fires*, ed. by P.J. Crutzen and J.G. Goldammer, John Wiley & Sons, Chichester, 77-88.

Justice, C.O., E. Vermote, J.R.G. Townshend, R. DeFries, D.P. Roy, D.K. Hall, V.V. Salomonson, J.L. Privette, G. Riggs, A. Strahler, W. Lucht, R.B. Myneni, Y. Knyazikhin, S.W. Running, R.R. Nemani, Z. Wan, A.R. Huete, W. van Leeuwen, R.E. Wolfe, L. Giglio, J.-P. Muller, P. Lewis, and M.J. Barnsley, 1998: The Moderate Resolution Imaging Spectroradiometer (MODIS): Land remote sensing for global change research. *IEEE Trans. Geosci. Remote Sens.*, **36**, 1228-1249.

Kaufman, Y.J., and B.C. Gao, 1992: Remote sensing of water vapor in the near IR from EOS/MODIS. *IEEE Trans. Geosci. Remote Sens.*, **30**, 871–884.

Kaufman, Y.J., and L.A. Remer, 1994: Remote sensing of vegetation in the mid-IR: The 3.75 μm channels. *IEEE Trans. Geosci. Remote Sens.*, **32**, 672–683.

Kaufman, Y.J., and C. Sendra, 1988: Algorithm for automatic atmospheric corrections to visible and near-IR satellite imagery. *Int. J. Remote Sens.*, **9**, 1357–1381.

Kaufman, Y.J., C.J. Tucker, and I. Fung, 1990: Remote sensing of biomass burning in the tropics. *J. Geophys. Res.*, **95** (D7), 9927-9939.

Kaufman, Y.J., D. Tanré, H.R. Gordon, T. Nakajima, J. Lenoble, R. Frouin, H. Grassl, B.M. Herman, M.D. King, and P.M. Teillet, 1997a: Passive remote sensing of tropospheric aerosol and atmospheric correction for the aerosol effect. *J. Geophys. Res.*, **102** (D14)**,** 16,815-16,830.

Kaufman, Y.J., D. Tanré, L. Remer, E. Vermote, A. Chu, and B.N. Holben, 1997b: Operational remote sensing of tropospheric aerosol over land from EOS-moderate resolution imaging spectroradiometer. *J. Geophys. Res.*, **102** (D14), 17,051-17,067.

Kaufman Y.J., C.O. Justice, L.P. Flynn, J.D. Kendall, E.M. Prins, D.E. Ward, P. Menzel, and A.W. Setzer, 1998a: Potential global fire monitoring from EOS-MODIS. *J. Geophys. Res.*, **103**, 32,215-32,238.

Kaufman, Y.J., R.G. Kleidman, and M.D. King, 1998b: SCAR-B fires in the tropics: Properties and remote sensing from EOS-MODIS. *J. Geophys. Res.*, **103** (D24), 31,955-31,968.

Kiefer, D.A., and R.A. Reynolds, 1992: Advances in understanding phytoplankton fluorescence and photosynthesis. In *Primary Productivity and Biogeochemical Cycles in the Sea*, ed. by P.G. Falkowski and A.D. Woodhead, Plenum, New York, 155-174.

King, M.D., 1987: Determination of the scaled optical thickness of clouds from reflected solar radiation measurements. *J. Atmos. Sci.*, **44**, 1734-1751.

King, M.D., ed., 1999: *EOS Science Plan: The State of Science in the EOS Program*, NASA Goddard Space Flight Center, Greenbelt, MD, 397 pp.

King, M.D., and R. Greenstone, 1999: *1999 EOS Reference Handbook: A Guide to NASA's Earth Science Enterprise and the Earth Observing System*, NASA Goddard Space Flight Center, Greenbelt, MD, 361 pp.

King, M.D., Y.J. Kaufman, W.P. Menzel, and D. Tanré, 1992: Remote sensing of cloud, aerosol, and water vapor properties from the Moderate Resolution Imaging Spectroradiometer (MODIS). *IEEE Trans. Geosci. Remote Sens.*, **30**, 2-27.

King, M.D., W.P. Menzel, P.S. Grant, J.S. Myers, G.T. Arnold, S.E. Platnick, L.E. Gumley, S.C. Tsay, C.C. Moeller, M. Fitzgerald, K.S. Brown, and F.G. Osterwisch, 1996: Airborne scanning spectrometer for remote sensing of cloud, aerosol, water vapor and surface properties. *J. Atmos. Oceanic Technol.*, **13**, 777-794.

King, M.D., S.C. Tsay, S.A. Ackerman and N.F. Larsen, 1998: Discriminating heavy aerosol, clouds, and fires during SCAR-B: Application of airborne multispectral MAS data. *J. Geophys. Res.*, **103**, 31,989-32,000.

King, M.D., Y.J. Kaufman, D. Tanré, and T. Nakajima, 1999: Remote sensing of tropospheric aerosols from space: Past, present, and future. *Bull. Amer. Meteor. Soc.*, **80**, 2229-2260.

Kleepsies, T.J., and L.M. McMillan, 1984: Physical retrieval of precipitable water using the split window technique. *Proc. Conf. on Satellite Meteorology/ Remote Sensing and Applications*, Amer. Meteor. Soc., Boston, MA, 55-57.

Klein, A.G., and D.K. Hall, 2000: Snow albedo determination using the NASA MODIS instrument. *Proc. 56th Annual Eastern Snow Conference*, 2-4 June 1999, Fredericton, New Brunswick, Canada, 77-85.

Klein, A.G., D.K. Hall, and G.A. Riggs, 1998: Improving snow-cover mapping in forests through the use of a canopy reflectance model. *Hydrological Processes*, **12** (10-11), 1723-1744.

Knap, W.H., and J. Oerlemans, 1996: The surface albedo of the Greenland ice sheet: satellite-derived and in situ measurements in the Søndre Strømfjord area during the 1991 melt season. *J. Glaciol.*, **42** (141), 364-374.

Knyazikhin, Y., J.V., Martonchik, R.B. Myneni, D.J. Diner, and S.W. Running, 1998a: Synergistic algorithm for estimating vegetation canopy leaf area index and fraction of absorbed photosynthetically active radiation from MODIS and MISR data. *J. Geophys. Res.*, **103**, 32,257-32,275.

Knyazikhin, Y., J.V. Martonchik, D.J. Diner, R.B. Myneni, M.M. Verstraete, B. Pinty, and N. Gobron, 1998b: Estimation of vegetation canopy leaf area index and fraction of absorbed photosynthetically active radiation from atmosphere-corrected MISR data. *J. Geophys. Res.*, **103**, 32,239-32,256.

Kratz, D.P., and Z. Li, 1995: Clouds and the Earth's Radiant Energy System (CERES) Algorithm Theoretical Basis Document. Volume III - Cloud Analyses and Determination of Improved Top of Atmosphere Fluxes (Subsystem 4), Subsystem 4.6.1 - Estimation of Longwave Surface Radiation Budget from CERES, NASA Ref. Pub. 1376, Vol. III, 213-216.

Krummel, J.R., R.H. Gardner, G. Sugihara, R.V. O'Neill, and P.R. Coleman, 1987: Landscape patterns in a disturbed environment. *Oikos*, **48**, 321-324.

Kummerow, C., W.S. Olson, and L. Giglio, 1996: A simplified scheme for obtaining precipitation and vertical hydrometeor profiles from passive microwave sensors. *IEEE Trans. Geosci. Remote Sens.*, **34**, 1213-1232.

Kummerow, C., W. Barnes, T. Kozu, J. Shiue, and J. Simpson, 1998: The Tropical Rainfall Measuring Mission (TRMM) sensor package. *J. Atmos. Oceanic Technol.*, **15**, 808-816.

Kuo, C.C., D.H. Staelin, and P.W. Rosenkranz, 1994: Statistical iterative scheme for estimating atmospheric relative humidity profiles. *IEEE Trans. Geosci. Remote Sens.*, **32**, 254-260.

Kyle, H.L., R.J. Curran, W.L. Barnes, and D. Escoe, 1978: A cloud physics radiometer. Third Conference on Atmospheric Radiation, Davis, CA, 107-109.

Lakshmi, V, J. Susskind, and B.J. Choudhury, 1998: Determination of land surface skin temperatures and surface air temperature and humidity from TOVS HIRS2/MSU data. *Adv. Space Res.*, **22** (5), 629-636.

Lambin, E.F., and A.H. Strahler, 1994a: Change-vector analysis in multitemporal space: A tool to detect and categorize land-cover change processes using high temporal-resolution satellite data. *Remote Sens. Environ.*, **48**, 231-244.

Lambin, E.F., and A.H. Strahler, 1994b: Indicators of land-cover change for change-vector analysis in multitemporal space at coarse spatial scales. *Int. J. Remote Sens.*, **15**, 2099-2119.

Lambrigtsen, B., 1996: AIRS Algorithm Theoretical Basis Document L1B Part 2: Microwave Instruments, version 1.2, Jet Propulsion Laboratory, California Institute of Technology, Pasadena, California, 46 pp.

Ledley, T.S., 1991: Snow on sea ice: Competing effects in shaping climate. *J. Geophys. Res.*, **96**, 17,195-17,208.

Lee, Z.P., K.L. Carder, T.G. Peacock, C.O. Davis, and J.L. Mueller, 1996: Method to derive ocean absorption coefficients from remote sensing reflectance. *Appl. Opt.*, **35** (3), 453-462.

Lee III, R.B., M.A. Gibson, R.S. Wilson, and S. Thomas, 1995: Long-term total solar irradiance variability during sunspot cycle 22. *J. Geophys. Res.*, **100**, 1667-1675.

Lee III, R.B., B.R. Barkstrom, G.L. Smith, J.E. Cooper, L.P. Kopia, and R.W. Lawrence, 1996: The Clouds and Earth's Radiant Energy System (CERES) sensors and preflight calibration plans. *J. Atmos. Oceanic Technol.*, **12**, 300-313.

Letelier, R.M., M.R. Abbott, and D.M. Karl, 1997: Chlorophyll natural fluorescence response to upwelling events in the Southern Ocean. *Geophys. Res. Lett.*, **24**, 409-412.

Levine, J.S., ed., 1991: *Global Biomass Burning*, MIT Press, Cambridge, MA, 569 pp.

Li, X., A. H. Strahler and C. E. Woodcock, 1995: A hybrid geometric optical-radiative transfer approach for modeling albedo and directional reflectance of discontinuous canopies. *IEEE Trans. Geosci. Remote Sens.,* **33**, 466-480.

Li, Z., and H. Leighton, 1993: Global climatologies of solar radiation budgets at the surface and in the atmosphere from 5 years of ERBE data. *J. Geophys. Res.*, **98**, 4919-4930.

Li, Z., H.G. Leighton, K. Masuda, and T. Takashima, 1993: Estimation of SW flux absorbed at the surface from TOA reflected flux. *J. Climate*, **6**, 317-330.

Liang, S., A.H. Strahler, and C.W. Walthall, 1999: Retrieval of land surface albedo from satellite observations: A simulation study. *J. Appl. Meteorol.*, **38**, 712-725.

Liou, K.-N., 1992: *Radiation and Cloud Processes in the Atmosphere*, Oxford University Press, Oxford, UK, 487 pp.

Lipes, R.G., R.L. Bernstein, V.J. Cardone, K.B. Katsaros, E.G. Njoku, A.L. Riley, D.B. Ross, C.T. Swift, and F.J. Wentz, 1979: SEASAT scanning multichannel microwave radiometer: Results of the Gulf of Alaska workshop. *Science*, **204**, 1415-1417.

Liu, G., and J. Curry, 1993: Determination of characteristic features of cloud liquid water from satellite microwave measurements. *J. Geophys. Res.*, **98**, 5069-5092.

Liu, W.T., W. Tang, and F.J. Wentz, 1992: Precipitable water and surface humidity over global oceans from SSM/I and ECMWF. *J. Geophys. Res.*, **97**, 2251-2264.

Llewellyn-Jones, D.T., P.J. Minnett, R.W. Saunders, and A.M. Zavody, 1984: Satellite multichannel infrared measurements of sea surface temperature of the N.E. Atlantic Ocean using AVHRR/2. *Quart. J. Roy. Meteor. Soc.*, **110**, 613-631.

Lorenzen, C.J., and S.W. Jeffrey, 1980: Determination of chlorophyll in sea water, UNESCO Tech. Paper. *Marine Science*, No. 35, 20 pp.

Los, S.O., C.O. Justice, and C.J. Tucker, 1994: A global 1° by 1° NDVI data set for climate studies derived from the GIMMS continental NDVI data. *Int. J. Remote Sens.*, **15**, 3493-3518.

Lucht, W., 1998: Expected retrieval accuracies of bidirectional reflectance and albedo from EOS-MODIS and MISR angular sampling. *J. Geophys. Res.*, **103**, 8763-8778.

Lucht, W., and P. Lewis, 2000: Theoretical noise sensitivity of BRDF and albedo retrieval from the EOS-MODIS and MISR sensors with respect to angular sampling. *Int. J. Remote Sens.*, **21** (1), 81-98.

Lucht, W., C.B. Schaaf, and A.H. Strahler, 2000: An algorithm for the retrieval of albedo from space using semiempirical BRDF models. *IEEE Trans. Geosci. Remote Sens.*, **38** (2), 977-998.

Ma, X.L., W.L. Smith, and H.M. Woolf, 1984: Total ozone from NOAA satellites—A physical model for obtaining observations with high spatial resolution. *J. Climate Appl. Meteor.*, **23**, 1309-1314.

Markus, T., 1999: Results from an ECMWF-SSM/I forced mixed layer model of the Southern Ocean. *J. Geophys. Res.*, **104**, 15,603-15,620.

Markus, T., and D.J. Cavalieri, 1998: Snow depth distribution over sea ice in the Southern Ocean from satellite passive microwave data. In *Antarctic Sea Ice: Physical Processes, Interactions and Variability*, Antarctic Research Series, Volume 74, American Geophysical Union, Washington, DC, 19-39.

Markus, T., and D.J. Cavalieri, 2000: An enhancement of the NASA Team sea ice algorithm. *IEEE Trans. Geosci. Remote Sens.*, **38** (3), 1387-1398.

McClain, E.P., W.G. Pichel, C.C. Walton, 1985: Comparative performance of AVHRR-based multichannel sea surface temperatures. *J. Geophys. Res.*, **90** (C6), 11,587-11,601.

McMillin, L.M., L.J. Crone, M.D. Goldberg, and T.J. Kleespies, 1995: Atmospheric transmittance of an absorbing gas. OPTRAN: a computationally fast and accurate transmittance model for absorbing gases with fixed and variable mixing ratios at variable viewing angles. *Appl. Opt.*, **34** (N27), 6269-6274.

Mehta, A., and J. Susskind, 1999: Outgoing longwave radiation from the TOVS Pathfinder Path A Data Set. *J. Geophys. Res.*, **104** (D10), 12,193.

Ménard, Y., L-L. Fu, P. Escudier, and G. Kunstmann, 2000: Cruising the ocean from space with Jason-1 in the 2000s. *EOS, Trans. Amer. Geophys. Union*, in press.

Minnett, P.J., 1991: Consequences of sea surface temperature variability on the validation and applications of satellite measurements. *J. Geophys. Res.*, **96**, 18,475-18,489.

Minnett, P.J., 1995: Sea surface temperature measurements from the Along-Track Scanning Radiometer on ERS-1. In *Oceanographic Applications of Remote Sensing*, ed. by M. Ikeda and F. Dobson, CRC Press Inc., Boca Raton, FL, 131-143.

Minnis, P., and E.F. Harrison, 1984: Diurnal variability of regional cloud and clear-sky radiative parameters derived from GOES data, Part III: November 1978 radiative parameters. *J. Climate Appl. Meteor.*, **23**, 1033-1051.

Minnis, P., D.P. Kratz, J.A. Coakley, Jr., M.D. King, R. Arduini, D.P. Garber, P.W. Heck, S. Mayor, W.L. Smith, Jr., and D.F. Young, 1995: Cloud optical property retrieval (Subsystem 4.3). *Clouds and the Earth's Radiant Energy System (CERES) Algorithm Theoretical Basis Document, Volume III: Cloud Analyses and Radiance Inversions (Subsystem 4)*, NASA Ref. Pub. 1376, Vol. III, ed. by the CERES Science Team, 135-176.

Minnis, P., D.P. Garber, D.F. Young, R.F. Arduini, and Y. Takano, 1998: Parameterization of reflectance and effective emittance for satellite remote sensing of cloud properties. *J. Atmos. Sci.*, **55**, 3313-3339.

Minnis, P., D.F. Young, B.A. Wielicki, P.W. Heck, S. Sun-Mack, and T.D. Murray, 1999: Cloud properties Derived from VIRS for CERES. *Proc. AMS 10th Conf. Atmos. Rad.*, Madison, WI, June 28-July 2, 21-24.

Mognard, N.M., 1984: Swell in the Pacific Ocean observed by Seasat radar altimeter. *Mar. Geodesy*, **8**, 183-209.

Mognard, N.M., and B. Lago, 1988: The computation of wind speed and wave heights from Geos 3 data. *J. Geophys. Res.*, **93**, 2285-2302.

Monteith, J.L., 1972: Solar radiation and productivity in tropical ecosystems. *J. Appl. Ecology*, **9**, 747-766.

Moody, A., and C. E. Woodcock, 1995: The influence of scale and the spatial characteristics of landscapes on land-cover mapping using remote sensing. *Landscape Ecology*, **10**, 363-379.

Morel, A., and J.M. Andre, 1991: Pigment distribution and primary production in the Western Mediterranean as derived and modeled from Coastal Zone Color Scanner observations. *J. Geophys. Res.*, **96**, 12,685-12,698.

Myneni, R.B., C.D. Keeling, C.J. Tucker, G. Asrar, R.R. Nemani, 1997a: Increased plant growth in the northern high latitudes from 1981 to 1991. *Nature*, **386**, 698-702.

Myneni, R.B., R.R. Nemani, and S.W. Running, 1997b: Estimation of global leaf area index and absorbed PAR using radiative transfer model. *IEEE Trans. Geosci. Remote Sens.*, **35**, 1380-1393.

Naderi, F.M., M.H. Freilich, and D.G. Long, 1991: Spaceborne radar measurement of wind velocity over the ocean—An overview of the NSCAT scatterometer system. *Proc. IEEE*, **79**, 850-866.

Nakajima, T.Y., and T. Nakajima, 1995: Wide-area determination of cloud microphysical properties from NOAA AVHRR measurements for FIRE and ASTEX regions. *J. Atmos. Sci.*, **52**, 4043-4059.

Nemani, R.R., and S.W. Running, 1989: Estimation of regional surface resistance to evapotranspiration from NDVI and thermal-IR AVHRR data. *J. Appl. Meteor.*, **28** (4), 276-284.

Nemani, R.R., and S.W. Running, 1995: Satellite monitoring of global land-cover changes and their impact on climate. *Climatic Change*, **31**, 395-413.

Nemani, R.R., L. Pierce, S. Running, and S. Goward, 1993: Developing satellite-derived estimates of surface moisture status. *J. Appl. Meteor.*, **32** (3), 548-557.

Nerem, R.S., D.P. Chambers, E.W. Leuliette, G.T. Mitchum, and B.S. Giese, 1999: Variation in global mean sea level associated with the 1997-1998 ENSO event: Implications for measuring long-term sea level change. *Geophys. Res. Lett.*, **26**, 3005-3008.

Nilsson, M., 1996: Estimation of tree heights and stand volume using an airborne lidar system. *Remote Sens. Environ.*, **56**, 1-7.

Njoku, E., 1994: Surface temperature estimation over land using satellite microwave radiometry. In *Passive Microwave Remote Sensing of Land-Atmosphere Interactions*, ed. by B. Choudhury, Y. Kerr, E. Njoku, and P. Pampaloni, VSP Press, Utrecht, The Netherlands, 509-530.

Njoku, E.G., and O.B. Brown, 1993: Sea surface temperature. In *Atlas of Satellite Observations Related to Global Change*, ed. by R.J. Gurney, J.L. Foster, and C.L. Parkinson, Cambridge Univ. Press, Cambridge, UK, 237-249.

Njoku, E.G., and D. Entekhabi, 1996: Passive microwave remote sensing of soil moisture. *J. Hydrology*, **184**, 101-129.

Njoku, E., and L. Li, 1999: Retrieval of land surface parameters using passive microwave measurements at 6 to 18 GHz. *IEEE Trans. Geosci. Remote Sens.*, **37**, 79–93.

Nordberg,W., J. Conaway, D.B. Ross, and T.T. Wilheit, 1971: Measurement of microwave emission from a foam covered wind driven sea. *J. Atmos. Sci.*, **38**, 429-433.

NSIDC, The National Snow and Ice Data Center DAAC, 1996: DMSP SSM/I Brightness Temperature and Sea Ice Concentration Grids for the Polar Regions, User's Guide, CIRES, University of Colorado, Boulder, CO, second revised edition.

Oliver, C.D., and B.C. Larson, 1990: *Forest Stand Dynamics*, McGraw Hill, New York, 520 pp.

Olson, W., C.D. Kummerow, Y. Hong, and W.K. Tao, 1999: Atmospheric latent heating distributions in the tropics derived from satellite passive microwave radiometer measurements. *J. Appl. Meteor.*, **38**, 633-664.

Palmer, M.W., 1988: Fractal geometry: A tool for describing spatial patterns of plant communities. *Vegetatio*, **75**, 91-102.

Paltridge, G.W., and C.M.R. Platt, 1976: *Radiative Processes in Meteorology and Climatology*, Elsevier, Amsterdam, 318 pp.

Parker, D.E., C.K. Folland, and M. Jackson, 1995: Marine surface temperature: Observed variations and data requirements. *Climate Change*, **31**, 559-600.

Parkinson, C.L., 1997: *Earth from Above: Using Color-Coded Satellite Images to Examine the Global Environment*, University Science Books, Sausalito, California, 176 pp.

Parkinson, C.L., J.C. Comiso, H.J. Zwally, D.J. Cavalieri, P. Gloersen, and W.J. Campbell, 1987: *Arctic Sea Ice, 1973-1976: Satellite Passive-Microwave Observations*, NASA Spec. Pub. 489, National Aeronautics and Space Administration, Washington, D.C., 296 pp.

Penner, J.E., R.E. Dickinson, C.A. O'Neill, 1992: Effects of aerosol from biomass burning on the global radiation budget. *Science*, **256**, 1432-1434.

Pierson, W.J., 1990: Examples of, reasons for, and consequences of, the poor quality of wind data from ships for the marine boundary layer: Implications for remote sensing. *J. Geophys. Res.*, **95**, 13,313-13,340.

Platnick, S., P.A. Durkee, K. Nielson, J.P. Taylor, S.C. Tsay, M.D. King, R.J. Ferek, P.V. Hobbs, and J.W. Rottman, 2000: The role of background cloud microphysics in the radiative formation of ship tracks. *J. Atmos. Sci.*, **57**, 2607-2624.

Platt, T.C., C. Caverhill, and S. Sathyendranath, 1991: Basin scale estimates of oceanic primary production by remote sensing: The North Atlantic. *J. Geophys. Res.*, **96** (15), 147-149.

Poe, G.A., 1990: Optimum interpolation of imaging microwave radiometer data. *IEEE Trans. Geosci. Remote Sens.*, **28**, 800-810.

Prabhakara, C., B.J. Conrath, and R.A. Hanel, 1970: Remote sensing of atmospheric ozone using the 9.6 micron band. *J. Atmos. Sci.*, **26**, 689-697.

Price, J.C., 1983: Estimating surface temperature from satellite thermal infrared data—a simple formulation for the atmospheric effect. *Remote Sens. Environ.*, **13**, 353-361.

Price, J.C., 1984: Land surface temperature measurements from the split window channels of the NOAA 7 Advanced Very High Resolution Radiometer. *J. Geophys. Res.*, **89**, 7231-7237.

Priestley, K.J., B.R. Barkstrom, R.B. Lee III, R.N. Green, S. Thomas, R.S. Wilson, P.C. Spence, J. Paden, D.K. Pandey, and A. Al-Hajjah, 2000: Post-launch radiometric validation of the Clouds and the Earth's Radiant Energy System (CERES) proto-flight model on the Tropical Rainfall Measuring Mission (TRMM) spacecraft through 1999. *J. Appl. Meteor.*, in press.

Prince, S.D., and S.N. Goward, 1995: Global primary production: A remote sensing approach. *J. Biogeography*, **22**, 815-835.

Ramanathan, V., 1986: Scientific use of surface radiation budget for climate studies. *Surface Radiation Budget for Climate Applications*, ed. by J.T. Suttles and G. Ohring, NASA Ref. Pub. 1169, Washington, DC, 58-86.

Ramanathan, V., 1987: The role of Earth radiation budget studies in climate and general circulation research. *J. Geophys. Res.*, **92**, 4075-4095.

Ramanathan, V., 1988: The greenhouse theory of climate change: a test by an inadvertent global experiment. *Science*, **240**, 293-298.

Ramanathan V., R.D. Cess, E.F. Harrison, P. Minnis, B.R. Barkstrom, E. Ahmad, and D. Hartmann, 1989: Cloud-radiative forcing and climate: Results for the Earth Radiation Budget Experiment. *Science*, **243**, 57-63.

Randall, D.A., Harshvardhan, D.A. Dazlich, and T.G. Corsetti, 1989: Interactions among radiation, convection, and large-scale dynamics in a general circulation model. *J. Atmos. Sci.*, **46**, 1943-1970.

Rao, C.R.N., L.L. Stowe, and E.P. McClain, 1989: Remote sensing of aerosols over the oceans using AVHRR data: Theory, practice, and applications. *Int. J. Remote Sens.*, **10**, 743–749.

Remer, L.A., and Y.J. Kaufman, 1998: Dynamic aerosol model: Urban/industrial aerosol. *J. Geophys. Res.*, **103** (D12), 13,859-13,871.

Remer, L.A., Y.J. Kaufman and B.N. Holben, 1996: The size distribution of ambient aerosol particles: Smoke vs. urban/industrial aerosol. In *Global Biomass Burning*, ed. by J. S. Levine, The MIT Press, Cambridge, MA, 519-530.

Remer, L.A., S. Gassó, D.A. Hegg, Y.J. Kaufman, and B.N. Holben, 1997: Urban/industrial aerosol: Ground-based sun/sky radiometer and airborne in situ measurements. *J. Geophys. Res.*, **102** (D14), 16,849-16,859.

Remer, L.A., Y.J. Kaufman, B.N. Holben, A.M. Thompson, and D. McNamara, 1998: Biomass burning aerosol size distribution and modeled optical properties. *J. Geophys. Res.*, **103** (D24), 31,879-31,891.

Rencz, A., ed., 1999: *Remote Sensing for the Earth Sciences*. Volume 3 of the *Manual of Remote Sensing*, Third Edition, ed. by R.A. Ryerson, John Wiley & Sons, New York, 707 pp.

Reynolds, R.W., and T.M. Smith, 1994: Improved global sea surface temperature analyses using optimum interpolation. *J. Climate*, **7**, 929-948.

Robinson, J.M., 1991: Fire from space: Global fire evaluation using infrared remote sensing. *Int. J. Remote Sens.*, **12** (1), 3-24.

Robinson, W.D., C. Kummerow, and W.S. Olson, 1992: A technique for enhancing and matching the resolution of microwave measurements from the SSM/I instrument. *IEEE Trans. Geosci. Remote Sens.*, **30**, 419-429.

Rosenkranz, P.W., 1995: A rapid atmospheric transmittance algorithm for microwave sounding channels. *IEEE Trans. Geosci. Remote Sens.*, **33**, 1135-1140.

Rosenkranz, P.W., 1998: Water vapor microwave continuum absorption: A comparison of measurements and models. *Radio Sci.*, **33**, 919-928.

Rossow, W.B., and L.C. Garder, 1993: Cloud detection using satellite measurements of infrared and visible radiances for ISCCP. *J. Climate*, **6**, 2341-2369.

Ruf, C.S., S.J. Keihm, B. Subramanya, and M.A. Janssen, 1994: TOPEX/POSEIDON microwave radiometer performance and calibration. *J. Geophys. Res.*, **99**, 24,915-24,926.

Rufenach, C.L., and W.R. Alpers, 1978: Measurement of ocean wave heights using the Geos 3 altimeter. *J. Geophys. Res.*, **83**, 5001-5018.

Ruimy, A., B. Saugier, and G. Dedieu, 1994: Methodology for the estimation of terrestrial net primary production from remotely sensed data. *J. Geophys. Res.*, **99** (D3), 5263-5283.

Running, S.W., 1990: Estimating terrestrial primary productivity by combining remote sensing and ecosystem simulation. In *Remote Sensing of Biosphere Functioning*, ed. by R. Hobbs and H. Mooney, New York: Springer-Verlag, 65-86.

Running, S.W., R.R. Nemani, D.L. Peterson, L.E. Band, D.F. Potts, L.L. Pierce, and M.A. Spanner, 1989: Mapping regional forest evapotranspiration and photosynthesis by coupling satellite data with ecosystem simulation. *Ecology*, **70**, 1090-1101.

Running, S.W., C. Justice, V. Salmonson, D. Hall, J. Barker, Y. Kaufmann, A. Strahler, A. Huete, J-P. Muller, V. Vanderbilt, Z. Wan, P. Teillet, and D. Carneggie, 1994: Terrestrial remote sensing science and algorithms planned for EOS/MODIS. *Int. J. Remote Sens.*, **15**, 3587-3620.

Running, S.W., T.R. Loveland, L.L. Pierce, R.R. Nemani, and E.R. Hunt, 1995: A remote sensing based vegetation classification logic for global land cover analysis. *Remote Sens. Environ.*, **51**, 39-48.

Salisbury, J.W., and D.M. D'Aria, 1992: Emissivity of terrestrial materials in the 8-14 mm atmospheric window. *Remote Sens. Environ.*, **42**, 83-106.

Salomonson, V.V., D.K. Hall, and J.Y.L. Chien, 1995: Use of passive microwave and optical data for large-scale snow-cover mapping. *Proc. Second Topical Symposium on Combined Optical-Microwave Earth and Atmospheric Sensing*, 3-6 April 1995, Atlanta, GA, 35-37.

Sarmiento, J.L., J.R. Toggweiler, and R. Najjar, 1988: Ocean carbon-cycle dynamics and atmospheric CO_2. *Phil. Trans. Roy. Soc. Lond. A*, **325**, 3-21.

Saunders, R.W., and K.T. Kriebel, 1988: An improved method for detecting clear-sky and cloud radiances for AVHRR data. *Int. J. Remote Sens.*, **9**, 123-150.

Schluessel, P., and H. Luthardt, 1991: Surface wind speeds over the North Sea from Special Sensor Microwave/Imager Observations. *J. Geophys. Res.*, **96**, 4845-4853.

Schluessel, P., W.J. Emery, H. Grassl, and T. Mammen, 1990: On the bulk-skin temperature difference and its impact on satellite remote sensing of sea surface temperatures. *J. Geophys. Res.*, **95**, 13,341-13,356.

Schubert, S.D., R.B. Rood, and J. Pfaendtner, 1993: An assimilated dataset for earth science applications. *Bull. Amer. Meteor. Soc.*, **74**, 2331-2342.

Sellers, P.J., 1987: Canopy reflectance, photosynthesis and transpiration. *Int. J. Remote Sens.*, **6**, 1335-1372.

Shapiro, M.A., A.J. Krueger, and P.J. Kennedy, 1982: Nowcasting the position and intensity of jet streams using a satellite borne total ozone mapping spectrometer. In *Nowcasting*, ed. by K. A. Browning, Academic Press, London, UK, 137-145.

Shinell, D., D. Rind, and P. Lonergan, 1998: Increased polar ozone losses and delayed eventual recovery owing to increasing green-house gas concentrations. *Nature*, **392**, 589.

Sikes, S., and V. Fabry, 1994: Photosynthesis, $CaCO_3$ deposition, coccolithophorids and the global carbon cycle. In *Photosynthetic Carbon Metabolism and Regulation of Atmospheric CO_2 and O_2*, ed. by N.E. Tolbert and J. Preiss, Oxford University Press, London, 217-233.

Slater, P.N., S.F. Biggar, R.G. Holm, R.D. Jackson, Y. Mao, M.S. Moran, J.M. Palmer, and B. Yuan, 1987: Reflectance-based and radiance-based methods for the in-flight absolute calibration of multi-spectral sensors. *Remote Sens. Environ.*, **22**, 11-37.

Smith, A.H., R.W. Saunders, and A.M. Zavody, 1994: The validation of ATSR using aircraft radiometer data over the tropical Atlantic. *J. Atmos. Oceanic Technol.*, **11**, 789-800.

Smith, E.A. and 26 others, 1998: Results of WetNet PIP-2 Project. *J. Atmos. Sci.*, **55**, 1483-1536.

Smith, G.L., R.N. Green, E. Raschke, L.M. Avis, J.T. Suttles, B.A. Wielicki, and R. Daview, 1986: Inversion methods for satellite studies of the Earth's radiation budget: Development of algorithms for the ERBE mission. *Rev. Geophys.*, **24**, 407-421.

Smith, G.L., K.A. Bush, F.E. Martino, III, R. Hazra, N. Manalo-Smith, and D. Rutan, 1995: Clouds and the Earth's Radiant Energy System (CERES) Algorithm Theoretical Basis Document. Volume IV - Determination of Surface and Atmosphere Fluxes and Temporally and Spatially Averaged Products (Subsystems 5-12), Subsystem 9.0—Grid TOA and Surface Fluxes for Instantaneous Surface Product, NASA Ref. Pub. 1376, Vol. IV, 129-138.

Smith, R.C., and K.S. Baker, 1977: The bio-optical state of ocean waters and remote sensing. Scripps Institution of Oceanography, Ref. 77-2, 36 pp.

Smith, R.C., and K.S. Baker, 1982: Oceanic chlorophyll concentrations as determined by satellite (Nimbus-7 Coastal Zone Color Scanner). *Marine Biology*, **66**, 269-279.

Smith, R.C., and W.H. Wilson, 1981: Ship and satellite bio-optical research in the California Bight. In *Oceanography from Space*, ed. by J.F.R. Gower, Plenum, New York, 281-294.

Smith, W.L., and H.M. Woolf, 1976: The use of eigenvectors of statistical covariance matrices for interpreting satellite sounding radiometer observations. *J. Atmos. Sci.*, **33**, 1127-1140.

Smith, W.L., and F.X. Zhou, 1982: Rapid extraction of layer relative humidity, geopotential thickness and atmospheric stability from satellite sounding radiometer data. *Appl. Opt.*, **21**, 924-928.

Smith, W.L., H.M. Woolf, and A.J. Schreiner, 1985: Simultaneous retrieval of surface and atmospheric parameters: A physical and analytically direct approach. In *Advances in Remote Sensing Retrieval Methods*, ed. by A. Deepak, H.E. Fleming, and M.T. Chahine, A. Deepak Publishing, Hampton, VA, 221-232.

Smith, W.L., R.O. Knuteson, H.E. Revercombe, W. Feltz, H.B. Howell, W.P. Menzel, N.R. Nalli, O.B. Brown, J. Brown, P.J. Minnett and W. McKeown, 1996. Observations of the infrared radiative properties of the ocean—implications for the measurement of sea-surface temperature via satellite remote sensing. *Bull. Amer. Meteor. Soc.*, **77** (1), 41-51.

Snyder, W., and Z. Wan, 1996: Surface temperature correction for active infrared reflectance measurements of natural materials. *Appl. Opt.*, **35** (13), 2216-2220.

Sohn, B.-J., and F.R. Robertson, 1993: Intercomparison of observed cloud radiative forcing: A zonal and global perspective. *Bull. Amer. Meteor. Soc.*, **74**, 997-1006.

Solomon, S., M. Mills, L.E. Heidt, W.H. Pollock, and A.F. Tuck, 1992: On the evaluation of ozone depletion potentials. *J. Geophys. Res.*, **97** (D1), 825-842.

Solomon, S., R.W. Portmann, R.R. Garcia, L.W. Thomason, L.R. Poole, and M.P. McCormick, 1996: The role of aerosol variations in anthropogenic ozone depletion at northern midlatitudes. *J. Geophys. Res.*, **101** (D3), 6713-6727.

Solomon, S., S. Bormann, R.R. Garcia, R. Portmann, L. Thomason, L.R. Poole, D. Winker, and M.P. McCormick, 1997: Heterogeneous chlorine chemistry in the tropopause region. *J. Geophys. Res.*, **102**, 21,411-21,429.

Staelin, D.H., and F.W. Chen, 2000: Precipitation observations near 54 and 183 GHz using the NOAA-15 satellite. *IEEE Trans. Geosci. Remote Sens.*, in press.

Staelin, D.H., K.F. Kunzi, R.L. Pettyjohn, R.K.L. Poon, R.W. Wilcox, and J.W. Waters, 1976: Remote sensing of atmospheric water vapor and liquid water with the Nimbus-5 microwave spectrometer. *J. Appl. Meteor.*, **15**, 1204-1214.

Stogryn, A., 1978: Estimates of brightness temperatures from scanning radiometer data. *IEEE Trans. Antennas Propag.*, **5**, 720-726.

Stolarski, R.S., and H.L. Wesoky, ed., 1993: *The Atmospheric Effects of Stratospheric Aircraft: A Third Program Report*, NASA Ref. Pub. 1313, National Aeronautics and Space Administration, Washington, D.C., 422 pp.

Stowe, L.L., E.P. McClain, R. Carey, P. Pellegrino, G. Gutman, P. Davis, C. Long, and S. Hart, 1991: Global distribution of cloud cover derived from NOAA/AVHRR operational satellite data. *Adv. Space Res.,* **11**, 51-54.

Stowe, L., P. Ardanuy, R. Hucek, P. Abel, and H. Jacobowitz, 1993: Evaluating the design of an earth radiation budget instrument with system simulations. Part I: Instantaneous estimates. *J. Atmos. Oceanic Tech.*, **10**, 809-826.

Strabala, K.I., S.A. Ackerman, and W.P. Menzel, 1994: Cloud properties inferred from 8-12 micron data. *J. Appl. Meteor.*, **33**, 212-229.

Strahler, A., A. Moody, and E. Lambin, 1995: Land cover and land-cover change from MODIS. *Proc. 15th Int. Geosci. and Remote Sens. Symp.*, Florence, Italy, July 10-14, 1995, vol. 2, 1535-1537.

Stroeve, J., A. Nolin, and K. Steffen, 1997: Comparison of AVHRR-derived and in situ surface albedo over the Greenland Ice Sheet. *Remote Sens. Environ.*, **62**, 262-276.

Strong, A.E., and E.P. McClain, 1984: Improved ocean surface temperature from space—comparisons with drifting buoys. *Bull. Amer. Meteor. Soc.*, **65** (2), 138-142.

Strow, L.L., D.C. Tobin, W.W. McMillan, S. E. Hannon, W.L. Smith, H.E. Revercomb, and R. Knuteson, 1998: Impact of a new water vapor continuum and line shape model on observed high resolution infrared radiances. *J. Quantitative Spectroscopy and Radiative Transfer*, **59** (3-5), 303-317.

Suarez, M., L.L. Takacs, A. Molod, and T. Wang, 1994: Documentation of the Goddard Earth Observing System (GEOS) General Circulation Model, Version 1. NASA Tech. Memo. 104606, NASA, Goddard Space Flight Center, Greenbelt, MD, 106 pp.

Sullivan, J., L. Gandin, A. Gruber, and W. Baker, 1993: Observation error statistics for NOAA-10 temperature and height retrievals. *Mon. Wea. Rev.*, **121**, 2578-2587.

Susskind, J., and D. Reuter, 1985: Retrieval of sea surface temperatures from HIRS2/MSU. *J. Geophys. Res.*, **90**, 11,602-11,608.

Susskind, J., J. Joiner, and M.T. Chahine, 1993: Determination of temperature and moisture profiles in a cloudy atmosphere using AIRS/AMSU. In NATO ASI Series, Vol. 19. High spectral resolution infrared remote sensing for Earth's weather and climate studies, ed. by A. Chedin, M.T. Chahine, and N.A. Scott, Springer Verlag, Berlin Heidelberg, 149-161.

Susskind, J., D. Reuter, and M.T. Chahine, 1997: Cloud fields derived from analysis of HIRS2/MSU sounding data. *J. Geophys. Res.*, **92**, 4035-4050.

Susskind, J., J.C. Barnet, and J. Blaisdell, 1998: Determination of atmospheric and surface parameters from simulated AIRS/AMSU/HSB data: Retrieval and cloud clearing methodology. *Adv. Space Res.*, **21** (3), 369-384.

Suttles, J.T., and G. Ohring, 1986: Surface radiation budget for climate applications. NASA Ref. Pub. 1169, Washington, DC, 136 pp.

Tanré D., M. Herman and Y.J. Kaufman, 1996: Information on the aerosol size distribution contained in the solar reflected spectral radiances. *J. Geophys. Res.*, **101**, 19,043–19,060.

Tanré, D., Y.J. Kaufman, M. Herman, and S. Mattoo, 1997: Remote sensing of aerosol properties over oceans using the MODIS/EOS spectral radiances. *J. Geophys. Res.*, **102** (D14), 16,971-16,988.

Tian, Y., Y. Zhang, Y. Knyazikhin, R.B. Myneni, J.M. Glassy, D. Dedieu, and S.W. Running, 2000: Prototyping of MODIS LAI and FPAR algorithm with LASUR and LANDSAT data. *IEEE Trans. Geosci. Remote Sens.*, in press.

Topliss, B.J., and T. Platt, 1986: Passive fluorescence and photosynthesis in the ocean: Implications for remote sensing. *Deep Sea Res.*, **33**, 849-864.

Townshend, J.R.G., and C.O. Justice, 1988: Selecting the spatial resolution of satellite sensors required for global monitoring of land transformations. *Int. J. Remote Sens.*, **9**, 187-236.

Townshend, J.R.G., C.O. Justice, W. Li, C. Gurney, and J. McManus, 1991: Global land cover classification by remote sensing: Present capabilities and future possibilities. *Remote Sens. Environ.*, **35**, 243-256.

Trenberth, K.E., 1998: Atmospheric moisture residence times and cycling: implications for rainfall rates and climate change. *Climate Change*, **39**, 667-694.

Ustin, S.L., M.O. Smith, and J.B. Adams, 1993: Remote sensing of ecological processes: A strategy for developing and testing ecological models using spectral mixture analysis. In *Scaling Physiological Processes Leaf to Globe*, ed. by J.R. Ehleringer and C.B. Field, Academic Press, New York, 339-357.

van Leeuwen, W.J.D., A.R. Huete, and T.W. Laing, 1999: MODIS vegetation index compositing approach: A prototype with AVHRR data. *Remote Sens. Environ.*, **69**, 264-280.

Vermote, E.F., N. El Saleous, C.O. Justice, Y.J. Kaufman, J.L. Privette, L. Remer, J.C. Roger, and D. Tanré, 1997: Atmospheric correction of visible to middle-infrared EOS-MODIS data over land surfaces: Background, operational algorithm and validation. *J. Geophys. Res.*, **102** (D14), 17,131-17,141.

Vladimer, J.A., P. Jastrzebski, M.C. Lee, P.H. Doherty, D.T. Decker, and D.N. Anderson, 1999: Longitude structure of ionospheric total electron content at low latitudes measured by the TOPEX/Poseidon satellite. *Radio Sci.*, **34** (5), 1239-1260.

Vonder, O.W. and J.P.G.W. Clevers, 1998: *Multisensor RS Capabilities Land—Report 1: Applications of Present and Future Optical Remote Sensing Satellite Sensors*, Wageningen Agricultural University, Netherlands, USP-2 98-25, BCRS, ISBN 90 5411 263-8, web address: http://137.224.135.82/cgi/projects/bcrs/multisensor/report1/intro.htm.

Vorosmarty, C., A. Grace, B. Moore III, B. Choudhury, and C.J. Willmott, 1991: A strategy to study regional hydrology and terrestrial ecosystem processes using satellite remote sensing, ground-based data, and computer modeling. *Acta Astronautica*, **25**, 785-792.

Wan, Z., and J. Dozier, 1996: A generalized split-window algorithm for retrieving land-surface temperature from space. *IEEE Trans. Geosci. Remote Sens.*, **34** (4), 892-905.

Wan, Z., and Z.-L. Li, 1997: A physics-based algorithm for retrieving land-surface emissivity and temperature from EOS/MODIS data. *IEEE Trans. Geosci. Remote Sens.*, **35**, 980-996.

Wang, J.R., and B.J. Choudhury, 1995: Passive microwave radiation from soil: Examples of emission models and observations. In *Passive Microwave Remote Sensing Research Related to Land-Atmosphere Interactions,* ed. by B.J. Choudhury, Y.H. Kerr, E.G. Njoku, and P. Pampaloni, VSP Press, The Netherlands, 423-460.

Wang, M., and H.R. Gordon, 1994: Estimating aerosol optical properties over the oceans with MISR: Some preliminary studies. *Appl. Opt.*, **33**, 4042-4057.

Wanner, W., X. Li, and A.H. Strahler, 1995: On the derivation of kernels for kernel-driven models of bidirectional reflectance. *J. Geophys. Res.*, **100**, 21,077-21,090.

Wanner, W., A.H. Strahler, B. Hu, X. Li, C.L. Barker Schaaf, P. Lewis, J.-P. Muller, and M.J. Barnsley, 1997: Global retrieval of bidirectional reflectance and albedo over land from EOS MODIS and MISR data: Theory and algorithm. *J. Geophys. Res.*, **102**, 17,143-17,162.

Webster, P.J., 1994: The role of hydrological processes in ocean-atmosphere interactions. *Rev. Geophys.*, **32**, 427-476.

Weeks, W.F., 1981: Sea ice: The potential of remote sensing. *Oceanus*, **24**, 39-48.

Weng, F., and N.C. Grody, 1994: Retrieval of cloud liquid water using the special sensor microwave imager (SSM/I). *J. Geophys. Res.*, **99**, 25,535-25,551.

Wentz, F.J., 1975: A two-scale scattering model for foam-free sea microwave brightness temperatures. *J. Geophys. Res.*, **80**, 3441-3446.

Wentz, F.J., 1983: A model function for ocean microwave brightness temperatures. *J. Geophys. Res.*, **88**, 1892-1908.

Wentz, F.J., 1992: Measurement of oceanic wind vector using satellite microwave radiometers. *IEEE Trans. Geosci. Remote Sens.*, **30**, 960-972.

Wentz, F.J., 1997: A well-calibrated ocean algorithm for SSM/I. *J. Geophys. Res.*, **102**, 8703-8718.

Wentz, F.J., and D.K. Smith, 1999: A model function for the ocean-normalized radar cross section at 14 GHz derived from NSCAT observations. *J. Geophys. Res.*, **104**, 11,499-11,514.

Wentz, F.J., and R.W. Spencer, 1998: SSM/I rain retrievals within a unified all-weather ocean algorithm. *J. Atmos. Sci.*, **55**, 1613-1627.

Wharton, S.W., and M.F. Myers, eds, 1997: *1997 MTPE/EOS Data Products Handbook, Vol. 1, TRMM & AM-1*, NASA Goddard Space Flight Center, Greenbelt, MD, 266 pp.

Whitlock, C.H., T.P. Charlock, W.F. Staylor, R.T. Pinker, I. Laszlo, A. Ohmura, H. Gilgen, T. Konzelman, R.C. DiPasquale, C.D. Moats, S.R. LeCroy, and N.A. Ritchey, 1995: First global WCRP shortwave surface radiation budget dataset. *Bull. Amer. Meteor. Soc.*, **76**, 905-922.

Wielicki, B.A., R.D. Cess, M.D. King, D.A. Randall, and E.F. Harrison, 1995: Mission to Planet Earth: Role of clouds and radiation in climate. *Bull. Amer. Meteor. Soc.*, **76**, 2125-2153.

Wielicki, B.A., B.R. Barkstrom, E.F. Harrison, R.B. Lee III, G.L. Smith, and J.E. Cooper, 1996: Clouds and the Earth's Radiant Energy System (CERES): An Earth Observing System experiment. *Bull. Amer. Meteor. Soc.*, **77,** 853-868.

Wielicki, B.A., B.R. Barkstrom, and 21 others, 1998: Clouds and the Earth's Radiant Energy System (CERES): Algorithm overview. *IEEE Trans. Geosci. Remote Sens.*, **36**, 1127-1141.

Wilheit, T.T., 1990: An algorithm for retrieving water vapor profiles in clear and cloudy atmospheres from 183 GHz radiometric measurements: Simulation studies. *J. App. Meteor.*, **29**, 508-515.

Wilheit, T.T., and A.T.C. Chang, 1980: An algorithm for retrieval of ocean surface and atmospheric parameters from the observations of the Scanning Multichannel Microwave Radiometer (SMMR). *Radio Sci.*, **15**, 525-544.

Wilheit, T.T., and M.G. Fowler, 1977: Microwave radiometric determination of wind speed at the surface of the ocean during BESEX. *IEEE Trans. Antennas Propag.*, **AP-25**, 111-120.

Wilheit, T.T., A.T.C. Chang, and L.S. Chiu, 1991: Retrieval of monthly rainfall indices from microwave radiometric measurements using probability distribution functions. *J. Atmos. Oceanic Technol.*, **8**, 118-136.

Willson, R.C., 1984: Measurements of solar total irradiance and its variability. *Space Sci. Rev.*, **38**, 203-242.

Willson, R.C., 1997: Total solar irradiance trend during solar cycles 21 and 22. *Science*, **277**, 1963-1965.

Willson, R.C., S. Gulkis, M. Janssen, H.S. Hudson, and G.A. Chapman, 1981: Observations of solar irradiance variability. *Science*, **211**, 700.

Willson, R.C., and A.V. Mordvinov, 1999: Time-frequency analysis of total solar irradiance variations. *J. Geophy. Res.*, **26**, 3613-3616.

World Meteorological Organization (WMO), 1992: Scientific assessment of ozone depletion: 1991, *Global Ozone Research and Monitoring Project*, World Meteorological Organization Report 25, 311 pp.

World Meteorological Organization (WMO), 1995: Scientific assessment of ozone depletion: 1994, Global Ozone Res. and Monit. Proj., WMO Report 37, 326 pp.

Woodard, M., and H.S. Hudson, 1983: Frequencies, amplitudes and linewidths of solar oscillations from total irradiance observations. *Nature*, **305**, 589-593.

Wu, M., and L.-P. Chang, 1992: Longwave radiation budget parameters computed from ISCCP and HIRS2/MSU products. *J. Geophy. Res.*, **97**, 1083-1101.

Wunsch, C., and E.M. Gaposchkin, 1980: On using satellite altimetry to determine the general circulation of the oceans with application to geoid improvement. *Rev. Geophys. Space Phys.*, **18**, 725-745.

Wunsch, C., and D. Stammer, 1998: Satellite altimetry, the marine geoid, and the oceanic general circulation. *Ann. Rev. Earth Planet. Sci.*, **26**, 219-253.

Wylie, D.P., and W.P. Menzel, 1998: Eight years of global high cloud statistics using HIRS. *J. Climate*, **12**, 170-184.

Yoder, J.A., C.R. McClain, G.C. Feldman, and W.E. Esaias, 1993: Annual cycles of phytoplankton chlorophyll concentrations in the global ocean, A satellite view. *Global Biogeochem. Cycles*, **7**, 181-193.

Young, D.F., E.F. Harrison, B.A. Wielicki, P. Minnis, G.G. Gibson, B.R. Barkstrom, T.P. Charlock, D.R. Doelling, A.J. Miller, O.C. Smith, and J.C. Stassi, 1995a: Clouds and the Earth's Radiant Energy System (CERES) Algorithm Theoretical Basis Document. Volume IV - Determination of Surface and Atmosphere Fluxes and Temporally and Spatially Averaged Products (Subsystems 5-12), Subsystem 7.0 - Time Interpolation and Synoptic Flux Computation for Single and Multiple Satellites, NASA Ref. Pub. 1376, Vol. IV, 69-108.

Young, D.F., E.F. Harrison, and E. Singh, 1995b: Clouds and the Earth's Radiant Energy System (CERES) Algorithm Theoretical Basis Document. Volume IV - Determination of Surface and Atmosphere Fluxes and Temporally and Spatially Averaged Products (Subsystems 5-12), Subsystem 8.0 - Monthly Regional, Zonal, and Global Radiation Fluxes and Cloud Properties, NASA Ref. Pub. 1376, Vol. IV, 109-128.

Young, D.F., P. Minnis, D. Baumgardner, and H. Gerber, 1998: Comparison of in situ and satellite-derived cloud properties during SUCCESS. *Geophys. Res. Lett.*, **25**, 1125-1128.

Zhan, X., R. DeFries, J.R.G. Townshend, C. DiMiceli, M. Hansen, C. Huang, and R. Sohlberg, 2000: The 250m global land cover change product from the Moderate Resolution Imaging Spectroradiometer of NASA's Earth Observing System. *Int. J. Remote Sens.*, **21**, 1433-1460.

Zhan, X., R. DeFries, M. Hansen, C. DiMiceli, R. Sohlberg, and C. Huang. 1999: Algorithm Theoretical Basis Document of the MODIS Enhanced Land Cover and Land Cover Change Product (MOD 29), update available at http://eospso.gsfc.nasa.gov/atbd/modistables.html.

Zhang, Y., Y. Tian, Y. Knyazikhin, J.V. Martonchick, D.J. Diner, M. Leroy, and R.B. Myneni, 2000: Prototyping of MODIS LAI and FPAR algorithm with POLDER data over Africa. *IEEE Trans. Geosci. Remote Sens.*, in press.

Zwally, H.J., J.C. Comiso, C.L. Parkinson, W.J. Campbell, F.D. Carsey, and P. Gloersen, 1983: *Antarctic Sea Ice, 1973-1976: Satellite Passive-Microwave Observations*, NASA Spec. Pub. 459, National Aeronautics and Space Administration, Washington, D.C., 206 pp.

Appendix D: Acronyms and Abbreviations

A

ACRIM	Active Cavity Radiometer Irradiance Monitor
ACRIMSAT	ACRIM Satellite
ADEOS	Advanced Earth Observing Satellite
ADM	Angular Distribution Model
AEM	Applications Explorer Mission
AERONET	Aerosol Robotic Network
AGC	Automatic Gain Control
AIRS	Atmospheric Infrared Sounder
AMI	Active Microwave Instrument
AMS	American Meteorological Society
AMSR	Advanced Microwave Scanning Radiometer
AMSR-E	Advanced Microwave Scanning Radiometer for EOS
AMSU	Advanced Microwave Sounding Unit
APAR	Absorbed Photosynthetically Active Radiation
APOLLO	AVHRR Processing scheme Over Cloud Land and Ocean
AREAS	Altimeter Return Echo Analysis System
ARM	Atmospheric Radiation Measurement
ARP	Absorbed Radiation by Phytoplankton
ASF	Alaska SAR Facility
ASTER	Advanced Spaceborne Thermal Emission and Reflection Radiometer
ASTEX	Atlantic Stratocumulus Transition Experiment
ATBD	Algorithm Theoretical Basis Document
ATSR	Along Track Scanning Radiometer
AVG	Name used for the CERES average Monthly Regional Radiative Fluxes and Cloud product
AVHRR	Advanced Very High Resolution Radiometer
AVIRIS	Airborne Visible-Infrared Imaging Spectrometer

B

BDS	Bi-Directional Scan
BGC	Biogeochemical
BIOME	Biogeochemical Information Ordering Management Environment
BOREAS	Boreal Ecosystems Atmosphere Study
BRDF	Bidirectional Reflectance Distribution Function
BUAN	Baseline Upper Air Network

C

CAGEX	CERES/ARM/GEWEX Experiment
CART	Cloud and Radiation Testbed
CCN	Cloud Condensation Nuclei
CDDIS	Crustal Dynamics Data Information System
CDOM	Colored (or Chromomorphic) Dissolved Organic Matter
CEES	Committee on Earth and Environmental Sciences
CERES	Clouds and the Earth's Radiant Energy System
CFC	Chlorofluorocarbon
CH_4	Methane
CHEM-1	Chemistry Mission-1 (now Aura)
CLAVR	Cloud Advanced Very high resolution Radiometer
ClO_x	Oxides of chlorine
CNES	Centre National d'Etudes Spatiales (France)
CO	Carbon monoxide
CPF	Calibration Parameter File
CRS	Clouds and Radiative Swath
CZCS	Coastal Zone Color Scanner

D

DAAC	Distributed Active Archive Center
DAO	Data Assimilation Office
DEM	Digital Elevation Model
DIS	Data and Information System
DMSP	Defense Meteorological Satellite Program
DoE	Department of Energy
DOM	Dissolved Organic Matter
DORIS	Doppler Orbitography and Radiopositioning Integrated by Satellite
DPH	Data Products Handbook
DTED	Digital Terrain Elevation Data

E

EASE	Equal-Area Scalable Earth, a grid for data mapping
ECMWF	European Centre for Medium-Range Weather Forecasts
ECS	EOSDIS Core System
EDC	EROS Data Center
ENSO	El Niño-Southern Oscillation
ENVISAT	Environmental Satellite, ESA
EO-1	Earth Observing 1
EOS	Earth Observing System
EOS PM	EOS afternoon-crossing satellite (now Aqua)
EOSDIS	EOS Data and Information System
EOSPSO	EOS Project Science Office
EP	Earth Probe
EPGN	EOS Polar Ground Network
ERB	Earth Radiation Budget
ERBE	Earth Radiation Budget Experiment
ERBS	Earth Radiation Budget Satellite
EROS	Earth Resources Observation System
ERS	European Remote Sensing Satellite
ERS-1	European Remote Sensing Satellite-1
ERTS	Earth Resources Technology Satellite
ES	EOS Science, a product identification code for CERES data products
ESA	European Space Agency
ESDIS	Earth Science Data and Information System
ESE	Earth Science Enterprise
ESMR	Electrically Scanning Microwave Radiometer
ESSP	Earth System Sciences Pathfinder
ET	Evapotranspiration
ETM	Enhanced Thematic Mapper
ETM+	Enhanced Thematic Mapper Plus
EVI	Enhanced Vegetation Index

F

FIFE	First ISLSCP Field Experiment
FIRE	First ISCCP Regional Experiment
FOV	Field of View
FPAR	Fraction of Photosynthetically Active Radiation
FSW	Name used for the CERES Monthly Gridded Radiative Fluxes and Clouds product
FTP	File Transfer Protocol

G

GCM	General Circulation Model (also Global Climate Model)
GDR	Geophysical Data Record
GEOS	Goddard Earth Observing System
GEOSAT	Geodetic Satellite
GEWEX	Global Energy and Water cycle Experiment
GOES	Geostationary Operational Environmental Satellite
GPCP	Global Precipitation Climatology Project
GPS	Global Positioning System
GRACE	Gravity Recovery And Climate Experiment
G/S	Ground Station
GSFC	Goddard Space Flight Center

H

HDF	Hierarchical Data Format
HIRDLS	High-Resolution Dynamics Limb Sounder
HIRS	High-Resolution Infrared Radiation Sounder
HO_x	Hydrogen oxides
HRPT	High-Resolution Picture Transmission
HSB	Humidity Sounder for Brazil

I

ICEMAP Ice-Mapping Algorithm

ICESat Ice, Clouds, and Land Elevation Satellite

ID Identification

IES Instrument Earth Scans

IFOV Instantaneous Field of View

IfSAR Interferometric Synthetic Aperture Radar

IGBP International Geosphere-Biosphere Programme

IGDR Interim Geophysical Data Record

IGS International Ground Station

IPAR Instantaneous Photosynthetically-Active Radiation

IPCC Intergovernmental Panel on Climate Change

IR Infrared

IR/MW Infrared/microwave

ISCCP International Satellite Cloud Climatology Project

ISLSCP International Satellite Land Surface Climatology Project

ITPP International TOVS Processing Package

J

JMR Jason-1 Microwave Radiometer

JPL Jet Propulsion Laboratory

K

Kbps Kilobits per second

L

LAI Leaf Area Index

Landsat Land Remote Sensing Satellite

LaRC Langley Research Center

LASE Laser Atmospheric Sensing Experiment

LI Lifted Index

LIS Lightning Imaging Sensor

LP Level Processors

LST Land Surface Temperature

Ltyp Spectral radiance at typical conditions

LVIS Laser Vegetation Imaging Sensor

LW Longwave

M

MAS MODIS Airborne Simulator

MB Megabyte

MBLA Multi-Beam Laser Altimeter

Met. data Meteorological data

METEOSAT Meteorology Satellite (an ESA geosynchronous satellite)

MISR Multi-angle Imaging Spectroradiometer

MIT Massachusetts Institute of Technology

MLR Multiple Linear Regression

MLS Microwave Limb Sounder

MMS Multi-mission Modular Spacecraft

MOA Meteorological Ozone and Aerosol

MOBY Marine Optical Buoy

MODIS Moderate Resolution Imaging Spectroradiometer

MODLAND MODIS Land science team

MOLA Mars Orbiter Laser Altimeter

MOPITT Measurements of Pollution in the Troposphere

MSE Mean squared error

MSFC Marshall Space Flight Center

MSS Multispectral Scanner

MSU Microwave Sounding Unit

MVI Modified Vegetation Index

MW Microwave

MW/IR Microwave/infrared

MWP Microwave Water Path

N

N/A Not Applicable

NASA National Aeronautics and Space Administration

NASDA National Space Development Agency (Japan)

NBAR Nadir BRDF-Adjusted Reflectance

NCEP National Centers for Environmental Prediction

NCSA National Center for Supercomputing Applications (at the University of Illinois)

NDVI Normalized Difference Vegetation Index

NE	Noise Equivalent
NESDIS	National Environmental Satellite, Data, and Information Service
NIR	Near Infrared
NISN	NASA Integrated Services Network
NMC	National Meteorological Center
NOAA	National Oceanic and Atmospheric Administration
NOHRSC	National Operational Hydrologic Remote Sensing Center
NORAD	North American Aerospace Defense Command
NO_x	Nitrogen oxides (NO, NO_2, NO_3)
NPOESS	National Polar-orbiting Operational Environmental Satellite System
NPP	Net Primary Production
NSCAT	NASA Scatterometer
NSIDC	National Snow and Ice Data Center
NWS	National Weather Service

O

OClO	Chlorine dioxide
OI	Optimum Interpolation
OLR	Outgoing Longwave Radiation
OMI	Ozone Monitoring Instrument
ORNL	Oak Ridge National Laboratory
OSDR	Operational Sensor Data Record
O_x	Oxides

P

PAR	Photosynthetically-Active Radiation
PDF	Portable Document Format
pdf	Probability density function
PEB	Phycoerythrobilin
PGE	Product Generation Executive
PICASSO	Pathfinder Instruments for Cloud and Aerosol Spaceborne Observations
PICASSO-CENA	Pathfinder Instruments for Cloud and Aerosol Spaceborne Observations-Climatologie Etendue des Nuages et des Aerosols
POCC	Project Operation Control Center
PO.DAAC	Physical Oceanography Distributed Active Archive Center (at the Jet Propulsion Laboratory)
POES	Polar Orbiting Environmental Satellite
POLDER	Polarization and Directionality of the Earth's Reflectance
PP	Pre-Processor
ppm	Parts per million
ppmv	Parts per million by volume
PR	Precipitation Radar
PSC	Polar Stratospheric Cloud
PSN	Photosynthesis
PUB	Phycourobilin

Q

QA	Quality Assurance
QuikScat	Quick Scatterometer
QuikTOMS	Quick Total Ozone Mapping Spectrometer

R

RAOBS	Radiosonde Observations
RMS	Root Mean Square
RSMAS	Rosenstiel School of Marine and Atmospheric Science, University of Miami
RSS	Root Sum Square

S

SAGE	Stratospheric Aerosol and Gas Experiment
SAM	Stratospheric Aerosol Measurement
SAR	Synthetic Aperture Radar
SARB	Surface and Atmospheric Radiation Budget
SASS	SEASAT-A Satellite Scatterometer
SBRS	Santa Barbara Remote Sensing
S/C	Spacecraft
SCAR-B	Smoke, Cloud, and Radiation-Brazil
SCF	Scientific Computing Facility
SEASAT	Sea Satellite
SeaWiFS	Sea-viewing Wide Field-of-view Sensor
SEDAC	Socioeconomic Data and Applications Center
SERCAA	Support of Environmental Requirements for Cloud Analysis and Archive
SFC	Surface Fluxes and Clouds

SGDR	Sensor Geophysical Data Record
SGP	Southern Great Plains
SI	Systeme Internationale
SIM	Spectral Irradiance Monitor
SIPS	Science Investigator-led Processing System
SLA	Shuttle Laser Altimeter
SLR	Satellite Laser Ranging
SMM	Solar Maximum Mission
SMMR	Scanning Multichannel Microwave Radiometer
SNOMAP	Snow-Mapping Algorithm
SNR	Signal-to-Noise Ratio
SOHO	Solar Heliospheric Observatory
SORCE	Solar Radiation and Cloud Experiment
SPOT-2	Systeme Pour l'Observation de la Terre-2
SRB	Surface Radiation Budget
SRBAVG	Name for CERES Monthly TOA/Surface Averages product
SRTM	Shuttle Radar Topography Mission
SSALTO	Segment Sol Multimission Altimetry and Orbitography
SSF	Single Scanner Footprint*
SSM/I	Special Sensor Microwave/Imager
SST	Sea Surface Temperature
SW	Shortwave
SWE	Snow Water Equivalent
SWH	Significant Wave Height
SWIR	Shortwave Infrared
SWS	SeaWinds Standard
SYN	Name for CERES Synoptic Radiative Fluxes and Clouds product

T

TARFOX	Tropospheric Aerosol Radiative Forcing Observational Experiment
Tb	Brightness temperature
TCP	Topographic Control Points
TEC	Total Electron Content
TES	Tropospheric Emission Spectrometer
TIM	Total Irradiance Monitor
TIMED	Thermosphere, Ionosphere, Mesosphere, Energetics, and Dynamics
TIR	Thermal Infrared
TLSCF	Team Leader Science Computing Facility
TM	Thematic Mapper
TMI	TRMM Microwave Imager
TMR	TOPEX Microwave Radiometer
TOA	Top Of the Atmosphere
TOGA	Tropical Ocean Global Atmosphere
TOMS	Total Ozone Mapping Spectrometer
TOPEX	Ocean Topography Experiment
TOPEX/ Poseidon	Ocean Topography Experiment/ Poseidon (U.S.-France)
TOVS	TIROS Operational Vertical Sounder
T/P	TOPEX/Poseidon
TRMM	Tropical Rainfall Measuring Mission
T_s	Sea surface temperature
TSI	Total Solar Irradiance
TSIM	Total Solar Irradiance Mission
TT	Total Totals
Ttyp	Temperature at typical conditions

U

UARS	Upper Atmosphere Research Satellite
UMD	University of Maryland
UNESCO	United Nations Educational, Scientific, and Cultural Organization
USGS	United States Geological Survey
USNO	United States Naval Observatory
UT	Universal Time
UTC	Universal Time Coordinate
UV	Ultraviolet

V

VCL	Vegetation Canopy Lidar
VDC	VCL Data Center
VDIS	Vertical Distribution of Intercepted Surfaces
VI	Vegetation Index
VIRGO	Variability of solar Irradiance and Gravity Oscillations
VIRS	Visible Infrared Scanner
VIS	Visible
VISSR	Visible Infrared Spin-Scan Radiometer
VNIR	Visible and Near Infrared
VPGS	VCL Precision Geolocation System

*SSF is also used in the Product ID for the CERES Single Scanner TOA/Surface Fluxes and Clouds product

W

WCRP	World Climate Research Program
WINCE	Winter Cloud Experiment
WMO	World Meteorological Organization
WN	Window

Z

ZAVG	Name for CERES Monthly Zonal and Global Radiative Fluxes and Clouds product

Appendix E: Data Products Index

Poseidon-2 (on Jason-1)

Poseidon-2/JMR/DORIS (on Jason-1)

SAGE III (on Meteor 3M)

SeaWinds (on QuikScat)

TOMS (on QuikTOMS)

EOS
http://eos.nasa.gov/

EOSDIS
http://spsosun.gsfc.nasa.gov/New_EOSDIS.html

ACRIMSAT
- ACRIM III

Aqua
- AIRS
- AMSR-E
- AMSU-A
- CERES
- HSB
- MODIS

Jason-1
- DORIS
- JMR
- Poseidon-2

Landsat 7
- ETM+

Meteor 3M
- SAGE III

QuikScat
- SeaWinds

QuikTOMS
- TOMS

VCL
- MBLA

National Aeronautics and
Space Administration

NP-2000-5-055-GSFC